

**A Genetic Investigation of the
Muscle and Neuronal
Channelopathies: From Sanger
to Next – Generation
Sequencing**

Alice Gardiner

MRC Centre for Neuromuscular Diseases and UCL Institute
of Neurology

Supervised by Professor Henry Houlden and Professor
Mike Hanna

Declaration

I, Alice Gardiner, confirm that the work presented in this thesis is my own. Where information has been derived from other sources, I confirm that this has been indicated in the thesis.

Signature.....*Alice*.....

Date.....*24/03/2016*.....

Abstract

The neurological channelopathies are a group of hereditary, episodic and frequently debilitating diseases often caused by dysfunction of voltage-gated ion channels. This thesis reports genetic studies of carefully clinically characterised patient cohorts with different episodic neurological and neuromuscular disorders including paroxysmal dyskinesias, episodic ataxia, periodic paralysis and episodic rhabdomyolysis.

Genetic and clinical heterogeneity has in the past, using traditional Sanger sequencing methods, made genetic diagnosis difficult and time consuming. This has led to many patients and families being undiagnosed. Here, different sequencing technologies were employed to define the genetic architecture in the paroxysmal disorders.

Initially, Sanger sequencing was employed to screen the three known paroxysmal dyskinesia genes in a large cohort of paroxysmal movement disorder patients and smaller mixed episodic phenotype cohort. A genetic diagnosis was achieved in 39% and 13% of the cohorts respectively, and the genetic and phenotypic overlap was highlighted.

Subsequently, next-generation sequencing panels were developed, for the first time in our laboratory. Small custom-designed amplicon-based panels were used for the skeletal muscle and neuronal channelopathies. They offered considerable clinical and practical benefit over traditional Sanger sequencing and revealed further phenotypic overlap, however there were still problems to overcome with incomplete coverage. Large custom and non-custom pull-down panels were used to investigate patients with recurrent rhabdomyolysis patients. The contribution of genetic abnormalities was determined, and it was concluded that while the contribution of the *RYR1* was substantial, it was minimal for the classic voltage-gated ion channels *SCN4A* and *CACNA1S*.

Lastly, whole-exome sequencing was applied to two large undiagnosed possible channelopathy families. One family was found to indeed harbour a channelopathy mutation, whilst the other did not.

Overall, next-generation sequencing proved to be a more thorough and efficient method for channelopathy genetic diagnosis and several novel findings throughout the thesis expanded the current knowledge within the field.

Acknowledgements

I would first like to thank my supervisors Professor Henry Houlden and Professor Mike Hanna for their support, encouragement and scientific guidance of me and my project throughout the last four years. I am deeply grateful for the opportunity, time and supervision that they have given me, and without which I could not have succeeded.

I am also hugely grateful to my friends and family; in particular to my parents for their unwavering belief in me, their constant assistance in all things, for providing a lovely place for me to write when I needed to escape London, and to my mum for taking the time to read through this thesis. I thank my sister, Jenny, for her encouragement, wisdom, and the benefit of her scientific experience and my twin, Robert, for his constant non-scientific support. I also thank all of my friends for keeping me sane and for making the move to London one that I have not for a second regretted. I am especially indebted to Andy and Elaine for opening their house to me, first, when I needed somewhere to live three years ago and more recently when I needed somewhere to write, away from the builders.

This PhD would have not been possible without unending help and insight from everyone within Molecular Neurosciences, the MRC centre for Neuromuscular Diseases and the Neurogenetics team, in particular Renata, Amelie, Fatima, Josh, Mark, Klaus, Cath, Ros, Rob, Roope, Alan, Debbie and Karen, to whom I express my sincerest gratitude. Special thanks go to Ellen, Siobhan and Qiang, with whom sharing an office has been a pleasure, for their entertainment, advice and friendship.

Lastly, I would like extend my thanks to the Muscular Dystrophy Campaign, who funded this project, and to all of the patients and their families who have taken part in this research.

Table of Contents

Declaration	2
Abstract	3
Acknowledgements.....	4
Table of Contents	5
List of Figures	13
List of Tables	16
List of Abbreviations	19
Publications Arising from this Thesis.....	23
Chapter 1: Introduction	26
1. Voltage-Gated Ion Channels.....	26
1.1. Action Potentials.....	27
1.2. Structure of Voltage-Gated Ion Channels	27
1.3. Families of Voltage-Gated Ion Channels.....	30
1.3.1. Voltage-Gated Sodium Channels (VGSCs)	31
1.3.2. Voltage-Gated Calcium Channels (VGCCs)	31
1.3.3. Voltage-Gated Chloride Channels	31
1.3.4. Voltage-Gated Potassium Channels (VGKCs).....	31
1.4. Ryanodine Receptors (RyRs)	39
2. Channelopathies.....	39
2.1. The Skeletal Muscle Channelopathies.....	40
2.1.1. The Non-Dystrophic Myotonias.....	43
2.1.2. The Periodic Paralyse.....	45
2.2. The Neuronal Channelopathies	48
2.2.1. Episodic Ataxia	50
2.2.2. Familial Hemiplegic Migraine	53
2.2.3. The Paroxysmal Dyskinesias.....	55
2.3. Non-Channel Channelopathies	63
3. Rhabdomyolysis	64

3.1.	Channelopathies.....	66
3.1.1.	MHS1 – RYR1.....	66
3.1.2.	MHS5 – CACNA1S.....	67
3.1.3.	SCN4A	67
3.2.	Metabolic Muscle Disorders.....	67
3.2.1.	Glycogen Storage Diseases	68
3.2.2.	Fatty Acid Metabolism Disorders	75
3.3.	Muscular Dystrophy Genes.....	78
3.3.1.	ANO5	78
3.3.2.	FKRP.....	78
3.3.3.	DMD.....	78
3.3.4.	SGCA and SGCB.....	79
3.3.5.	DYSF.....	79
3.4.	Miscellaneous Genes	79
3.5.	Common Polymorphisms.....	81
4.	Mutation Detection.....	84
4.1.	Methods of Mutation Detection	84
4.1.1.	Sanger Sequencing	84
4.1.2.	Linkage Analysis.....	84
4.1.3.	Genome-Wide Association Studies.....	85
4.1.4.	MLPA and CGH Array	86
4.1.5.	Next-Generation Sequencing.....	87
4.2.	Determining Pathogenicity.....	94
4.2.1.	Splice Site Prediction.....	94
4.2.2.	Bioinformatic Tools	95
4.2.3.	Population Frequency Databases.....	95
4.2.4.	Functional Investigations	96
5.	Thesis Aims.....	97
	Chapter 2: Materials and Methods	98
1.	Patients	98

2.	PCR and Sanger Sequencing.....	98
2.1.	PCR and Product Purification	98
2.2.	Sequencing Reaction.....	99
2.3.	Mutation Nomenclature.....	100
3.	Functional Studies – HEK293 Cells and Fibroblasts	100
3.1.	Vector Transformation and Amplification	100
3.2.	Mutagenesis	101
3.3.	Transfection of Vector into HEK293 Cells and Cell Harvesting	101
3.4.	Western Blot.....	102
3.5.	RNA Extraction from Fibroblasts.....	102
3.6.	Reverse Transcription and cDNA Sequencing.....	103
4.	Next-Generation Sequencing.....	103
4.1.	TruSeq Custom Amplicon.....	103
4.1.1.	Library Preparation Protocol	103
4.2.	TruSight One	105
4.2.1.	Library preparation protocol.....	106
4.3.	Whole Exome Library Preparation and Sequencing.....	108
4.4.	Primary Data Analysis	109
4.5.	Variant Filtering	109
4.6.	Determination of Coverage.....	109
5.	Electrophysiology.....	109
5.1.	RNA Preparation	109
5.2.	<i>Xenopus</i> Oocyte Collection, Preparation and Injection	110
5.3.	Two-Electrode Voltage Clamp Recording	110
5.4.	TEVC Data Analysis	111
Chapter 3: Screening of the Paroxysmal Dyskinesia Genes		112
1.	Introduction.....	112
2.	Chapter Aims.....	113
3.	Patients and Methods.....	114
3.1.	Patient Cohorts.....	114

3.1.1.	Mixed Paroxysmal Dyskinesia Cohort.....	114
3.1.2.	Related Episodic Cohort.....	115
3.2.	Genetic Investigations	115
3.2.1.	Paroxysmal Dyskinesia Gene Screening	115
3.2.2.	<i>SNAP25</i> Screening.....	115
3.2.3.	Results Collection from Departmental Colleagues	115
3.3.	Functional Investigations	117
3.3.1.	Expression of Wild type and Mutant <i>PRRT2</i> Protein in HEK293 cells..	117
3.3.2.	Investigation of Nonsense-Mediated Decay in Patient Fibroblasts.....	118
3.3.3.	Determination of Neuronal Expression Levels of PxD and Related Genes 119	
4.	Results	119
4.1.	Frequency of Mutations in <i>PRRT2</i> , <i>PNKD</i> and <i>SLC2A1</i>	119
4.1.1.	<i>PRRT2</i> Screening in the PxD Cohort.....	119
4.1.2.	<i>PRRT2</i> Screening in the Further Episodic Phenotype Cohort.....	120
4.1.3.	<i>PNKD</i> Screening in the PxD Cohort.....	124
4.1.4.	<i>PNKD</i> Screening in the Further Episodic Phenotype Cohort.....	124
4.1.5.	<i>SLC2A1</i> Screening in the PxD Cohort	124
4.1.6.	<i>SLC2A1</i> Screening in the Further Episodic Phenotype Cohort	125
4.1.7.	Cohort-Wide Results – PxD Cohort	130
4.1.8.	Cohort-Wide Results – Non-PxD Cohort.....	130
4.2.	Additional Mutations Identified Within the Department in <i>PRRT2</i> , <i>SLC2A1</i> , and <i>PNKD</i> 130	
4.3.	<i>SNAP25</i> Screening.....	131
4.4.	Mutation Analysis	131
4.4.1.	<i>PRRT2</i> Mutations	131
4.4.2.	<i>PNKD</i> Mutations.....	137
4.4.3.	<i>SLC2A1</i> Mutations.....	137
4.5.	Functional Analysis.....	141
4.5.1.	Over-Expression of Wild type and Mutant <i>PRRT2</i>	141

4.5.2.	cDNA Sequencing to Investigate the Occurrence of Nonsense-Mediated Decay of PRRT2 mRNA	141
4.5.3.	cDNA Sequencing to Investigate the Occurrence of Nonsense-Mediated Decay of PNKD mRNA	144
5.	Discussion	144
Chapter 4: Investigating Channel Panels for Diagnosis of the Channelopathies		151
1.	Introduction.....	151
2.	Chapter Aims.....	152
3.	Patients and Methods	152
3.1.	Patients	152
3.1.1.	Patients and Controls used for the Brain Channel Panel Trial.....	152
3.1.2.	Patients and Controls used for the Muscle Channel Panel Trial.....	153
3.2.	Panels	153
3.2.1.	Panel Design	153
3.2.2.	Library Preparation and Sequencing.....	153
3.2.3.	Primary Data Analysis and Coverage Determination	153
3.2.4.	Variant Filtering	154
3.2.5.	Variant Confirmation.....	154
3.3.	Sensitivity and Specificity Calculations	155
4.	Results	155
4.1.1.	Brain Channel Panel Design.....	155
4.1.2.	Muscle Channel Panel Design.....	155
4.2.	Brain Channel Panel Results	158
4.2.1.	Positive Controls.....	158
4.2.2.	False Positive Calls	159
4.2.3.	Patient Results	160
4.2.4.	Clinical Benefit.....	165
4.2.5.	Coverage.....	165
4.3.	Muscle Channel Panel Results	167
4.3.1.	Positive Controls.....	167

4.3.2.	False Positive Calls	168
4.3.3.	Patient Results – Genetically Undiagnosed Patient Cohort.....	169
4.3.4.	Patient Results – Single Recessive <i>CLCN1</i> Mutation Patients.....	175
4.3.5.	Clinical Benefit.....	175
4.3.6.	Clinical ‘Likelihood’ Ratings	175
4.3.7.	Coverage.....	176
5.	Discussion	177
Chapter 5: Panel Sequencing in a Large Cohort of Patients with Rhabdomyolysis and Exercise Intolerance		
		180
1.	Introduction.....	180
2.	Chapter Aims.....	181
3.	Methods.....	182
3.1.	Patients	182
3.2.	Panels	182
3.2.1.	TruSeq Custom Amplicon Panel Design, Library Preparation and Sequencing.....	182
3.2.2.	TruSight One Library Preparation and Sequencing.....	183
3.2.3.	Primary Data Analysis and Coverage Determination	183
3.3.	Variant Filtering	183
3.4.	Variant Confirmation.....	183
3.5.	Known Polymorphism Analysis.....	184
3.6.	Enolase Activity Assay.....	184
3.7.	Western Blot.....	184
4.	Results	185
4.1.	TruSeq Custom Amplicon Rhabdomyolysis Panel	185
4.1.1.	Panel Design	185
4.1.2.	Failed samples	187
4.1.3.	Coverage.....	187
4.1.4.	Decision to Change Sequencing Method.....	187
4.2.	TruSight One Panel	187

4.2.1.	Gene Selection.....	187
4.2.2.	Library Quality	190
4.2.3.	Coverage.....	192
4.3.	Patient Results	192
4.3.1.	Channelopathy Genes.....	192
4.3.2.	Glycogen Storage Disorder Genes	204
4.3.3.	Fatty Acid Metabolism Genes	209
4.3.4.	Muscular Dystrophy Genes	212
4.3.5.	Miscellaneous Genes	219
4.3.6.	Overall.....	224
4.4.	Polymorphism Analysis - Previously Reported Risk Factors	225
4.4.1.	<i>ACTN3</i> p.(Arg577*) - rs1815739.....	225
4.4.2.	<i>MYLK</i> p.(Pro21His) - rs28497577	226
5.	Discussion	226
Chapter 6: Whole Exome Sequencing in Two Genetically Unexplained Possible Channelopathy Families		
		232
1.	Introduction.....	232
2.	Aims	233
3.	Methods.....	234
3.1.	Whole Exome Sequencing and Primary Data Analysis	234
3.2.	Sequencing of <i>KCNA1</i>	234
3.3.	Expression of Wild type and Mutant <i>KCNA1</i> RNA in Oocytes.....	234
3.4.	Electrophysiological Investigation of Wild Type and mutant <i>KCNA1</i>	235
3.5.	Two-Electrode Voltage-Clamp (TEVC) Protocols.....	235
3.6.	Analysis	236
4.	Results	236
4.1.	Project One – Whole Exome Sequencing in a Large Paroxysmal Exercise-Induced Dyskinesia Pedigree.....	236
4.1.1.	Clinical Presentation and Family Tree of Family A.....	236
4.1.2.	Index Case Whole Exome Sequencing.....	237

4.1.3.	Candidate Gene Screening Result.....	239
4.1.4.	Screening of <i>KCNA1</i> in a Cohort of 190 Mixed Channelopathy Patients 239	
4.1.5.	Hypothesis – A Gating Pore Current?.....	241
4.1.6.	Two-Electrode Voltage-Clamp.....	243
4.1.7.	Crude Currents Test.....	243
4.1.8.	Quantification of Steady-State Currents at Different WT:MT Ratios.....	244
4.1.9.	Pathology of p.(Arg298Thr) Mutation Discussion.....	246
4.2.	Project Two - Exome Sequencing in a Complex Myopathy Family.....	248
4.2.1.	Clinical Presentation and Family Tree of Family B.....	248
4.2.2.	Whole Exome Sequencing of Three Family Members.....	249
4.2.3.	Shared Variants Between all Three Members.....	251
4.2.4.	Shared Variants between Two Family Members.....	252
4.2.5.	Analysis of only the Sisters.....	257
4.2.6.	Analysis of only RW.....	258
5.	Discussion.....	259
	Chapter 7: General Conclusions.....	262
1.	Chapter Three.....	262
2.	Chapter Four.....	264
3.	Chapter Five.....	265
4.	Chapter Six.....	266
5.	Overall.....	268
	Appendices.....	272
	Appendix 1 – Target and Designed Amplicon Coordinates and Target Coverage of Brain Channel Panel.....	272
	Appendix 2 – Target and Designed Amplicon Coordinates and Target Coverage of Muscle Channel Panel.....	278
	Appendix 3 – Negative Patients included on the Brain and Muscle Channel Panels .	284
	Appendix 4 –Variants Identified by the Rhabdomyolysis Panel.....	286
	References.....	306

List of Figures

Figure 1.1 – The stages involved in the creation and propagation of an action potential

Figure 1.2 – A schematic diagram of the 24 transmembrane domains of Na⁺ and Ca²⁺

Figure 1.3 – The channel genes in which mutations cause muscular and neuronal disease, divided by type of disorder and location of impact

Figure 1.4 – The genetic spectrum and diagnostic strategy for the skeletal muscle channelopathies

Figure 1.5 – A Venn diagram showing the phenotypic and genetic overlap of the neuronal channelopathies (including the Paroxysmal dyskinesias)

Figure 1.6 – *PNKD* schematic diagrams showing (a) the different isoforms and (b) the known mutations

Figure 1.7 – *SLC2A1* schematic diagrams showing the known mutations

Figure 1.8 – *PRRT2* schematic diagrams showing the known mutations

Figure 1.9 – A spider diagram to summarise the genetic and non-genetic causes of rhabdomyolysis

Figure 1.10 – The steps in the sequencing process used by Illumina NGS chemistry

Figure 1.11 – Examples of six different WES mutation detection strategies

Figure 2.1 – Overview of the TSCA library preparation process

Figure 3.1 – The structure of the pEF1-HA vector

Figure 3.2 – Chromatograms, nucleotide conservation and family trees for *PRRT2* mutations

Figure 3.3 – Chromatograms, nucleotide conservation and family trees for *PNKD* mutations

Figure 3.4 – Chromatograms, nucleotide conservation and family trees for *SLC2A1* mutations

Figure 3.5 – *PRRT2* schematic diagrams showing (a) the mutations identified here and (b) a *PRRT2* elongation mutation

Figure 3.6 – Chromatograms, nucleotide conservation and family trees for compound heterozygous *PRRT2* mutations

Figure 3.7 – *PNKD* schematic diagram showing the mutations identified here

Figure 3.8 – *SLC2A1* schematic diagram showing the mutations identified here

Figure 3.9 – The western blot of HA-tagged *PRRT2* expression in soluble fractions of transfected HEK 293 cells

Figure 3.10 – The predicted consequence of mutations on the *PRRT2* protein

Figure 3.11 – A schematic diagram of the WT and truncated *PNKD-L*, the result of the P341Pfs*2 mutation

Figure 3.12 – A suggested synaptic mechanism for the paroxysmal dyskinesias

Figure 3.13 – The regional distribution of *CACNA1A*, *KCNA1*, *PNKD*, *PRRT2*, *SLC2A1* and *SNAP25* mRNA expression in the normal human brain

Figure 4.1 – (a) A screenshot of Illumina Design Studio software and (b) an example of designed amplicons covering the *PRRT2* gene

Figure 4.2 – Chromatograms and genome browser visualisations of a selection of mutations found by the brain channel panel

Figure 4.3 – The average percentage coverage for each exon of each gene included in the brain channel panel

Figure 4.4 – Chromatograms and genome browser visualisations of a selection of mutations found by the muscle channel panel

Figure 4.5 – The average percentage coverage for each exon of each gene included in the muscle channel panel

Figure 5.1 – The TruSight One library fragments as shown on the bioanalyzer

Figure 5.2 – The enolase activity assay, showing that there is a significant lag of reaction completion between the sample of patient 5.70 and controls

Figure 5.3 – The levels of caveolin-3 and β -dystroglycan in three patients with *CAV3* mutations

Figure 6.1 – The family tree of family A

Figure 6.2 – A flow diagram to show the candidate gene strategy employed for mutation discovery in family A

Figure 6.3 – The (a) chromatogram and conservation and (b) segregation of the *KCNA1* mutation found in family A

Figure 6.4 – A schematic diagram to show how neutralisation of an S4 arginine can result in a gating pore current

Figure 6.5 – The currents produced in response to protocol one by homotetrameric (a) WT and (b) p.(Arg298Thr) (MT) $K_v1.1$ channels

Figure 6.6 – The (a) mean and (b) largest currents produced in response to protocol two by the varying subunit ratios

Figure 6.7 – The ratios of each of the five types of $K_v1.1$ channel

Figure 6.8 – The family tree of family B

Figure 6.9 – A flow diagram to show shared variant strategy employed for mutation discovery in family B

Figure 6.10 – Visualisations of the difference between (a) a variant that was covered but not present and (b) a variant that was not covered

Figure 6.11 – The chromatograms of three family members and nucleotide conservation for the *DES* mutation c.735+1G>A

List of Tables

Table 1.1 – An overview of the human sodium channel alpha subunits

Table 1.2 – An overview of the human calcium channel subunits

Table 1.3 – An overview of the human chloride alpha subunits

Table 1.4 – An overview of the human potassium channel subunits

Table 1.5 – A summary of the skeletal muscle channelopathies

Table 1.6 – A summary of the neuronal channelopathies

Table 1.7 – An overview of EA3 – EA7

Table 1.8 – The features of the paroxysmal dyskinesias

Table 1.9 – A summary of the glycogen storage diseases

Table 1.10 – A summary of the fatty acid metabolism disorders that cause rhabdomyolysis

Table 1.11 – ‘Miscellaneous’ rhabdomyolysis genes

Table 1.12 – The common polymorphisms that have been reported be associated with raised CK or rhabdomyolysis

Table 1.13 – The details of different next-generation sequencing platforms

Table 3.1 – The primer sequences used to screen *PNKD*, *PRRT2* and *SLC2A1*

Table 3.2 – The primer sequences used to screen *SNAP25*

Table 3.3 – The mutagenesis primer sequences used to introduce two mutations into the *PRRT2* gene

Table 3.4 –Primer sequences used to sequence regions of *PNKD* and *PRRT2* cDNA

Table 3.5 – The mutations identified in *PRRT2* in the paroxysmal dyskinesia cohort

Table 3.6 – The mutations identified in *PRRT2* in the mixed episodic phenotype cohort

Table 3.7 – The mutations identified in *PNKD* in the paroxysmal dyskinesia cohort

Table 3.8 – The mutations identified in *SLC2A1* in the paroxysmal dyskinesia cohort

Table 3.9 – The mutations identified in *SLC2A1* in the mixed episodic phenotype cohort

Table 3.10 – Mutations in the three PxD genes found within the department

Table 3.11 – The Polyphen-2, SIFT, EVS and 1000genome scores for the novel variants found in *PRRT2*

Table 3.12 – The Polyphen-2, SIFT, EVS and 1000genome scores for the novel variants found in *SLC2A1*

Table 4.1 – The genes, exons and amplicons included in the brain channel panel

Table 4.2 –The final brain channel panel design metrics

Table 4.3 – The genes, exons and amplicons included in the muscle channel panel

Table 4.4 –The final muscle channel panel design metrics

Table 4.5 – The positive controls included on the brain channel panel

Table 4.6 – The possible pathogenic mutations identified by the brain channel panel

Table 4.7 – The positive controls included on the muscle channel panel

Table 4.8 – The possible pathogenic mutations identified by the muscle channel panel

Table 5.1 – The genes, exons and amplicons included in the TSCA rhabdomyolysis panel

Table 5.2 –The final TSCA rhabdomyolysis panel design metrics

Table 5.3 – The genes included in the revised gene list and so analysed on the TruSight One rhabdomyolysis panel

Table 5.4 – The rare variations found in *RYR1*

Table 5.5 – The rare heterozygous mutations found in *CACNA1S*

Table 5.6 – The rare heterozygous mutations found in *SCN4A*

Table 5.7 – The recessive mutations found in *PYGM*

Table 5.8 – The recessive mutations found in *PFKM*

Table 5.9 – The possible pathogenic mutations found in *PHKA1*

Table 5.10 – The recessive mutations found in *CPT2*

Table 5.11 – The recessive mutations found in *ACADVL*

Table 5.12 – The recessive mutations found in *ANO5*

Table 5.13 – The recessive mutations found in *DYSF*

Table 5.14 – The mutations that fit the described criteria found in *DMD*

Table 5.15 – The mutations found in *CAV3*

Table 5.16 – The clinical features of the five patients with *CAV3* mutations

Table 5.17 – The patients in whom pathogenic and possibly pathogenic mutations were found by the rhabdomyolysis panel

Table 6.1 – The primer sequences used to screen *KCNA1*

Table 6.2 – The mutagenesis primer sequences used to create the wild type and p.(Arg298Thr) *KCNA1* vector

Table 6.3 – The volumes of WT RNA, mutant RNA and water used to create varying WT: mutant ratios

Table 6.4 – The WES metrics for patient A.I.2

Table 6.5 – The WES metrics for patients B.IV.8, B.IV.9 and B.IV.5

Table 6.6 – The shared variants between patients B.IV.5, B.IV.8 and B.IV.9

Table 6.7 – The shared variants between patients B.IV.5 and B.IV.9 but not patient B.IV.8

Table 6.8 – The variations found in patients B.IV.8 and B.IV.9 that are in regions not covered by WES in patient B.IV.5

Table 7.1 – A revised summary of the genes involved in neuronal channelopathies

List of Abbreviations

AD	Autosomal dominant
ADHD	Attention deficit hyperactivity disorder
AR	Autosomal recessive
ADP	Adenosine diphosphate
ATP	Adenosine triphosphate
ATS	Andersen-Tawil Syndrome
BMD	Becker's muscular dystrophy
BSA	Bovine serum albumin
cDNA	Complementary deoxyribonucleic acid
CGH	Comparative genomic hybridisation
CHCT	Caffeine-halothane contracture test
CK	Creatine kinase
CNS	Central nervous system
CRBL	Cerebellum
CSD	Cortical sensory depression
CSF	Cerebrospinal fluid
CNV	Copy number variation
DTX	Dendrotoxin
DHAP	dihydroxyacetone phosphate
DMD	Duchenne's muscular dystrophy
DNA	Deoxyribonucleic acid
dNTP	Deoxynucleosidetriphosphate
DTT	Dithiothreitol
EA	Episodic ataxia
EC	Excitation-contraction
ECL	Electrochemiluminescence
EDTA	Ethylenediaminetetraacetic acid
EEG	Electroencephalogram
EGTA	Ethylene glycol tetraacetic acid
ERDB	Elicited repetitive daily blindness
EMHG	European malignant hyperthermia group
EMG	Electromyography
EVS	Exome variant server
ExAC	Exome aggregation consortium

FALS	Familial amyotrophic lateral sclerosis
FCTX	Frontal cortex
F/H	Family history
FHM	Familial hemiplegic migraine
FPU	Filter plate assembly unit
GFP	Green fluorescent protein
GLUT1 DS1	GLUT1 deficiency syndrome 1
GSD	Glycogen storage disease
GWAS	Genome-wide association study
HA	Human influenza hemagglutinin
HEK	Human embryonic kidney
HIPP	Hippocampus
HM	Hemiplegic migraine
HVA	High voltage-activated
HyperPP	Hyperkalemic periodic paralysis
HypoPP	Hypokalemic periodic paralysis
ICCA	Infantile convulsions and choreoathetosis
IF	Intermediate filament
ION	Institute of Neurology
IPSC	Induced pluripotent stem cell
IVCT	In vitro contracture test
IVG	Integrative genomics viewer
K+	Potassium ion
LB	Luria broth
LGMD	Limb-girdle muscular dystrophy
LOD	Logarithm of odds
LVA	Low voltage-activated
MADD	Multiple acylcoenzyme A dehydrogenase deficiency
MAF	Minor allele frequency
MBS	Modified barth's saline
MC	Myotonia congenita
MD	Muscular dystrophy
MEDU	Medulla
MHE	Malignant hyperthermia equivocal
MHN	Malignant hyperthermia negative
MHS	Malignant hyperthermia susceptibility
MLPA	Multiplex ligand-dependent probe amplification
NMD	Nonsense-mediated decay

MT	Mutant
MP	Membrane potential
MRC	Medical Research Council
Na ⁺	Sodium ion
NAD	Nicotinamide adenine dinucleotide
NADP	Nicotinamide adenine dinucleotide phosphate
NEB	New England Biolabs
NGS	Next-generation sequencing
NHNN	National Hospital for Neurology and Neurosurgery
OCTX	Occipital cortex
OMIIM	Online Mendelian Inheritance in Man
PBS	Phosphate-buffered saline
PCR	Polymerase chain reaction
PMC	Paramyotonia congenita
PP	Periodic Paralysis
PED	Paroxysmal exercise-induced dyskinesia
PKD	Paroxysmal kinesigenic dyskinesia
PNKD	Paroxysmal non-kinesigenic dyskinesia
PxD	Paroxysmal dyskinesia
PUTM	Putamen
RM	Rhabdomyolysis
RMD	Rippling muscle disease
RNA	Ribonucleic acid
RT	Room temperature
RyRs	Ryanodine receptors
SCM	Sodium channel myotonia
SDS	Sodium dodecyl sulphate
SEM	Standard error of the mean
SNIG	Substantia nigra
SNP	Single nucleotide polymorphism
T1	Tetramerisation
TCTX	Temporal cortex
TEVC	Two-electrode voltage clamp
THAL	Thalamus
TSCA	TruSeq custom amplicon
TM	Transmembrane
TPP	Thyrotoxic periodic paralysis
UCL	University College London

UTR	Untranslated region
UV	Ultra violet
VGCC	Voltage-gated calcium channel
VGIC	Voltage-gated ion channel
VGKC	Voltage-gated potassium channel
VGSC	Voltage-gated sodium channel
VLCAD	Very long-chain acyl-CoA dehydrogenase
VSD	Voltage sensing domain
WES	Whole-exome sequencing
WGS	Whole-genome sequencing
WHMT	White matter
WT	Wild type

Publications Arising from this Thesis

Familial PRRT2 mutation with heterogeneous paroxysmal disorders including paroxysmal torticollis and hemiplegic migraine.

Dale RC, **Gardiner A**, Antony J, Houlden H.

Dev Med Child Neurol. 2012 Oct;54 (10):958-60.

PMID:22845787

PRRT2 gene mutations: from paroxysmal dyskinesia to episodic ataxia and hemiplegic migraine.

Gardiner AR, Bhatia KP, Stamelou M, Dale RC, Kurian MA, Schneider SA, Wali GM, Counihan T, Schapira AH, Spacey SD, Valente EM, Silveira-Moriyama L, Teive HA, Raskin S, Sander JW, Lees A, Warner T, Kullmann DM, Wood NW, Hanna M, Houlden H.

Neurology. 2012 Nov 20;79 (21):2115-21.

PMID:2307702

Clinical features of childhood-onset paroxysmal kinesigenic dyskinesia with PRRT2 gene mutations.

Silveira-Moriyama L, **Gardiner AR**, Meyer E, King MD, Smith M, Rakshi K, Parker A, Mallick AA, Brown R, Vassallo G, Jardine PE, Guerreiro MM, Lees AJ, Houlden H, Kurian MA

Dev Med Child Neurol. 2013 Apr;55 (4):327-34

PMID:23363396

A dominant mutation in FBXO38 causes distal spinal muscular atrophy with calf predominance.

Sumner CJ, d'Ydewalle C, Wooley J, Fawcett KA, Hernandez D, **Gardiner AR**, Kalmar B, Baloh RH, Gonzalez M, Züchner S, Stanescu HC, Kleta R, Mankodi A, Cornblath DR, Boylan KB, Reilly MM, Greensmith L, Singleton AB, Harms MB, Rossor AM, Houlden H

Am J Hum Genet. 2013 Nov 7;93 (5):976-83.

PMID:24207122

Paroxysmal Kinesigenic Dyskinesia May Be Misdiagnosed in Co-occurring Gilles de la Tourette Syndrome

Christos Ganos, Niccolo Mencacci, **Alice Gardiner**, Roberto Erro, Amit Batla, Henry Houlden and Kailash P. Bhatia

MOVEMENT DISORDERS CLINICAL PRACTICE. 2014 APR;1 (1):84-86

Benefit of carbamazepine in a patient with hemiplegic migraine associated with PRRT2 mutation.

Dale RC, **Gardiner A**, Branson JA, Houlden H.

Dev Med Child Neurol. 2014 Sep;56 (9):910.

PMID:24506539

Rhabdomyolysis: a genetic perspective.

Scalco RS, **Gardiner AR**, Pitceathly RD, Zanoteli E, Becker J, Holton JL, Houlden H, Jungbluth H, Quinlivan R.

Orphanet J Rare Dis. 2015 May 2;10 (1):51.

PMID:25929793

Under Review:

Frequency, genotype and phenotype of PRRT2, SLC2A1 and PNKD mutations in a paroxysmal movement disorder cohort

Alice Gardiner, Fatima Jaffer, Russell Dale, Robyn Labrum, Roberto Erro, Esther Meyer, Georgia Xiromerisiou, Maria Stamelou, Matthew Walker, Dimitri Kullmann, Tom Warner, Paul Jarman, Carlos DeSousa, Mike Hanna, Manju A Kurian, Kailash Bhatia, Henry Houlden

Published Abstracts:

Mutations in PRRT2 Gene Cause Episodic Diseases: From Paroxysmal Dyskinesia to Episodic Ataxia and Hemiplegic Migraine

Alice Gardiner, Dimitri Kullmann, Nicholas Wood, Louis Ptacek, Michael Hanna and Henry Houlden

Movement disorders society conference, 2012; Ataxia UK conference, 2012; Queen's square symposium, 2012

Next Generation Sequencing of Ion Channels in Neurological disorders

Alice Gardiner, Fatima Jaffa, Alan Pittman, Josh Hersheson, Vaneesha Gibbons, Nick Wood, Mike Hanna, Henry Houlden

British society of human genetics conference, 2012; UK neuromuscular translational research conference, 2012;

Searching for Genetic Causes of Muscle Channelopathies

Alice Gardiner, Nicholas Wood, Mike Hanna and Henry Houlden

Muscular Dystrophy Campaign Conference, 2012

Next Generation Sequencing of Ion Channels in Skeletal Muscle Channelopathies

Alice Gardiner, Dipa Raja Rayan, Alan Pittman, Nick Wood, Henry Houlden, Mike Hanna

UK neuromuscular translational research conference, 2013; Neuromics meeting, 2014

Searching for Genetic Causes of Muscle Channelopathies

Alice Gardiner, Nicholas Wood, Mike Hanna and Henry Houlden

Muscular Dystrophy Campaign Conference, 2013

Functional Investigation of a Novel Mutation Causing a New Phenotype for the KCNA1 Gene

Alice R Gardiner, Roope Mannikko, Mike Hanna, Henry Houlden

UK neuromuscular translational research conference, 2014; Queen's square symposium 2014; Neuromics meeting 2014

Next generation sequencing of ion channels in the neuronal and skeletal muscle channelopathies

Alice Gardiner, Alan Pittman, Nick Wood, Henry Houlden, Mike Hanna

MRC centre for neuromuscular disease scientific advisory board meeting, 2014

Chapter 1: Introduction

Hereditary diseases can be highly debilitating, and providing genetic diagnosis to patients is important for many reasons, including treatment management, genetic counselling, peace of mind and benefit entitlements. This thesis will explore the genetic diagnosis of patients with neuromuscular and neuronal disorders that are paroxysmal or episodic, stemming usually from ion channel and ion-channel-related protein dysfunction. In this chapter, first voltage-gated ion channels and their function will be introduced. Next, the classic 'channelopathies' - diseases caused by mutations in these ion channels - will be discussed, and the current knowledge surrounding their genetic basis established. Recurrent rhabdomyolysis (RM) can be a fatal condition sometimes caused by ion channel dysfunction, and so this, along with its other genetic causes, will be presented. Lastly, the different methods used to investigate genetic causes of disease will be discussed.

1. Voltage-Gated Ion Channels

Ion channels are pore-forming proteins that span the cell membrane and, when activated, selectively facilitate the transduction of charged ions along a concentration and electrostatic gradient. Two factors differentiate ion channels from other ion transporters: transport occurs at high rate (faster than that of diffusion) and without the input of energy such as ATP (Bertil 2001). Ion channels can be divided according to the factors that control their gating; they open and close in response to stimuli such as ligand binding, light or pressure. This thesis will only focus on ion channels that are gated by a change in membrane potential (the difference between the charge outside and inside a cell), known as voltage-gated ion channels (VGICs). VGICs are further subdivided by the type of ion they are selective for; there are calcium (Ca^{2+}), potassium (K^+), sodium (Na^+) and chloride (Cl^-) channels. VGICs are composed primarily of alpha subunits, often with additional auxiliary subunits. A distinct family of proteins, the ryanodine receptors (RyRs) share similar structural and functional features to classic VGICs and will be reviewed section 1.4 of this introduction.

1.1. Action Potentials

VGICs are the hallmark of excitable cells (such as muscle cells and neurones), and are required for the generation and propagation of action potentials. There is an electrostatic gradient between the cytoplasm of a cell and the extracellular fluid, caused by sodium-potassium pumps which use active transport to transfer Na^+ out of the cell and K^+ into the cell. However, K^+ can pass back out through leak channels, thus a mammalian cell has a negative resting membrane of about -70mV , which is maintained by the cell's lipid-based plasma membrane. A stimulus can cause a voltage-gated sodium channel to open, allowing Na^+ into the cell and so raising the membrane potential. If the membrane potential increases above a threshold, an action potential is triggered (the stages of an action potential are shown in Figure 1.1). In the rising phase, more sodium channels open and the membrane is depolarised so that the inside of the cell has a positive charge relative to the outside. This has a knock-on effect on neighbouring sodium channels, thus the action potential can travel along the neurone. Once it reaches a neuro-muscular junction, the positive charge is passed on to the sarcolemma (membrane of the muscle fibre), and the depolarisation continues along the muscle in the same way.

Once the action potential reaches its peak, the sodium channels close and voltage-gated potassium channels open. The combination of K^+ leaving the cell and no more Na^+ entering causes the membrane potential to fall. The membrane actually repolarises beyond the resting membrane potential, allowing for a refractory phase in which the cell recovers and cannot be depolarised again.

The above is a simplistic description of an action potential; however the reality is far more complex. There are additional calcium VGICs, which conduct Ca^{2+} into the cell and so assist in the membrane depolarisation, and chloride VGICs which help stabilise the cell's electrical charge. There are also several of each class of VGIC; in total there are more than 100 alpha subunits, as well as many more auxiliary subunits, and thus the expression profile of a cell will drastically impact the pattern, size and shape of the action potentials it conducts (Bean 2007), allowing fine tuning within each cell. We are still a long way from understanding all of the subtleties of the varying contributions of different VGICs.

1.2. Structure of Voltage-Gated Ion Channels

With the exception of chloride channels, all voltage-gated ion channels have a common structure comprising of 24 transmembrane (TM) alpha helices. For Na^+ and Ca^{2+} channels this 1800 amino acid subunit is encoded by a single gene. It contains four

homologous repeat domains (DI – DIV) of six TM helices named S1 – S6 (Figure 1.2). Each domain can be divided into two distinct structural and functional regions. The S1 – S4 segments comprise the voltage sensing domain (VSD), which detects the cell's membrane potential, and when triggered, can initiate a conformational change to open the channel. The most important part of the VSD is the S4 which contains 5 – 7 positively charged hydrophilic amino acids (usually arginines), interspersed with hydrophobic amino acids. The S5 and S6, along with the P loop that connects them, are responsible for the main pore and selectivity filter (James Kew 2010). The eight S5 and S6 segments come together to form the central pore of the channel, through which the ions can travel when the channel is open. Meanwhile, their connecting P loops contain four amino acid motifs that confer selectivity to the channel. On sodium channels this motif reads DEKA (Heinemann et al. 1992), whilst for calcium channels the amino acids are EEEE (Sather and McCleskey 2003).

Voltage-gated potassium channel genes encode only one of the four domains, and so each subunit has six TM regions. Four subunits come together to form a tetramer, and thus the resultant ion channel still has 24 TM helices. Each subunit has an additional domain required for tetramerisation (T1) on the N-terminal, and either similar subunits can form homotetramers, or different channel subunits can form heterotetramers. Therefore a large amount of different potassium channels can be formed. The selectivity motif on the P loop in K⁺ channels reads TVGYG (Jiang et al. 2002).

Voltage-gated chloride channels are structurally unrelated to the other VGICs. Each subunit, encoded by one chloride channel gene, contains 12 TM regions, and two subunits together form a homodimer. Within the dimer, however, each subunit forms a pore which functions independently of the other; thus the protein is described as having a 'double barrel' configuration (Steinmeyer et al. 1994).

Further detail on the structure of voltage-gated ion channels can be found in 'Ion channels: from structure to function' by James Kew and Curie Davies (2009).

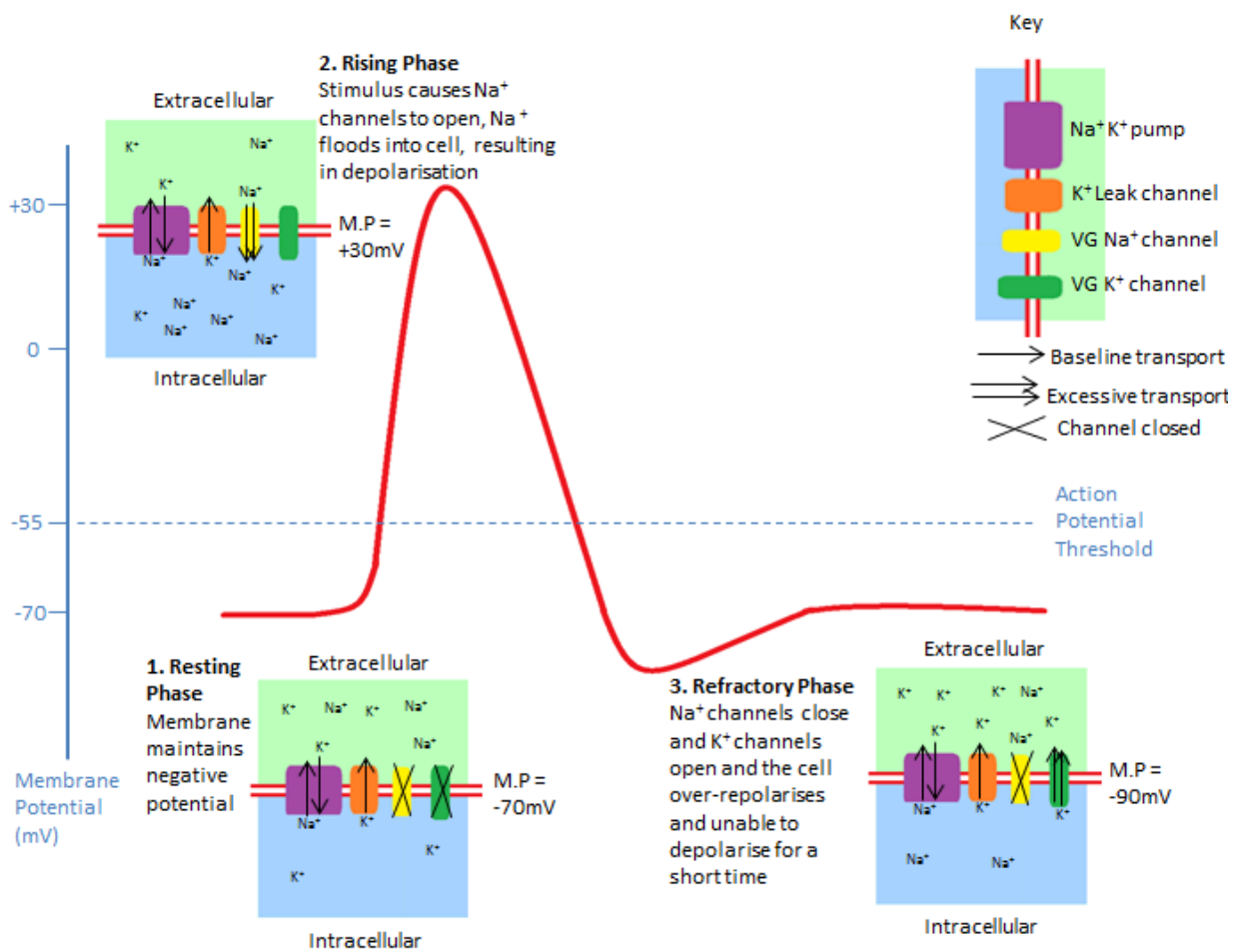


Figure 1.1 – The stages involved in creation and propagation of an action potential. The stages are overlaid onto the correlating voltages of the cell during the action potential. The blue dashed line indicates the voltage at which the action potential is triggered. M.P = membrane potential

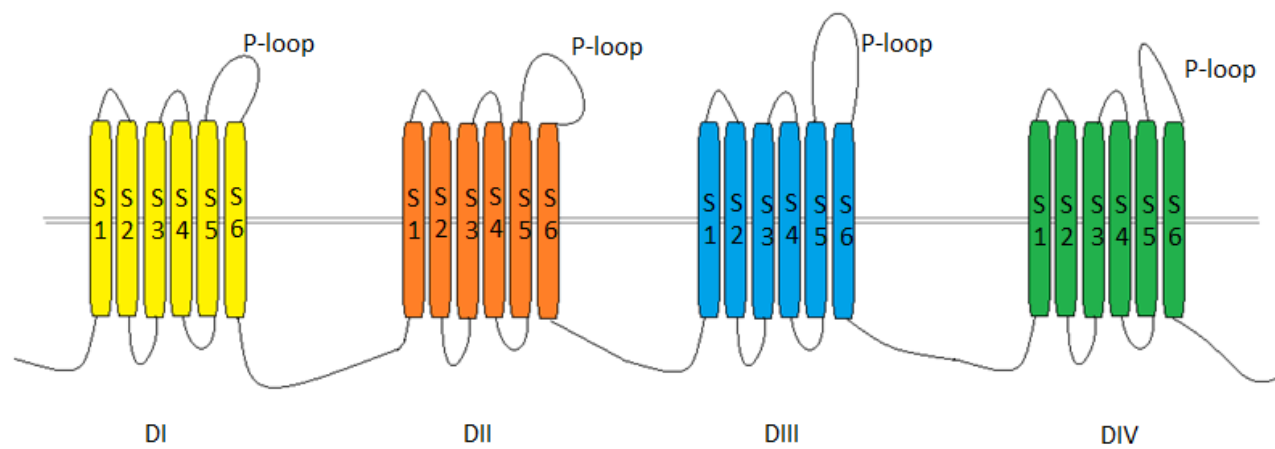


Figure 1.2 – Schematic of the 24 transmembrane domains of Na⁺ and Ca²⁺ VGICs, divided into four homologous repeat domains. VGKC subunits consist of only one repeat domain

1.3. Families of Voltage-Gated Ion Channels

As mentioned previously, there are four main VGIC families (Na^+ , Ca^{2+} , K^+ and Cl^-). Calcium and potassium channels are divided into further subfamilies based on their properties. Genomic mutation events in VGICs can often lead to diseases known as channelopathies, and, as can be expected, the phenotypic range of these is huge. This section contains only a broad overview of most channel families, members and links to disease (overview in Figure 1.3). Channelopathies that are most relevant to this thesis will be discussed in more detail in section 2.

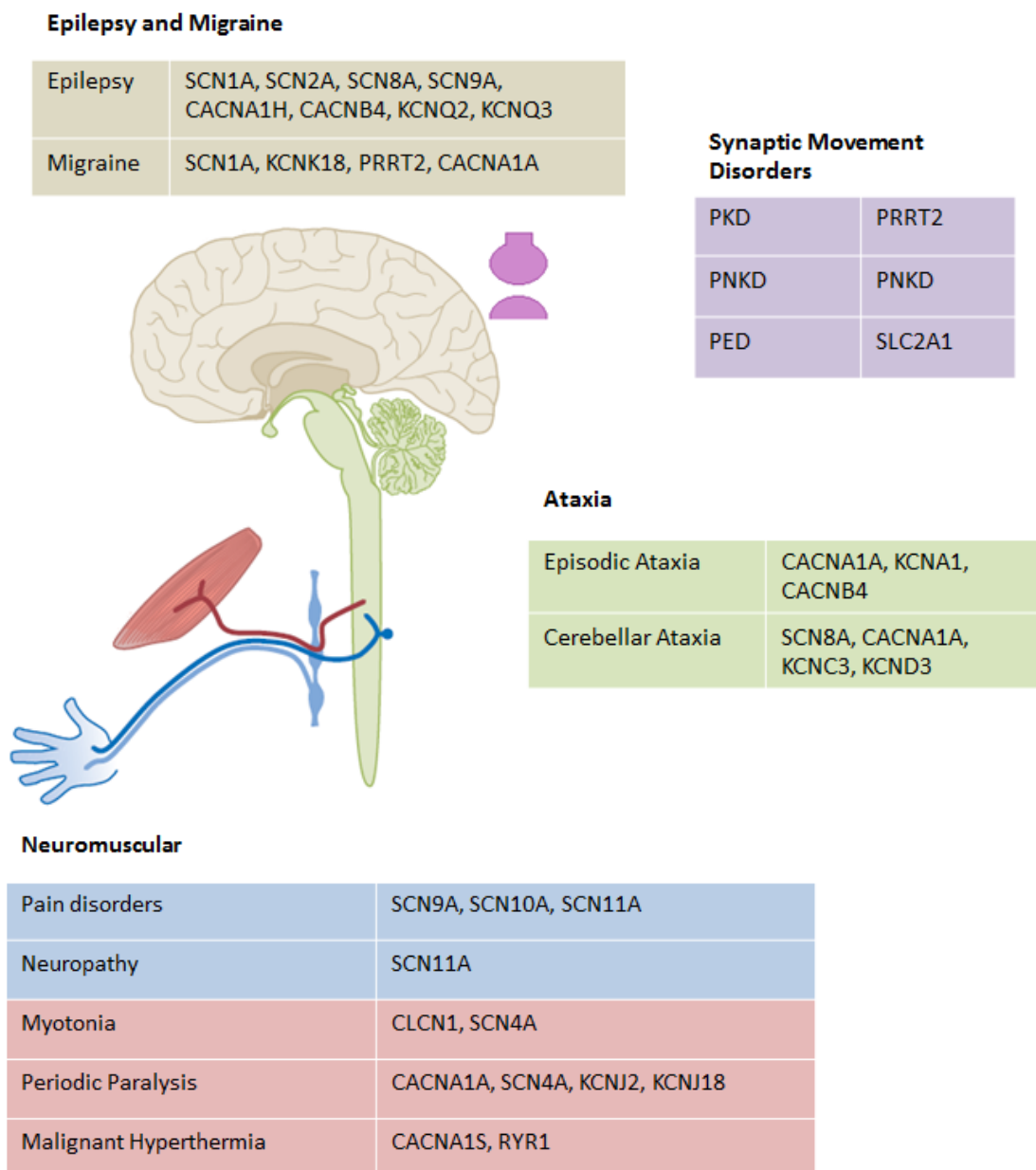


Figure 1.3 – The channel genes in which mutations cause muscular and neuronal disease, divided by type of disorder and location of impact. The paroxysmal dyskinesias are also included. Adapted from (Kullmann 2010)

1.3.1. Voltage-Gated Sodium Channels (VGSCs)

There are nine different VGSC alpha subunits from the same family ($Na_v1.x$), several of which contribute to disease; their details are given in Table 1.1.

1.3.2. Voltage-Gated Calcium Channels (VGCCs)

There are three families of classic VGCC alpha subunits. The existing ten channels were initially divided into two groups, based on their activation voltage dependence; low voltage-activated (LVA) channels respond to small depolarisations whilst high voltage-activated (HVA) channels require a greater depolarisation event. LVA channels belong to the $Ca_v3.x$ family, and are also known as T-type channels. More recently, HVA channels have further been classified by their response to various pharmacological substances into L- ($Ca_v1.x$ family), and R-, N- and P/Q-type ($Ca_v2.x$ family) channels (James Kew 2010). Details of these ten alpha subunits, along with additional auxiliary subunits (α_2d , β and γ) which form a 1:1:1:1 complex with the alpha subunit and thus are required for channel function, are given in Table 1.2.

1.3.3. Voltage-Gated Chloride Channels

Voltage-gated chloride channels fall into two groups; those expressed on the cell's plasma membrane, and those instead expressed on intracellular organelles which are actually classed as chloride transporters. Only the four membrane chloride channels are included in Table 1.3.

1.3.4. Voltage-Gated Potassium Channels (VGKCs)

The VGKC family is much larger and more diverse than the others, and includes 13 subfamilies; $K_v1 - K_v12$, and K_{2p} . $K_v1 - K_v6$ and $K_v8 - K_v9$ (not K_v7) are collectively known as K_v family, and have fast channel kinetics. As mentioned previously, potassium channel subunits form homo- or heterotetramers, and generally each subfamily contains subunits that will assemble with each other to create channels with properties and functions distinct for that subfamily. K_v2 subunits however can assemble with subunits from K_v5 , 6, 8 or 9, none of which can form channels by themselves. For this reason, they are sometimes included as members of the K_v2 family. There are also three $K_v\beta$ auxiliary subunits which bind 1:1 with K_v1 proteins. K_v7 instead have slow channel kinetics, and, unlike the K_v family, have their T1 domains at the C-terminal (Wehling et al. 2007). They, again, form homo- or heterotetramers within their subfamily. $K_v10 - K_v11$ channels are collectively known as the EAG potassium channel family. They share a similar structure to the K_v family, but have an additional PAS domain of unknown function in the N-terminal (Chen et al. 1999). Lastly, the K_{2p} family

have a completely different structure to the other potassium channels, with each subunit containing four TM domains and two P-loops (hence the name). They act as the 'leak' channels mentioned earlier that facilitate the cell's negative membrane potential. Details of all of these channels are in Table 1.4.

Channel Subunit	Gene	OMIM#	Disease Association	References
Na _v 1.1	SCN1A	182389	Hemiplegic migraine, epilepsy/ seizures	(Baulac et al. 1999; Dichgans et al. 2005)
Na _v 1.2	SCN2A	182390	Epilepsy/ seizures	(Berkovic et al. 2004)
Na _v 1.3	SCN3A	182391	None	
Na _v 1.4	SCN4A	603967	Periodic paralysis, myotonia (see section 2.1)	(Ptacek et al. 1991; McClatchey et al. 1992)
Na _v 1.5	SCN5A	600163	Cardiac pathologies	(Remme 2013)
Na _v 1.6	SCN8A	600702	Epilepsy /seizures, cognitive impairment (with or without ataxia)	(Trudeau et al. 2006; Veeramah et al. 2012)
Na _v 1.7	SCN9A	603415	Erythromelalgia, epilepsy/ seizures, extreme pain disorder, indifference to pain	(Yang et al. 2004; Cox et al. 2006; Furtleman et al. 2006; Singh et al. 2009)
Na _v 1.8	SCN10A	604427	Episodic pain disorder	(Faber et al. 2012)
Na _v 1.9	SCN11A	604385	Neuropathy, episodic pain disorder	(Leipold et al. 2013), (Zhang et al. 2013)

Table 1.1 – An overview of the human sodium channel alpha subunits. For simplicity, all epilepsy types are described as epilepsy/ seizures

Channel Subunit	Subunit/ channel type	Gene	OMIM#	Disease Association	References
Ca _v 1.1	α, HVA, L-type	<i>CACNA1S</i>	114208	Periodic paralysis (see section 2.1.2.2), malignant hyperthermia (see section 3.3.2)	(Fontaine et al. 1994), (Monnier et al. 1997)
Ca _v 1.2	α, HVA, L-type	<i>CACNA1C</i>	114205	Timothy syndrome, Brugada syndrome	(Splawski et al. 2004), (Antzelevitch et al. 2007)
Ca _v 1.3	α, HVA, L-type	<i>CACNA1D</i>	114206	Primary aldosteronism, deafness	(Baig et al. 2011), (Scholl et al. 2013)
Ca _v 1.4	α, HVA, L-type	<i>CACNA1F</i>	300110	Sight pathologies	(Doering et al. 2007)
Ca _v 2.1	α, HVA, P/Q-type	<i>CACNA1A</i>	601011	Episodic ataxia, hemiplegic migraine, cerebellar ataxia (see section 2.2.1.1.)	(Ophoff et al. 1996), (Zhuchenko et al. 1997)
Ca _v 2.2	α, HVA, N-type	<i>CACNA1B</i>	601012	None	
Ca _v 2.3	α, HVA, R-type	<i>CACNA1E</i>	601013	None	
Ca _v 3.1	α, LVA, T-type	<i>CACNA1G</i>	604065	None	
Ca _v 3.2	α, LVA, T-type	<i>CACNA1H</i>	607904	Epilepsy/ seizures	(Chen et al. 2003)
Ca _v 3.3	α, LVA, T-type	<i>CACNA1I</i>	608230	None	
Ca _v a ₂ d1	α ₂ δ subunit	<i>CACNA2D1</i>	114204	None	
Ca _v a ₂ d2	α ₂ δ subunit	<i>CACNA2D2</i>	607082	None	
Ca _v a ₂ d3	α ₂ δ subunit	<i>CACNA2D3</i>	606399	None	
Ca _v a ₂ d4	α ₂ δ subunit	<i>CACNA2D4</i>	608171	Retinal cone dystrophy	(Wycisk et al. 2006)
Ca _v β1	β subunit	<i>CACNB1</i>	114207	None	
Ca _v β2	β subunit	<i>CACNB2</i>	600003	Brugada syndrome	(Antzelevitch et al. 2007)

Ca _v β3	β subunit	CACNB3	601958	None	
Ca _v β4	β subunit	CACNB4	601949	Episodic ataxia, epilepsy/ seizures (see section 2.2.1)	(Escayg et al. 2000)
Ca _v γ ₁	γ subunit	CACNG1	114209	None	

Table 1.2 – An overview of the human calcium channel subunits. For simplicity, all epilepsy types are described as epilepsy/ seizures

Channel Subunit	Gene	OMIM#	Disease Association	References
CLC-1	<i>CLCN1</i>	118425	Myotonia congenita (see section 2.1.1.1)	(Koch et al. 1992)
CLC-2	<i>CLCN2</i>	600570	Leukoencephalopathy with ataxia	(Depienne et al. 2013)
CLC-Ka	<i>CLCNKA</i>	602024	Bartter syndrome	(Schlingmann et al. 2004)
CLC-Kb	<i>CLCNKB</i>	602023	Bartter syndrome	(Simon et al. 1997)

Table 1.3 – An overview of the human chloride alpha subunits

Channel Subunit	Subfamily	Gene	OMIM#	Disease Association	Refs
K _v 1.1	K _v 1	<i>KCNA1</i>	176260	Episodic ataxia (see section 2.2.1.2)	(Browne et al. 1994)
K _v 1.2	K _v 1	<i>KCNA2</i>	176262	None	
K _v 1.3	K _v 1	<i>KCNA3</i>	176263	None	
K _v 1.4	K _v 1	<i>KCNA4</i>	176266	None	
K _v 1.5	K _v 1	<i>KCNA5</i>	176267	Atrial fibrillation	(Olson et al. 2006)
K _v 1.6	K _v 1	<i>KCNA6</i>	176257	None	
K _v 1.7	K _v 1	<i>KCNA7</i>	176268	None	
K _v 1.8	K _v 1	<i>KCNA10</i>	602420	None	
K _v 2.1	K _v 2	<i>KCNB1</i>	600397	Epileptic encephalopathy	(Torkamani et al. 2014)
K _v 2.2	K _v 2	<i>KCNB2</i>	607738	None	
K _v 5.1	K _v 2	<i>KCNF1</i>	603787	None	
K _v 6.1	K _v 2	<i>KCNG1</i>	603788	None	
K _v 6.2	K _v 2	<i>KCNG2</i>	605696	None	
K _v 6.3	K _v 2	<i>KCNG3</i>	606767	None	
K _v 6.4	K _v 2	<i>KCNG4</i>	607603	None	
K _v 8.1	K _v 2	<i>KCNV1</i>	608164	None	
K _v 8.2	K _v 2	<i>KCNV2</i>	607604	Retinal cone dystrophy	(Wu et al. 2006)
K _v 9.1	K _v 2	<i>KCNS1</i>	602905	None	
K _v 9.2	K _v 2	<i>KCNS2</i>	602906	None	
K _v 9.3	K _v 2	<i>KCNS3</i>	603888	None	
K _v 3.1	K _v 3	<i>KCNC1</i>	176258	None	
K _v 3.2	K _v 3	<i>KCNC2</i>	176256	None	
K _v 3.3	K _v 3	<i>KCNC3</i>	176264	Spinocerebellar ataxia	(Waters et al. 2006)
K _v 3.4	K _v 3	<i>KCNC4</i>	176265	None	
K _v 4.1	K _v 4	<i>KCND1</i>	300281	None	
K _v 4.2	K _v 4	<i>KCND2</i>	605410	None	
K _v 4.3	K _v 4	<i>KCND3</i>	605411	Spinocerebellar ataxia	(Lee et al. 2012)
K _v 7.1	K _v 7	<i>KCNQ1</i>	607542	Cardiac pathologies	(Peroz et al. 2008)
K _v 7.2	K _v 7	<i>KCNQ2</i>	602235	Epilepsy/ seizures	(Singh et al. 1998)

K _v 7.3	K _v 7	<i>KCNQ3</i>	602232	Epilepsy/ seizures	(Charlier et al. 1998)
K _v 7.4	K _v 7	<i>KCNQ4</i>	603537	Deafness	(Kubisch et al. 1999)
K _v 7.5	K _v 7	<i>KCNQ5</i>	607357	None	
K _v 10.1	K _v 10	<i>KCNH1</i>	603305	None	
K _v 10.2	K _v 10	<i>KCNH5</i>	605716	None	
K _v 11.1	K _v 11	<i>KCNH2</i>	152427	Long QT syndrome	(Curran et al. 1995)
K _v 11.2	K _v 11	<i>KCNH6</i>	608168	None	
K _v 11.3	K _v 11	<i>KCNH7</i>	608169	None	
K _v 12.1	K _v 12	<i>KCNH8</i>	608260	None	
K _v 12.2	K _v 12	<i>KCNH3</i>	604527	None	
K _v 12.3	K _v 12	<i>KCNH4</i>	604528	None	
K _{2P} 1.1	K _{2P}	<i>KCNK1</i>	601745	None	
K _{2P} 2.1	K _{2P}	<i>KCNK2</i>	603219	None	
K _{2P} 3.1	K _{2P}	<i>KCNK3</i>	603220	Pulmonary hypertension	(Ma et al. 2013)
K _{2P} 4.1	K _{2P}	<i>KCNK4</i>	605720	None	
K _{2P} 5.1	K _{2P}	<i>KCNK5</i>	603493	None	
K _{2P} 6.1	K _{2P}	<i>KCNK6</i>	603939	None	
K _{2P} 7.1	K _{2P}	<i>KCNK7</i>	603940	None	
K _{2P} 9.1	K _{2P}	<i>KCNK9</i>	605874	None	
K _{2P} 10.1	K _{2P}	<i>KCNK10</i>	605873	None	
K _{2P} 12.1	K _{2P}	<i>KCNK12</i>	607366	None	
K _{2P} 13.1	K _{2P}	<i>KCNK13</i>	607367	None	
K _{2P} 15.1	K _{2P}	<i>KCNK15</i>	607368	None	
K _{2P} 16.1	K _{2P}	<i>KCNK16</i>	607369	None	
K _{2P} 17.1	K _{2P}	<i>KCNK17</i>	607370	None	
K _{2P} 18.1	K _{2P}	<i>KCNK18</i>	613655	Migraine with or without aura (see section 2.2.2.4)	(Lafreniere et al. 2010)
K _v β1	β subunit	<i>KCNAB1</i>	601141	None	
K _v β2	β subunit	<i>KCNAB2</i>	601142	None	
K _v β3	β subunit	<i>KCNAB3</i>	604111	None	

Table 1.4 – An overview of the human potassium channel subunits. For simplicity, all epilepsy types are described as epilepsy/ seizures

1.4. Ryanodine Receptors (RyRs)

The RyRs are a family of three homologous intracellular VGCCs (RyR1, RyR2 and RyR3). Their main function is their crucial role in excitation-contraction (EC) coupling, as they are needed to convert the electrical signal from the action potential to the chemical signal. They do this by facilitating Ca^{2+} release into excitable cells from internal stores, thus are vital for electrical signalling, and are present on the surface of the sarcoplasmic reticulum in skeletal muscle (RyR1) and cardiac muscle (RyR2), and on the endoplasmic reticulum in neurones (RyR3). With highly complex gating, RyRs can both initiate and amplify Ca^{2+} signals, as they interact with many modifying proteins, as well as detect intracellular Ca^{2+} levels (Van Petegem 2015). RyR1 (encoded by *RYR1*) is also believed to directly interact with $\text{Ca}_v1.1$, and the conformational change caused by the opening of the calcium channel results in RyR1 opening (Rios and Brum 1987).

RyRs share the 24 TM structure of the VGICs, with four subunits containing six TM domains forming a homotetramer. However, the large proteins also have additional domains. Recent crystallographic studies of RyR1 have revealed a 'mushroom' like scaffold structure (Hwang et al. 2012; Efremov et al. 2015; Yan et al. 2015; Zalk et al. 2015).

The ryanodine receptors are included in this thesis because of their structural and functional similarity with the classic VGICs, but also their link with episodic disease. *RYR1* mutations are known to cause a range of skeletal muscle diseases, most notably for this work, malignant hyperthermia (Gillard et al. 1991) (see section 3.1.1), whereas *RYR2* mutations can result in cardiac defects (Priori et al. 2001). RyR3 has not currently been associated with disease.

2. Channelopathies

VGICs are clearly vital for normal function of excitable cells. It is therefore unsurprising that disruption of their activity can cause diseases, known collectively as the channelopathies. Channelopathies can be either be acquired, for example in an autoimmune disorder or as the result of a toxin, or caused by a genetic mutation. This mutation could be in the channel subunit itself or in an auxiliary protein, and could lead to alteration in the channel's structure, interactions or expression level. Only genetic channelopathies will be discussed in this thesis.

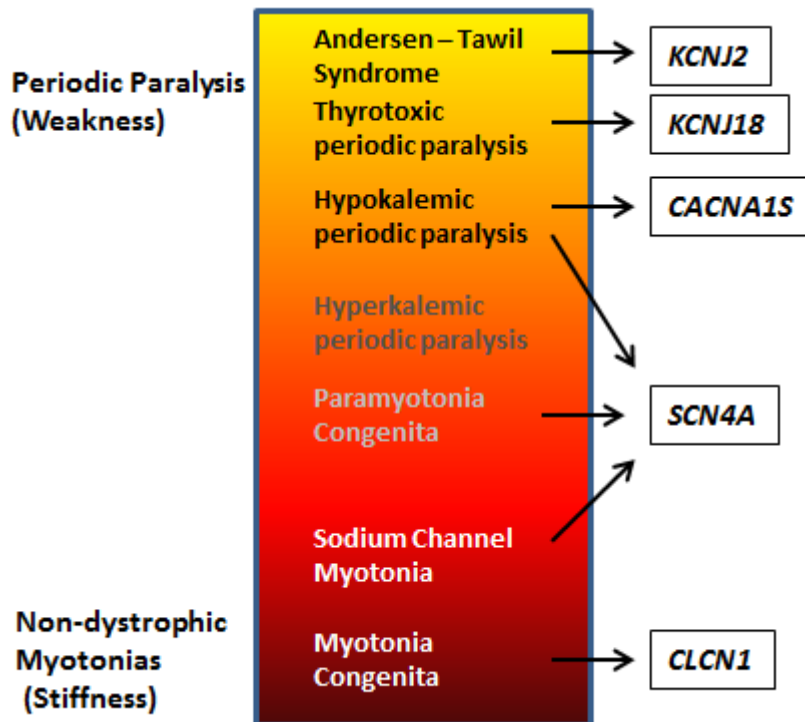
There are two main types of classic channelopathy, classified according to where the channel proteins are expressed; skeletal muscle channelopathies and neuronal channelopathies (cardiac channelopathies are not usually included, and are not relevant to this thesis). Although the clinical presentations are distinct, the two groups share classic channelopathy features including episodic attacks, normal muscle/ nerve function between attacks and an autosomal dominant inheritance pattern. Each will be discussed in detail below.

2.1. The Skeletal Muscle Channelopathies

Channelopathies of the skeletal muscle alter muscle excitability, as the affected VGICs are expressed in the skeletal muscle cells. They are sub-divided into two main groups based on the overriding symptoms; the non-dystrophic myotonias, in which the main symptom is myotonia (experienced as stiffness) and the periodic paralyses, in which the main symptom is muscle weakness. Each of these groups is further divided based on symptoms and genetic cause, although all of the skeletal muscle channelopathies exist as part of a spectrum from muscle inexcitability to muscle hyperexcitability, and there is great deal of crossover between the disorders. This is shown in Figure 1.4, along with the current strategy for genetic diagnosis (Rayan and Hanna 2010). Table 1.5 provides a summary of the main features and genetics of each disease.

The prevalence of skeletal muscle channelopathies is estimated to be about 1/100,000 (Emery 1991), however reports vary depending on the country. A large amount is already known about the genetics of these diseases, yet about 20% of patients are still without a genetic diagnosis. There is also much known about the pathology of skeletal muscle channelopathies, which is hoped will help understanding the pathology of the other types of channelopathy further.

a)



b)

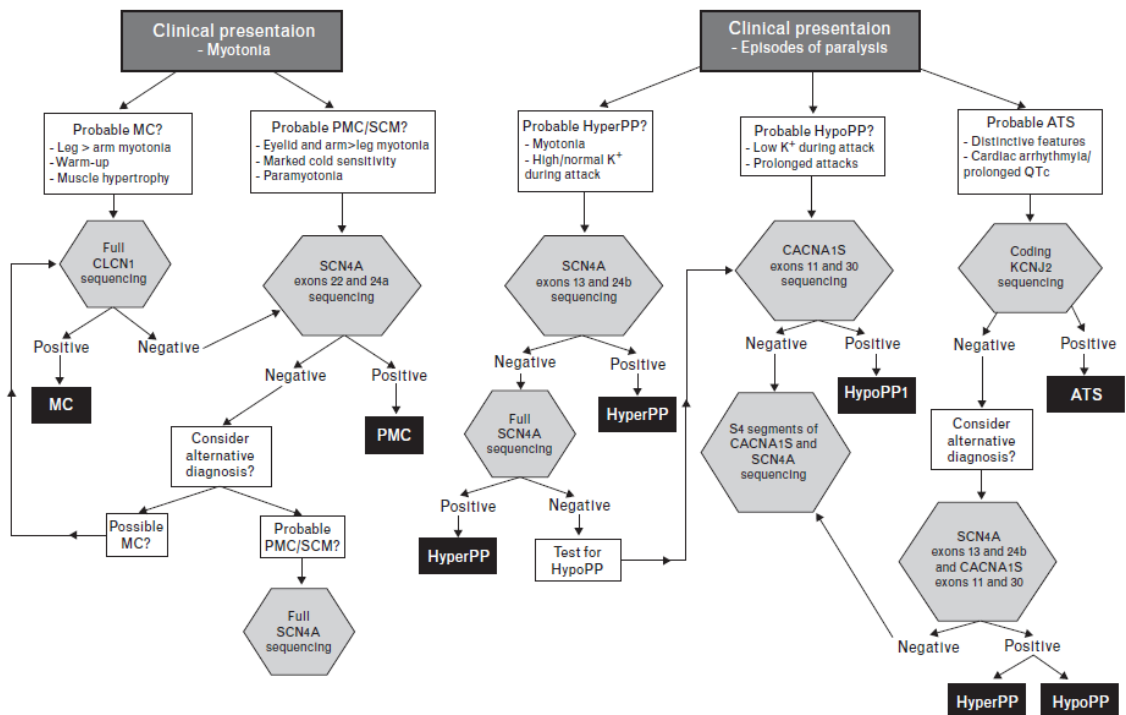


Figure 1.4 – (a) The spectrum of skeletal muscle channelopathies from weakness (yellow) to stiffness (red), and associated genes. (b) The current genetic diagnosis strategy for the skeletal muscle channelopathies. Taken from (Rayan and Hanna 2010)

Disease	OMIM#	Main symptom	Gene responsible	Main phenotypic features
Thompson's myotonia congenita	160800	Myotonia	<i>CLCN1</i> (dominant)	Stiffness with 'warm up' phenomenon and no weakness.
Becker's myotonia congenita	255700	Myotonia	<i>CLCN1</i> (recessive)	Stiffness with 'warm up' phenomenon and no weakness. More severe than Thompson's.
Sodium channel myotonia	170390	Myotonia	<i>SCN4A</i>	Stiffness with 'warm up' phenomenon and no weakness. Sensitivity to potassium.
Paramyotonia congenita	168300	Myotonia	<i>SCN4A</i>	Stiffness made worse with repeated movement. Sometimes with weakness.
Hyperkalemic periodic paralysis	170500	Periodic paralysis	<i>SCN4A</i>	Weakness with increased potassium levels. Sometimes with stiffness. Attacks are shorter and less severe than HypoPP but more frequent.
Hypokalemic periodic paralysis	613345 170400	Periodic paralysis	<i>SCN4A</i> <i>CACNA1S</i>	Weakness with reduced potassium levels. No stiffness. Attacks are longer and more severe than HyperPP but less frequent.
Thyrotoxic periodic paralysis	613239	Periodic paralysis	<i>KCNJ18</i>	Attacks indistinguishable from HypoPP, but there is associated thyrotoxicity
Andersen-Tawil syndrome	170390	Periodic paralysis	<i>KCNJ2</i>	Triad of features; PP, cardiac and skeletal defects.

Table 1.5 – A summary of the skeletal muscle channelopathies

For each of the non-dystrophic myotonias and the periodic paralyses, the main sub-diseases will be addressed separately, detailing the symptoms, known genetic causes and what is understood of the disease mechanism.

2.1.1. The Non-Dystrophic Myotonias

The non-dystrophic myotonias are one of the two classes of skeletal muscle channelopathy. They are characterised by delayed muscle relaxation after contraction, thus after an action potential, the muscle continues to fire in a phase known as ‘after-depolarisation’, and the patient experiences muscle stiffness. The non-dystrophic myotonias are divided into three clinically distinct disorders; myotonia congenita (MC), paramyotonia congenita (PMC) and sodium channel myotonia (SCM). As the genetic etiology of PMC and SCM are similar, they will be discussed together.

2.1.1.1. Myotonia Congenita

MC is the most common of the skeletal muscle channelopathies. It is characterised by attacks of myotonia, usually present in the first decade of life and typically triggered by sudden voluntary movements such as standing after a period of sitting down. The myotonia subsides after repeated movements in a phenomenon known as the ‘warm up’ effect. MC exists in two forms, distinguished by inheritance. Thomsen’s disease (OMIM #160800) is the autosomal dominant form, while Becker’s disease (OMIM #255700) is autosomal recessive, the only recessive disorder of the channelopathies. Becker’s disease tends to have a much more severe phenotype than Thomsen’s disease, and can often be accompanied by muscle hypertrophy.

Both of the forms of MC are caused by mutations in the *CLCN1* gene, which encodes CLC-1, the main chloride channel that is expressed in skeletal muscle. It was first found to be the causative gene in 1992 (Koch et al. 1992), (George et al. 1993), and since, over 150 different mutations have been reported that are spread throughout the whole of the 23 exon gene, although there is a mutation hot spot for dominant mutations in exon eight (Fialho et al. 2007). The CLC-1 channel is a homo-dimer and consequently dominant mutations often cause disease by disrupting dimer formation (Duffield et al. 2003). All reported dominant mutations are missense, or occasionally nonsense, changes. Recessive mutations are spread throughout the gene and can be nonsense, missense, splice site, insertions, deletions, or, as recently reported, whole exonic deletions or duplications (Rayan et al. 2012). Many families have previously unreported private (only seen in that family) mutations and compound heterozygosity is relatively common, with some of the alleles being present in as much as 1% of the population (Papponen et al. 1999). Interestingly, some mutations can present with

either a dominant or recessive inheritance pattern (Kubisch et al. 1998). The reason for this is unknown, although it is speculated that it could be because of varying levels of allelic expression. There are also recessive pedigrees with only one *CLCN1* mutation identified, and again the reason for this is not clear; it could be due to a mutation in another gene, a deep intronic mutation in *CLCN1*, or a copy number variant (CNV) that has not yet been identified. Indeed, a co-occurrence of a *CLCN1* mutation with a *DMPK* expansion (the gene known to cause myotonic dystrophy one) has recently been reported (Kassardjian and Milone 2014). About 25% of MC patients are without genetic diagnosis (Meyerkleine et al. 1995).

Skeletal muscles have a uniquely high level of chloride conductance, which acts as a buffer for depolarisation of the cell. A mutation preventing the channel from conducting chlorine will decrease the cell's conductance, and if this is by more than 70%, the buffering system fails and myotonia occurs (Furman and Barchi 1978). This explains why a single recessive mutation does not usually cause myotonia, as the conductance will only be decreased by 50%. A dominant mutation, however, will decrease it by 75% and will be sufficient to cause pathogenicity. Therefore, both dominant and recessive *CLCN1* mutations are loss-of-function mechanisms.

2.1.1.2. Paramyotonia Congenita and Sodium Channel Myotonia

PMC (OMIM# 168300) is similar to MC, the main distinction being that there is no 'warm up' effect; in PMC the myotonia worsens with repeated movement, giving rise the name 'paradoxical' MC, and so PMC. It is precipitated by cold and exertion. Unlike MC, PMC can be accompanied by attacks of periodic paralysis-like weakness. SCM is a fairly new term incorporating three previously separate diseases; myotonia fluctuans, myotonia permanens and potassium aggravated myotonia, which were combined due to their genetic and phenotypic similarity (Matthews et al. 2010). The SCM phenotype is similar to MC as it is usually not associated with weakness, and can have the 'warm up affect', but is clinically distinct as it is often potassium sensitive.

PCM and SCM are allelic diseases; they are both caused by mutations in the *SCN4A* gene, encoding the alpha subunit of the main skeletal muscle sodium channel, Na_v1.4. The first mutation in the gene was identified in 1992 after linkage studies (McClatchey et al. 1992), (Koch et al. 1991). The majority of PMC mutations have been found in exons 22 and 24 of the 24 exon gene, with the most common causative mutations being c.3938C>T p.(Thr1313Met) and a range of substitutions at Arg1448. SCM mutations are often in the same exons as PMC, but the same mutation has never been reported to cause both diseases. All mutations reported in the literature for both

diseases have been point mutations, with the exception of an intronic insertion of a guanine in a patient with PMC (Kubota et al. 2011). The most common mutations that are known to cause SCM are c.4765G>A p.(Val1589Met) and mutations at p.Gly1306 (Ptacek et al. 1992), (Yang et al. 1994). For 20% of suspected PMC patients a causative mutation cannot be found in the *SCN4A* gene, but when the *CLCN1* gene is also screened the amount of patients without a genetic diagnosis is reduced to 7%, highlighting the phenotypic overlap with MC (Trip et al. 2008).

Both PMC and SCM are traditionally autosomal dominant diseases, although one recessive mutation has been seen to cause PMC, which, like Becker's disease, produces a more severe phenotype than the dominant disease (Arzel-Hezode et al. 2010). Furthermore, Furby et al described five cases which seemed to have phenotypic features of both MC and PMC, and had seemingly pathogenic mutations in both genes, suggesting a digenic cause (Furby et al. 2014). The pathogenic mutations that cause PMC and SCM in *SCN4A* are found in functionally important regions which control channel inactivation; they are gain-of-function mutations that cause an increased Na⁺ inward current, and consequently, enhanced channel recovery from inactivation and the presence of myotonia (Plassart-Schiess et al. 1998).

2.1.2. The Periodic Paralyses

The periodic paralyses (PP) are at the opposite end of the spectrum to the non-dystrophic myotonias; mutations cause abnormal depolarisation of membrane potential, preventing the firing of action potentials and causing the muscle to be unable to contract. This is experienced by the patient as transient episodes of weakness. Whilst patients are described as having normal muscle activity between attacks, they can develop fixed proximal myopathy, and can eventually become wheel-chair bound (Miller et al. 2004). The two main sub-types of periodic paralysis are distinguished by the serum potassium levels approaching an attack; hyperkalemic PP (HyperPP) which is precipitated by increased potassium levels, and hypokalemic PP (HypoPP), precipitated by decreased potassium levels. These have different mechanisms of disease. There are also two additional diseases that come under the PP heading which will be discussed: thyrotoxic periodic paralysis (TPP) and Andersen-Tawil syndrome (ATS).

2.1.2.1. Hyperkalemic Periodic Paralysis

HyperPP (OMIM #170500) usually presents as attacks of paralysis or weakness in the first decade of life. It is precipitated by high potassium levels, and so can be triggered by eating potassium-rich food or prolonged fasting. In 75% of cases paralysis is

accompanied by myotonia as a secondary symptom, seen either clinically or by electrical testing (Miller et al. 2004).

HyperPP was the first of the skeletal muscle channelopathies in which the genetic cause was identified; in 1990 Fontaine et al used linkage analysis to find that *SCN4A* was the responsible gene (Fontaine et al. 1990). Consequently, it is allelic with PMC and SCM. The overlap with PMC is evident; patients will often have both weakness and stiffness, but they are classified by the predominant symptom. Relatively few mutations have been reported to cause HyperPP, only 11 thus far. This is because many patients share two common mutations; c.2111C>T p.(Thr704Met) accounts for 60% of cases and c.4774A>G p.(Met1592Val) for 30% (Vicart et al. 2005). 60% of distinct mutations are seen in either exon 13 or 24 of the gene (Jurkat-Rott and Lehmann-Horn 2007), however this is biased due to selective exon screening during diagnostic genetic tests. Again, almost all of mutations reported are point mutations, with the exception of one double mutation (two mutations on the same allele), where an insertion and a deletion were seen in two families. This led to an abnormal phenotype; the PP was present with additional malignant hyperthermia susceptibility (Bendahhou et al. 2000).

As expected from the overlap in phenotypes and genetics, the disease mechanism for HyperPP is similar to that for PCM and SCM. It is a gain-of-function, with an increased inward Na⁺ current delaying channel inactivation. In HyperPP however, the current is larger, shifting the membrane resting potential and thus preventing channel activation (Wagner et al. 1997).

2.1.2.2. Hypokalemic Periodic Paralysis

Patients with HypoPP have attacks of paralysis or weakness associated with reduced serum potassium levels. Attacks are clinically distinct from HyperPP as they tend to be longer and more severe but less frequent. Secondary myotonia is never seen. Attacks are often triggered by large meals and can be alleviated by ingestion of oral potassium. There are two subtypes of HypoPP based on the causative gene; HypoPP1 (OMIM #170400) and HypoPP2 (OMIM #613345). Patients with HypoPP1 and HypoPP2 are clinically indistinguishable. HypoPP is currently the only skeletal muscle channelopathy with known genetic heterogeneity; although as more causative genes are discovered this may not remain the case.

HypoPP was first linked to the *CACNA1S* gene (HypoPP 1) in 1994 by Fontaine et al (Fontaine et al. 1994). This gene encodes the calcium channel Ca_v1.1. Mutations in *CACNA1S* were only found to account for about 70% of cases, and in 1999 a

causative mutation was also found in *SCN4A*, giving rise to HypoPP2, which now accounts for 10% of cases. The majority of mutations are localised to the same regions of the two genes, the S4 segments (within the VSD). This is unlike mutations seen in the other skeletal muscle channelopathies. In the S4 regions of these channels, every third amino acid is a positively charged arginine. It has long been known that HypoPP mutations often neutralise this charge (Matthews et al. 2009) but it was unclear how this could cause disease until 2007 when both the Catterall and Cannon labs showed that there was an alternative and aberrant ionic leak through the VSD into the cell, causing its depolarisation (Sokolov et al. 2007), (Struyk and Cannon 2007). This is known as the gating pore leak, and is a fundamentally different mechanism of disease to all of the other skeletal muscle channelopathies. There is only one reported HypoPP mutation in *CACNA1S* which does not affect an S4 arginine (Ke et al. 2009); the mechanism of this mutation is unclear. Thus, it appears that loss-of-function variations in *CACNA1S* are not frequently pathogenic, as they are in *CACNA1A* (section 2.2.1.2). This could be due to a compensatory interaction with the ryanodine receptor, *RYR1*, which can also trigger calcium-mediated calcium release (Protasi et al. 2002) (discussed further in sections 1.4 and 3.1.1.). There have even been case reports of *RYR1* mutations causing atypical PP or PP with MHS, demonstrating the overlap between the genes (Marchant et al. 2004; Zhou et al. 2010).

As with the other skeletal muscle channelopathies, about 20% of HypoPP cases are still genetically undiagnosed. This could be because only S4 segments of these genes are routinely screened, because the mutations are intronic or large scale deletions and are missed, or because an as yet unknown gene is causing the same phenotype.

2.1.2.3. Thyrotoxic Periodic Paralysis

TPP (OMIM #613239) is a sporadic form of periodic paralysis accompanied by hyperthyroidism. It is more common in people with Asian and Hispanic ethnicity than Caucasians. The paralysis attacks in TPP are indistinguishable from patients with HypoPP. The gene responsible for causing TPP has only recently been identified; in 2010 Ryan et al found that mutations in *KCNJ18* caused the disease (Ryan et al. 2010). This gene encodes the inwardly rectifying potassium channel kir2.6 and is transcriptionally regulated by thyroid hormones. To date, seven mutations have been identified in *KCNJ18* that cause TPP, as well as two more which cause sporadic HypoPP without hyperthyroidism (Cheng et al. 2011). *KCNJ18* is 98% similar to the gene *KCNJ12*, which makes its sequencing problematic.

2.1.2.4. Andersen-Tawil Syndrome

ATS (OMIM #170390) is different to other skeletal muscle channelopathies because it affects other systems as well as the muscle; patients can also have heart and skeletal abnormalities. These, along with periodic paralysis are known as the 'triad of symptoms', although not all three symptoms are always present; there is huge variability between patients in terms of severity and phenotype. ATS is rare, and only accounts for about 10% of PP cases (Haruna et al. 2007).

ATS is known to be caused by mutations in the *KCNJ2* gene which encodes Kir1.2, another inwardly rectifying potassium channel, the function of which is to stabilise membrane potential. Although over 50 mutations have been reported, spanning the entire gene, there does not appear to be a correlation between genotype and phenotype. It is reported that about 40% of ATS cases do not have a mutation in *KCNJ2*, making it highly likely that there is another causative gene that has not yet been identified (Kimura et al. 2012).

2.2. The Neuronal Channelopathies

The other main class of channelopathies is the neuronal channelopathies, which are the result of mutations in VGICs expressed in neuronal cells in the brain or peripheral nervous system. These channelopathies are much less clearly defined and grouped than the skeletal muscle channelopathies as the phenotypes are varied and overlapping. Furthermore, they can be genetically heterogeneous, and can be caused by mutations in other types of channel or transporter proteins. Similar to skeletal muscle channelopathies, most neuronal channelopathies have episodic symptoms, with periods of normal function between attacks as well as the occurrence of associated progressive symptoms. To date, all neuronal channelopathies that have been reported have been sporadic or with an autosomal dominant inheritance pattern.

Broadly, there are three main classes of neuronal channelopathy; episodic ataxia (EA), familial hemiplegic migraine (FHM) and epilepsy: EA and FHM will be addressed separately; however, the epilepsies will not be covered here as their causes are complex and varied, and epileptic patients are not included in this work. Additionally, as they are phenotypically and functionally related, the paroxysmal dyskinesias will be included although they are not, strictly speaking, channelopathies. The main phenotypic and genetic features of the neuronal channelopathies are summarised in Table 1.6, and their genetic heterogeneity is shown in a Venn diagram in Figure 1.5.

Disease	OMIM#	Gene responsible	Phenotypic feature
EA1	160120	<i>KCNA1</i>	Short attacks of ataxia with myokymia, sometimes associated with seizures
EA2	108500	<i>CACNA1A</i>	Longer attacks of ataxia without myokymia, sometimes associated with nausea, headaches or cognitive impairment
FM1	141500	<i>CACNA1A</i>	Migraine with hemiplegia (subtypes are clinically indistinct)
FM2	602481	<i>ATP1A2</i>	Migraine with hemiplegia (subtypes are clinically indistinct)
FM3	609634	<i>SCN1A</i>	Migraine with hemiplegia (subtypes are clinically indistinct)
Migraine with aura	613656	<i>KCNK18</i>	Migraine without hemiplegia, with aura
PNKD	118800	<i>PNKD</i>	Long attacks (hours) of dyskinesia triggered by alcohol, coffee or strong emotion
PED	612126	<i>SLC2A1</i>	Mid-length attacks (minutes) of dyskinesia triggered by prolonged exercise
PKD	128200	<i>PRRT2</i>	Short frequent attacks (seconds) of dyskinesia triggered by sudden movements

Table 1.6 – A summary of the neuronal channelopathies

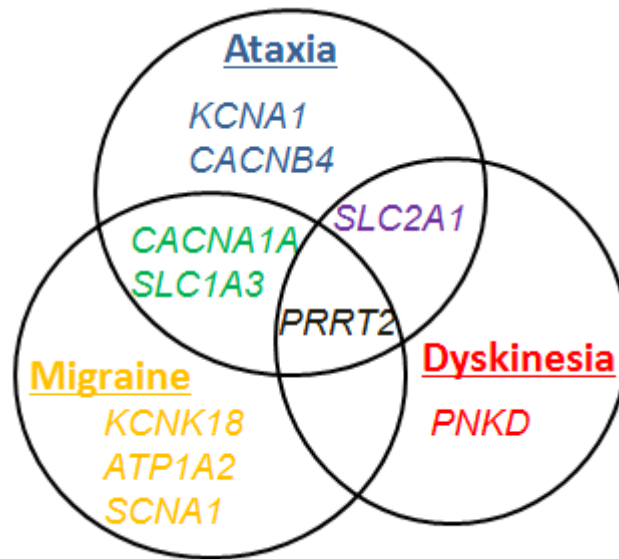


Figure 1.5 – A Venn diagram showing the phenotypic and genetic overlap of the neuronal channelopathies (including the paroxysmal dyskinesias)

2.2.1. Episodic Ataxia

First described clinically in 1975 (Vandyke et al. 1975), patients with episodic ataxia (EA) experience intermittent attacks of cerebellar dysfunction, which can manifest as a range of phenotypes, often including disco-ordination, dizziness, vertigo, aura and nystagmus. There are currently seven described types of EA (EA1 – EA7), although little is known about EA3 – EA7 as they have only been identified in a small number of cases (sometimes only one family). As with the skeletal muscle channelopathies, there are still many EA patients (one third of EA2 patients (Tomlinson et al. 2009)) without a genetic diagnosis and therefore it is likely there are causative genes that have not been identified. The majority of known EA patients have EA1 or EA2, and only these are discussed in depth; details of the others can be found in Table 1.7 and are reviewed by Jen (Jen 2008).

EA Type	Patients EA has been described in	Gene or locus	Clinical features	References
EA3	One large family	Chr1 q42	Brief attacks lasting minutes with kinesigenic triggers. Vertigo, tinnitus, headache	(Steckley et al. 2001)
EA4	Two families (likely related)	Unknown	Long attacks lasting hours. Vertigo, diplopia, nystagmus.	(Farmer and Mustian 1963), (Damji et al. 1996)
EA5	One family	<i>CACNB4</i>	Long attacks lasting hours. Vertigo, nystagmus, seizures.	(Escayg et al. 2000)
EA6	One family and one singleton	<i>SLC3A1</i>	Long attacks lasting hours triggered by hyperpyrexia (fever with elevated body temperature). Progressive ataxia as well as episodic. Seizures, hemiplegia, migraine, cognitive impairment.	(Jen et al. 2005), (de Vries et al. 2009)
EA7	One family	Chr19 q13	Long attacks lasting hours but reducing in frequency with age and triggered by exertion. Vertigo, weakness, dysarthria (trouble speaking).	(Kerber et al. 2007)

Table 1.7 – An overview of EA3 – EA7

2.2.1.1. Episodic Ataxia 1

The first case of EA1 (OMIM #160120) was described in 1975 as 'periodic ataxia with myokymia' (Vandyke et al. 1975). This is because in nearly the entirety of cases of EA1 ataxia is accompanied by neuromyotonia (twitching of muscles, known as myokymia), the extent of which can range from mild to severe. Attacks of ataxia are typically brief and unaccompanied by headache, but are sometimes associated with seizures. They can be precipitated by emotional stress, illness, sudden movements or a startle. Onset is usually in the first or second decade of life. As with other channelopathies, symptoms are variable, and can be different within the same family and even between identical twins (Graves et al. 2010).

KCNA1, encoding the VGKC K_v1.1, was identified as the causative gene for EA1 in 1994 by Browne et al (Browne et al. 1994). Since, 30 mutations have been reported in the gene; one causing hypomagnesemia, three causing myokymia without EA, and the remainder responsible for EA1 with varying associated symptoms and severities. The mutations are missense, with the exception of one nonsense mutation, one small in-frame deletion and one large scale deletion covering the whole gene. Mutations are generally associated with an autosomal dominant family history, although there is one reported *de novo* mutation in the literature responsible for EA with cognitive delay (Demos et al. 2009). Mutations are spread over the S1 – S6 segments and C terminus; however no mutations have yet been reported in the N terminus which contains the T1 tetramerisation domain (see section 1.2) (Tomlinson et al. 2009).

K_v1.1 regulates the excitability of neurones. EA1 mutations cause disease by affecting the fast inactivation of Kv1.1, and this can lead to neurones becoming excessively excitable (Imbrici et al. 2011). It is thought that this happens in different ways depending on the mutation, either by reducing surface expression of the channel, or by reducing the affinity of Kv1.1 for Kv1.4. This is a dominant-negative mechanism of disease.

2.2.1.2. Episodic Ataxia 2

EA2 (OMIM #108500) was first recognised as a distinct disorder from EA1 in 1986 (Gancher and Nutt 1986). Although age of onset is similar, attacks differ clinically as they have a longer duration (hours to days instead of seconds to minutes), and can be associated with nausea and headaches or cognitive impairment. Triggers include alcohol, stress, exertion and caffeine. Myokymia is never a symptom of EA2, although

again, there is large variation in phenotype and severity. EA2 is more common than EA1.

The genetic cause for EA2 was discovered after EA1 – *CACNA1A* was found to be responsible in 1996, although the chromosomal location had been known for some time (Ophoff et al. 1996). *CACNA1A* encodes the Ca²⁺ channel Ca_v2.1. EA2 is allelic with familial hemiplegic migraine1 (FHM1 – section 2.2.2.1) and spinocerebellar ataxia type six (SCA6) – a non-episodic form of ataxia (the SCAs are beyond the scope of this thesis). To date almost 100 mutations have been reported in *CACNA1A* that cause EA2; a combination of missense, nonsense, small and large insertions and deletions, splice sites, a rearrangement and even a repeat variation which would normally be associated with SCA6 (Jodice et al. 1997). Mutations span the whole gene; therefore genetic diagnostic testing is lengthy and expensive as the gene contains 48 exons.

Ca_v2.1 is widely expressed in the central nervous system. Pre-synaptic membrane depolarisation results in Ca²⁺ influx via these channels, which allows for the release of neurotransmitters. The range of mutations as well as phenotypes suggests that there are multiple mechanisms of disease depending on the effect of the mutation on the structure of the channel. However, many of the mutations result in either a truncated protein or nonsense mediated decay so it is likely that haploinsufficiency plays an important role in many cases of EA2, and thus the mutations are loss-of-function.

2.2.2. Familial Hemiplegic Migraine

Migraine is common and will be experienced by 43% of women and 18% of men at some point in their lifetime (Stewart et al. 2008). It is often accompanied by aura, photophobia and phonophobia. There are a variety of causes and an undoubted genetic link in some families; genome-wide association studies (GWAS, discussed in section 4.1.3) have implicated several genes in various types of migraine without Mendelian inheritance (McClatchey et al. 1992; Anttila et al. 2010), (Chasman et al. 2011); however they are beyond the scope of this thesis.

One rare form of migraine however, familial hemiplegic migraine (FHM), has autosomal dominant inheritance, and some of the causative genes have been identified. FHM is a severe form of migraine with aura and motor weakness (hemiplegia), and can also be associated with ataxia and seizures. It is a genetically heterogeneous disease with three forms currently described relating to the three genes known to be responsible, although the phenotypes are clinically indistinct.

2.2.2.1. Familial Hemiplegic Migraine 1

As mentioned above, FHM1 (OMIM #141500) is caused by mutations in the *CACNA1A* gene encoding $Ca_v2.1$ and is allelic with EA2; in fact both diseases were reported in the initial paper (Ophoff et al. 1996). There is substantial phenotypic and genetic overlap between the two disorders; to date around 35 mutations have been reported to cause FHM1, of which about 25% are also reported to cause EA2. The mutations are spread throughout the gene and are nonsense, missense and small and large deletions. In contrast to EA2 mutations, the majority of FHM1 mutations are gain-of-function and are thought to reduce the threshold for activation of the channel. This favours initiation and propagation of a cortical sensory depression (CSD) – a burst of depolarisation that spreads through the cortex and is widely believed to be responsible for many cases of migraine with aura (Raouf et al. 2010).

2.2.2.2. Familial Hemiplegic Migraine 2

FHM2 (OMIM #602481) was first described in 2003 by Du Fusco et al as FHM caused by mutations in the Na^+/K^+ pump $\alpha 2$ subunit *ATP2A1* (De Fusco et al. 2003). As this gene is not a VGIC, it is not strictly a channelopathy, however the Na^+/K^+ pump is vital for the generation and propagation of action potentials and so mutations can have channelopathy-like effects. Since its discovery, more than 70 mutations causing FHM2 have been reported in this gene, the majority of which are missense, although two nonsense, one splice site and five indels (small insertions or deletions) have been seen. It is thought that the altered pump action could cause disease by either increased extracellular potassium or cellular calcium levels resulting in higher chance of CSD (Raouf et al. 2010).

2.2.2.3. Familial Hemiplegic Migraine 3

The final type of FHM, FHM3 (OMIM #609634) is caused by mutations in the voltage gated sodium channel gene *SCN1A* (Dichgans et al. 2005). This gene is well known as a cause of several types of epilepsy, but is a rare cause of FHM, with only five mutations being reported to date, all of which are missense. Of the five only two caused pure FHM (Vanmolkot et al. 2007), while one caused FHM with epilepsy (Castro et al. 2009) and two FHM with elicited repetitive daily blindness (ERDB) (Vahedi et al. 2009).

2.2.2.4. The *KCNK18* gene

TRESK is a two-pore domain potassium channel encoded by the *KCNK18* gene which has been linked to migraine with aura, although not FHM. This channel is a

homodimer. In 2010 Lafreniere et al discovered a two base pair deletion (c.414_415delCT, p.(Phe139Trpfs*24)), leading to a premature stop codon, and showed it had a dominant negative effect on the channel (Lafreniere et al. 2010), by co-expressing the mutant with the wild type, leading to the channel showing marked reduction in conductance. However, recently, missense variants found in equal amounts in both migraineurs and controls were examined functionally and one in particular, c.328T>C p.(Cys110Arg) was found to result in complete loss-of-function and a similar dominant-negative effect as the deletion. These results question the direct cause of *KCNK18* mutations in migraine as a Mendelian disorder, and more understanding is needed before the mechanism can be determined (Andres-Enguix et al. 2012).

2.2.3. The Paroxysmal Dyskinesias

The paroxysmal dyskinesias (PxDs) are a group of movement disorders characterised by involuntary movements lasting for a brief duration. Typically patients present with episodic attacks of pure or mixed choreic, ballistic, athrtoic or dystonic features. As mentioned previously the PxDs are not channelopathies as they are not caused by mutations in VGICs. However, they share neuronal channelopathy features such as episodic attacks interspersed with periods of normal activity and an autosomal dominant inheritance pattern. Furthermore, there can be phenotypic overlap including migraine with aura, hemiplegic migraine, seizures and even ataxia. Therefore for the purpose of this study they are considered to be in the spectrum of neuronal channelopathies and thus they are included in this work.

PxDs are rare, and one study estimated them to only account for 0.76% of movement disorder patients (Blakeley and Jankovic 2002), although their episodic nature could leave them under-reported. They can be hereditary or acquired, however only PxDs with a genetic cause will be addressed. There are three types which are nominally by divided attack trigger, but they also differ in attack length and causative gene. These are paroxysmal non-kinesigenic dyskinesia (PNKD) paroxysmal kinesigenic dyskinesia (PKD), and paroxysmal exercise-induced dyskinesia (PED). The main features of these three conditions are shown in Table 1.8.

	Paroxysmal Kinesigenic Dyskinesia	Paroxysmal Exercise-Induced Dyskinesia	Paroxysmal Non-Kinesigenic Dyskinesia
Abbreviation	PKD	PED	PNKD
Trigger	Sudden voluntary movements, e.g. standing up from sitting down	Physical exertion after long periods of exercise	Alcohol, coffee, strong emotion
Age of onset	First two decades of life	First two decades of life	First decade of life
Associated symptoms	Infantile seizures (ICCA), migraine (can be hemiplegic)	migraine, hemiplegia, ataxia and epilepsy	Premonitory aura
Attack length	~ 30 seconds	2 – 5 minutes	10 minutes – 1 hour
Attack Frequency	20 times per day	1 or 2 per months	A few per year
Gene	<i>PRRT2</i>	<i>SLC2A1</i>	<i>PKND</i> (formerly <i>MR-1</i>)

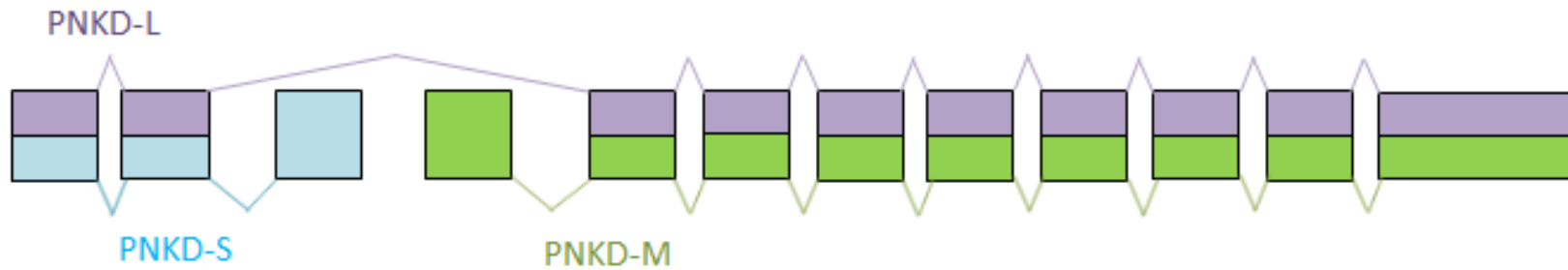
Table 1.8 – The features of the paroxysmal dyskinesias

2.2.3.1. Paroxysmal Non-Kinesigenic Dyskinesia

PNKD (OMIM #118800) was the first PxD condition to be reported in the literature, in 1940 (Mount and Reback 1940). PNKD refers to a paroxysmal movement disorder which is not triggered by movement as the others are, but instead by alcohol, coffee or strong emotion (Forssman 1961). Attacks of PNKD usually last between 10 minutes and one hour, but can be for as long as 12 hours. They tend to be relatively infrequent, and are only experienced a few times a year. Attacks can be preceded by a premonitory aura, but other associated symptoms are not usually experienced. Onset is generally in the first decade of life (Mount and Reback 1940).

The gene responsible for PNKD was identified as the *MR-1* gene in 2004 (Rainier et al. 2004), but it is now referred to as *PNKD*. Its protein of unknown function, thought to have three isoforms of varying length: PNKD-S, PNKD-M and PNKD-L (Figure 1.6a). To date three mutations have been reported in this gene to cause PNKD; c.20C>T p.(Ala7Val), c.26C>T p.(Ala9Val) and c.97G>C p.(Ala33Pro) (Figure 1.6b), the first two which have been found in multiple unrelated patients (Lee et al. 2004; Ghezzi et al. 2009). All three mutations are in exon one and therefore occur in the highly conserved N-terminus of the protein (present in PNKD-L and PNKD-S). Mutations in *PNKD* seem to account for about 70% of PNKD patients (Bruno et al. 2007), and four unaffected carriers have been reported in the literature, thus the penetrance is thought to be at about 95% (Erro et al. 2014). Emerging evidence, predominantly from the Ptacek lab, suggests that the protein has an important role in the synapse; it is found in neurones, associated with the cell membrane but is not a transmembrane protein, and PNKD-L was found in pre and post synaptic fractions of mouse neurones (Lee et al. 2015). A role in the exocytosis of neurotransmitters has been postulated as PNKD-L forms protein-protein interactions with RIM1 and RIM2, proteins which also regulate exocytosis of neurotransmitters. Furthermore, WT PNKD appears to inhibit this exocytosis whilst the mutant failed to do so (Shen et al. 2015). Interestingly given the attack triggers, a C-terminal enzymatic domain, found in PNKD-L and PNKD-M, is homologous to hydroxyacylglutathione hydrolase, an enzyme which detoxifies methylglyoxal; a compound found in coffee, alcohol and produced in oxidative stress. However, PNKD is unable to catalyse this reaction (Shen et al. 2011).

a.



b.

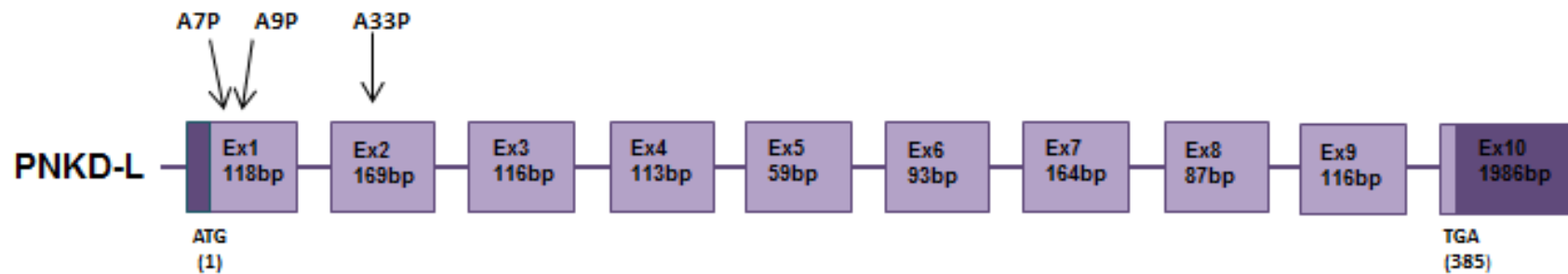


Figure 1.6 – Schematic diagrams to show (a) how differential splicing creates three PNKD isoforms: PNKD-S, PNKD-M and PNKD-L and (b) the structure of the longest isoform, PNKD-L, showing where the reported disease-causing mutations are found (described in terms of protein change)

2.2.3.2. Paroxysmal Exercise-induced Dyskinesia

PED (OMIM #612126) was first recognised as a separate and 'intermediate' form of PxD by Lance in 1977 (Lance 1977) and is the rarest. Attacks are induced by physical exertion after long periods of exercise and usually last between two and five minutes, although they can be up to two hours (Bhatia 2011). They have a frequency of about once or twice per month. The condition can be associated with migraine, hemiplegia, ataxia and epilepsy (Neville et al. 1998).

Mutations in the *SLC2A1* gene, which encodes the glucose transporter type1 protein, have recently been found to be responsible for causing PED (sometimes referred to as GLUT1 deficiency syndrome 2), and since the first discovery in 2008 the mutations reported total 10, all of which are missense or small indels (Weber et al. 2008) (Figure 1.7). However mutations in the gene are phenotypically heterogeneous, and in total more than 160 mutations have been reported, causing a range of phenotypes from one presentation of episodic ataxia (Ohshiro-Sasaki et al. 2014), alternating hemiplegia of childhood, pure dystonia, epilepsy and most commonly, GLUT1 deficiency syndrome 1 (GLUT1 DS1). GLUT1 DS1 is itself a phenotypically variable disorder with symptoms including ataxia, cognitive impairment, seizures, developmental delay and, essentially, low serum glucose levels. Although classed as different disorders, clinically distinguishing GLUT DS1 and GLUT DS2 can be problematic, and manifestations can be age dependent. Mutations in the *SLC2A1* gene only appear to account for up to 20% of PED cases (Schneider et al. 2009).

As the name of the protein suggests, *SLC2A1* encodes a transporter of glucose across the blood brain barrier. Expression of the PED mutant proteins result in reduced glucose transport into the brain, thus it is thought that these mutations have a loss of function mechanisms. Therefore it seems that the energy deficit caused by prolonged exertion, coupled with the reduced glucose transport can result in the movement disorder (Weber et al. 2008). If a *SLC2A1* mutation is suspected, cerebrospinal fluid (CSF) glucose levels should be investigated. However, there are PED families without mutations in *SLC2A1* and so it is likely that there is another gene responsible for this disorder.

2.2.3.3. Paroxysmal Kinesigenic Dyskinesia

PKD (OMIM #128200) is the most common of the PxDs. Attacks are brief, only lasting seconds, but frequent with most patients experiencing up to 20 per day. They are triggered by sudden movement such as standing from a sitting position or increasing speed from a walk to run to catch a bus. Onset varies but is usually in the first two

decades of life. The condition was first recorded in the literature as being a separate disorder from PNKD in 1967 by Kertesz (Kertesz 1967). PKD can be familial or sporadic, and sporadic cases are four times more common in men than women. PKD is often accompanied by infantile seizures in a disorder known as ICCA (infantile convulsions and paroxysmal choreoathetosis OMIM #602066) (Swoboda et al. 2000), and can also be accompanied by migraines with or without hemiplegia. 70% of patients experience an aura-like sensation prior to the attack, and some can use this to suppress it (Bruno et al. 2004). There is often large phenotypic variety between family members and although the disease is autosomal dominant there can be reduced penetrance.

The gene causing PKD has been elusive for many years. Families with pure PKD and ICCA were both mapped to the same region of chromosome 16, but examination of the genes contained within did not yield any positive results (Kikuchi et al. 2007). Sporadic PKD patients were also mapped to chromosome 16, but to a different region (Valente et al. 2000). However, recently several groups simultaneously used whole-exome sequencing as well as the previous linkage data to identify the gene as *PRRT2*, a small gene of unknown function (Chen et al. 2011; Wang et al. 2011; Li et al. 2012), (Lee et al. 2012). Since this discovery more groups have screened cohorts of PKD and ICCA patients and to date about 60 mutations have been reported (Figure 1.8). Mutations are spread throughout the gene, however there is a hotspot within a string of cytosines in exon two, including by far the most common mutation in this gene, c.649dupC p.(Arg217Pfs*8), an insertion of a cytosine that results in a premature stop codon. It has been suggested that this sequence could potentially form a hairpin, and this would account for the high rate of mutations occurring in the region (Heron and Dibbens 2013). It has been shown that this common mutation results in nonsense mediated decay (NMD) and so it is thought that the mechanism of disease is haploinsufficiency (Wu et al. 2014). Microdeletions covering the whole gene and causing PKD add evidence to this theory (Dale et al. 2012), however some missense mutations have been reported and it is unclear how they are incorporated. *PRRT2* mutations have been since been seen in families with only hemiplegic migraine or benign seizures. Reports of the percentage of PKD patients who harbour a *PRRT2* mutation vary from 23% – 65%, likely due to the thoroughness of the clinical diagnosis (Erro et al. 2014). The vast majority of *PRRT2* mutations are heterozygous, however, the rare reports of homozygous and one compound heterozygous case describe a marked increase in severity of the disorder (Delcourt et al. 2015).

Although much is unknown about the PRRT2 protein, it is known that it contains two transmembrane regions, is expressed throughout the brain and spinal cord, and interacts with the presynaptic protein SNAP25 (Stelzl et al. 2005). SNAP25 is a SNARE protein which is involved in both transporting vesicles from the golgi apparatus and forming a complex for vesicle docking prior to exocytosis (Lee et al. 2015). Lee et al showed that the p.*Arg217Pfs*8) mutation prevented this PRRT2 – SNAP25 interaction from occurring presumably because of absence of PRRT2 due to NMD (Lee et al. 2012). Therefore PRRT2 could also be involved in regulating vesicle exocytosis, and disruption of this could in turn cause PKD.

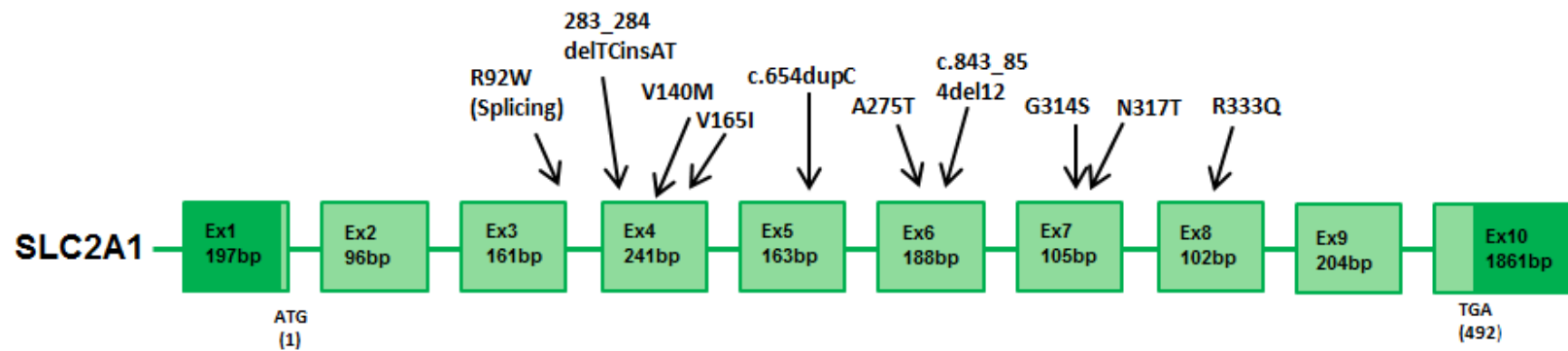


Figure 1.7 –A schematic diagram to show the structure of the SLC2A1 gene, identifying where the reported PED disease-causing mutations are found (described in terms of protein change unless indicated otherwise)

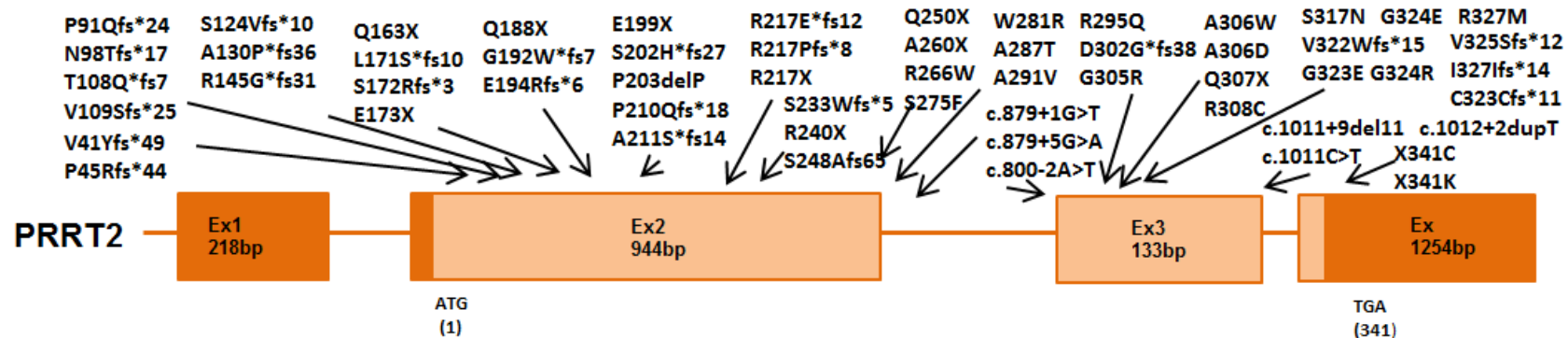


Figure 1.8 –A schematic diagram to show the structure of the PRRT2 gene, identifying where the reported PKD disease-causing mutations are found (described in terms of protein change unless indicated otherwise)

2.2.3.4 Phenotypic and Genetic Overlap

A small amount of genetic overlap has been reported between the PxDs, highlighted by a recent review which consolidated the 500 genetically confirmed cases that have been published (Erro et al. 2014). It found that of patients with *PRRT2* mutations, 98% did have PKD, but 2% had either PED or PNKD, and 99% of the patients with *PNKD* mutations did have PNKD, but 1% had PED, and an additional 6% had exercise as secondary trigger. Furthermore, whilst 95% of the patients with *SLC2A1* mutations did have PED, 5% had PNKD. Therefore overall, 98% of genetically diagnosed PxD patients had a mutation in the expected gene. It should be taken into account however, that the majority of patients in these studies would have only been screened for the gene that their condition is associated with, and so the true number may actually be higher. Interestingly, PKD cases were never found with mutations in the other two genes.

2.3. Non-Channel Channelopathies

Although traditionally hereditary channelopathies are caused by VGIC dysfunction, it is increasingly being recognised that channel-interacting proteins can be equally important for normal channel function. Consequently, disruption of the function of these auxiliary proteins can also result in the 'channelopathy' phenotypes, as demonstrated by the paroxysmal dyskinesias. This area is the subject of a review by Lee *et al*, in which non-channel genes such as *NOL3*, *GPS98*, *CK1δ* as well as the PxD genes, are described as causing electrical disorders usually attributed to channelopathies (Lee et al. 2015).

3. Rhabdomyolysis

Rhabdomyolysis (RM) is a term that refers to the breakdown of damaged skeletal muscle tissue, resulting in leakage of cellular components into the circulation. These contents, especially myoglobin, can be toxic, and produce symptoms such as vomiting, confusion, muscle pain, and in severe cases acute kidney failure. Therefore RM episodes can be potentially life-threatening.

There are several environmental causes of a RM episode including alcohol, drug abuse, medication, extreme exertion, infection and crush injury. However, there can also be underlying genetic causes, especially if the RM is recurrent (two or more episodes). The sources of RM are summarised in Figure 1.9 (adapted from (Scalco et al. 2015)). Despite the varied triggers, all episodes of RM share a common pathophysiology. As discussed in section 1.1, resting muscle sustains an electrical gradient across the sarcolemma, with sodium-potassium pumps maintaining a high intercellular K^+ and high extracellular Na^+ and Ca^+ levels. Insufficient energy production can cause pump dysfunction and increased membrane permeability, eventually resulting in high intracellular Ca^+ ; the same consequence occurs in the event of muscle damage. The raised Ca^+ level triggers increased production of proteases and phosphatases, and leads to muscular breakdown (Zutt et al. 2014). It is unclear why muscle is more susceptible to such damage than neuronal cells.

There are mixed reports as to prevalence of RM. One study found that there are 26,000 cases annually in the USA (Graves and Gillum 1997), though mild occurrences may cause events to be underreported. There is also no strict definition of an episode of RM, however, they are characterised by increased serum creatine kinase (CK) levels (although there is controversy over whether levels should increase to five or ten times the normal range), with a rapid return to baseline, and often myoglobinuria (myoglobin in the urine causing it to have a dark 'coca cola' colour), as well as weakness and myalgia (Zutt et al. 2014).

Exercise intolerance is a term which is often used alongside RM, especially when caused by genetic factors. It refers to a condition in which a patient is unable to exercise at a level which would be expected for their general physical condition, usually because of muscle pain or fatigue, and will often accompany an exercise-induced RM event due to a shared underlying pathway.

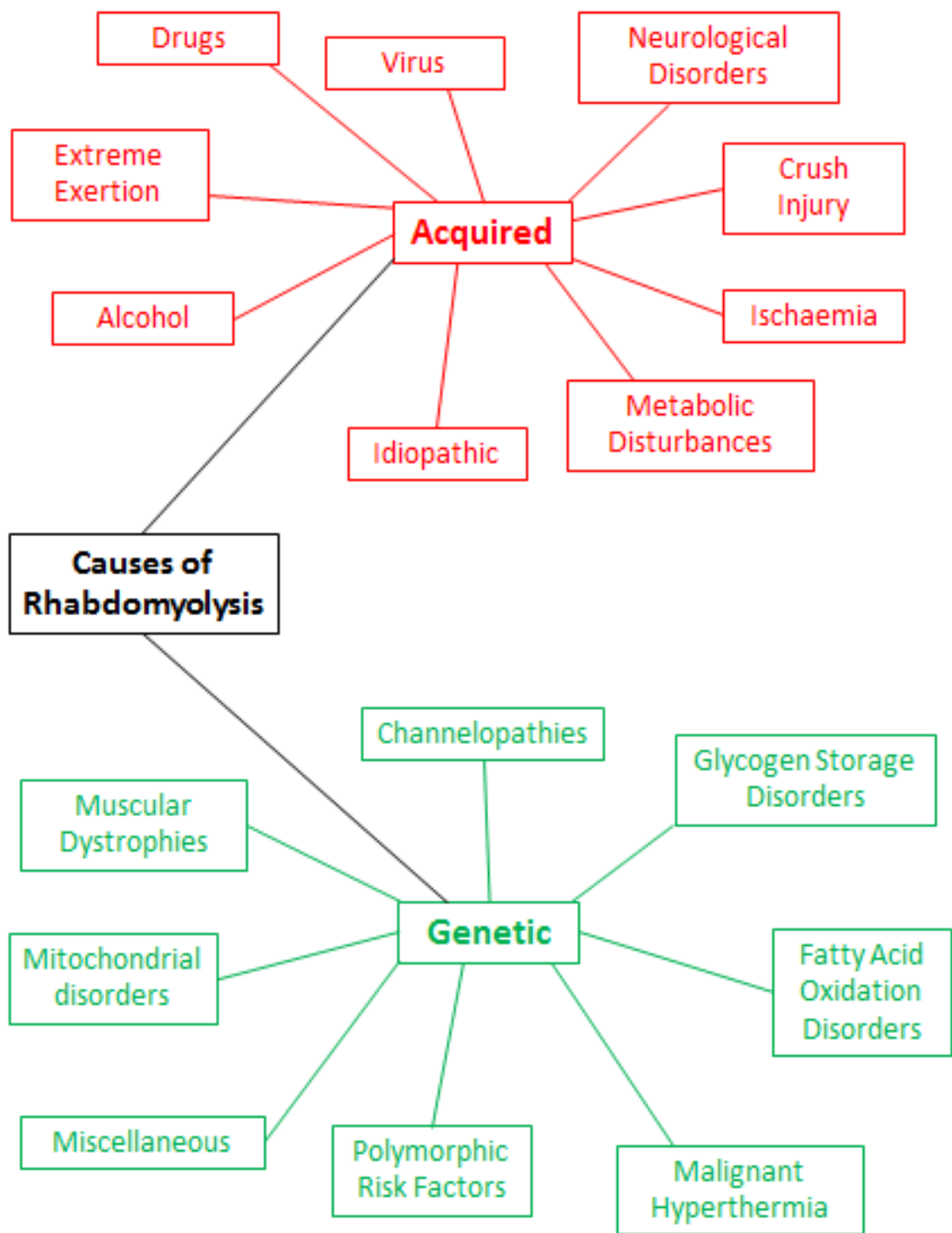


Figure 1.9 – A spider diagram to summarise the genetic and non-genetic causes of rhabdomyolysis. Adapted from (Scalco et al. 2015)

Genetically diagnosing patients with recurrent RM can be difficult, as there are many known genetic causes, huge phenotypic variability, sometimes non-Mendelian genetic causes and usually little or no family history. However, it is also crucial as appropriate clinical advice can prevent future life-threatening episodes. Genetic defects that are known to cause recurrent RM and exercise intolerance can be broadly divided into channelopathies, disorders of glycogen metabolism, disorders of fatty acid metabolism, muscular dystrophies and miscellaneous genes (Nance and Mammen 2015; Scalco et al. 2015). Here, the underlying genetic causes of RM will be discussed in further detail.

3.1. Channelopathies

Skeletal muscle ion channel dysfunction has been reported to cause recurrent RM, usually as a separate presentation to the channelopathy phenotypes described above, although there have been a very small number of patients reported to demonstrate both sets of symptoms (Marchant et al. 2004). The majority of RM due to ion channel impairment is as a result of malignant hyperthermia.

Malignant hyperthermia is a condition in which apparently unaffected patients have an adverse reaction to anaesthesia with symptoms including hyperthermia, tachycardia, tachypnea, increased oxygen consumption, acidosis, muscle rigidity, and RM. If left untreated the condition can be fatal, and so diagnosing it is of the utmost importance as then triggers can be avoided. It is usually an autosomal dominant disease, although not fully penetrant, and thus the genetic condition is referred to as malignant hyperthermia susceptibility (MHS). It is thought that the incidence of MHS variants in the population could be as high as 1:2000 (Rosenberg et al. 2007). Linkage studies have identified six disease loci (MHS1-MHS6), however thus far only two MHS genes have been discovered: *RYR1* and *CACNA1S* (Stowell 2014). Although traditionally anaesthesia is the trigger for RM in MHS, there is increasing evidence that patients with MHS can also have episodes triggered by heat, infection, and, importantly, exercise (Capacchione and Muldoon 2009). There are two useful diagnostic tools for MHS – the in vitro contracture test (IVCT) and the caffeine-halothane contracture test (CHCT), however both are invasive as they require a muscle biopsy (Stowell 2014). A predictive genetic test would instead be ideal; however there is much that is still unknown about its genetic basis.

3.1.1. MHS1 – *RYR1*

As discussed in section 1.4, *RYR1* encodes the ryanodine receptor 1, a calcium release channel the sarcoplasmic reticulum of skeletal muscle. It is coupled with the voltage-gated calcium channel $Ca_v2.1$, and opens in response to increased intracellular

Ca²⁺, amplifying the signal, therefore acts as a VGIC in muscle fibres. In an MH episode, the channel opening is prolonged, resulting in excessive intracellular Ca²⁺ (Schneiderbanger et al. 2014). *RYR1* is a huge gene, consisting of 107 exons, and mutations in it are thought to account for 50 – 70% of MHS cases. It is also a phenotypically heterogeneous gene, and, aside from MHS, mutations (recessive or dominant, depending on the phenotype) can be responsible for central core disease, multi-minicore disease, centronuclear myopathy and congenital fibre type disproportion (Scalco et al. 2015). There has also been one case report of a patient with atypical periodic paralysis due to mutations in the gene (Zhou et al. 2010). This heterogeneity can make *RYR1* mutations hard to interpret.

3.1.2. MHS5 – *CACNA1S*

The only other gene currently known to be a cause of MHS is *CACNA1S*, encoding the voltage-gated calcium channel Ca_v2.1. This gene is also a known cause of the skeletal muscle channelopathy, HypoPP (see section 2.1.1.1). The gene was first identified as a cause of MHS in 1997, and to date only four mutations have been found to cause the condition (Monnier et al. 1997). *CACNA1S* mutations are thought to account for only about 1% of MHS patients (Carpenter et al. 2009). Given that the channel is coupled to the ryanodine receptor, it is unsurprising that mutations in the gene can cause MHS.

3.1.3. *SCN4A*

There has been one report in the literature of a patient presenting with fixed, progressive weakness and recurrent RM due to an *SCN4A* mutation, c.4774A>G p.(Met1592Val) (Lee and Chahin). This mutation had previously been reported to cause HyperPP, a condition well known to be associated with the gene (see section 2.1.2.1). The RM attacks occurred biannually and were triggered by stress, exercise and emotion. Additionally, a family was reported with two *SCN4A* mutations on the same allele manifesting as MHS with PP (Anderson et al. 2002) (mentioned previously in section 2.1.21), No other such cases have been reported with mutations in the gene, although linkage analysis of MHS and MHS/ PP families have suggested *SCN4A* as a potential disease locus (Moslehi et al. 1998).

3.2. Metabolic Muscle Disorders

In genetic metabolic muscle disorders, generally the mutated gene encodes an enzyme in one of the energy-producing pathways, resulting in insufficient energy and thus exercise intolerance and exercise-induced RM episodes. The mutations tend to be loss-of-function, and are usually recessive. There are two pathways that can be

affected – the glycolysis pathway or the fatty acid metabolism pathway. The two are distinguishable by the circumstances surrounding the onset of symptoms; in glycogen metabolism disorders symptoms begin within minutes of intense or aerobic exercise, whereas prolonged exercise (e.g. 45 minutes) is required to trigger symptoms for fatty acid oxidation disorders. With careful clinical consideration the correct pathway should be identifiable.

3.2.1. Glycogen Storage Diseases

Glycogen metabolism is an important source of energy for skeletal muscle during exercise, and so it is unsurprising that deficiency of the enzymes required for glycogen breakdown can result in RM and exercise intolerance. Diseases in which the activity of these enzymes is diminished are called glycogen storage diseases (GSD), and there are 21, although not all affect skeletal muscle. The GSDs are summarised in Table 1.9. Each of the GSDs that cause RM and/ or exercise intolerance will be briefly discussed in terms of genetic causes and phenotype.

3.2.1.1. GDSV – McArdle’s Disease

McArdle’s Disease is the most common of the muscle GSDs. It is caused by recessive mutations in the *PYGM* gene which encodes muscle glycogen phosphorylase, resulting in enzyme deficiency. The function of this enzyme is to convert glycogen into glucose-1-phosphate, so GDSV patients accumulate glycogen in skeletal muscle (Andreu et al. 2007). To date more than 140 mutations have been reported in the gene, the most common being c.148C>T p.(Arg50*), which present in between 43% and 81% of genetically diagnosed patients, depending on ethnic background (Andreu et al. 2007). Patients experience exercise intolerance manifesting as muscle cramps, myalgia, and fatigue, with associated raise in CK and myoglobinuria. After a short rest they can continue exercising with more ease, in their characteristic ‘second wind’. Lack of muscle glycogen phosphorylate can be seen biochemically (Scalco et al. 2015).

3.2.1.2. GSDVII – Tarui’s Disease

Recessive mutations in *PFKM*, encoding muscle phosphofructokinase, are responsible for GSDVII. This enzyme catalyses the production of fructose-1-6-dipsosphate from fructose-6-phosphate, and its deficiency impairs glycolysis. More than 20 mutations in the gene have been reported to cause the rare disorder. Symptoms of Tarui’s disease are similar to McArdle’s disease, with exercise intolerance, muscle cramping, and exertional myopathy, however, unlike McArdle’s disease there is no warm-up

phenomenon. There is also additional haemolytic anaemia. A biochemical assay will demonstrate reduced enzymatic activity (Musumeci et al. 2012; Scalco et al. 2015).

3.2.1.3. GSDIX

GSDIX is a glycogen storage disorder that is caused by mutations in 4 genes: *PHKA2* (GSDIXa), *PHKB* (GSDIXb), *PHKG2* (GSDIXc), and *PHKA1* (GSDIXd), encoding alpha1, beta, gamma1 and alpha2 subunits respectively. Together, four copies of each of four subunits (alpha, beta, gamma and delta) come together to form phosphorylase kinase. This enzyme has a regulatory role in glycogen metabolism (Goldstein et al.). The different subunits are differentially expressed in different tissues, thus, while mutations in all four genes cause glycogen storage disease symptoms, only mutations in *PHKB* and *PHKA1* lead to a muscle phenotype (although there are two patients reported in which *PHKG2* mutations cause weakness after extreme exercise (Bali et al. 2014)). RM has only been reported in conjunction with mutations in *PHKA1*. This gene is on the X-chromosome, so the disease has an X-linked recessive inheritance pattern. Symptoms tend to be mild and include exercise-induced myalgia, cramps, fatigue and myoglobinuria, and in one case, raised CK. RM is only triggered following intense exercise (Scalco et al. 2015). Again, a biochemical assay can show reduced enzymatic activity in muscle.

3.2.1.4. GSDX

Recessive mutations in the gene *PGAM2* cause the rare glycogen storage disorder GSDX. *PGAM2* encodes the muscle phosphoglycerate mutase enzyme, and its deficiency results in a block in glycogenolysis. The gene was first identified in 1993, yet fewer than ten mutations have been reported (Tsujino et al. 1993). The phenotype for GSDX is relatively mild, with patients only usually experiencing symptoms after intense exercise. As well as RM episodes, symptoms include muscle cramps and exercise intolerance. A muscle biopsy may show glycogen accumulation and tubular aggregates, and enzymatic activity should be markedly reduced (Tonin et al. 2009).

3.2.1.5. GDSXI

LDHA recessive mutations are the genetic basis for GDSXI. These mutations result in insufficient levels of lactate dehydrogenase, which catalyses the production of lactate from pyruvate. GDSXI patients experience easy fatigue, exercise intolerance, cramps and occasionally RM. It should be noted that mutations in the gene have not been reported in those patients with RM episodes; however they do have reduced serum

LDH levels similar to those with a genetic diagnosis (Kanno et al. 1980), (Maekawa et al. 1990).

3.2.1.6. GSDXII

GSDXII is caused by recessive mutations in the *ALDOA* gene, encoding the enzyme fructose-1,6-bisphosphate aldolase A; responsible for the conversion of fructose-1,6-bisphosphate into dihydroxyacetone phosphate (DHAP) and glyceraldehyde-3-phosphate. Again, enzymatic deficiency results in impaired glycolysis in muscle, but additionally, the enzyme is expressed in erythrocytes. It is a rare disorder, with few reported patients. Most patients with aldolase A deficiency present with haemolytic anaemia and mental retardation and myopic features are unusual but include muscle pain, exercise intolerance and RM triggered by childhood infection. One consanguineous family has been reported with only a muscle presentation (Mamoune et al. 2014). Reduced aldolase activity can be seen biochemically.

3.2.1.7. GSDXIII

GSDXIII is a highly rare glycogen storage disorder, only being reported in three families to date (Musumeci et al. 2014). It is due to mutations in the beta-enolase gene, *ENO3*. Beta-enolase converts 2-phosphoglyceric acid into phosphoenolpyruvate and is important in terminal glycolysis. Recessive mutations result in strenuous exercise-triggered myalgia, cramps, and, in two of the cases, RM. Beta-enolase activity is markedly reduced.

3.2.1.8. GSDXIV – Congenital Disorder of Glycosylation 1

Congenital disorder of glycosylation type one is a highly heterogeneous, multisystem disorder, with huge variety in severity and manifesting symptoms. It is known to be caused by recessive mutations in *PGM1*, the predominant phosphoglucomutase in most cell types. The function of this enzyme is to transfer the phosphate group of glucose from the one position to the six position. GSDXIV patients can have congenital features such as cleft palate, bifid uvula, and short stature as well or instead of endocrine disorders, liver disease, hypoglycaemia, cardiomyopathy exercise intolerance, cramps and RM episodes (Tegtmeyer et al. 2014). Enzymatic activity of phosphoglucomutase is reduced.

3.2.1.9. GSD0B

Recessive mutations in the *GYS1* gene which encodes the muscle form of the enzyme glycogen synthase are responsible for GSD0B. This enzyme enables the addition of

glucose monomers to glycogen and thus is essential for glycogen synthesis. Few cases have been reported, but those that have describe patients with exercise intolerance and, often fatal, hypertrophic cardiomyopathy. One patient experienced epilepsy; it is unclear whether this is related or coincidental. No patients have yet been reported to have RM episodes (Kollberg et al. 2007). Patients have a complete deficiency in muscle glycogen.

3.2.1.10. Phosphoglycerate Kinase 1 Deficiency

Although not classed as a glycogen storage disorder, phosphoglycerate kinase 1 deficiency is included as phosphoglycerate kinase catalyses the conversion of 1,3-diphosphoglycerate to 3-phosphoglycerate during glycolysis, thereby producing ATP. Recessive mutations in the X-chromosome gene *PGK1* cause the disease, of which more than 20 have been reported. Clinical presentations are various and patients can have one, two or all of three distinct phenotypes: hemolytic anaemia, myalgia with exercise intolerance and RM, or developmental delay. Biochemically, PGK activity is reduced (Scalco et al. 2015).

Name	OMIM#	Gene/ Enzyme	RM?	Phenotypic Features	Reference
GSDIa (von Gierke's disease)	232200	<i>G6PC</i> / glucose-6-phosphatase	No	Growth retardation, delayed puberty, lactic acidemia, hyperlipidemia, hyperuricemia	(Lei et al. 1993)
GSDIb	232220	<i>SLC37A4</i> / glucose-6-phosphate translocase	No	Like GSDIa, but with recurrent infections and neutropenia	(Gerin et al. 1997)
GSDII (Pompe's disease)	232300	<i>GAA</i> / acid alpha-1,4-glucosidase	No	Cardiomyopathy and muscular hypotonia, often premature death	(Pompe 1932), (Martiniuk et al. 1990)
GSDIII (Cori's or Forbes' disease)	232400	<i>AGL</i> / glycogen debrancher enzyme	No	Hepatomegaly, hypoglycaemia, growth retardation, muscle weakness, cardiomyopathy	(Shen et al. 1996)
GSDIV (Andersen's disease)	232500	<i>GBE1</i> / glycogen branching enzyme	No	Liver disease progressing to lethal cirrhosis, with heterogeneous additional symptoms	(Andersen 1956; Bao et al. 1996)
GSDV (McArdle's disease)	232600	<i>PYGM</i> / muscle glycogen phosphorylase	Yes	Exercise intolerance, muscle cramps, myalgia 'second wind' phenomenon	(Mc 1951; Tsujino et al. 1993)
GSDVI (Her's disease)	232700	<i>PYGL</i> / liver glycogen phosphorylase	No	Hypoglycaemia, mild ketosis, growth retardation, and prominent hepatomegaly	(Hers 1959; Burwinkel et al. 1998)
GSDVII (Tarui's disease)	232800	<i>PFKM</i> / muscle phosphofructokinase	Yes	Exercise intolerance, muscle cramps, myalgia, no 'second wind', haemolytic anaemia	(Tarui et al. 1965), (Nakajima et al. 1990)
GSDIXa	306000	<i>PHKA2</i> / hepatic phosphorylase kinase,	No	Usually mild. hepatomegaly, short stature, liver dysfunction, hypoglycaemia, and mild motor delay	(Hendrickx et al. 1995)

		alpha 2			
GSDIXb	261750	<i>PHKB</i> / phosphorylase kinase, beta	No	Hepatomegaly, hypoglycaemia following fasting, growth delay, mild muscle signs	(Burwinkel et al. 1997)
GSDIXc	613027	<i>PHKG2</i> / hepatic phosphorylase kinase, gamma 2	No	Hepatomegaly, hypotonia, growth retardation in childhood, and liver dysfunction	(Maichele et al. 1996)
GSDIXd	300559	<i>PHKA1</i> / muscle phosphorylase kinase, alpha 1	Yes	Variable exercise-induced muscle weakness or stiffness, cramps and myalgia	(Wehner et al. 1994)
GSDX	261670	<i>PGAM2</i> / muscle phosphoglycerate mutase	Yes	Mild phenotype with intolerance to strenuous exercise and exercise-induced cramps	(Tsujino et al. 1993)
GSDXI	612933	<i>LDHA</i> / lactate dehydrogenase	Yes	Easy fatigue, muscle cramps and stiffness	(Maekawa et al. 1990)
GSDXII	611881	<i>ALDOA</i> / fructose-1,6-bisphosphate aldolase A	Yes	Hemolytic anaemia, mental retardation, increased hepatic glycogen. Occasionally with associated myopathy	(Kishi et al. 1987)
GSDXIII	612932	<i>ENO3</i> / beta-enolase	Yes	Exercise intolerance, muscle cramps and tenderness, myalgia	(Comi et al. 2001)
GSDXIV (Congenital disorder of	171900	<i>PGM1</i> / phosphoglucomutase	Yes	Varied; cleft lip, bifid uvula, hepatopathy, hypoglycaemia, short stature, exercise intolerance,	(Stojkovic et al.)

glycosylation, 1)				cardiomyopathy	
GSDXV	613507	GYG1/ glycogenin-1	No	Myopathy with slowly progressive weakness. Cardiomyopathy in one case, raised CK in one case	(Malfatti et al. 2014), (Moslemi et al. 2010)
GSD0A	240600	GYS2/ hepatic glycogen synthase-2	No	Infantile hypoglycaemia, hepatic glycogen deficiency	(Orho et al. 1998)
GSD0B	611556	GYS1/ muscle glycogen synthase-1	No	Cardiomyopathy, exercise intolerance, muscle glycogen deficiency, premature death, seizures.	(Kollberg et al. 2007)
Phosphoglycerate kinase 1 deficiency	300653	PGK1/ Phosphoglycerate kinase 1	Yes	Varied, one or all of hemolytic anaemia, myopathy, and developmental delay	(Fujii and Yoshida 1980)

Table 1.9 – A summary of the glycogen storage diseases

3.2.2. Fatty Acid Metabolism Disorders

During prolonged exercise, when glucose reserves have been depleted, the body relies on lipid metabolism; in the mitochondria, long-chain fatty acids are oxidised to provide an energy source for skeletal muscles. Defects of the enzymes involved in this oxidation process can result in a group of diseases called the fatty acid metabolism disorders, characterised by episodes of RM and exercise intolerance induced by prolonged periods of aerobic exercise. Patients can also experience RM episodes triggered by other factors such as drugs, stress, fasting and general anaesthesia (Scalco et al. 2015). There are seven genes known to cause RM and exercise intolerance as a result of impaired fatty acid oxidation, summarised in Table 1.10.

3.2.2.1. VLCAD Deficiency

Very long-chain acyl-CoA dehydrogenase (VLCAD) is an enzyme that acts upon only very long-chain fatty acids within the mitochondria. Recessive mutations in the *ACADVL* gene are responsible for the metabolic disorder VLCAD deficiency. This disease presents in three forms of differing severity. The most severe form has early onset of cardiomyopathy, liver disease and hypotonia, often leading to premature death. The intermediate consists of childhood onset of hypoketotic hypoglycaemia and hypotonia, sometimes with liver disease. Finally, the mildest form has adult-onset and myopathy, with exercise intolerance, cramps and RM episodes. There is a clear genotype-phenotype correlation, with mutations resulting in complete reduction of VLCAD resulting in a more severe disease than those leaving residual enzymatic activity (Spiekerkoetter 2010). Well over 100 mutations have been reported in the gene.

3.2.2.2. CPTII Deficiency

CPTII deficiency is the most common of the fatty acid metabolism disorders, and over 80 mutations have been reported in the causative gene, *CPT2*. 60% of genetically diagnosed patients have the common c.338C>T p.(Ser113Leu) mutation (Thuillier et al. 2003) and mutations are recessive. *CPT2* encodes carnitine palmitoyltransferase II, an enzyme involved in the translocation of long-chain fatty acids from the cytosol to the mitochondria. Similarly to VLCAD, presentation is seen in three forms of increasing severity, from a fatal neonatal form, to an intermediate infantile form with muscle and cardiac features, to lastly an adult-onset myopathic form with RM and exercise intolerance. Again, mutations resulting in complete enzyme depletion lead to a more severe presentation (Fanin et al. 2012).

3.2.2.3. MADD (Multiple Acylcoenzyme A Dehydrogenase Deficiency)

MADD, also known as glutaric academia II, is caused by clinically indistinct recessive mutations in three different genes, *ETF A*, *ETF B* (which encode the electron transfer flavoprotein subunits A and B respectively), and *ETFDH* (which encodes electron transfer flavoprotein dehydrogenase). Both enzymes are required to transfer electrons from the dehydrogenase into the electron transport chain. Once again, mutations result in three separate clinical manifestations: a neonatal form with high likelihood of mortality, hypotonia, hepatomegaly, hypoglycaemia and congenital abnormalities, an infant-onset form with no congenital abnormalities, and a milder adult-onset form with symptoms including hypoglycaemia, exercise intolerance, myalgia, weakness and RM (Grunert 2014). The severity of the condition is not related to which of the three genes is mutated.

3.2.2.4. Trifunctional Protein Deficiency

The mitochondrial trifunctional protein is an enzyme which catalyses three steps of the oxidation of fatty acids in the mitochondria with three different enzymatic activities. It is composed of eight subunits, four alpha and four beta, encoded by *HADHA* and *HADHB* respectively. Recessive mutations in either of these genes results in trifunctional protein deficiency (indistinguishable by genetic cause); a disorder with, again, three severities. A neonatal onset leading to sudden death syndrome is the worse, an infantile liver condition is the intermediate, and the mildest is an adolescent-onset skeletal myopathy with exercise induced RM and a peripheral neuropathy (Spiekerkoetter et al. 2003). It is again though that the more residual enzyme, the milder the phenotype (Purevsuren et al. 2009).

Name	OMIM#	Gene/ Enzyme	RM?	Phenotypic Features	Reference
VLCAD deficiency	201475	<i>ACADVL</i> / very long-chain acyl-CoA dehydrogenase	Yes	Severity and symptoms vary; cardiomyopathy, premature death, hypoketotic hypoglycaemia, exercise intolerance.	(Aoyama et al. 1995)
CPTII deficiency	255110	<i>CPT2</i> / carnitine palmitoyltransferase II	Yes	Severity and symptoms vary; early sudden death, dysmorphic features, hepatomegaly, cardiomegaly, hypoketotic hypoglycaemia, exercise intolerance	(Taroni et al. 1993)
MADD, Glutaric aciduria type IIA	231680	<i>ETFAL</i> / electron transfer flavoprotein, alpha	Yes	Severity and symptoms vary; congenital abnormalities, hypotonia, hepatomegaly, hypoglycaemia, premature death, myopathy, exercise intolerance	(Indo et al. 1991)
MADD, Glutaric aciduria type IIB	231680	<i>ETFB</i> / electron transfer flavoprotein, beta			(Colombo et al. 1994)
MADD, Glutaric aciduria type IIC	231680	<i>ETFDH</i> / electron transfer flavoprotein dehydrogenase			(Beard 1993)
Trifunctional protein deficiency	609015	<i>HADHA</i> / mitochondrial trifunctional protein, alpha subunit	Yes	Severity and symptoms vary; sudden death syndrome, hepatic Reye-like syndrome, skeletal myopathy, cardiomyopathy	(Brackett et al. 1995)
		<i>HADHB</i> / mitochondrial trifunctional protein, beta subunit			(Spiekerkoetter et al. 2003)

Table 1.10 – A summary of the fatty acid metabolism disorders that cause rhabdomyolysis

3.3. Muscular Dystrophy Genes

The muscular dystrophies (MDs) are characterised by progressive skeletal muscle degeneration and weakness and are highly heterogeneous, both genetically and clinically. There are nine main types (Duchenne, Becker, limb-girdle, congenital, facioscapulohumeral, myotonic, oculopharyngeal, distal and Emery-Dreifuss), although subtypes total more than 30, with more than 30 causal genes. The muscle damage involved in MD can result in RM episodes (Scalco et al. 2015); however, usually MDs are distinct from primary RM and thus are recognisable. They are therefore beyond the scope of this review. Nevertheless, there is a small number of MD genes for which there are known instances of RM or exercise intolerance being the presenting feature, which will be discussed briefly here.

3.3.1. *ANO5*

ANO5 encodes anoctamin-5, an eight TM protein that is suggested to be important for the development of the musculoskeletal system (Mizuta et al. 2007). Recessive mutations in the gene are a known cause of Miyoshi MD type 3, and limb-girdle dystrophy type 2L. However, RM and exercise intolerance can be the main presenting feature, accompanied with severe myalgia and variable muscle weakness RM episodes do not appear to have a discernible trigger (Milone et al. 2012), (Lahoria et al. 2014).

3.3.2. *FKRP*

Recessive mutations in the *FKRP* gene, encoding the fukutin-related protein, cause two types of muscular dystrophy: limb-girdle MD type 2I and congenital MD type 1C. LGMD2I is known to be occasionally accompanied by RM episodes, and some patients have also been reported to have exercise-induced RM and myalgia episodes as the presenting feature. The c.826C>A p.(Leu276Ile) mutation is by far the most common in the gene (Lindberg et al. 2012).

3.3.3. *DMD*

The X-chromosome gene *DMD* encodes the dystrophin protein, shortening of or full reduction in which is the cause of Becker's or Duchenne's MD respectively. This is because the majority (65%) of the almost 3000 mutations reported in the gene are large deletions, which maintain the reading frame in Becker's MD and do not in Duchenne's (Monaco et al. 1988). Nonsense, splice site and a small number of missense changes have also been reported (Tuffery-Giraud et al. 2005). Becker's MD

can have associated exercise-induced RM, cramps and exercise intolerance, and these have been known to be the presenting symptoms (Doriguzzi et al. 1993). Mutations in this gene also cause X-linked dilated cardiomyopathy (Muntoni et al. 1993).

3.3.4. *SGCA* and *SGCB*

The sarcoglycanopathies are a subset of limb-girdle MDs, caused by recessive mutations in one of four genes that code for the sarcoglycan protein subunits, *SGCA*, *SGCB*, *SGCD*, *SGCG*, resulting in LGMD2C – F. Whilst the phenotypes of some of the others have been reported to include RM, mutations in the gene encoding the alpha and beta subunits, *SGCA* and *SGCB* respectively, are the only ones with the condition as a presenting feature. The RM episode reported was triggered by infection in *SGCA* mutations (Ceravolo et al. 2014) and by exercise in *SGCB* mutations (Cagliani et al. 2001).

3.3.5. *DYSF*

Recessive mutations in *DYSF* gene, which encodes dysferlin, result in a varied group of presentations known as the dysferlinopathies. These include Miyoshi MD type 1, limb-girdle MD type 2B and distal myopathy. Whilst not usually associated with RM episodes, there is a report of a LGMD2B patient presenting with acute renal failure as a result of RM (Moody and Mancias 2013). Dysferlin is involved in calcium-mediated sarcolemma repair (Han and Campbell 2007).

3.4. Miscellaneous Genes

There are several genes which can harbour RM or exercise intolerance causing mutations, but do not fit into the above categories. These genes are summarised in Table 1.11.

Gene/ Protein	Disease	OMIM#	Inheritance	Features of RM/ exercise intolerance episodes	Ref
ISCU/ iron-sulphur cluster scaffold protein	Myopathy with lactic acidosis	255125	AR	Childhood onset of exercise intolerance with muscle tenderness, cramping, dyspnea, lactic acidosis and, RM. Only two mutations reported: one missense and one intronic.	(Sanaker et al. 2010)
LPIN1/ phosphatidic acid phosphatase 1	Acute recurrent myoglobinuria	268200	AR	Common cause of recurrent RM. Onset is before six, episodes are triggered by infection, not exercise.	(Zeharia et al. 2008)
SIL1/ nucleotide exchange factor SIL1	Marinesco-Sjogren syndrome	248800	AR	A multisystem disorder with symptoms including cataracts, cerebellar atrophy, ataxia, hypotonia, development delay, weakness, peripheral neuropathy. RM is rare and triggered by infection.	(Lagier-Tourenne et al. 2003)
CAV3/ caveolin-3	Rippling muscle disease	606072	AD/AR	Allelic with LGMD1C. Rippling muscles with myalgia, weakness and exercise-induced cramps and stiffness. One case reported with myoglobinuria.	(Aboumoussa et al. 2008), (Torbergson 1975)
TSFM/ elongation factor Ts, mitochondrial	Combined oxidative phosphorylation deficiency 3	610505	AR	A severe mitochondrial disease. Symptoms include hypotonia, weakness, severe lactic acidosis, RM, often premature death.	(Smeitink et al. 2006)

Table 1.11 – ‘Miscellaneous’ rhabdomyolysis genes

3.5. Common Polymorphisms

The genes discussed above all assume a Mendelian inheritance pattern for genetically-caused RM episodes or exercise intolerance. However, there is a large body of evidence to suggest that some common polymorphisms could increase a person's susceptibility for getting the condition, or at least an increased CK level, and so are classed as genetic risk factors. For some of the polymorphisms there are differing reports, making it unclear as to whether or not there is an association. The polymorphisms and surrounding literature are detailed in Table 1.12.

Gene	Exercise related symptoms	Rs# (dbSNP)	Amino acid change	Reference
<i>ACE</i>	Dose dependent increased CK levels following exercise	rs4340	None – intronic deletion/ insertion	(Yamin et al. 2007)
	No association	rs4340	None – intronic deletion/ insertion	(Heled et al. 2007)
	No association	rs4340	None – intronic deletion/ insertion	(Deuster et al. 2013)
<i>ACTN3</i>	Exertion RM	rs1815739	p.Arg577*	(Deuster et al. 2013)
	Lower baseline CK	rs1815739	p.Arg577*	(Clarkson et al. 2005)
<i>CCL2</i>	Exercise-induced skeletal muscle damage	rs3917878, rs13900, rs1024611, rs1860189	None – all in either 5' or 3' UTR	(Hubal et al. 2010)
<i>CCR2</i>	Exercise-induced skeletal muscle damage	rs3918358, rs768539, rs1799865,	None, either in 5' UTR or synonymous	(Hubal et al. 2010)
<i>CKM</i>	Exertion RM	rs1803285	None – in 3' UTR	(Deuster et al. 2013)
	Increased CK following exertion	rs1803285	None – in 3' UTR	(Heled et al. 2007)
<i>IGF-2</i>	Muscle damage following extreme exercise	rs3213221, rs680, rs7924316, rs2132570	None – in promoter, intron, 3'UTR or 3' downstream	(Devaney et al. 2007)
<i>IL6</i>	Dose dependent increased CK levels following exercise	rs13447445	None – in promoter region	(Yamin et al. 2008)
	No association	rs13447445	None – in promoter region	(Deuster et al. 2013)
<i>MYLK</i>	No association	rs2700352	None – in 5'UTR	(Deuster et al. 2013)
	Muscle damage following extreme exercise	rs2700352, rs28497577	None - in 5'UTR p.Pro21His	(Clarkson et al. 2005)

	Exertion RM	rs28497577	p.Pro21His	(Deuster et al. 2013)
<i>TNF</i>	Increased CK levels following extreme exercise	rs361525	None – in promoter region	(Yamin et al. 2008)

Table 1.12 – Common polymorphisms that have been reported be associated with raised CK or rhabdomyolysis. Adapted from (Scalco et al. 2015)

4. Mutation Detection

4.1. Methods of Mutation Detection

Within both the channelopathies and RM there are numerous patients without a genetic diagnosis. However, mutation detection is imperative for patients with genetic diseases, as it can inform treatment and improve understanding of the disease etiology. There are several methods employed when undertaking the finding of a patient's causative mutation which are explained below. The method chosen depends on the phenotype of the patient, the family history, the budget of the project and the technology available.

4.1.1. Sanger Sequencing

Traditionally, when determining the sequence of DNA, the Sanger sequencing method is used, invented by Frederick Sanger in 1977 (Sanger et al. 1977). This involves the combination of normal deoxynucleotidetriphosphates (dNTPS) with those that are modified and unable to be extended upon (ddNTPS). Therefore, as the DNA polymerase moves along the template, it will either add a dNTP, in which case the sequence can be elongated, or a ddNTP and the sequence will be terminated. This combination produces fragments of different sizes, which can be resolved on a gel or, more recently, by capillary electrophoresis. By comparing the resultant sequence to a reference, or to other samples of the same sequence, mutations can be identified.

Sanger sequencing is considered the gold standard in sequencing methods, and is still widely used in mutation detection. However, it has limitations; samples are processed individually, and usually each exon is amplified and examined separately. Therefore it is a lengthy and labour-intensive process. Furthermore, only single nucleotide polymorphisms (SNPs) and small-scale insertions and deletions will be identified by Sanger sequencing. Lastly, it is a candidate gene approach, and thus only genes which have been considered likely to harbour a mutation are investigated, leaving little scope for unexpected findings.

4.1.2. Linkage Analysis

Genetic linkage was first discovered in 1904 by William Bateson (William Bateson 1904). It is the principle that the closer two genes are on a chromosome, the more likely they are to be co-inherited and so they are 'linked'. Used in mutation detection for Mendelian diseases, it assumes that within a pedigree, the area of DNA that contains the disease-causing mutation will segregate so that affected members possess the

area and unaffected do not. Markers consisting of common polymorphisms are genotyped for family members and a marker that is linked to the mutation will therefore co-segregate with the mutation. A statistical test known as a LOD (logarithm of odds) test is used to determine if the mutation is likely to be linked to a given marker (Morton 1955). The more family members used and the more recombination events presents (i.e. the family members are more distantly related), the more powerful the linkage analysis is.

Linkage analysis has been a highly successful tool, and assisted in the mapping of more than 1000 monogenic diseases in the 20th century (Peltonen and McKusick 2001). It also has the benefit that, unlike candidate gene approaches, it is not biased by expected results. However it has restrictions. It relies on a large pedigree and family members with clear affected/ unaffected status. Therefore it is only useful for diseases with fairly early onset, which do not reduce reproductivity, and which are fully penetrant. Furthermore, investigating complex non-Mendelian diseases with linkage analysis is challenging. Lastly, a typical analysis with 400 markers will produce a linkage area of about 10 – 20 million bases, covering several hundred genes, and so more analysis will be needed to determine the disease mutation.

4.1.3. Genome-Wide Association Studies

As discussed, linkage analysis is much less helpful when determining the causes of complex diseases, such as schizophrenia and diabetes, as they are polygenic, influenced by environmental factors, and single mutations have less of a consequence. In 1996 it was suggested that association studies are more useful for investigating these conditions (Risch and Merikangas 1996), in which the probability of having a polymorphism by chance is compared with the frequency of that polymorphism in patients. Associations in complex diseases are often investigated using GWAS. Typically, in a GWAS, more than 100,000 SNP markers are genotyped in a large cohort of patients with a disease, as well as in a size-matched group of unaffected people. The frequency of each SNP in the affected population is compared to the frequency in the control population to determine if any are significantly higher amongst the patients. The first GWAS that successfully identified disease loci was a 2005 study into age-related macular degeneration with a cohort of 96 patients (Klein et al. 2005). Since then, hundreds more have been published, with a trend of increasing cohort size and SNP number, up to a study of 200,000 cases of high blood pressure and 2.5 million SNPs (Ehret GB 2011).

GWAS have been very powerful. Again, they do not employ a candidate gene strategy and so produce unbiased results. Many of the findings have been intergenic or intronic, possibly influencing gene expression, and would have been missed by other methods. Furthermore, they allow investigation into diseases that would have been difficult previously. However, as always, the method has limitations. False positive and false negative results are relatively common. The more stringent the analysis, the more likely to eliminate the false positive results, but also the more likely to exclude real results and so create false negatives. Additionally, sample size can be an issue; large cohorts can be required to get results but are not always achievable. Lastly, they do not take into account environmental factors, which can often be important in these diseases (Pearson and Manolio 2008).

4.1.4. MLPA and CGH Array

Genetic disease is often thought of as being caused by small genomic changes that affect a single base or a few bases. However, it can also be caused by larger deletions or duplications, known as copy number variations (CNVs) which can range from a single exon, to a whole gene, to many genes. These changes are not identified by Sanger sequencing and so can be overlooked without additional detection methods such as MLPA and CGH arrays.

Multiplex ligand-dependent probe amplification (MLPA) is a PCR-based method, first developed in 2002 (Schouten et al. 2002). Two oligonucleotides are designed to bind to adjacent sites on genomic region of interest. One contains a forward primer binding site, and the other a reverse primer binding site. Only when both oligonucleotides bind to the DNA, and ligation between them occurs, is the probe a complete PCR template and can be amplified. Therefore, MLPA measures the presence or absence of a small fragment of DNA. If probes are designed for every exon in a gene, single exon deletions or duplications can be identified; and, by comparing to a reference, dosage can be determined (i.e. if someone has one, two or three copies.) Furthermore, the probes can be designed to be specific sizes, and then resolved by size of the amplified region (amplicon), meaning that many reactions can take place simultaneously. Depending on the location and number of probes used, MLPA can have further applications such as detecting trisomy or SNPs (Schouten et al. 2002). However, it is a candidate gene approach, as it would be impossible to use MLPA for detecting CNVs over the whole genome.

Comparative genomic hybridisation (CGH) is an alternative method used for detecting CNVs. First developed in 1992 (Kallioniemi et al. 1992), it involves the

fluorescent labelling of genomic DNA, using different coloured fluorophores for the sample and for a reference. These were originally hybridised to metaphase chromosomes, and the fluorescence signals were measured and compared to determine if the sample signal is increased or decreased relative to the reference, identifying a duplication or deletion respectively. In 1997, the method was improved such that the fluorescent DNA was hybridised to a chip instead of chromosomes (Solinas-Toldo et al. 1997), giving higher resolution. The chip contains a matrix consisting of genomic probes, and thus CNVs over the whole genome can be detected. Alternatively, custom targeted chips can be designed for specific areas of interest. Despite improvement, the resolution is still limited to about 1Kbp, and so CGH array technology is not suitable for detecting single exon changes (Evangelidou et al. 2013). However it can give a good estimate of the size of the CNV, which MLPA cannot unless the change is small or many probes are used.

Both MLPA and CGH arrays are useful tools for identifying CNVs, and they both have benefits and disadvantages that make them suitable for different purposes.

4.1.5. Next-Generation Sequencing

Sanger sequencing, known as 'first-generation sequencing', while still used widely, is slow and inefficient for large-scale sequencing projects. In 1990, the human genome project began, in which the whole human genome was sequenced, and this massive venture encouraged the development of faster, automated sequencing methods, consequently the majority of the thirteen-year project was completed in the final two years (Marziali and Akeson 2001), (Human Genome Sequencing 2004). Subsequently, there was a shift to develop new sequencing technologies that move away from Sanger sequencing, these are called 'next-generation sequencing' (NGS) technologies. They aim to provide fast, low-cost, high-throughput sequencing which provide large volumes of genetic data quickly (Jarvie 2005). Additionally, incorporation of identifiable index sequences to samples enables multiplexing and thus many samples can be combined and sequenced simultaneously. In the last ten years this field has progressed enormously, and presently there are several different types of chemistry and sequencing platforms, which are summarised in Table 1.13.

The next-generation sequencing performed this thesis will utilise the Illumina sequencing chemistry, and consequently this method will be explained in further detail and used as a general example of the principles of NGS. There are four steps to this process, shown in Figure 1.10.

1. Library Preparation – In any NGS process, the first step is to fragment the DNA. Illumina do this using an enzymatic approach, and with their tagmentation technology, also simultaneously add adapter sequences to each end of the sheared DNA. Next further motifs are added; unique indexes for multiplexing, sequencing primer binding sites and sequences which bind to the flow cell oligonucleotides. If only a subset of the genome is being sequenced (for example whole-exome sequencing or panel sequencing – discussed in sections 4.1.5.1, and 4.1.5.2), probes are then used to enrich for the regions of interest, known as ‘capturing’ (Head et al. 2014). The libraries are qualitatively assessed and the concentrations are quantified.

2. Cluster Generation – The library is loaded to a flow cell for cluster generation. The surface of the flow cell contains two types of oligonucleotides which are complementary to the adapter sequence. First, one of the adapters binds to the flow cell, and DNA polymerase creates a reverse complement copy. The original fragment is washed away, and the unattached end of the reverse strand binds to the other type of oligonucleotide on the flow cell surface to create a bridge. DNA polymerase creates another copy by isothermal amplification, one end detaches, and the steps repeated many times to create a cluster of identical copies of the original DNA fragment, in a process called clonal amplification (Buermans and den Dunnen 2014). The copies detach at one end and reverse strands are washed away to leave single stranded forward copies to be sequenced.

3. Sequencing by Synthesis – The primers sites are extended against the forward template, one base at a time. Each of the four bases has a different fluorescent signal, and after every addition a light source excites the most recently added base. The flow cell is imaged, and so the colour of the signal is recorded. In this way, the sequence is determined as it is built up, and so the process is called sequence by synthesis. All of the strands in each cluster, and the clusters on the flow cell, are added to and imaged simultaneously. Once the template strand has been sequenced, the read product is washed away and the index is sequenced in the same way. The template strand’s unattached end then again binds to the free oligonucleotide on the flow cell to create a bridge. The second index is read.

4. Sequencing the Reverse Strand – DNA polymerase creates another reverse complement copy of the forward template, and again the strands detach, but this time the forward copies are cleaved and washed away. The reverse strand is sequenced by the same method as previously. This is paired-end sequencing

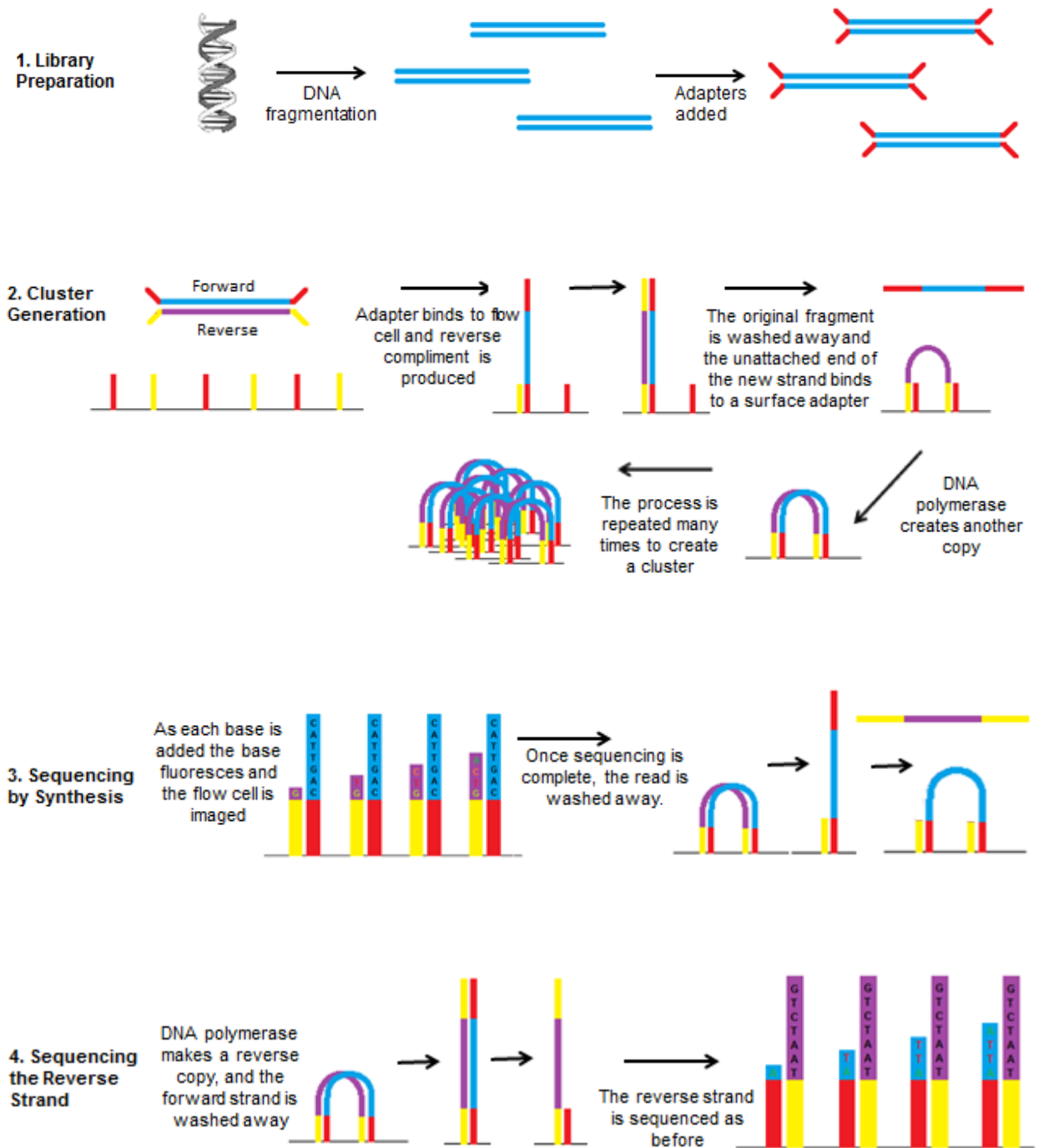


Figure 1.10 – The steps in the sequencing process used by Illumina NGS chemistry. The steps are described in detail in section 4.1.5.

Once the sequence has been determined, it must be processed computationally. How this is done depends on the application of the sequencing, but in the case of variant determination, a bioinformatic pipeline will align the sequences to a reference genome, identify the variants and annotate them with positional information.

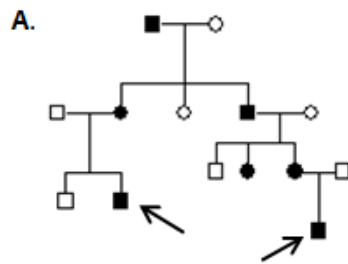
NGS has revolutionised the way that genetic studies are carried out. There are many applications that are beyond the scope of this thesis, for example RNA sequencing, ChIP-seq and de novo genome assembly. Only applications relevant to mutation detection will be discussed here.

4.1.5.1. Whole-Exome Sequencing and Whole-Genome Sequencing

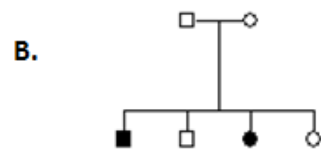
Whole-exome sequencing and whole-genome sequencing (WES and WGS respectively) are useful tools for finding causative mutations. As the name suggests, in WGS, a person's entire DNA is sequenced. This sequence is then compared to a reference genome to determine what variations they have; if they have a genetic disease, one of these variants may be causing it. The exome (protein-coding portion of the genome), however, accounts for less than 2% of the genome, yet harbours about 85% of known disease mutations (Choi et al. 2009), therefore it is often more efficient and cost effective to only sequence the exome. This is carried out by targeted enrichment of exonic regions. Since the process was first performed in 2009 (Ng et al. 2009), more than 150 disease genes have been found using the technology (Rabbani et al. 2014). WES also provides data that is easier to interpret because the sequences usually have higher conservation. Furthermore, it is simpler to try and predict the effect of the change. Despite this, a person's exome will still harbour roughly 23,000 variations, and so discovering the true pathogenic mutation is difficult unless an already known mutation is found. Variants can be filtered by the structural effect they have, their frequency in the population and the gene function, but this will still leave many candidates. Therefore, like linkage analysis, multiple family members are usually required for successful mutation discovery by segregation analysis. An effective strategy is triome analysis, where an affected child has unaffected parents. This circumstance suggests either a de novo, compound heterozygous or homozygous mutation and so there will be fewer candidates. Another successful method is to combine linkage and WES data to reduce the candidate genes. Strategies for gene discovery using WES are shown in Figure 1.11. Determining the pathogenicity of variation is discussed further in section 4.2

Company	Platform	Sequencing method	Detection method	Reads/run	Output /run
Roche	GS FLX Titanium XL+	Synthesis, single end	Pyrophosphate detection	1 Million	700Mb
	GS Junior system	Synthesis, single end	Pyrophosphate detection	0.1 Million	40Mb
Life Technologies	Ion torrent	Synthesis, single end	Proton release	4 Million	1.5 – 2Gb
	Proton	Synthesis, single end	Proton release	60 - 80 Million	8 – 10Gb
	Abi/solid	Ligation, single and paired end	Fluorescence detection of di-base probes	2.7 Billion	300Gb
Illumina/ Solexa	Hiseq 2000/2500	Synthesis, single and paired end	Fluorescence: reversible terminators	3 Billion	600Gb
	Miseq	Synthesis, single and paired end	Fluorescence: reversible terminators	25 Million	15Gb
Pacific Biosciences	RSII	Single molecule synthesis, single end	Fluorescence: terminally phospholinked	0.8Million	5Gb
Helicos	Heliscope	Single molecule synthesis, single end	Fluorescence: virtual terminator	500 Million	15Gb

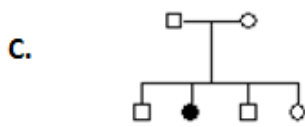
Table 1.13 – Details of different next-generation sequencing platforms. Adapted from (Buermans and den Dunnen 2014)



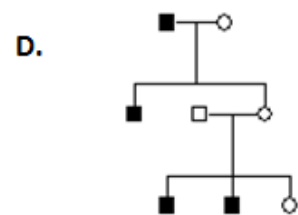
Large Autosomal Dominant Pedigree – Either use multiple family members for segregation, or distantly related affected members (the two shown by the arrows will only share 6.25% of DNA)



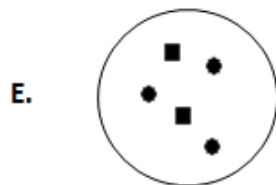
Recessive Pedigree – If two or more affected children and unaffected parents, can filter for only homozygous or compound heterozygous (especially if non-consanguineous)



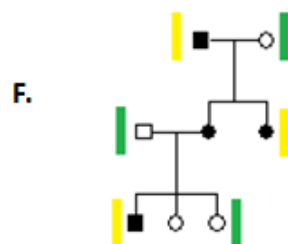
Likely De Novo – If one child is affected, and disease is usually caused by dominant mutations, heterozygous variants only in the child can be filtered for. If this is unsuccessful it could be recessive



X-Linked – If only males are affected and females are carriers it is likely to be X-linked, in which case only X chromosome variants need to be considered



Cohort of Similar Patients – Singletons are usually difficult to interpret, but if there is a cohort of patients with similar phenotypic features, a shared gene can be looked for



Using Linkage Analysis – If linkage has been performed to leave a small genomic area, genes not in the linkage region can be filtered out

Figure 1.11 – Examples of six different WES mutation detection strategies.

Despite the obvious advantages of speed, thoroughness and the potential for new discoveries WES and WGS have some disadvantages. They are expensive, although costs are constantly falling. They can also have some coverage gaps which can lead to false negatives and they can occasionally produce false positives, especially in areas of lower coverage, and so all findings must be confirmed using Sanger sequencing (Rehm 2013). Furthermore they require bioinformatic expertise to process the data and render it accessible for the average scientist. Finally, they do not easily identify CNVs, however, some complex software is beginning to make that possible.

4.1.5.2. Targeted Gene Panels

Despite being cheaper than WGS, WES is still expensive, and thus the next step is targeted gene panels. Here, only specific genes are sequenced. These are often disease-specific, and so only genes known to be relevant to a certain condition are investigated. There is a different emphasis when using these panels compared to WES; instead of gene discovery they are more useful for genetic diagnosis in known genes. Disease-specific sequencing panels are particularly useful for diseases with genetic heterogeneity, when it is not clear from the phenotype which gene may be responsible. Panels can be custom-designed, such as Illumina's Truseq Custom Amplicon (TSCA) technology. TSCA does not use standard Illumina sequencing chemistry; instead target regions are amplified using a PCR-based method. Alternatively pre-designed, off the shelf products can be used (Balabanski et al. 2014), (LaDuca et al. 2014) such as the Illumina TruSight One. Here, targets are again enriched and thus the product is essentially a reduced exome.

4.1.5.3. Association Studies

As discussed above (section 4.1.3.), complex, non-Mendelian genetic disease can be caused by polymorphisms, and so GWAS have traditionally been used to analyse these diseases. However, NGS can also be used for this purpose; it has the added benefit of not being limited to the SNPs chosen for the study. With large enough cohorts, polymorphisms that are too rare to be included in GWAS can be analysed. In recent years, several studies utilising this methodology have been published (Panoutsopoulou et al. 2013). Furthermore, NGS comparison studies can be used to investigate less complex diseases which are still difficult to assess using segregation studies. An example of this is familial amyotrophic lateral sclerosis (FALS); due to the late-onset nature of the disease, segregation studies are often impossible. A recent study performed WES on 363 FALS probands and looked for genes with a significantly

higher rate of rare variations than seen in control databases (burden analysis). This technique identified a new potential gene for FALS (Smith et al. 2014). However, this method requires large numbers of patients to undergo NGS, and thus is expensive.

4.2. Determining Pathogenicity

Every human genome has roughly 23,000 exonic variants, and the majority will have no functional impact. Many will be synonymous (not cause an amino acid change), and if they are not at a potential splice site can be assumed to be benign. Determining pathogenicity of unknown non-synonymous variants of unknown significance, however, has always been a challenge, and the introduction of WES and WGS has made it even more so. For Mendelian diseases, segregation in large families will always be the most convincing tool for proving pathogenicity, but in the absence of family members, there are other methods that are used.

4.2.1. Splice Site Prediction

Splice sites are the areas of the gene which govern how the gene will be spliced, i.e. the non-coding intronic parts removed to only leave the protein-coding exons. Mutations which disrupt splices can cause introns to be retained and exons to be missed (skipped), both of which will have a structural effect on the protein. Additionally, mutations can introduce new aberrant splice sites, which could again affect protein structure. Predicating if a variation will affect or cause a splice site is therefore an important step in determining its pathogenicity.

Within an intron, the particular areas of importance for splicing are the donor site (a region at the immediate 5' end invariably starting with GU) and the acceptor site (a region at the 3' end usually ending with AG). In addition, the polypyrimidine tract (rich in Us and Cs, upstream of the acceptor site) and the branch point (further upstream) are also important (Black 2003). It follows those variations in these regions, especially the GU and AG, can be pathogenic. There several are bioinformatic tools which can assess variations around these regions for pathogenicity. These include the Human Splicing Finder (Desmet et al. 2009) (<http://www.umd.be/HSF3/>), Spliceman (Lim et al. 2011) (<http://fairbrother.biomed.brown.edu/spliceman/>) and Spliceport (Dogan et al. 2007) (<http://spliceport.cbcb.umd.edu/>) which all use different algorithms based on sequence motifs, positional data and conservation to predict pathogenicity. As with all prediction tools, they can be useful but should be treated with caution as

they are not always correct. Analysis of a patient's RNA is the only accurate way to determine how a splice site is affected.

4.2.2. Bioinformatic Tools

Bioinformaticians have developed software that predicts the pathogenicity of amino acid substitutions. The two most commonly used of these are SIFT and PolyPhen-2. SIFT will find homologous sequences for a query, and using multiple alignments of the sequences, predict which substitutions at which positions are likely to be not tolerated (Ng and Henikoff 2001). This program therefore assumes that homologous sequences are likely to share functions. PolyPhen-2 also uses multiple sequence alignment of homologous sequences, but additionally uses structural information and conservation scores (Adzhubei et al. 2010). Other less-used programs include SuSPect (Yates et al. 2014) and MutationT@ster (Schwarz et al. 2014). While all of these tools can be useful for giving an idea of pathogenicity, there is plenty of anecdotal evidence of their unreliability. Therefore, many people now choose not to use them at all, and if they are used they should be done so with caution.

4.2.3. Population Frequency Databases

A useful method for investigating pathogenicity is by determining a variation's frequency in the general population. Public databases are available containing WES variation data, and so when a change is found it is useful to look it up in these databases. The two that are most used are the 1000genomes (roughly 2,500 genomes from Asia, Europe, Africa and America) (Altshuler et al. 2010), and the exome variant server (EVS – 6,500 exomes of American cardiac patients, divided into African or European ancestry (<http://evs.gs.washington.edu/EVS>)). Recently, the ExAC (Exome aggregation consortium) browser, containing WES data from over 60,000 unrelated individuals sequenced as part of various disease-specific and population genetic studies has become publically available (<http://exac.broadinstitute.org/>), and is another useful resource. These websites can provide invaluable insights into the potential pathogenicity of a variant of unknown consequence but, again, should be used with caution; if a variant is present it will not necessarily mean it could not be pathogenic. They should be treated as a representation of population genetic variation, and not as a list of benign variants. However, they are useful for filtering out common SNPs; when looking for a dominant mutation, a user can be relatively certain that anything present in more than one percent of the population will not be causative.

4.2.4. Functional Investigations

Often, the only way to be sure of the effect of a genomic variation is through functional studies, where the consequences of the mutation are investigated in a biological model, either *in vitro* (for example in cell lines) or *in vivo* (for example in an animal model such as mice or flies).

The simplest *in vitro* model is pre-existing cell lines. A mutation can be introduced by the transfection of a vector containing the gene of interest, harbouring the mutation. The cell will then translate this gene into the altered protein, and experiments such as western blots can determine the effects on the cell. This is known as an overexpression study. It is the easiest way to investigate a mutation, but is often criticised due to lack of biological relevance, i.e. it is not simulating the true conditions (Prelich 2012).

A more relevant model is patient-derived cells, such as fibroblasts. These will harbour the mutation already; therefore the endogenous protein will have the altered structure. These cell lines will provide a more accurate picture of the functional consequence of the mutation, although, as they are derived from skin cells they are often not the correct cell type for the disease. Induced pluripotent stem cells (iPSCs), created from fibroblasts, can be reprogrammed to become other, more applicable, cell types, so in the case of neurological disease, they can become neurones. This provides an even more biologically relevant model with which to study the mutation. Furthermore, they have the advantage of harbouring the genetic profile of the patient they were taken from and so accurately representing how the protein of interest will interact within the cell (Okano and Yamanaka 2014). However, generating iPSC-derived neurones is highly time consuming, taking months, and so not practical for testing all variations.

Animal models can be useful for studying particular genes through the development, for example, of transgenic mice. These either have additional genes, which may harbour a mutation, and overexpress the altered protein of interest (Gordon et al. 1980), or alternatively, edit an existing gene to knock it out or introduce a mutation (Thomas and Capecchi 1987). However, this is again a lengthy and expensive technique and so not realistic for investigating genetic variants.

5. Thesis Aims

The overall aim of this work is to improve the genetic diagnosis for patients with diseases caused by ion channel, or ion channel related protein dysfunction; both through identifying new genetic causes, as well as investigating new methods for genetic diagnosis. This task will be presented in the results chapters under four aims:

Chapter Three – To investigate the frequency of PxD gene mutations in a large paroxysmal dyskinesia series, as well as a smaller mixed episodic cohort. This will ascertain the degree of phenotypic and genetic overlap amongst these diseases, and help inform future genetic diagnosis protocols in these patients. Additionally, it may improve the limited understanding of the etiology of these diseases.

Chapter Four – To trial the use of custom next-generation sequencing panels as an alternative for Sanger sequencing in the genetic diagnosis of the classic channelopathies. This will establish the benefits and pitfalls of this new technology with a view to translation into a diagnostic laboratory setting.

Chapter Five – To utilise two different panel sequencing technologies to investigate the more genetically complex conditions episodic rhabdomyolysis and exercise intolerance. Through this, the prevalence of ion channel dysfunction as a cause for these conditions will be determined. It will allow comparison and assessment of the technologies for this purpose, and exploration of the genetic underpinnings of the diseases.

Chapter Six – To use whole-exome sequencing to attempt to uncover the genetic basis of two undiagnosed families with channelopathy or related neuromuscular diseases, and thus establish the benefit of WES as a method for genetically diagnosing complex channelopathy patients.

Chapter 2: Materials and Methods

1. Patients

Patients and unaffected family members were recruited through the Neurogenetics Laboratory and from collaborators of Professors Mike Hanna, Ros Quinlivan and Henry Houlden with patient consent for analysis and ethical approval (NHNN studies 06/N076 and 07/Q0512/26).

2. PCR and Sanger Sequencing

The following method was used as standard for all Sanger sequencing.

2.1. PCR and Product Purification

DNA was previously extracted by the standard phenol chloroform method from blood at the National Hospital of Neurology and Neurosurgery. It was measured for concentration and quality using a nanodrop spectrophotometer and the concentration was adjusted to 50ng/μl where possible, using autoclaved nanopure water. Exons were amplified using primers that were designed using Primer3 software (Rozen and Skaletsky 2000). The components of each reaction were as follows; 10μl of autoclaved nanopure water, 12.5μl of Roche PCR MasterMix (Roche), 0.75μl of forward primer (10ng/μl), 0.75μl of reverse primer (10ng/μl) and 1μl of DNA (50ng/μl). The PCR conditions were as follows (unless stated otherwise);

95°C for 15 minutes

35 cycles of: 95° for 30 seconds

60°C for 30 seconds (-0.4°C per cycle)

72°C for 45 seconds

72°C for 10 minutes

Hold at 4°C

The PCR products were run on a 1% agarose gel (5µl of PCR product and 3µl of loading dye) at 60V with for 20 minutes to confirm that the PCR was successful and that no contamination occurred. The size of the fragment was confirmed using a 1kb ladder.

Before February 2013, the PCR products were purified using a filter plate (Millipore) by adding 80µl of autoclaved nanopure water, putting onto a vacuum for five minutes, repeating, and then resuspending in 50µl of autoclaved nanopure water by shaking for 30 minutes. After February 2013, the Millipore filter plates were deemed unsuitable due to contamination potential. Instead, Exosap was used. 1ml Exosap aliquots were made (50µl Exo1, 200µl Fast-AP (both Life Technologies), 750µl autoclaved nanopure water) and stored at -20°C. 5µl of PCR product was combined with 2µl of Exosap and placed on a PCR machine programmed as follows:

37°C for 30 minutes

80°C for 15 minutes

Hold at 4°C

The clean PCR products were stored at 4°C if to be used within three days or -20°C otherwise.

2.2. Sequencing Reaction

The PCR products were sequenced using BigDye chemistry (Applied Biosystems) with reverse and forward primers (unless stated otherwise). The components of each sequencing reaction were; 2.7µl autoclaved nanopure water, 2µl 5x terminator buffer, 1µ primer (3.2ng/µl), 0.5µl Big Dye v3.1, and 3.8µl clean PCR product. They were put onto a PCR machine set as follows:

25 cycles of: 96°C for 10 seconds

50°C for 5 seconds

60°C for 4 minutes

Hold at 4°C

As with PCR, before February 2013 the sequencing products were purified using a filter plate (Millipore), with the same method. Subsequently, sephadex plates were used instead. Sephadex plates were prepared as follows: per plate, 40ml autoclaved distilled

water was added to 2.9g Sephadex G-50 (Sigma) and mixed thoroughly by vigorous shaking. The mixture was left to hydrate for at least 30 minutes and, when ready, 350µl was added to each well of a Corning FiltrEX 96 well filter plates (Sigma). Each plate was then spun at 700xg for 3 minutes on top of an empty collection plate to finish plate preparation. All 10µl of the sequencing reactions were added and the plate was spun for 5 minutes at 910xg on top of a clean, labelled PCR plate to collect the purified products. They were then run on an ABI3730XL (Applied Biosystems) sequencer immediately, or else frozen until use.

The sequencing data was analysed using SeqScape v2.5 software (Applied Biosystems). Where a possible pathogenic mutation was found, the PCR and sequencing of the appropriate exon were repeated in both the forward and reverse directions in the sample in question. Samples that had poor quality sequencing or areas that were missed were repeated.

2.3. Mutation Nomenclature

The variations discussed in this thesis are named based on published cDNA sequences, using standard nomenclature from the Human Genome Variation Society (Dunnen and Antonarakis 2000) (<http://www.hgvs.org/mutnomen/>). Variations mentioned in the text for the first time in a chapter are written with respect to both the nucleotide change and amino acid change (denoted by c. and p. respectively), and afterwards only the amino acid change is used. Variations in tables and figures are written in the protein from unless otherwise specified.

3. Functional Studies – HEK293 Cells and Fibroblasts

3.1. Vector Transformation and Amplification

Vectors were received on filter paper and cut out using a sterile blade. They were removed from the paper by adding 50µl of nanopure water, leaving for 10 minutes and then centrifuging for one minute at 12,000 rpm. The quality and concentration were determined using a nanodrop spectrophotometer.

Each vector was then transformed into competent *E.Coli* bacteria. 10ng of vector was put into a round-bottomed tube with 25µl of bacteria cells, and the mixture was incubated for 30 minutes on ice. It was heat-shocked at 42°C for 35 seconds using

a water bath, and then moved back to the ice for a further two minutes. 200µl of fresh LB was then added, and the cells were then put into a 37°C incubator for one hour, with shaking. 100µl of the bacteria was then plated onto ampicillin–agar plates and incubated at 37°C overnight.

The next day 4ml of LB with 1/1000 ampicillin in a round-bottomed tube was inoculated with a single colony from the plate and grown at 37°C overnight with shaking. The plasmid was then extracted from the bacteria using a GenElute MiniPrep Kit and protocol (Sigma) and the concentration was determined using a nanodrop spectrophotometer. It was frozen until further use.

3.2. Mutagenesis

Mutagenesis primers were designed using QuikChange Primer Design Program (Agilent Technologies). Site-directed mutagenesis was carried out on 10ng of DNA with QuikChange II XL Site-Directed Mutagenesis Kit and protocol (Agilent Technologies). The resulting vector was then digested with *Dnp1* for one hour and then transformed, amplified and extracted using the same method as above. The vector was subsequently sequenced by the UCL sequencing facility to confirm that correct mutagenesis had taken place, and stored at -20°C until further use.

3.3. Transfection of Vector into HEK293 Cells and Cell Harvesting

HEK293 cells were thawed and grown in Dulbecco's Modified Eagle Medium (Gibco) in a T75 flask. 2.5×10^5 cells were pipetted into each well of 6-well plate and incubated at 37°C to grow overnight (about 18 hours). The next day the cells were transfected using the Effectene Reagent and protocol (Qiagen). The cells were incubated at 37° for 24 hours. After that time, transfection was confirmed by the presence of green GFP-tagged cells under a UV light.

The cells were then harvested. The plate was placed on ice, the media removed and 1ml of PBS added and removed. 70µl of lysis buffer (1ml = 50µl of 1M Tris (pH7.4), 1µl of 100mM EGTA (pH 7.4), 2µl 50mM EDTA (pH 7.4), 10µl Triton x100, 0.092g sucrose, 100µl protease inhibitor, 100µl phosphatase inhibitor, 1µl beta-mercaptoethanol, made up to 1ml with nanopure water) was added to the surface and the cells were scraped with a cell scraper for five minutes and frozen at -80°C for further cell lysis.

3.4. Western Blot

Protein levels in lysed cells were determined by western blot. The lysed cells were first spun at 13,200 rpm to separate the pellet and supernatant fractions of the cell. The supernatant was removed, and the overall protein concentration was determined by Bio-Rad DC Protein Assay and protocol (Bio-Rad). Samples were adjusted to 1mg/ml and made up 100µl with 25µl 4xSDS, 1µl 1M DTT and the necessary volume of lysis buffer. All samples were heated at 70°C.

10µl of each sample was loaded onto a 15-well 4-10% Bis-Tris Nupage gel (Life Technologies) and electrophoresed at 120V for 10 minutes and then at 180V for a further 90 minutes. The samples were then transferred onto a nitrocellulose membrane at 35V for two hours. They were then blocked with 5% milk for one hour at room and in incubated with the primary antibody overnight at 4°C (primary antibody details are given the relevant chapter).

The next day, the membranes were washed with PBS-Tween for 10 minutes three times, and then incubated with the secondary anti-rabbit antibody at a concentration of 1/5000 for one hour at room temperature. After three more washes with PBS-Tween, an ECL Chemiluminescence kit (Thermo-Scientific) was used to detect the antibody binding to the protein of interest, and developed onto X-ray film (Fujifilm).

The membrane was then washed again with PBS-Tween three times, and the same process was carried out to probe for actin as a control that the same amount of protein was loaded for each sample. This was done using a mouse actin primary (Sigma) antibody and an anti-mouse secondary antibody raised in goat (Santa Cruz).

3.5. RNA Extraction from Fibroblasts

Fibroblasts were taken with informed consent from affected patients and unaffected controls. Cells were grown in Dulbecco's Modified Eagle Medium (Gibco) in a T75 flask. 2.5×10^5 cells were pipetted into each well of 6-well plate and incubated at 37°C to grow overnight (about 18 hours) or until confluent. Media was aspirated and cells were harvested in 700µl Qiazol (Qiagen) by scraping. RNA was extracted in a fume hood using an miRNA kit (Qiagen) and following the kit protocol. RNA was eluted in 30µl RNase-free water and stored at -80°C.

3.6. Reverse Transcription and cDNA Sequencing

cDNA was synthesised from mRNA with SuperScript II reverse transcriptase (Life Technologies) according to the manufacturer's protocol, 1000ng of mRNA was used as template with random oligonucleotide primers. cDNA was stored at -20°C until used.

One microliter of the resulting cDNA product was then used as a template, and PCR and sequencing reactions were carried out as detailed in section 2.1 and 2.2 of the this chapter with primers designed to only amplify cDNA and not genomic DNA.

4. Next-Generation Sequencing

4.1. TruSeq Custom Amplicon

TruSeq Custom Amplicon (Illumina) technology was used for the brain channel panel, the skeletal muscle channel panel, and the first rhabdomyolysis panel. Oligonucleotides are designed against custom targets, and created by Illumina. The library design and cohort selection for the TSCA panels are discussed in chapters four and five. Possible pathogenic variations were confirmed used Sanger sequencing.

4.1.1. Library Preparation Protocol

The DNA concentration for each sample was determined using a Qubit fluorometer (Life Technologies) and plated out at 50ng/μl. The library was then prepared following the Illumina protocol in a number of steps as detailed below (a general outline of library preparation method is shown in Figure 2.1).

Hybridisation of oligonucleotide pool – 5μl of each sample was combined with 5μl of the custom amplicon oligonucleotide mixture. 40μl of hybridisation solution was added and the plate was placed on a heat block at 95°C and left to cool to 40°C, in which time the oligonucleotides hybridised to the DNA.

Removal of unbound oligonucleotides – The contents of the plate was transferred to a provided the filter plate, which was attached via a metal collar to a deep-well plate to make a filter plate assembly unit (FPU). The FPU was spun at 2,400g for two minutes at 20°C (all subsequent spins using the filter plate were under the same conditions). It was then washed with a 45μl of a stringent wash solution and spun, and this step was

repeated. 45µl of a universal buffer solution was then added and the FPU was spun again. This left just the oligos bound to DNA in the filter plate.

Extension-ligation of bound oligos – 45µl of extension-ligation mix was added to each well and the FPU was incubated for 45 minutes at 37°C.

PCR amplification – The FPU was first spun, and then 25µl of 50mM NaOH was added to each well and it was incubated at room temperature for five minutes. This eluted the oligonucleotides bound to DNA. The content of each well was then transferred from the FPU to a plate containing 22µl PCR Master Mix, as well as unique combination of i5 and i7 indices in each well (4µl of each). The PCR conditions were as follows:

95°C for 3 minutes

25 cycles of: 95°C for 30 seconds

62°C for 30 seconds

72°C for 60 seconds

72°C for 5 minutes

Hold at 10°C

Selected sample of the PCR products were run on a 4% agarose gel to ensure successful PCR. At this point the plate could be stored at 4°C for up to two days.

PCR clean-up – The PCR products were purified using AMPure XP beads (Beckman Coulter). 45µl was added and the mixture was transferred to a round-bottomed deep well plate. The plate was shaken at 1,800 rpm (all shaking took place at the same speed) for two minutes and then incubated at room temperature for 10 minutes, to allow the beads to bind to the PCR product. It was then placed on a magnetic stand so that the beads formed rings around the edges of the wells. When the supernatant had cleared it was removed. The beads were washed twice with 800µl of 80% ETOH, and then allowed to air dry for 10 minutes. The PCR products were eluted with 30µl of elution buffer by shaking at for two minutes, incubating at room temperature for two minutes and then putting onto the magnetic stand and transferring the cleared supernatant to a new round-bottomed deep well plate.

Library normalisation – The amount of PCR products for each sample was next normalised. To each well 45µl of normalisation beads were added. The plate was shaken for 30 minutes at 1800 rpm. It was then put onto the magnetic stand and the

cleared supernatant was removed. It was washed twice with 45µl of library normalisation wash, each time with five minutes of shaking at 1800 rpm. The beads were then eluted in 30µl of 0.1M NaOH by shaking for five minutes, put into the magnetic stand and the cleared supernatant being transferred to a new PCR plate. 30µl of library normalisation storage buffer was added to each well and the plate was frozen if not loaded immediately onto the MiSeq.

Library pooling and MiSeq sample loading – 5µl of each sample was combined into an Eppendorf tube and mixed thoroughly. 6µl of the resultant mixture was transferred to a new tube containing 594µl of hybridisation buffer, and the tube was heated to 96°C for two minutes and then put on ice for five minutes. It was finally then loaded into a thawed MiSeq reagent cartridge, put into the MiSeq to be run.

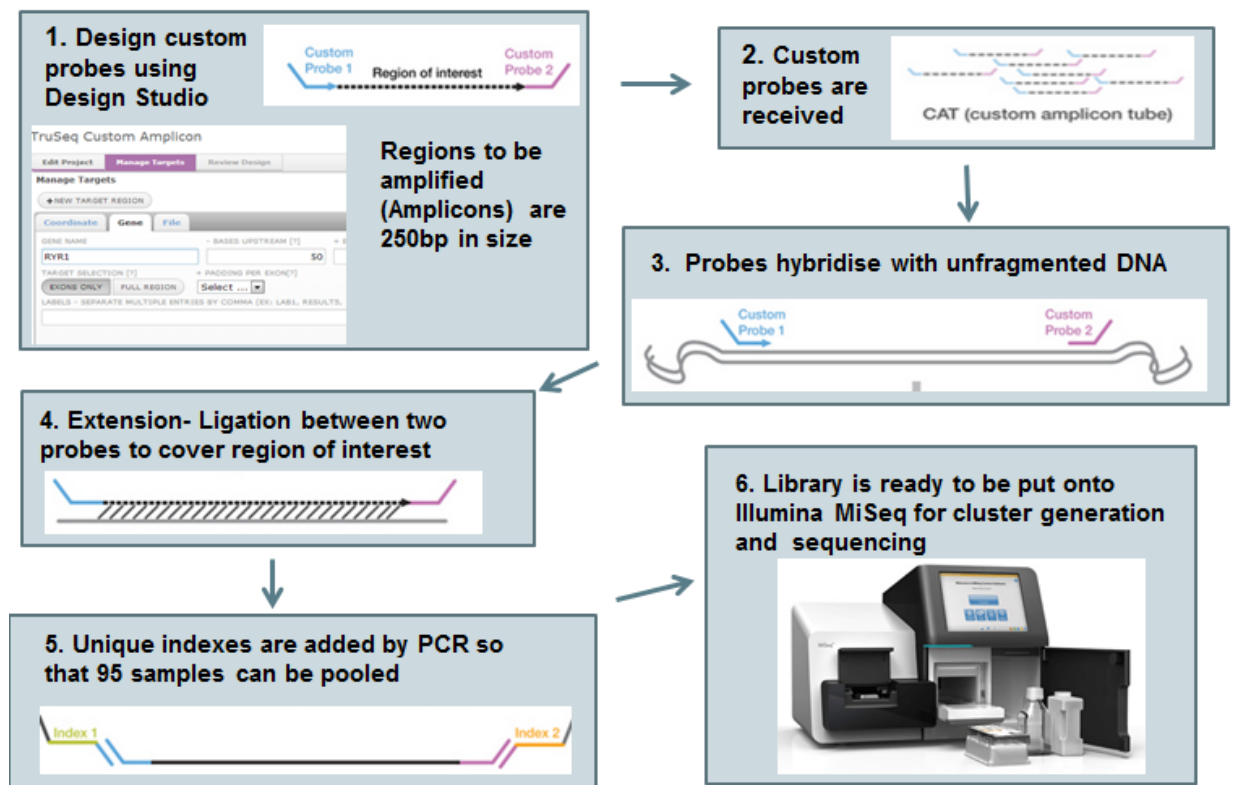


Figure 2.1 Overview of the TSCA library preparation process, adapted from the Illumina website (<http://www.illumina.com>)

4.2. TruSight One

TruSight One technology (Illumina) was used for the second, third and fourth rhabdomyolysis panels. These are standard, non-custom sequencing panels consisting

of 4813 genes with known clinical phenotypes. The genes included in these panels can be found at <http://www.illumina.com/products/trusight-one-sequencing-panel>.

4.2.1. Library preparation protocol

Sample Preparation – Sample requirement is 50ng of DNA at 5ng/μl. It is important that DNA concentration is accurate, so a two-step normalisation method was used; the concentration was quantified using the Qubit fluorometer (Life Technologies) diluted to 10ng/μl, quantified again and diluted to a final concentration of 5μl/ml. 72 samples (2 x 36 TruSight One kits) were prepared and run simultaneously.

Tagment DNA – to 50ng of DNA 25μl tagment DNA buffer, 5μl tagment DNA enzyme 1, and 10μl PCR-grade water was added. The plate was mixed and placed in a microheating system at 58°C for 10 minutes. 15μl of stop tagment buffer was added to each well; the plate was mixed and incubated at room temperature (RT) for 4 minutes.

Clean Up Tagmented DNA – 65μl of vortexed sample preparation beads was added to each well. The plate was sealed, shaken and incubated at RT for 8 minutes before being placed on a magnetic stand and the discarding of the cleared supernatant. With the plate on the magnet, the beads were washed twice with 200μl 80% ETOH, ensuring all residual ETOH was removed by air drying for 10 minutes. The beads were resuspended in 22.5μl resuspension buffer by shaking at 1800 rpm for 1 minute and placing back onto the magnet. The cleared eluate was removed into a new plate.

First PCR amplification – To each well of eluate, 5μl each of an i5 and an i7 index was added so that every sample within a group of 36 had a unique combination of indices. 20μl of nextera library amplification mix was added, and a PCR reaction took places with the following conditions:

72°C for 3 minutes

98°C for 30 seconds

10 cycles of: 98°C for 10 seconds

60°C for 30 seconds

72°C for 30 seconds

72°C for 5 minutes

Hold at 10°C

At this point the plate can be stored at 4°C for up to two days.

First PCR clean up – The PCR products were transferred into a deep-well plate, and 90µl of sample purification beads were added to each well, mixed, and incubated at RT for 10 minutes. After placing on the magnetic stand and removing the cleared supernatant, the beads were washed twice with 200µl ETOH and air dried. The beads were resuspended in 27.5µl resuspension buffer with 1 minute of shaking at 1800 rpm. On the magnet, the supernatant was removed and kept. The Qubit fluorometer (Life Technologies) was used to quantify the concentration of the libraries, and 500ng of each library in a row (12 in total – each with a unique i7 index) were pooled. If the volume of the pool exceeded 40µl, an Amicon Ultra-0.5 centrifugal filter unit (MerckMillipore) was used to reduce the volume. The quality of the libraries was assessed with a 2100 bioanalyzer (Agilent Technologies).

First hybridisation – 40µl of library pool was combined with 50µl of hybridisation buffer, and 10µl of TruSight One oligonucleotides and, after mixing, put onto a PCR machine for hybridisation with the following conditions:

95°C for 10 minutes

18 1 minute incubations, starting at 94°C, and then decreasing 2°C per incubation

Hold at 58°C (for at least 90 minutes, but not more than 24 hours. The plate must stay at 58°C until used)

First capture – After hybridisation, the plate contents were transferred to a deep well plate, and 250µl of well-mixed streptavidin magnetic beads were added and mixed by 5 minutes of shaking 1200 rpm. The plate was incubated for 25 minutes at RT, and then placed onto the magnetic stand. The cleared supernatant was discarded. The beads were washed twice by thorough resuspension in enrichment wash solution, incubation at 50°C for 30 minutes, immediate placement onto the magnet and removal of cleared supernatant. The libraries were eluted from the beads in 23.5µl elution pre-mix consisting of enrichment elution buffer 1 and HP3, and combined with 4µl elute target buffer 2. At this point the plate can be stored at -20°C for up to seven days.

Second hybridisation and second capture – The steps for the first hybridisation and capture were repeated, with the modification that after hybridisation the plate remained at 58°C for at least 14.5 hours, but not longer than 24 hours.

Capture sample clean up – The clean-up method was the same as for the first PCR clean up, except with 45µl of sample preparation beads. The result is 25µl of sample in resuspension buffer which can be stored at -20°C for up to seven days.

Second PCR amplification and clean up – To each well, 5µl PRC primer cocktail and 20µl Nextera Enrichment Amplification Mix were added. The PRC conditions were:

98°C for 30 seconds

10 cycles of: 98°C for 10 seconds

60°C for 30 seconds

72°C for 30 seconds

72°C for 5 minutes

Hold at 10°C

The clean-up method was the same as for the first PCR clean up, except 32.5µl resuspension buffer was used.

Validate libraries – The Bioanalyzer 2100 was again used to assess library quality and to determine the average library size. This number, along with the concentration in ng/µl (determined using the Qubit fluorometer) was used to calculate the concentration in nM using the following formula:

$$\frac{(\text{concentration in ng/}\mu\text{l}) \times 10^6}{(660\text{g/mol} \times \text{average library size})} = \text{concentration in nM}$$

10pM was loaded onto a rapid run flowcell, and run on the Illumina HiSeq 2500 with cBot clustering.

4.3. Whole Exome Library Preparation and Sequencing

The exonic regions of the genome were enriched using either the TruSeq 62mb capture or the Nextera focused 37mb capture (both Illumina), depending on when the sequencing was performed. Details of which capture was used for which sample are given in Chapter 6. Enrichment and library preparation followed the same protocol principles as described for library preparation of the TruSight One targeted panel (above), with a larger genomic capture area to cover all exonic regions. Sequencing was performed on the HiSeq 2000 or HiSeq 2500. Library Preparation and sequencing were carried out in-house by Dr Debbie Hughes at the UCL ION.

4.4. Primary Data Analysis

Primary data analysis was carried out in the same way for all NGS data. This included image analysis, base calling, alignment and variant calling, copy number variations and structural variations, and was performed in-house by Dr Alan Pittman at the UCL ION. Sequencing reads were mapped to the human reference genome build UCSC hg19 by Novoalign Software (Novocraft, Malaysia). After removal of PCR duplicates using Picard (<http://picard.sourceforge.net>) as well as reads without a unique mapping location, variants were extracted using the Maq model in SAMtools (<http://samtools.sourceforge.net>) and filtered by the following criteria: consensus quality >30, SNP quality >30 and root mean square mapping quality >30. Variants were further annotated using Annovar (<http://annovar.openbioinformatics.org/>).

4.5. Variant Filtering

Variant filtering was carried out by the author of this thesis, according to the filtering strategy described in each chapter.

4.6. Determination of Coverage

The percentage coverage of target regions was determined against exonic genomic coordinates using BedTools (<http://bedtools.readthedocs.org/>) with the assistance of Dr Joshua Hersheson.

5. Electrophysiology

5.1. RNA Preparation

Plasmid DNA was linearised using a restriction enzyme specific to the plasmid (linearisation conditions are dependent on the enzyme used, see results chapter for details). The DNA was then purified using QIAquick PCR purification kit (Qiagen,). 2µg of linearised DNA was used for transcription of RNA using Ambion T7 mMessage mMachinE kit (Life Technologies) in a reaction mixture containing: 10µl 2x NTP, 2µl 10x reaction buffer, 2µl enzyme mix and 2µg of linear template DNA, made up to 20µl with water. This reaction was incubated for 2 hours at 37°C, 1µl of DNase was added and incubation continued at 37 °C for a further 15 minutes. Lithium chloride precipitation was then used for RNA extraction using the following method; 30 µl of H₂O and 30 µl of LiCl precipitation solution were added to the reaction, the mixture was

placed at -20 °C overnight, and centrifuged for 15mins at 13,000 rpm and 4 °C. The supernatant was discarded and the pellet was washed with the addition of 500µl of 70% ethanol, further centrifugation and removal of the supernatant. The resultant pellet was resuspended in 20 µl of RNase free H₂O. RNA concentration was measured using nanodrop spectrometer.

5.2. *Xenopus* Oocyte Collection, Preparation and Injection

Stage V-VI *Xenopus laevis* oocytes were harvested from female *Xenopus laevis* frogs within UCL and stored in Modified Barth's Saline (MBS) (87mM NaCl, 1mM KCl, 1.68mM MgSO₄, 10mM HEPES, 0.94mM NaNO₃, 2.4mM NaHCO₃, 0.88mM CaCl₂, adjusted to pH 7.4 with NaOH). The follicular layer was removed by incubation with 25 2mg/ml Collagenase A (Roche diagnostics) in MBS for 90 minutes, removal of unhealthy oocytes, and further incubation with new collagenase. Healthy oocytes were selected and deposited into OR-2 media (82.5mM NaCl, 2mM KCl, 1mM MgCl₂, 5mM HEPES, adjusted to pH 7.4 with NaOH) with 100 U/ml penicillin-streptomycin and stored at 16 °C.

Within 24 hours of harvest oocytes were injected with RNA (RNA volume is experiment-dependent) using a Drummond Nanoject microinjector pipette (Drummond Scientific Company) 3.5" glass capillaries (Nanolitre replacement tubes, Drummond Scientific) were formed using a multistage-stage puller (Zeitz DMZ Universal Puller, AutoMate Scientific). The tip was broken manually to create sharp edge and the electrode backfilled with mineral oil (Sigma-Aldrich). RNA was microinjected into the oocyte cytoplasm and incubated at 18 °C in L-15 medium supplemented with Horse Serum, Pen/strep and Gentamycin for 48 hours.

5.3. Two-Electrode Voltage Clamp Recording

Electrophysiological experiments were carried out using the well-established two-electrode voltage-clamp (TEVC) technique (Stühmer 1998). The TEVC was controlled by an GeneClamp 500B amplifier (Axon Instrument) and was used to record the currents produced by the *Xenopus* oocytes. The amplifier was controlled and signals recorded using pClamp 7 software together with a DigiData1200A A/D converter (Axon Instruments). Microelectrodes were fabricated from borosilicate glass (Harvard Apparatus) using a multistage puller (AutoMate Scientific) to an O.D of 3-5µm for the voltage electrode and 7-9 µm for the current electrode. The tip resistance of the electrodes were <2MΩ and <1MΩ respectively with both electrodes filled with 3M KCl.

Ag⁺/AgCl coated electrodes were connected the amplifier headstage. See results chapter for details of TEVC protocols used.

5.4. TEVC Data Analysis

Data analysis was completed using Clampfit (from pCLAMP 9.2™, Axon instruments), Excel 2010 (Microsoft Office) and OriginPro 9.0 (OriginLab).

Chapter 3: Screening of the Paroxysmal Dyskinesia Genes

1. Introduction

The paroxysmal dyskinesias (PxDs) are a group of rare movement disorders, thought to account for under 1% of movement disorder patients (Blakeley and Jankovic 2002) however this is likely to be an underestimate. Patients experience episodic attacks of involuntary choreic, ballistic, athetoid or dystonic features, with normal neurological function in between attacks. Attack trigger divides the three subtypes into paroxysmal kinesigenic dyskinesia (PKD) paroxysmal non-kinesigenic dyskinesia (PNKD) and paroxysmal exercise-induced dyskinesia (PED). There has been significant overlap in the phenotype of these disorders and other neurological manifestations as associated such as migraine, epilepsy, ataxia and hemiplegic migraine. Details of the phenotypic features of each of these subtypes are given in Table 1.8.

Each of the three subtypes has an associated gene, dominant mutations in which are known to be responsible for causing the disease. Mutations in the *PNKD* gene account for about 70% of PNKD patients (Lee et al. 2004; Bruno et al. 2007), and to date only three mutations have been reported; c.20C>T p.(Ala7Val), c.26C>T p.(Ala9Val), and c.97G>C p.(Ala33Pro) (Figure 1.6b). Mutations in the glucose transporter gene *SLC2A1* cause PED in GLUT-1 DS2, a distinct condition from GLUT-1 DS1, the classic manifestation of mutations in this gene (Weber et al. 2008). Thus far ten mutations have been reported to cause PED in about 20% of cases (Figure 1.7) (Schneider et al. 2009). Lastly, mutations in *PRRT2* account for roughly 50% of PKD patients, the most common phenotype of the three (Chen et al. 2011; Wang et al. 2011; Lee et al. 2012; Li et al. 2012) Since its discovery in 2011, more than 60 mutations have been reported in the gene, although the majority of genetically confirmed cases have the common c.649dupC p.(Arg217Pfs*8) mutation (Figure 1.8).

Recent years have seen increased functional investigation into these three proteins, especially PNKD and PRRT2, as little was known about either before their association with the PxDs. PNKD is a protein with three differentially expressed isoforms of varying length; PNKD-S, PNKD-M and PNKD-L (Figure 1.6a). PNKD-S and PNKD-M are ubiquitous, while PNKD-L is only expressed in the brain (Lee et al. 2004). All of the reported mutations are found in the highly-conserved N-terminal region, which is present in PNKD-S and PNKD-L. The C-terminal contains an enzymatic domain of unknown consequence (Shen et al. 2011). Recent evidence suggests that PNKD has a role in the synapse, regulating the exocytosis of neurotransmitters (Shen et al. 2015).

The GLUT1 glucose transporter is known to be present on the blood-brain barrier and PED-causing mutations markedly reduce transport glucose into the brain (Weber et al. 2008). Thus the disease mechanism seems to be loss of function, and the movement disorder occurs due to the depletion of glucose after exercise, coupled with reduction of glucose transport into the brain.

The PRRT2 protein is also widely expressed in the brain and spinal cord. It is a TM protein known to interact with SNAP25, a protein important for vesicle docking and calcium-triggered exocytosis, and this interaction is disrupted by the p.(Arg217Pfs*8) mutation (De Meirleir et al. 2003; Lee et al. 2012). Therefore it is again suggested that PRRT2 has a role in synaptic exocytosis. Mutations appear to cause nonsense-mediated decay (NMD), and so it is thought the disease mechanism is haploinsufficiency (Wu et al. 2014).

There is some genetic overlap between the PxDs, identified by a recent review of 500 genetically confirmed cases (Erro et al. 2014). It showed that 2% of *PRRT2* patients had PED or PNKD, 1% of *PNKD* patients had PED, and 5% of *SLC2A1* patients had PNKD, totalling 2% of genetically diagnosed PxD patients having a mutation in an unexpected gene. All of the studies published previously are for the separate genes; no large study across all three genes has been performed.

2. Chapter Aims

At the NHNN there are 159 paroxysmal dyskinesia patients who have not yet been screened for mutations in the three PxDs genes. In this chapter, these patients will be screened to establish the frequency of PxD gene mutations in the cohort in the first ever large-scale screening study across all three genes. Furthermore this chapter will provide a novel, un-biased picture of the extent of genetic overlap amongst the PxDs. It

is also hoped that new mutations will be identified that could provide insight into the disease mechanisms of these proteins, therefore any novel mutations will be analysed in terms of their potential pathogenicity. Additionally, within the department, colleagues have identified a small number of mutations in the three genes; these will also be discussed.

It is well known that there is phenotypic overlap amongst the neuronal channelopathies. Furthermore, *PRRT2* mutations are already known for their marked phenotypic heterogeneity. Therefore, screening non-PxD episodic patients for mutations in these three genes could reveal new clinical manifestations for the PxD genes. This would expand the knowledge surrounding the genetic causes of the neuronal channelopathies, possibly allowing a higher rate of diagnosis in the future.

It is reported that around 50% of PKD patients do not harbour a *PRRT2* mutation, therefore it is likely that there is at least one other gene responsible for a proportion of these patients. There has been one report linking a *SNAP25* mutation to disease; in 2014 Shen et al reported a de novo change causing congenital myasthenia (Shen et al. 2014). *SNAP25* is known to interact with the *PRRT2* protein, and *PRRT2* disease-causing mutations disrupt this association (Lee et al. 2012). Therefore, mutations in the *SNAP25* gene could also cause PKD. To investigate this hypothesis, a sample of patients who are negative for the other PxD genes will be screened for *SNAP25* mutations in the hope of identifying a new PKD gene.

If interesting mutations are detected by the above screening studies, a small proportion will be investigated functionally to determine their pathogenicity and to further understand their disease mechanism. This will be done *in vitro*, using HEK293 cells, and *in vivo* with patient fibroblasts.

3. Patients and Methods

3.1. Patient Cohorts

3.1.1. Mixed Paroxysmal Dyskinesia Cohort

The mixed paroxysmal dyskinesia cohort consisted of 159 family probands or sporadic patients that had been sent for genetic diagnosis. The diagnosis of PKD, PED or PNKD was made using recognised criteria (Bruno et al. 2004; Bruno et al. 2007).

3.1.2. Related Episodic Cohort

The related episodic cohort consisted of 55 genetically undefined well-characterised probands with episodic ataxia, familial hemiplegic migraine (FHM) or benign infantile seizures that had again all been sent for genetic diagnosis. An additional 192 poorly characterised patients with episodic features were also included.

3.2. Genetic Investigations

3.2.1. Paroxysmal Dyskinesia Gene Screening

All three coding exons of *PRRT2*, ten coding exons of *SLC2A1* and exons one and two of *PNKD* were sequenced in the two cohorts. Primers for the aforementioned exons and flanking introns were designed against the longest transcript for each gene in Ensembl; *PRRT2*-001 – ENST00000358758, *SLC2A1*-001 – ENST00000426263 and *PNKD*-001 – ENST00000273077 using Primer3 software (Rozen and Skaletsky 2000). In cases where exons were close together, one primer pair was used to amplify and sequence two exons together. *PRRT2* exon two was very large and required two additional mid-exon sequencing primers for complete coverage (2RMID and 2FMID). Primer sequences for these genes are given in Table 3.1. PCR and sequencing procedures were carried out as described in section 2.1 and 2.2 of the materials and methods chapter.

3.2.2. SNAP25 Screening

A plate of 95 patients from the mixed PxD cohort, who were negative for mutations in the PxD genes were screened for the whole of the coding *SNAP25* gene as the encoded protein is known to interact with *PRRT2*. Exon one is non-coding, thus patients were sequenced for exons two to eight and flanking introns of the gene (excluding the non-coding region of exon eight) using primers designed against the longest transcript of the gene on Ensembl (<http://www.ensembl.org/index.html>); *SNAP25*-003 – ENST0000025497. PCR and sequencing procedures were carried out as described in section 2.1 and 2.2 of the materials and methods chapter. The *SNAP25* primer sequences are given in Table 3.2.

3.2.3. Results Collection from Departmental Colleagues

Within the department, there have been a small number of mutations in the PxD genes identified by Sam McCall, who has kindly agreed that they be included in this chapter for discussion purposes. Other than these mutations, all other sequencing was carried out by the thesis author.

Gene	Primer	Sequence (5' – 3')
<i>PRRT2</i>	2F	CCTATCTCCTCCTCTTCCAG
	2FMID	AAGAGGCCACTGCAGCCAG
	2R	CTCCAGAGGCTCTATTGCAG
	2RMID	TGGTTGAAGGGCTGGCTTG
	3F	CTTACCCGCCATCTATGG
	3R	AGGCTCCCTTGGTCCTTAGG
<i>PNKD</i>	1F	GGTCAAAGTCTAATTATCCG
	1R	GTCTGTAGGCAGGACGGAAG
	2F	TCCTCCCAAGCCCTTACTG
	2R	GAGAAGTTTCTAAGTCCTGC
<i>SLC2A1</i>	1F	GGAGTCAGAGTCGCAGTGG
	1R	AGGAGTCTGCGCCTTTGTT
	2F	CACAGAACTTGCCAGTCCA
	2R	ACTGTGGGCATGTGTGATGT
	3 and 4 F	AAGGAAAAGGAAGACTGGG
	3 and 4 R	CGGAAGAGAACTCTGCC
	5 and 6 F	CAGCAGCTGACACAAAGTAG
	5 and 6 R	CACCATGCACACTTGACC
	7 and 8 F	TCCCACATCCACTGCTAC
	7 and 8 R	CAGGCATTTTGGGATATG
	9F	TCTGGCCTCTGTAGCTTC
	9R	AGTTTCCTCCTCAGCATG
	10F	CAGCCAGGATGTAGGGTCAT
	10R	CCTGTGCTCCTGAGAGATCC

Table 3.1 - Primer sequences used to screen *PNKD*, *PRRT2* and *SLC2A1*

Gene	Primer	Sequence (5' – 3')
SNAP25	2F	TGGTCTTTGCACACACCTACA
	2R	CTCAGGCCTTCATCTTTTGC
	3F	CAAGATCTCTGGATCCTGCAC
	3R	GCCCAAGGAAACATCATAGC
	4F	GGGCTAATTGTCCCCTTACTG
	4R	CAAAGCGACCATCTGCGTAT
	5F	CCATCTGCTTCATTCTGTGG
	5R	GAGCTTGTCAAGGCTTGGAG
	6F	TGAGAGCTTGCTCCTCCAC
	6R	CACTCAGTTTTGGAGTTGTTTG
	7F	TGTCTTCTAAAACTTGCTCTTTGG
	7R	ATGCCCTTCACACTTCCTGT
	8F	GTGGTTTCACCCAAGAGGAA
	8R	CTATCTTGCCCGACAGCATT

Table 3.2 - Primer sequences used to screen SNAP25

3.3. Functional Investigations

3.3.1. Expression of Wild type and Mutant *PRRT2* Protein in HEK293 cells

The vector pEF1a-HA (Clontech Laboratories) with the *PRRT2* gene already cloned into it, along with the empty vector and the cloned vector with the common mutation, p.(Arg217Pfs*8), were received from the Ptacek group on filter paper (Lee et al. 2012). The plasmid structure is shown in Figure 3.1. The plasmids were removed from the filter paper and transformed into *E.Coli* and cloned. Two mutations (c.913G>T, p.(Gly305Trp) and the 4 base pair deletion, c.514_517delTCTG p.(Ser172Argfs*3)) were introduced into the wild type protein using mutagenesis, primer sequences for which are given in Table 3.3. HEK293 cells were transfected with one of the following:

1. The vector with the wild type *PRRT2* gene
2. The empty vector, with no *PRRT2* gene (negative control)
3. The vector with the p.(Arg217Pfs*8) mutation in the *PRRT2* gene
4. The vector with the p.(Ser172Argfs*3) mutation in the *PRRT2* gene
5. The vector with the p.(Gly305Trp) mutation in the *PRRT2* gene
6. A vector with a GFP tag (transfection control)

Subsequently, the cells were harvested and a western blot was used to detect PRRT2 protein using an anti-HA antibody raised in rabbit (abcam) at a concentration of 1/10,000. The above was carried out according to the protocol detailed in section 3 of the materials and methods chapter.

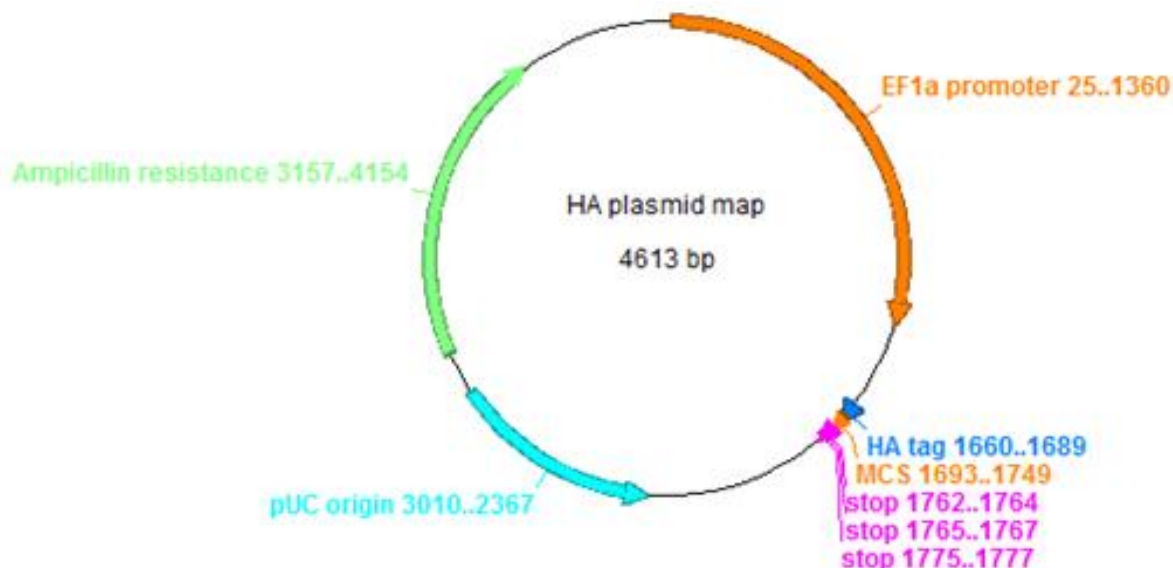


Figure 3.1 – The structure of the pEF1a-HA vector created in ApE A plasmid editor

Mutation	Primer	Sequence (5' – 3')
c.514_517delTCTG, p.Ser172Argfs*3	F	ACCCACCCCTGAGATTCTGAGAGTGTAGG
	R	CCTACTACTCTCAGAATCTCAGGGGTGGGGT
c.913G>T, p.Gly305Trp	F	GGGACGTGGACTGGGCCAGCGT
	R	ACGCTGGGCCAGTCCACGTCCC

Table 3.3 – Mutagenesis primer sequences used to introduce two mutations into the PRRT2 gene

3.3.2. Investigation of Nonsense-Mediated Decay in Patient Fibroblasts

Fibroblasts were taken with informed consent from patients 3.47, 3.49 and 3.70 and two unaffected controls including the mother of patient 3.47. RNA was extracted, reverse transcription made cDNA and it was sequenced as described in section 3.5 and 3.6 of the materials and method chapter. Sequencing was carried out for regions of *PNKD* and *PRRT2* using primer sequences given in Table 3.4.

Gene	Primer	Sequence (5' – 3')
<i>PRRT2</i>	3F	ACCTCGGGACTACATCATCC
	3R	AGAGGAGCCTGGCAAGATG
<i>PNKD</i>	10F	CTTCAGATCCGGGCCCTG
	10R	CGGGAGTAGTCATCATCCCC

Table 3.4 –Primer sequences used to sequence regions of *PNKD* and *PRRT2* cDNA

3.3.3. Determination of Neuronal Expression Levels of *PXD* and Related Genes

Regional distribution of *PRRT2*, *SLC2A1*, *PNKD*, *KCN1A*, *SNAP25* and *CACNA1A* mRNA expression in the normal human brain was determined using microarray analysis of human post-mortem brain tissue from the UK Human Brain Expression Consortium (<http://caprica.genetics.kcl.ac.uk:51519/BRAINEAC/>) (Trabzuni et al. 2011). Brain tissues originating from 134 control Caucasian individuals were collected by the Medical Research Council (MRC) Sudden Death Brain and Tissue Bank (Edinburgh, UK). The following brain regions were included in the analysis: cerebellum (CRBL), frontal cortex (FCTX), hippocampus (HIPPP), medulla (MEDU), occipital cortex (OCTX), putamen (PUTM), substantia nigra (SNIG), temporal cortex (TCTX), thalamus (THAL) and white matter (WHMT). Total RNA was isolated from these tissues using mRNeasy 96-well kit (Qiagen, UK) before processing with the Ambion WT Expression Kit and Affymetrix GeneChip Whole Transcript Sense Target Labelling Assay, and hybridization to the Affymetrix Exon 1.0 ST Array. This work was performed by Daniah Trabzuni.

4. Results

4.1. Frequency of Mutations in *PRRT2*, *PNKD* and *SLC2A1*

4.1.1. *PRRT2* Screening in the *PxD* Cohort

Heterozygous mutations in the *PRRT2* gene were found in 49 probands/ single cases (Table 3.5), which is 31% of the *PxD* cohort. 98% of *PxD* patients with a mutation in this gene (48 patients) had been diagnosed as having PKD, either alone or with additional features such as seizures or migraine (hemiplegic or normal). The remaining one *PxD* patient with a *PRRT2* mutation had PED. No patients with a *PRRT2* mutation had *PNKD*. Two pedigrees with mutations (patients 3.6 and 3.47) and accompanying chromatograms are shown in Figure 3.2.

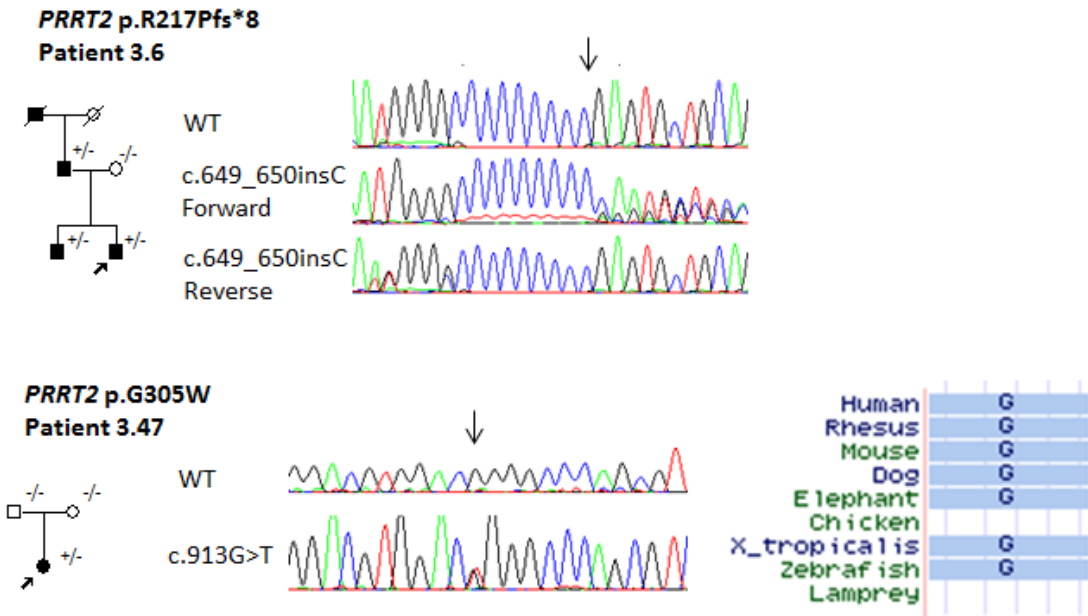


Figure 3.2 Chromatograms, nucleotide conservation and family trees for PRRT2 mutations found in patients 3.6 and 3.47 (nucleotide conservation is not given for p.(Arg217Pfs*8) as the mutation is not a substitution). Nucleotide conservation is taken from the UCSC genome browser (<https://genome-euro.ucsc.edu>)

4.1.2. PRRT2 Screening in the Further Episodic Phenotype Cohort

Five patients from the well characterised mixed non-PxD cohort (9%) had mutations in PRRT2 (Table 3.6). Four of the patients (patients 3.50, 3.52, 5.53 and 5.54) had infantile seizures (three with additional hemiplegic migraine), and the fifth (patient 5.51) had episodic ataxia with hemiplegic migraine (previously reported by us (Gardiner et al. 2012)), which is a completely novel phenotypic presentation for mutations in the gene. The patient had the p.(Arg217Pfs*8) mutation with episodic balance difficulties starting at the age of 18 years with unilateral headaches and hemiplegic episodes. She had frequent attacks every day of involuntary movement and balance problems, and cerebellar ataxia on examination but normal imaging. The mother had a past history of epilepsy and severe headaches, and one of her daughters had hemiplegic migraine. No patient from the poorly characterised cohort harboured a mutation.

Patient	Ethnicity	Age at onset/ current age	Phenotype	Family history	Genetics
3.1	Somalia	13/27	PKD with seizures	Affected sister	p.Ser172Argfs*3
3.2	British	15/32	PKD, migraine with aura	No family history	p.Pro215Arg
3.3	British	5/13	PKD, long and frequent episodes of dystonia, unusual tongue dystonia	No family history	p.Pro216His (also has <i>SLC2A1</i> mutation)
3.4	Black-British	7-8/12-16	PKD	Yes, affected sister,	p.Arg217*
3.5	Austrian	0.5-27/29-51	PKD	Yes, affected sister, father unaffected carrier	p.Arg217Pfs*8
3.6	Wales/ India	11/49	PKD, migraine with aura	Yes, affected paternal grandfather, father, brother with migraine	p.Arg217Pfs*8
3.7	Ireland	8/45	PKD	Yes, affected sister	p.Arg217Pfs*8
3.8	British	1/22	PKD	Yes, large autosomal dominant family	p.Arg217Pfs*8
3.9	Pakistan	14/33	PKD	Yes, affected sister	p.Arg217Pfs*8
3.10	British	10/26	PKD, meningitis and recurrent seizures as a child	Yes, brother and sister possibly affected, affected mother	p.Arg217Pfs*8
3.11	British	6-11/20-68	PKD with migraine	Large autosomal dominant family history. Seizures in one case.	p.Arg217Pfs*8
3.12	British	6/19	PKD	Probable, mother migraine	p.Arg217Pfs*8
3.13	Turkey	5/16	PKD	No family history	p.Arg217Pfs*8
3.14	British	12/18	PKD	No family history	p.Arg217Pfs*8
3.15	Pakistan	8/40	PKD	Yes, affected brother	p.Arg217Pfs*8
3.16	Malta	8-18/25-48	PKD with migraine	Yes, affected mother	p.Arg217Pfs*8
3.17	Pakistan	8/43	PKD with headaches	Yes, affected twin brother	p.Arg217Pfs*8
3.18	British	27/48	PKD	No	p.Arg217Pfs*8
3.19	Singapore	9/47	PKD	Yes, daughter has childhood seizures	p.Arg217Pfs*8
3.20	India	6-14/12-42	PED with migraine	Yes, affected brother and father, family history of seizures	p.Arg217Pfs*8
3.21	British	0.5-30/87	PKD, migraine with aura, HM, epilepsy	Yes, dominant, large number affected	p.Arg217Pfs*8
3.22	British	12/29	PKD	Yes, mother has migraine	p.Arg217Pfs*8

3.23	British	14/39	PKD	No family history	p.Arg217Pfs*8
3.24	India	7-13/9-60	PKD with seizures	Yes, large autosomal dominant family history	p.Arg217Pfs*8
3.25	India	8/52	PKD with migraine	Yes, father affected and seizures in paternal aunt	p.Arg217Pfs*8
3.26	British	8-12/28-76	PKD with HM and seizures	Yes, large autosomal dominant family history	p.Arg217Pfs*8
3.27	Slovakia	6/47	PKD with migraine burning hemiplegia	Yes, sister has migraine	p.Arg217Pfs*8
3.28	British	6/49	PKD	Yes, two affected relatives	p.Arg217Pfs*8
3.29	British	9/32	PKD	Yes, mother with migraine, uncle with infantile convulsion	p.Arg217Pfs*8
3.30	White-British	9/19	PKD	No family history	p.Arg217Pfs*8
3.31	White-British	11/20	PKD	Mother is carrier, she had single episode of torticollis but no paroxysmal movement disorder	p.Arg217Pfs*8
3.32	Pakistani	~10/18-69	PKD	Yes, affected father with PKD	p.Arg217Pfs*8
3.33	Irish	6-12/31-59	ICCA	Yes, affected brother, father mutation carrier but no history of ICCA	p.Arg217Pfs*8
3.34	British	39/63	PKD and episodic ataxia/ slurred speech	No family history	p.Arg217Pfs*8
3.35			PKD	No family history	p.Arg217Pfs*8
3.36	British	12/29	PKD	No family history	p.Arg217Pfs*8
3.37	Sri Lanka	6/16	PKD	No family history	p.Arg217Pfs*8
3.38	Afghanistan	8/15	PKD and HM	No family history	p.Arg217Pfs*8
3.39	Pakistan	8/27	PKD	No family history	p.Arg217Pfs*8
3.40	Australia	5/10	PKD and HM	Yes, father had HM	p.Arg217Pfs*8
3.41	British	14/33	PKC	Possible migraine	p.Arg217Pfs*8
3.42	British	7-12/9-32	PKC	Yes mother	p.Arg217Pfs*8
3.43	British	8-14/12-37	PKC	Yes mother	p.Arg217Pfs*8
3.44	Russian	Unknown	PKD	Yes, son with infantile spasms, affected aunt.	p.Arg217Pfs*8
3.45	British	Unknown/23	PKD	Yes, affected brother, mother with migraine	p.Arg217Pfs*8 + p.Gly258Glu

3.46	British	11/21	PKD	No	p.Arg240*
3.47	British	Unknown/23	PKD	No	p.Gly305Trp
3.48	India	14/46	PKD	Yes, father had seizures as a child	p.Cys332insAsp
3.49	British	12/35	PKD, migraine with aura (visual and hemisensory)	Yes, family history of migraine with aura and epilepsy	p.*341Leu

Table 3.5 – The mutations identified in PRRT2 in the paroxysmal dyskinesia cohort. Where age details are available for multiple family members, they are given

Patient	Ethnicity	Age at onset/ current age	Phenotype	Family history	Genetics
3.50	British	0.5/22	Benign familial infantile epilepsy, HM	Yes, father, sister and cousins affected with HM	p.Arg217Pfs*8
3.51	British	10/59	Episodic ataxia with familial hemiplegic migraine	Yes, affected mother and children with familial hemiplegic migraine	p.Arg217Pfs*8
3.52	Irish	6-12/31-59	Infantile convulsions with HM	Yes, Multiple affected members with PKD, infantile convulsions and/or HM	p.Arg217Pfs*8
3.53	British	0.5/2	Infantile seizures	Yes, affected father with PKD	p.Arg217Pfs*8
3.54	British	2/15	FHM and early benign seizures	Yes, several with FHM	c.1011C>T (exon 3 splice site)

Table 3.6 – The mutations identified in PRRT2 in the mixed episodic phenotype cohort

4.1.3. *PNKD* Screening in the PxD Cohort

Three heterozygous mutations were identified in PxD probands/ single cases in exons one and two of *PNKD*, accounting for 2% of the cohort (Table 3.7). These mutations (p.(Ala7Val), p.(Ala9Val)) are both well known to cause *PNKD* in multiple unrelated families (Shen et al. 2011). Here, two mutations caused *PNKD* (patient 3.56, 3.57), whilst the other was responsible for PKD (patient 3.55), a novel clinical manifestation for *PNKD* mutations. No mutations were found in patients with PED. Figure 3.3 shows pedigrees and chromatograms from patient 3.56 and patient 3.70 (from results section 4.2).

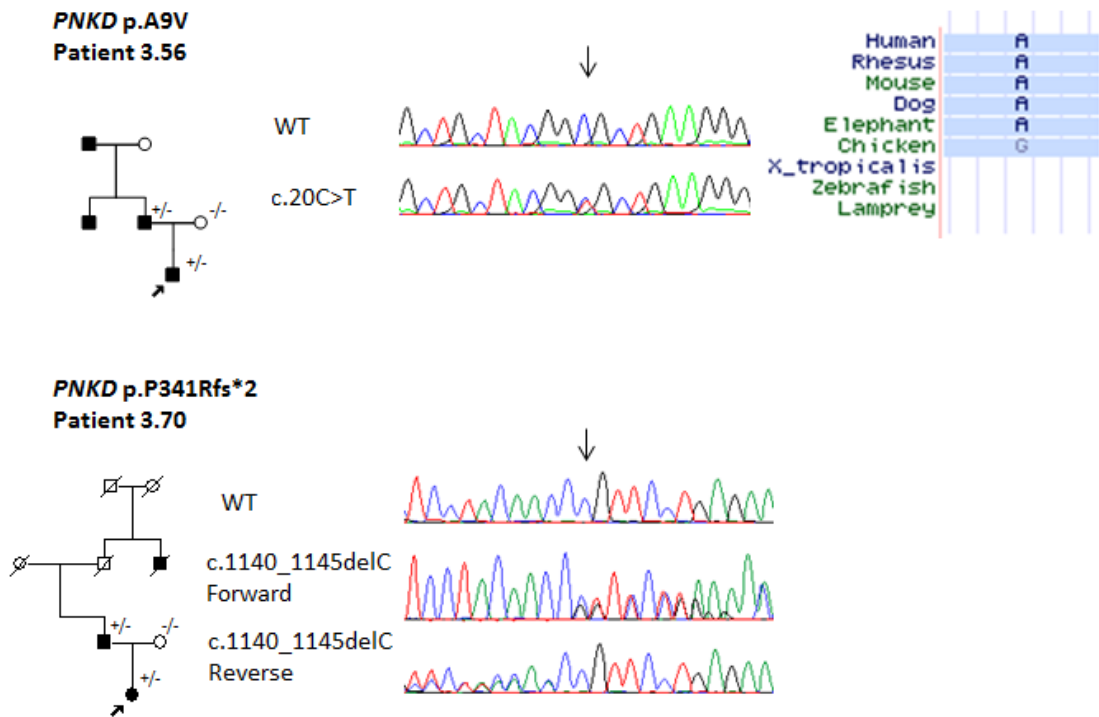


Figure 3.3. Chromatograms, nucleotide conservation and family trees for *PNKD* mutations found in patients 3.56 and 3.70 (nucleotide conservation is not given for c.1022delC p.(Pro341Argfs*3) as the mutation is not a substitution). Nucleotide conservation is taken from the UCSC genome browser (<https://genome-euro.ucsc.edu>)

4.1.4. *PNKD* Screening in the Further Episodic Phenotype Cohort

No patients from either the well-characterised non-PxD cohort or the poorly characterised cohort had mutations in exon one or two of *PNKD*.

4.1.5. *SLC2A1* Screening in the PxD Cohort

Ten *SLC2A1* mutations were identified in 11 probands/ single cases from the PxD cohort (7% of the cohort), with a range of phenotypes (Table 3.8). All were

heterozygous. Six had PED (patient 3.60 with PKD). Three had PKD (all with additional features), and one had PNKD (patient 3.61). The last patient had an interesting phenotype. Patient 3.58 was identified with a novel heterozygous mutation, c. 227G>T p.(Gly76Val). This patient was a 26 year old, diagnosed with ADHD as a child and since then has had episodes of 'wobbly' eyes, legs and arms, and abnormal arm posturing that lasted 10-20 minutes. Episode triggers included tiredness, sudden movement, infection or illness and excitement. Over the last twenty years he has on average two to three attacks a week. He experienced episodes of weakness and painful cramps in his hands and his legs. There was no relevant family history. He underwent repeat long exercise testing (McManis) repeated over several years and this showed significant decrement, accompanied by weakness of the exercised hand muscles. The decrement ranged from 51% to 66%. The clinical diagnosis at that time suggested a periodic paralysis phenotype but the problems with movement were not consistent with this.

4.1.6. *SLC2A1* Screening in the Further Episodic Phenotype Cohort

Two patients from the well-characterised cohort had mutations in *SLC2A1* (Table 3.9). This is 4% of the cohort. The first, patient 3.68, had a complex EA-type phenotype with unsteadiness, headaches, nystagmus, and vomiting, with the novel mutation, c.179C>T p.(Thr60Met). The second, patient 3.69, also had EA, this time with absence seizures, and the previously reported mutation .884C>T p.(Thr295Met). This mutation was also seen in the PxD cohort in a patient with PED and migraine. Figure 3.4 shows pedigrees and chromatograms from patient 3.58 and patient 3.68. No patient from the poorly characterised cohort harboured a mutation.

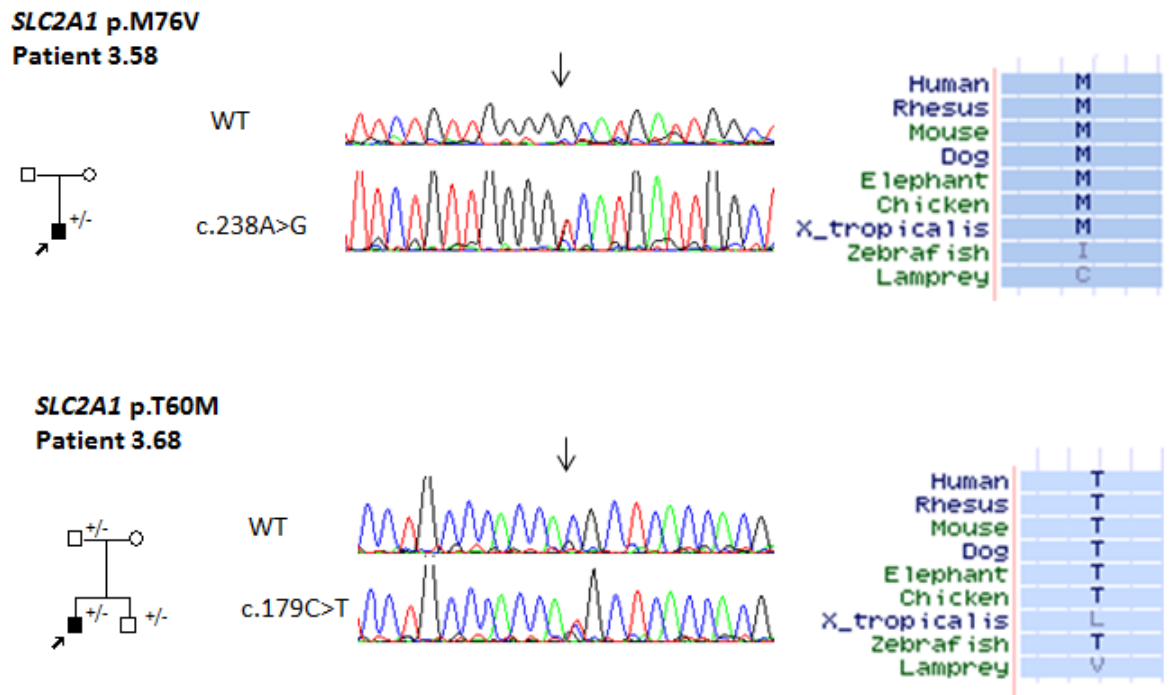


Figure 3.4. Chromatograms, family trees and nucleotide conservation for SLC2A1 mutations found in patients 3.58 and 3.68. Nucleotide conservation is taken from the UCSC genome browser (<https://genome-euro.ucsc.edu>)

Patient	Ethnicity	Age at onset/ current age	Phenotype	Family history	Genetics
3.55	German	Teens/20s	PKD	Four generation large family	p.Ala7Val
3.56	British	16/32	PNKD with atypical features	Yes, father, paternal uncle and grandmother	p.Ala9Val
3.57	British	8-22/20-64	PNKD	Several affected over three generations	p.Ala9Val

Table 3.7 – The mutations identified in PNKD in the paroxysmal dyskinesia cohort

Patient	Ethnicity	Age at onset /current age	Phenotype	Family history	Genetics	Previously reported? (reference)
3.58	British	8/28	Myotonia and dystonia	No	p.Gly76Val	No
3.59	British	6-13/18-78	PKD in three cases, PED in one. Attached more typical of PKD	Yes, family history of migraine.	p.RArg92Trp	Yes - causes PED (Schneider et al. 2009)
3.60	British	11/46	PED and PKD	Yes, AD family history	p.Met96Val	Yes - causes glut1 GLUT-1 DS1 (Leen et al. 2010)
3.61	British	Teens/49	PNKD	Affected mother	p.Cys201Arg	No
3.62	British	8/24	PKD with epilepsy	No	p.Arg223Trp	Yes - causes GLUT-1 DS1(Leen et al. 2010)
3.63	British	12/24	PED	Positive family history	p.Ala275Thr	Yes - causes PED (Weber et al. 2008)
3.64	British	4/17	PED and seizures	No	p.Ser285Pro	No
3.65	British	Child/36	PED/epilepsy	No	p.Thr295Met	Yes - causes PED (Weber et al. 2008)
3.3	British	5/13	PKD, long and frequent episodes of dystonia, unusual tongue dystonia	No	p.Arg333Gln + <i>PRRT2</i> (p.Pro216His)	Yes - causes PED (Schneider et al. 2009)
3.66	British	4/54	PED	No	p.Arg333Gln	Yes - causes PED (Schneider et al. 2009)
3.67	British	12/26	PED	Daughter affected	p.Arg333Trp	Yes - causes GLUT-1 DS1 (Wang et al. 2000)

Table 3.8 – The mutations identified in *SLC2A1* in the paroxysmal dyskinesia cohort

Patient	Ethnicity	Age at onset /current age	Phenotype	Family history	Genetics	Previously reported (reference)
3.68	Pakistan	1/9	Frequent paroxysmal episodes of unsteadiness, headaches, nystagmus, vomiting. MRI normal. Since baby.	The mutation is present in the father and brother but they are unaffected.	p.Thr60Met	No
3.69	Ireland	4/17	EA2, absence seizures	No	p.Thr295Met	Yes - causes GLUT-1 DS1 (Wang et al. 2005)

Table 3.9 – The mutations identified in SLC2A1 in the mixed episodic phenotype cohort

4.1.7. Cohort-Wide Results – PxD Cohort

Mutations in these three genes explained the paroxysmal dyskinesia in 62 (39.0%) patients out of a mixed PxD cohort of 159 patients. 31% had mutations in *PRRT2*, 7% in *SLC2A1*, and 2% in *PNKD*. Of the positive cases, 51 patients had PKD, seven patients had PED, and three had PNKD. The last had a novel phenotype that did not fit these categories (patient 3.58, discussed in section 4.1.5). 87% had mutations that have already been reported and 13% had novel mutations.

4.1.8. Cohort-Wide Results – Non-PxD Cohort

A further seven mutations were identified in our related episodic non-PxD cohort (13%). Three of these had an episodic ataxia- like phenotype, one had FHM and three had infantile seizures. No mutations were found in the poorly characterised cohort.

4.2. Additional Mutations Identified Within the Department in *PRRT2*, *SLC2A1*, and *PNKD*

A small number of additional mutations in these genes were found within the department by Sam McCall. These are included in this thesis for completeness and shown in Table 3.10. Four patients were found to have *PRRT2* mutations, both mutations identified have previously been reported, and have been found as part of the gene screening in this chapter in other patients. Unfortunately, fewer patient details are available for these patients. Additionally, a novel mutation was found in *PNKD*, in a patient with FHM-like presentation (a pedigree and chromatogram are shown in Figure 3.3). Attack symptoms in this patient, including cognitive dysfunction and impaired motor function, subsided after 2 hours leaving the patient with a severe headache. Stroke was excluded. No further *SLC2A1* mutations were found.

Patient	Phenotype	Gene	Mutation	Previously reported? (reference)
3.70	FHM	<i>PNKD</i>	p.Pro341Argfs*3	No
3.71	PKD	<i>PRRT2</i>	p.Arg217Pfs*8	Yes, common mutation
3.72	PKD	<i>PRRT2</i>	p.Arg217Pfs*8	Yes, common mutation
3.73	PKD	<i>PRRT2</i>	p.Arg217Pfs*8	Yes, common mutation
3.74	PKD	<i>PRRT2</i>	p.Arg217Pfs*8	Yes, by us (Gardiner et al. 2012)

Table 3.10 – Mutations in the three PxD genes found within the department by Sam McCall

4.3. *SNAP25* Screening

Screening of the seven coding exons of *SNAP25* in 95 PxD-gene negative paroxysmal dyskinesia patients identified no possible disease-causing mutations.

4.4. Mutation Analysis

4.4.1. *PRRT2* Mutations

Eleven different *PRRT2* mutations were found within this cohort (Table 3.5, Figure 3.5a). The male: female ratio in the *PRRT2* mutation cohort was 2:1. The patient demographic was 56% British, with a mixture of ethnicities comprising the other 44%; there was no common haplotype background. As widely reported, by far the most common mutation (48 patients of the 58 with mutations – 83%) was p.(Arg217Pfs*8), an insertion of a cytosine resulting in a frameshift and premature stop codon. It has been suggested that the sequence in this region of DNA may form a hairpin loop, which could make DNA replication more prone to error (Heron and Dibbens 2013), explaining the high frequency of this mutation. The remaining ten mutations accounted for one proband/ pedigree each (except p.(Ser172Argfs*3), accounting for two). Four had been reported previously in the literature, but only in small numbers, highlighting the relative infrequency of non-p.(Arg217Pfs*8) mutations in *PRRT2* (p.(Ser172Argfs*3) has been reported in one other case, c.1011C>T in two, p.(Arg217*) and p.(Arg240*) in four each (Yang et al. 2013)).

The remaining six mutations found were novel, and thus it cannot be certain that they are pathogenic. They are c.1022G>T p.(*341Leu) (which disrupts the stop codon and results in an elongated protein (Figure 3.5b)), c.773G>A p.(Gly258Glu) (seen alongside p.(Arg217Pfs*8) in the second ever case of compound heterozygosity in *PRRT2* mutations, Figure 3.6), c.644C>G p.(Pro215Arg), c.647C>A p.(Pro216His), p.(Gly305Trp), and c.997_998insATG p.(Cys332insAsp). They have all been reported, or are in the process of being, in publications arising from this work (Gardiner et al. 2012; Silveira-Moriyama et al. 2013).

The majority of the mutations reported in *PRRT2* to date have been nonsense or frameshift mutations, and this fact, coupled with functional work demonstrating NMD and reports of *PRRT2* microdeletions causing PKD, has provided fairly conclusive evidence that the disease mechanism is haploinsufficiency (Dale et al. 2012; Wu et al. 2014). None of the novel mutations found fit this disease model, as they are missense, a non-frameshift insertion and an elongation. Table 3.11 summarises their potential for pathogenicity using the *in silico* prediction tools Polyphen-2 and SIFT, and the

population frequency databases EVS, 1000genomes and ExAC. All novel variants found were absent or very rare in the population databases. Furthermore, all missense variants are predicted to be pathogenic by Polyphen-2, and all except p.(Gly258Glu) are by SIFT.

Variation	Polyphen-2 Prediction	SIFT Prediction	MAF EVS	MAF 1000g	MAF ExAC
p.Pro215Arg	Probably Damaging (0.999)	Damaging (0.02)	0.0006	0.002	0.0008
p.Pro216His	Probably Damaging (0.999)	Damaging (0)	0	0	0.0004
p.Gly258Glu	Probably Damaging (1)	Tolerated (1)	0	0	0.0006
p.Gly305Trp	Probably Damaging (1)	Damaging (0)	0	0	0
p.Cys332insAsp	n/a	n/a	0	0	0
p.*341Leu	n/a	n/a	0	0	0

Table 3.11 – The Polyphen-2, SIFT, EVS, 1000genome and ExAC scores for the novel variants found in PRRT2

The PRRT2 protein has two putative TM domains, consisting of the amino acids 286 – 290 and 315 – 337. Consequently, p.(Gly305Trp) is in a short linker region between the two domains, p.(Cys332insAsp) is in the middle of the second domain, and p.(*341Leu) is directly after it. Therefore all three mutations could interrupt these TM domains and thus prevent PRRT2 embedding into the cell membrane and performing its function. This would fit the loss of function hypothesis. Additionally, although not themselves previously reported, p.(Gly305Trp) and p.(*341Leu) are located at the same amino acids as disease-causing mutations that have been reported (c.913G>A p.(Gly305Arg) and c.1021T>C p.(*431Arg) (Liu et al. 2012; Djemie et al. 2014)). Two of the patients (3.48 and 3.49) have a positive family history segregating with the mutations found. Both of the parents of Patient 3.47 are unaffected, and neither harbour p.(Gly305Trp), therefore it is a de novo mutation. This combination of evidence suggests that all three of these mutations are disease causing.

The other three variants, however, are more ambiguous. As mentioned previously, the string of cytosines, from which p.(Pro215Arg) and p.(Pro216His) arise,

is prone to replication errors; and other more common variations, c. 643C>T p.(Pro215Ser), c. 645C>T/G/A p.(Pro215Pro) and c.647C>T p.(Pro216Leu), are also seen and are also predicted to be pathogenic by in silico tools. p.(Pro215Arg) and p.(Pro216His) are seen in population databases, although infrequently. Furthermore, patient 3.3, who has p.(Pro216His), also harbours a known-pathogenic *SLC2A1* mutation which is likely to account for his PKD; although p.(Pro216His) could be modifying the phenotype. This patient Therefore, both p.(Pro215Arg) and p.(Pro216His) should be considered variants of unknown consequence.

Patient 3.45, with p.(Gly258Glu), is an interesting case, as the variant is found in a pedigree alongside p.(Arg217Pfs*8) (for chromatograms, family tree and conservation see Figure 3.6). Patient 3.45 harbours both mutations, one inherited from each parent, whilst her brother, who has a milder phenotype, has p.(Arg217Pfs*8) but no p.(Gly258Glu). Both parents are unaffected by PKD, although the mother has a family history of migraine. Unexpectedly however, the father was the source of p.(Arg217Pfs*8), whilst p.(Gly258Glu) came from the maternal line.

a)

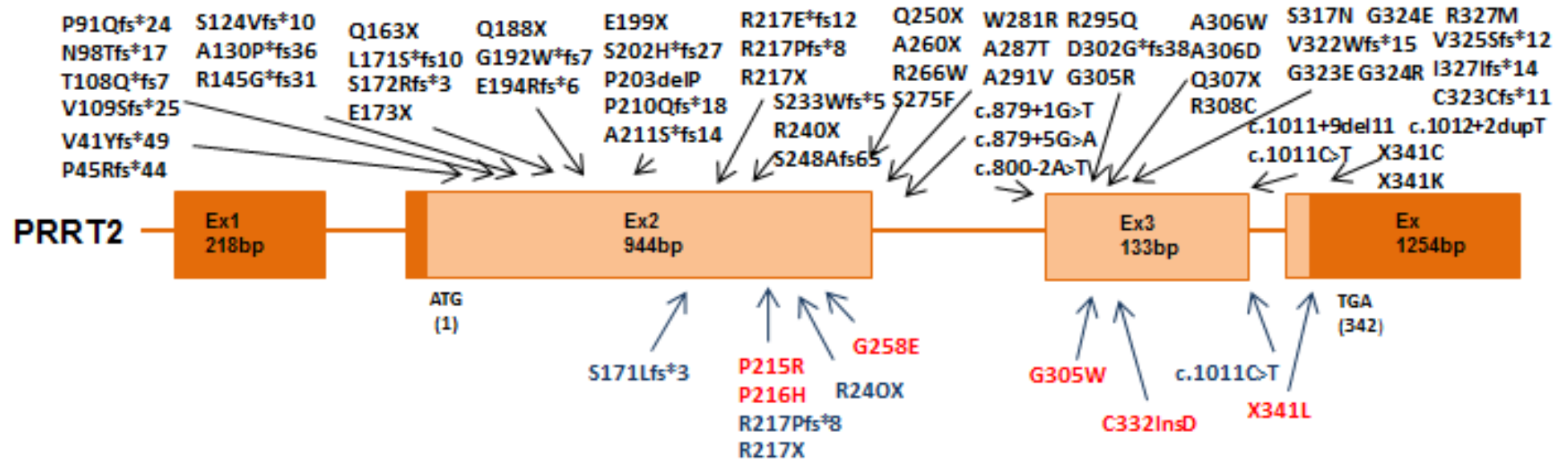


Figure 3.5 (a) - Schematic diagram of PRRT2 showing mutations that have been previously reported above the gene and mutations found in this study below the gene, (described in terms of protein change unless indicated otherwise, novel mutations are in red)

b)

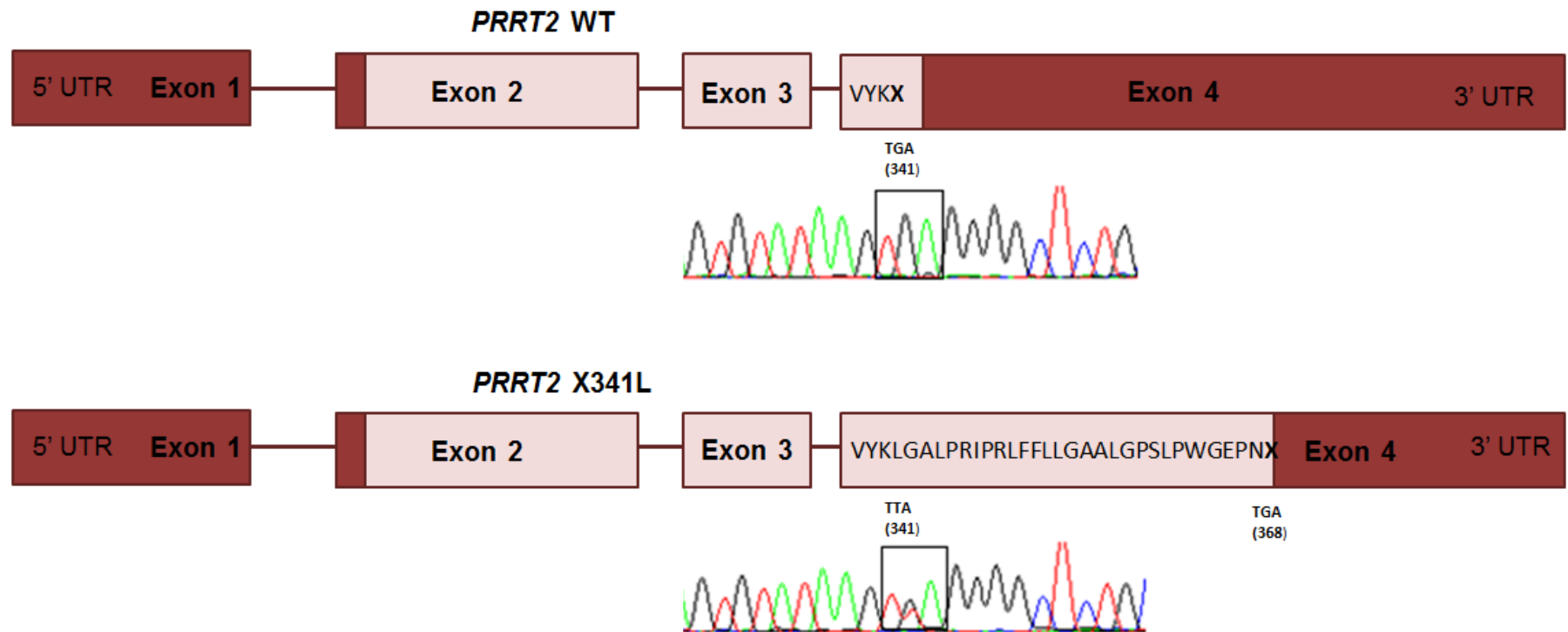


Figure 3.5 (b) - Schematic diagram of PRRT2 showing the elongation of the protein caused by p.(*341Leu), and the chromatogram identifying the mutation in the DNA of patient 3.49

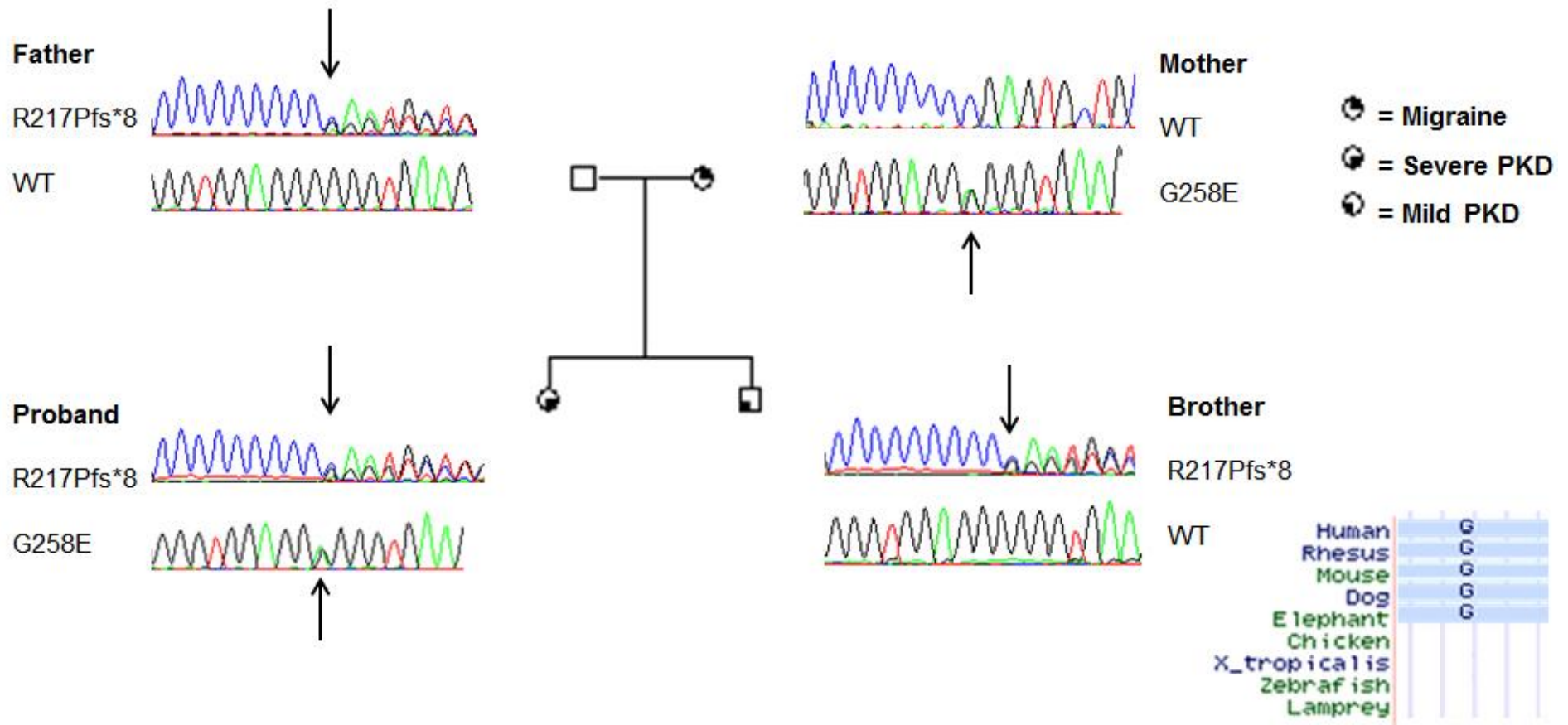


Figure 3.6 – The family tree and chromatograms of patient 3.45, possibly the second ever case of PRRT2 compound heterozygosity. Described in terms of protein change

4.4.2. *PNKD* Mutations

Two previously reported mutations and one novel variation were identified in *PNKD* (Table 3.7, Table 3.10, and Figure 3.7). The previously reported mutations, p.(Ala7Val) and p.(Ala9Val) have been widely seen and are known to be pathogenic (Ghezzi et al. 2009; Shen et al. 2011; Pons et al. 2012). The only other mutation to be reported in the gene is p.(Ala33Pro), thus all known mutations are located in the N-terminal of the protein. The novel mutation identified in this chapter, (c.1022delC p.(Pro341Argfs*3) in patient 3.70), however, was found in the C-terminal, and in a patient with FHM, a completely novel clinical manifestation. The variation segregates in three family members and is absent from all control population databases (a pedigree and chromatogram are shown in Figure 3.3). The variation results in a frameshift and thus a premature stop codon. This will either lead to NMD or a truncated protein. Other reported mutations in the gene are thought to cause a toxic gain of function, so identifying which of these potential disease mechanisms is the case is important in determining the pathogenicity of the mutation.

4.4.3. *SLC2A1* Mutations

Unlike *PRRT2*, there was no predominant mutation seen in the *SLC2A1* cohort; 11 different mutations (shown in Figure 3.8) were seen including two that were seen in two patients each (p.(Thr295Met) and c.998G>A p.(Arg333Gln)). Seven of the mutations have previously been reported as being pathogenic, the remaining four were novel; their potential pathogenicity shown in Table 3.12.

Variation	Polyphen-2	SIFT	MAF EVS	MAF 1000g	MAF ExAC
p.Thr60Met	Possibly damaging (0.823)	Tolerated (0.22)	0	0.0002	0.00002
p.Gly76Val	Probably damaging (1)	Damaging (0)	0	0	0
p.Cys201Arg	Benign (0.165)	Damaging (0.05)	0	0	0
p.Ser285Pro	Probably damaging (1)	Damaging (0)	0	0	0

Table 3.12 – The Polyphen-2, SIFT, EVS, 1000genome and ExAC scores for the novel variants found in *SLC2A1*

Pathogenic mutations in this gene are spread throughout *SLC2A1*; therefore it is difficult to predict the pathogenicity of these variations. However, p.(Gly76Val) and c.856T>C p.(Ser285Pro) are both in mutation hot-spots, as well as both being at the

same amino acid as reported pathogenic mutations themselves (Weber et al. 2008; Mosharov et al. 2015). The changes are also both predicted to be pathogenic, and not present in over 65,000 control genomes. It seems likely that both of these variations are disease-causing, however family members were not available for segregation analysis. Conversely, neither p.(Thr60Met) nor c. 604T>C p.(Cys201Arg) are in the immediate vicinity of other pathogenic amino acids, and their pathogenicity predictions are more ambiguous, as in both cases the programs disagree. However, it is widely believed that this software is unreliable. p.(Cys201Arg) is absent from EVS, 1000genomes and ExAC and segregates in the patient's affected mother and thus is likely to be pathogenic. p.(Thr60Met), however, is present in the population at a very low level, and was found in two unaffected family members, and thus it is unlikely this variation is disease-causing.

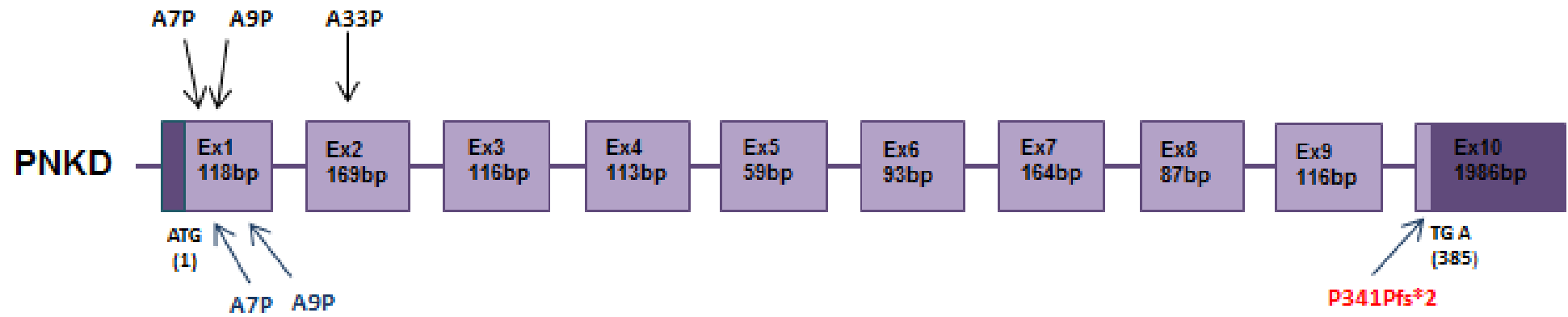


Figure 3.7 – Schematic diagram of PNKD showing mutations that have been previously reported above the gene and mutations found in this study below the gene, (described in terms of protein change, novel mutations are in red)

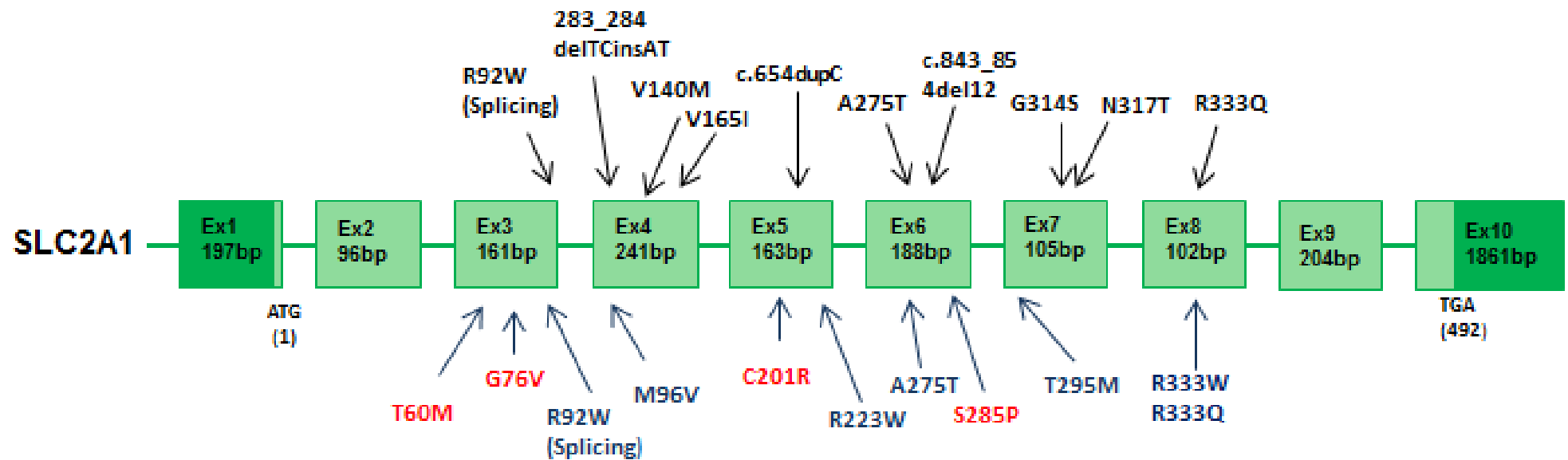


Figure 3.8 – Schematic diagram of SLC2A1 showing mutations that have been previously reported above the gene and mutations found in this study below the gene, (described in terms of protein change unless indicated otherwise, novel mutations are in red)

4.5. Functional Analysis

4.5.1. Over-Expression of Wild type and Mutant PRRT2

As mentioned previously, the majority of mutations in *PRRT2* are thought to cause disease through haploinsufficiency. To investigate this, a vector with an N-terminal HA tag containing either the WT or mutant *PRRT2* gene was transfected into HEK293 cells. The mutations investigated in this way were p.(Arg217Pfs*8), p.(Ser172Argfs*3) and p.(Gly305Trp). The cells were harvested and levels of PRRT2 were determined using a western blot, shown in Figure 3.9 (n=3). The blot shows that, as expected, p.(Arg217Pfs*8) and p.(Ser172Argfs*3) cause a complete reduction in PRRT2 levels, suggesting NMD. This replicates what has previously been shown for the common p.(Arg217Pfs*8) mutation (Lee et al. 2012). p.(Gly305Trp) however, had reduced, but present PRRT2 levels. This is, again, expected, as the mutation does not result in a premature stop codon.

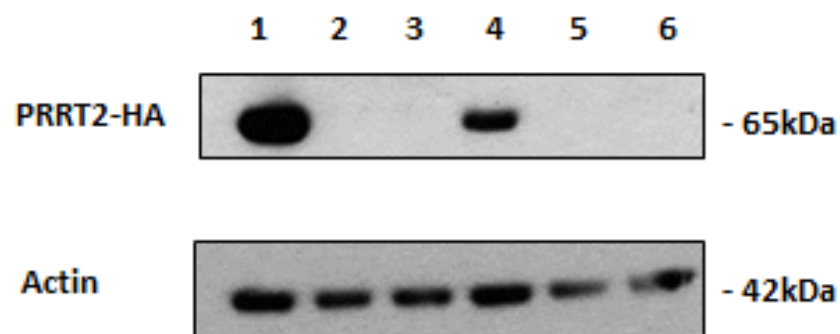


Figure 3.9 – Western blot of HA-tagged PRRT2 expression in soluble fractions of transfected HEK 293 cells. 1=WT, 2=empty vector (negative control), 3= p.Arg217Pfs*8, 4=p.Gly305Trp, 5=p.Ser172Argfs*3, 6=GFP transfection control. Actin was used as a loading control. N=3

4.5.2. cDNA Sequencing to Investigate the Occurrence of Nonsense-Mediated Decay of PRRT2 mRNA

It is known that the majority of *PRRT2* mutations result in NMD, and this has been unequivocally demonstrated at the cDNA level for previously reported mutations Q163X, G192WfsX8 and p.(Arg217Pfs*8) (Wu et al. 2014). To determine whether the novel mutations that we have identified as likely to be pathogenic also caused NMD, cDNA was sequenced from patients in question. Unfortunately, fibroblasts could not be obtained from the patient 3.48 harbouring p.(Cys332insAsp). Both the p.(Gly305Trp)

and p.(*341Leu) mutations were present at the mRNA level, demonstrating nonsense-mediated decay had not occurred. Based on these results, and on the previous study, Figure 3.10 shows the predicted presence or absence of NMD in all of our *PRRT2* mutations and the chromatograms of the cDNA sequencing.

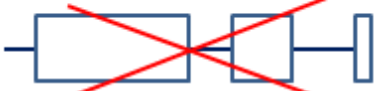
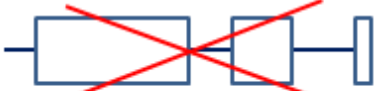
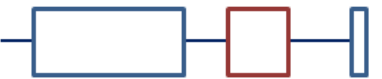
Mutation	Predicted Effect	Predicted PRRT2 Outcome
Wild Type	Normal Protein (cDNA sequencing is normal)	
R217Pfs*8	Has been shown previously that nonsense-mediated decay (NMD) will occur [ref]	
R217X	Predicted NMD (as has been shown for other exon 2 premature stop codon mutations)	
L171Lfs*3	Predicted NMD (as has been shown for other exon 2 premature stop codon mutations)	
R240X	Predicted NMD (as has been shown for other exon 2 premature stop codon mutations)	
G305W	cDNA shows no NMD. Mutation likely to disrupt TM domains	
c.996_998ins GAC	Insertion of polar aspartic acid into hydrophilic TM domain may disrupt region	
c.1011C>T	Likely to disrupt a splice site. Has previously been published as a de novo mutation	
X341L	cDNA shows no NMD. Extended protein may disrupt TM domains	

Figure 3.10 – The predicted consequence of mutations on the PRRT2 protein. Red cross=nonsense-mediated decay, burgundy=mutated exon. Chromatograms show presence of mutation in mRNA, excluding the possibility of nonsense-mediated decay. Changes are described in terms of protein change unless indicated otherwise

4.5.3. cDNA Sequencing to Investigate the Occurrence of Nonsense-Mediated Decay of PNKD mRNA

This study identified the first C-terminal frameshift mutation in PNKD. All mutations identified in the gene to date are gain-of-function. To determine whether this mutation resulted in nonsense-mediated decay or a truncated protein, patient and control cDNA was again sequenced. The mutation was present at the mRNA level of patient 3.70, suggesting nonsense-mediated decay had not occurred and that a functional truncated protein would be formed (Figure 3.11).

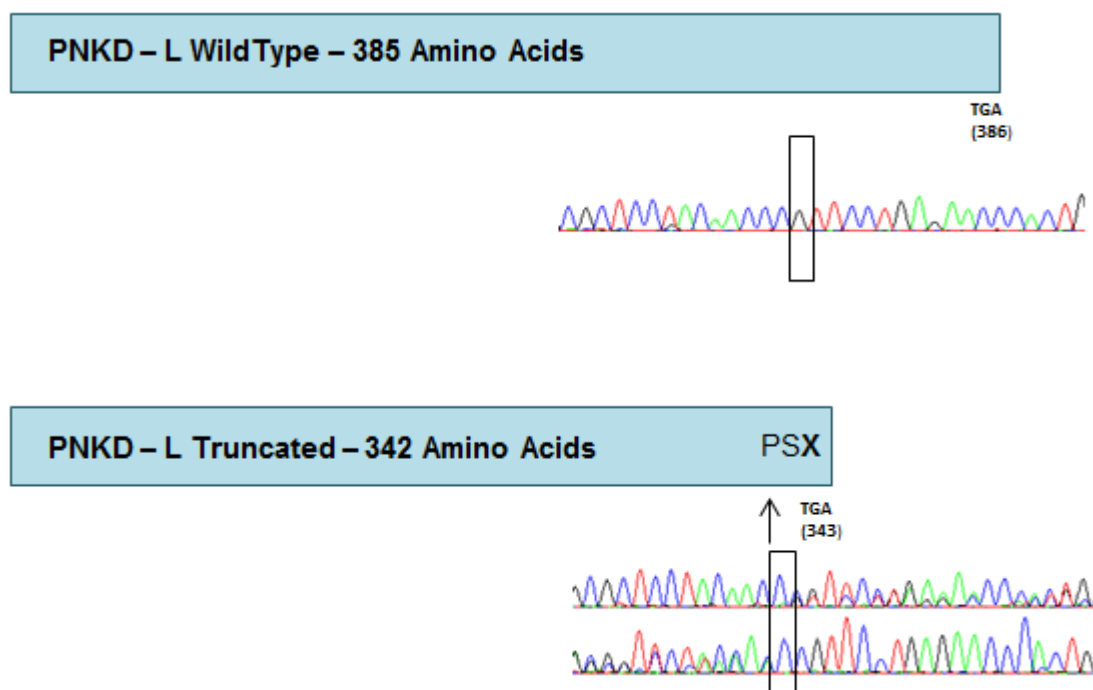


Figure 3.11 – A schematic diagram of the WT and truncated PNKD-L, the result of the *c.1022delC p.(Pro341Argfs*3)* mutation. The cDNA sequencing shows the mutation was present at the mRNA level and so excludes the possibility of nonsense-mediated decay

5. Discussion

In this chapter, a cohort of 159 patients with paroxysmal dyskinesia was screened for mutations in the entirety of the coding regions of *PRRT2* and *SLC2A1* and exons one and two of *PNKD* in the first large-scale sequencing project across all three genes. Mutations were identified in 62 patients, accounting for 39% of the cohort. By far the highest number of mutations was found in *PRRT2*, with mutations found in the gene in

49 patients (79% of mutations identified in PxD cases). This reflects the relatively high frequency of PKD compared to PED and PNKD in the population, and replicates a recent study consolidating all published genetically confirmed PxD cases which found that 75% of reported cases had *PRRT2* mutations (Erro et al. 2014). The same study showed that previously 2% of genetically confirmed PxDs had a mutation in one of the other two genes, and not the gene directly associated with the phenotype. In six patients in this cohort (10%) the mutation was found in one of the other two genes. Therefore, although the mutation is usually in the expected gene, it is considerably more likely that previously thought that the patient may have a mutation in the other PxD genes if the initial screening is negative. This highlights the genetic and phenotypic overlap amongst the PxDs and the importance of screening all three genes.

A further seven mutations in *PRRT2* and *SLC2A1* were identified in a cohort of 55 well-characterised patients with non-PxD episodic disorders including EA, FHM and infantile seizures. Additionally, one FHM patient not included in the cohort was found to have a *PNKD* mutation. No patient from the poorly characterised cohort harboured a mutation, showing the importance of good clinical phenotyping.

Novel phenotypes were identified for all three of the genes. One patient harbouring the common pathogenic *PRRT2* mutation, p.(Arg217Pfs*8), had an episodic ataxia like presentation (patient 3.51 described in results section 4.1.2), previously published by us (Gardiner et al. 2012). This is entirely novel and expands the clinical spectrum of *PRRT2* mutations. Likewise, two patients with *PNKD* mutations had novel phenotypes, although unlike *PRRT2*, *PNKD* is traditionally a phenotypically homogenous gene, with by far the majority of mutations reported causing PNKD. In this study, mutations were identified with patients with PKD and FHM, both again expanding the phenotypic spectrum of *PNKD* mutations.

The novel *PNKD* FHM mutation, P432Pfs*2 found in patient 3.70, is located in exon 10 of the gene, and results in a truncated protein and not nonsense-mediated decay, shown by patient cDNA sequencing (Figure 3.11). Alternate splicing of the *PNKD* results in three isoforms of the protein of varying length; PNKD-S, PNKD-M, (both expressed ubiquitously) and PNKD-L (expressed in the CNS) (Figure 1.6) (Shen et al. 2011). All previously reported mutations are thought to be gain-of-function and are located in 5' end of the gene, found in both PNKD-L and PNKD-S but not PNKD-M. As this mutation results in a truncated protein it is also likely to cause a gain-of-function disease mechanism, but, instead affects PNKD-L and PNKD-M. Additionally, it could disrupt the enzymatic domain that is present at the C-terminal of these transcripts. These factors could explain the novel phenotype of our family.

It is well established that *SLC2A1* is a highly phenotypically heterogeneous gene, as mutations in it can lead to classic PED, GLUT1 DS1, seizures alternating hemiplegia of childhood and intellectual disability, and in one case, a presentation of episodic ataxia (Ohshiro-Sasaki et al. 2014). Therefore, it is unsurprising that the thirteen patients harbouring *SLC2A1* mutations displayed a wide phenotypic range. Eleven of the patients had a PxD, six being the expected PED (only three without additional features). One had PNKD, three PKD, and one had myotonia with dystonia. PNKD has previously been reported in conjunction with this gene in two cases, therefore it is a known rare phenotype. PKD patients, however, have not been previously found with *SLC2A1* mutations, so this is a new clinical manifestation for the gene. Three of the Nine PxD cases had associated seizures or migraines; this is a common occurrence for *SLC2A1* mutations. Patient 3.58, discussed in results section 4.1.5, showed weakness on a McManis test. This is highly novel for *SLC2A1* mutations, and is an important finding as there are several genetically undiagnosed patients with similar McManis test results who could share a similar genetic basis.

While ataxia can often feature as part of the spectrum of GLUT1 DS1, it has only been seen as the sole presentation in one report (Ohshiro-Sasaki et al. 2014). In this study, two patients with *SLC2A1* mutations (patients 3.68 and 3.69) from the non-PxD cohort presented with episodic ataxia. Therefore, *SLC2A1* mutations may be a more common cause of EA than previously thought, and should be considered for EA patients if other genes are negative.

Interestingly four of the mutations had previously been reported to cause GLUT1 DS1, whereas here they were responsible for a movement disorder. Traditionally PED and GLUT-1 DS1 have been considered as distinct allelic disorders, however, it is increasingly being recognised that they are in fact both part of the same broad spectrum of GLUT1 phenotypes, due the range of clinical manifestations that have been described in recent years (Pearson et al. 2013). It has been suggested that there are three broad groups of symptoms caused by *SLC2A1* mutations – epilepsies, movement disorders and cognitive/behavioural disturbances. A patient with GLUT-1 DS could have symptoms from any of the groups, and will have symptoms from all three if they present with traditional GLUT-1 DS1 (Pearson et al. 2013). There is evidence that the severity of the condition is related to the level of reduction in glucose transport; 50% reduction (for example, a heterozygous nonsense mutation) results in classic GLUT1 DS1, whereas a 25% reduction results in a milder, episodic phenotype where glucose levels are sufficient unless reduced by exercise or fasting (Rotstein et al. 2010). However, as seen in this study, the same mutation can result in a range of

phenotypes and severities, thus there must be additional genetic and environmental factors involved (Leen et al. 2010).

Patient 3.3 was found to harbour both a novel *PRRT2* variation of unknown significance (p.Pro216His) and a known pathogenic *SLC2A1* mutation (p.Arg333Gln). This patient had atypical PKD, with longer episodes of dystonia and unusual tongue dystonia. As the *SLC2A1* mutation is known to be disease-causing, it is a safe assumption that this is contributing to the phenotype. It is unclear, however, what, if any, contribution p.(Pro216His) has towards the disease, and further investigation would be required to determine this. However, it is possible that the variation could account for the unusual PKD phenotype, in the first recorded case of a digenic paroxysmal dyskinesia. This patient should undergo an additional retrospective clinical assessment to more fully determine their phenotype in light of the genetic results. This finding again emphasises the importance of screening all three genes in these patients.

Additionally this study identified the second ever case of compound heterozygosity in *PRRT2* mutations in a family with a pair of affected siblings harbouring the common p.(Arg217Pfs*8) mutations inherited from their asymptomatic father. The more severe of the siblings, patient 3.45, also had p.(Gly258Glu), from the maternal line, where there is a family history of migraine (Figure 3.6). It is possible p.(Gly258Glu) could be modifying the phenotype of the proband to produce a more severe condition; it could disrupt the remaining copy of the protein left after NMD. Homozygous patients with severe phenotypes including mental retardation and EA have been reported, as well as one compound heterozygous case where p.(Arg217Pfs*8) was accompanied by a whole gene deletion (Delcourt et al. 2015). They would all result in no *PRRT2* protein remaining. This case, however, could be the first ever patient where one altered copy of the protein was present. The contribution of p.(Gly258Glu) to the maternal family history of migraines is unclear.

It was hypothesised that, as *PRRT2* is known to interact with the synaptic protein SNAP25 (Lee et al. 2012), that mutations in this gene could also cause paroxysmal dyskinesias. However, screening of the gene in 95 PxD-gene negative PxD patients did not identify any likely disease causing mutations. This could be because the important function of the protein means that mutations only cause the more severe previously reported condition congenital myasthenia (Shen et al. 2014). Alternatively, if the gene is cause of paroxysmal dyskinesias, it is clear that it is a very rare cause.

For several *PRRT2* mutations the protein effect was investigated. This was performed in two ways, either by over-expression and western blot, or by extraction of

patient mRNA and cDNA sequencing. The *PRRT2* exon two frameshift mutations p.(Arg217Pfs*8) and p.(Ser172Argfs*3) resulted in loss of protein (Figure 3.9), and the *PRRT2* mutations p.(Gly305Trp) and p.(*341Leu) resulted in altered proteins and not NMD (Figure 3.10). These results are as expected.

Whilst there is a great deal more to be understood, it seems likely that these three paroxysmal genes are acting on similar, possibly overlapping pathways, and thus can produce similar clinical manifestations. It has recently been reported that overexpression of wild-type PNKD in rat hippocampal cultures reduced neurotransmitter release in comparison to an empty vector, whereas overexpression of mutant PNKD did not. This suggested that PNKD has a role in regulating presynaptic exocytosis (Lee et al. 2015). It is also known that *PRRT2* interacts with *SNAP25*, a protein important in facilitating synaptic exocytosis (Lee et al. 2012). Therefore, we suggest a possible disease mechanism whereby both PNKD and *PRRT2* perform similar roles in restricting synaptic exocytosis. Disease causing mutations that either reduce levels of *PRRT2* or disrupt PNKD function reduce this restriction and result in excessive neurotransmitter release (Figure 3.12). It is unclear how *SLC2A1* mutations contribute to this theory, but it has been shown that they result in reduced glucose transport into the brain, so perhaps glucose is also involved in the regulation of exocytosis. There may also be overlap with other channelopathy genes such as *KCNA1*, *CACNA1A* and *SNAP25*. Interestingly, regional brain mRNA expression data shows correlating patterns for *PRRT2*, *CACNA1A*, *KCNA1* and *SNAP25* suggesting they could be operating in similar pathways. They share highest expression levels in the cerebellum, and with frontal, temporal and occipital cortices also featuring amongst the highest levels (Figure 3.13 – worked carried out by Daniah Trabzuni). However, although the *PNKD* expression pattern is similar, the cerebellar expression is unexpectedly the second lowest of all 10. Strangely, the *SLC2A1* pattern is reversed in comparison to the other genes with the highest expression regions being the substantia nigra and medulla. The functional consequences of these regional expression disparities remain to be seen but could indicate that *SLC2A1* and PNKD pathways are related more to dystonic genes located in the basal ganglia and brainstem.

This chapter has expanded the broad phenotypic spectrum of these paroxysmal movement disorders, suggesting where possible, as part of the investigative workup, all three genes should be analysed in these conditions. This study also emphasises the genetic and phenotypic overlap of the paroxysmal dyskinesias with other episodic disorders such as patients with episodic ataxia and familial hemiplegic migraine.

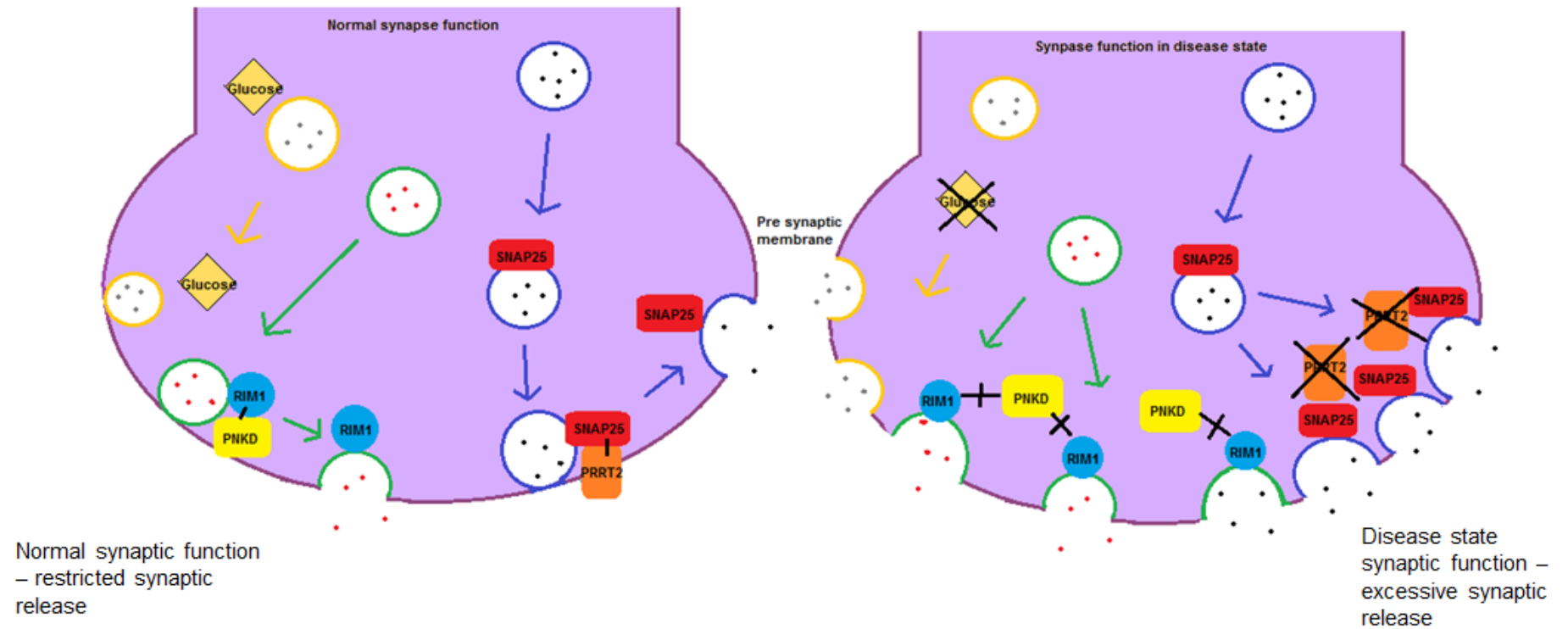


Figure 3.12 – A suggested mechanism for the paroxysmal dyskinesias, where mutations in PRRT2, PNKD and SLC2A1 result in disruption of neurotransmitter release regulation and thus excessive synaptic release. Circles indicate pre-synaptic vesicles containing neurotransmitter (dots). Yellow vesicles are affected by SLC2A1, green by PNKD and blue by PRRT2

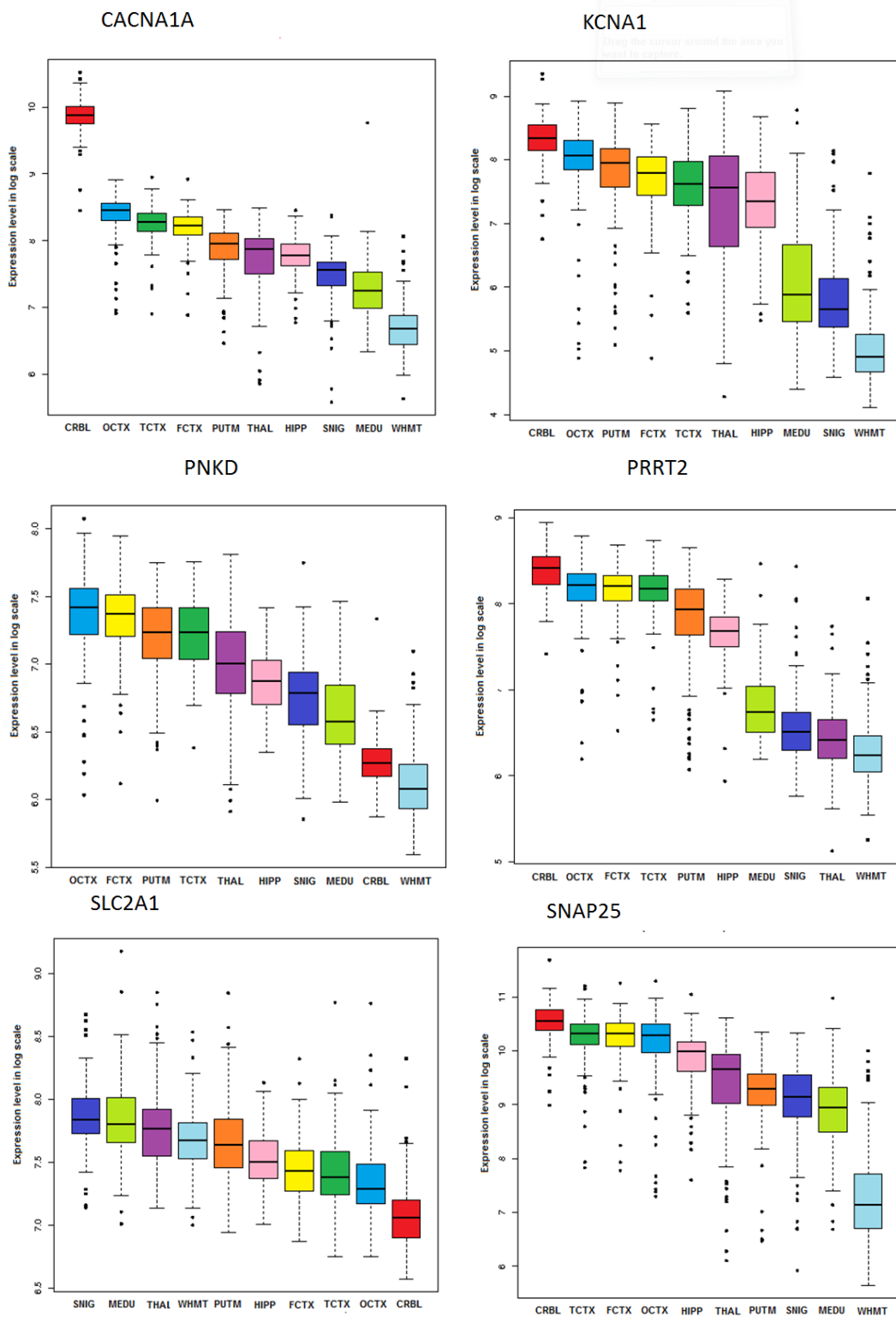


Figure 3.13 Regional distributions of CACNA1A, KCNA1, PNKD, PRRT2, SLC2A1 and SNAP25 mRNA expression in the normal human brain. Brain regions included in the analysis: red – cerebellum (CRBL), yellow - frontal cortex (FCTX), pink - hippocampus (HIP), light green - medulla (MEDU), mid blue - occipital cortex (OCTX), orange - putamen (PUTM), dark blue - substantia nigra (SNIG), dark green - temporal cortex (TCTX), purple - thalamus (THAL) and light blue - white matter (WHMT). This analysis was carried out by Daniah Trabzuni as part of a projet with UK Human Brain Expression Consortium (Trabzuni et al. 2011).

Chapter 4: Investigating Channel Panels for Diagnosis of the Channelopathies

1. Introduction

The channelopathies are a rare group of diseases caused by mutations in voltage-gated ion channel genes, resulting in channel dysfunction. They are phenotypically variable but share common features such as episodic or paroxysmal attacks interspersed with periods of normal nerve/ muscle function, no loss of consciousness during attacks and an autosomal inheritance pattern. There are two main classes of channelopathy, depending on the expression profile of the channel in question; if the channel is found in neurones in the brain it will cause a neuronal channelopathy, whereas if found in skeletal muscle, it will instead result in a skeletal muscle channelopathy.

The skeletal muscle channelopathies exist in a spectrum from episodic attacks of weakness (periodic paralysis) to stiffness (myotonia congenita), as shown in Figure 1.4a. There are five main genes responsible (*SCN4A*, *CACNA1S*, *CLCN1*, *KCNJ2*, *KCNJ18*), although there is genetic and phenotypic heterogeneity, which is summarised in Table 1.5. This can make genetic diagnosis difficult, as it is not always easy to identify the causative gene. Furthermore, the genes are large and mutations can be concentrated in hotspots, so deciding which exons to screen is not straightforward. The current strategy for genetic diagnosis is shown in Figure 1.4b (Rayan and Hanna 2010).

The neuronal channelopathies are also difficult to diagnose genetically. Patients present with symptoms such as episodic attacks of ataxia, and migraine, which can be hemiplegic or be preceded by aura. The paroxysmal dyskinesias are included in this work, as they too share features listed above, and can also be accompanied by migraine or aura. The neuronal channelopathies exhibit even more genetic

heterogeneity than the skeletal muscle channelopathies, with at least seven genetic causes for the EAs (Table 1.7) and three for FHM. The genes involved in the neuronal channelopathies are summarised in Table 1.6, and their phenotypic and genetic heterogeneity is shown in Figure 1.5.

Traditionally, all of these disorders are genetically diagnosed by sequential Sanger sequencing of candidate genes until a mutation is found. This is an inefficient and costly method of gene screening.

2. Chapter Aims

The current method of genetic diagnosis for both the neuronal and skeletal muscle channelopathies is slow, costly and inefficient. Here, Illumina's TruSeq Custom Amplicon (TSCA) technology will be used to design two custom sequencing panels; one that will screen all of the neuronal channelopathy genes simultaneously for 95 patients (referred to as the brain channel panel), and one that will do the same for the skeletal muscle channelopathies (referred to as the muscle channel panel). These panels will be trialled on cases and controls. The technology will be evaluated in terms of coverage, sensitivity, specificity and clinical benefit (defined here as the identification of mutations that would have been missed by Sanger sequencing), to establish its advantage over Sanger sequencing, and ultimately, its feasibility for implementation into a diagnostic lab. Interesting findings arising from the trials that contribute to the genetic knowledgebase surrounding the channelopathies will also be discussed.

3. Patients and Methods

3.1. Patients

3.1.1. Patients and Controls used for the Brain Channel Panel Trial

Included in the 95 samples were 79 patients with genetically undiagnosed brain channelopathies or movement disorders, as well as 16 positive controls with known disease causing mutations. The control group contained a mixture of missense mutations, nonsense mutations, splice-site mutations, small insertions or deletions and large scale mutations, which were located throughout the genes.

3.1.2. Patients and Controls used for the Muscle Channel Panel Trial

Similarly, in the 95 samples selected to trial the muscle channel panel were 16 positive controls harbouring a range of known disease-causing mutations. However, there were only 69 genetically undiagnosed skeletal muscle channelopathy patients. The final 10 samples were patients with myotonia congenita, but in whom only one recessive mutation had been identified, in the hope that another mutation in a different gene could be discovered. Unlike the brain panel patients, the genetically undiagnosed patients have been given a clinical 'likelihood' rating of the probability of their having a mutation in the muscle channelopathy genes. This is to ascertain the correlation between the perceived clinical chance of them having a mutations and their chance of genetic diagnosis. The four groups and the distribution are 'very probable' (22%), 'probable' (19%), possible (26%) and low probability (33%).

3.2. Panels

3.2.1. Panel Design

Both the brain and muscle channel panels were designed using the Illumina Design Studio online software (<http://designstudio.illumina.com/>). To use this software the user must upload the genomic coordinates of the targets to be sequenced, or else enter the names of the genes of interest. The software then designs oligonucleotides to sequence the targets in amplicons of 250bp, which can be ordered from Illumina. A screenshot of the software (a) and an example of how the amplicons cover a gene (b) are shown in Figure 4.1. Exact details of each of the panel designs are discussed in the results section of this chapter.

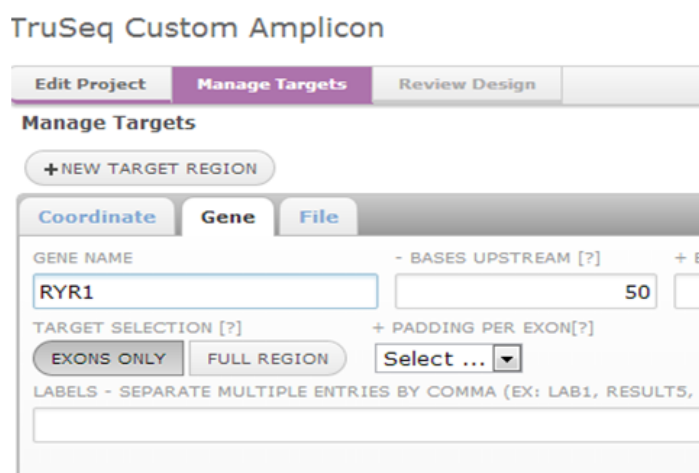
3.2.2. Library Preparation and Sequencing

95 patients or controls were used on each of the panels. 250ng of DNA was used for the library preparation for each sample; details of how the libraries were prepared and loaded onto the Illumina Miseq are given in section 4.1 of the materials and methods chapter.

3.2.3. Primary Data Analysis and Coverage Determination

Primary data analysis was carried out by Dr Alan Pittman, as described in section 4.4 of the materials and methods chapter. Percentage coverage at 20x of target exons was determined as described in section 4.6 of the same chapter with the help of Dr Joshua Hersheson.

a)



b)



Figure 4.1 – (a) Screenshot of Illumina Design Studio software and (b) example of designed amplicons covering the PRRT2 gene

3.2.4. Variant Filtering

For both panels, initially synonymous variants, which were not likely to affect splicing, were filtered out on the assumption that as they would not alter the protein structure they would not be disease causing. For the brain panel, a fully-penetrant, autosomal dominant inheritance model was adopted, and thus variants were filtered against $MAF \geq 0.01$ using 1000genomes and the exome variant server (both are discussed in section 4.2.2. of the introduction). For the muscle panel, the same filters were applied, with the exception of *CLCN1* variants, which can be recessive, and so a $MAF \geq 0.1$ filter was used. For this trial, depth or quality filters were not used, with the rationale that it was better to confirm false positives than miss real mutations. Any remaining variants that were present in more than 5% of samples were assumed to be artefacts of the library preparation and excluded.

3.2.5. Variant Confirmation

Variants remaining after the filtering process were confirmed using Sanger sequencing, using the protocols described in section 2 of the materials and methods chapter.

3.3. Sensitivity and Specificity Calculations

Sensitivity, also known as the true positive rate, measures the amount of positive controls identified by a test in comparison to the number of false positives (the positive controls that were not identified in the test). It is calculated by the following equation:

$$\text{Sensitivity} = \frac{\text{Number of true positives}}{(\text{Number of true positives} + \text{Number of false negatives})}$$

Specificity, on the other hand, measures false positives, and thus is known as the true negative rate. It calculates the number of real negative results in a test in comparison to the amount of false positives (mutations that were identified but not real upon Sanger sequencing) using the equation:

$$\text{Specificity} = \frac{\text{Number of true negatives}}{(\text{Number of true negatives} + \text{Number of false positives})}$$

4. Results

4.1.1. Brain Channel Panel Design

The genes included in the brain channel panel are shown in Table 4.1. They are the genes most associated with the neuronal channelopathies, with an emphasis on the episodic ataxias and paroxysmal movement disorders, as these patients comprise the majority of the cohort for this study. In the first instance, the genomic coordinates for the coding exons for each of the genes were used, plus or minus 25bp to allow for coverage of splicing variants and to ensure the entirety of the exon was covered. If this approach could not produce amplicon designs, for example if the targets were too GC rich, the given coordinates were shifted slightly in a process of trial and error until a design was realised. Three exons could not have amplicons designed against them; these were exons 36, 37 and 38 of *CACNA1A*. A further two exons had partial coverage gaps; *CACNA1A* exons 19 and 20. The metrics for the final brain channel panel design are shown in Table 4.2, and the coordinates of the amplicons and targets can be found Appendix 1.

4.1.2. Muscle Channel Panel Design

Ideally, the five genes known to cause the skeletal muscle channelopathies would have been included in the muscle channel panel (Table 1.5). However, it was impossible to design amplicons against *KCNJ18*, the gene recently found to be a cause of thyrotoxic

periodic paralysis. This was because the gene is 98% similar to the homologous gene *KCNJ12*, and so amplicons could not be designed that would distinguish between the two. Therefore, only the four other genes were included, shown in Table 4.3. The muscle channel panel was designed in the same way as described above for the brain channel panel. There were no exons that could not have amplicons designed against them. Three exons had partial gaps in coverage; these are *CLCN1* exons 11 and 21, and *SCN4A* exon 6. The muscle channel panel design metrics are shown in Table 4.4, and the coordinates of the amplicons and targets can be found in Appendix 2.

Gene	Associated disease	N° Target exons	N° Amplicons
<i>PRRT2</i>	PKD	3	7
<i>CACNA1A</i>	EA2/ FHM/ SCA6	47	66
<i>KCNA1</i>	EA1	1	10
<i>CACNB4</i>	EA5	14	18
<i>SLC2A1</i>	PED/ GLUT1 DS1	10	16
<i>SLC1A3</i>	EA6	10	16
<i>PNKD</i>	PNKD	10	13
<i>KCNK18</i>	Migraine	3	9

Table 4.1 – Genes, exons and amplicons included in the brain channel panel

Total number of target exons	98
Number of exons missed	3
Number exons with coverage gaps	2
Number of target bases	20,429
Number of bases missed	513
% of target covered	97.4%
Total number of amplicons	155

Table 4.2 – The final brain channel panel design metrics

Gene	Associated disease	N° Target exons	N° Amplicons
<i>CLCN1</i>	Myotonia congenita	23	37
<i>SCN4A</i>	PMC/ SCM/ HyperPP/ HypoPP	24	69
<i>CACNA1S</i>	HypoPP	44	73
<i>KCNJ2</i>	Andersen – Tawil syndrome	1	36

Table 4.3 – Genes, exons and amplicons included in the muscle channel panel

Total number of target exons	92
Number of exons missed	0
Number of exons with coverage gaps	3
Number of target bases	30,625
Number of bases missed	150
% of target covered	99.5%
Total number of amplicons	215

Table 4.4 – The final muscle channel panel design metrics

4.2. Brain Channel Panel Results

The brain panel was run on the patients and controls discussed above. The positive controls and false positive rates were used to determine the sensitivity and specificity of the panels. The mutations found were analysed in terms of pathogenicity and thus the clinical benefit of the panel was determined. Lastly, the panel's coverage of the target exons was established.

4.2.1. Positive Controls

16 positive controls were used on the brain panel, of which 11 were identified, therefore 69% of positive controls were found; they are shown in Table 4.5. Therefore the sensitivity for this panel is 0.69. There were two main reasons why the control mutations were not picked up by the panel. The first was that the mutation was a large deletion; in one case of one exon, in the other of a whole gene. Both are bigger than the amplicon size of 250bp, so would have meant that entire amplicons were not sequenced. These CNVs can be identified by some NGS analysis pipelines, but were not by the pipeline used here. Secondly, the remaining three missed mutations were all in the same area of *PRRT2*, in a region with poor coverage. This reflects a bias in the control mutation selection. Ideally, control mutations from each of the panel genes would have been used. However, unfortunately only mutations from four of the genes were available at the time of the panel trial, and so some of the mutations were concentrated into small genomic areas. If repeated, care would be taken to ensure each control mutations at least represented a different amplicon.

Gene	Mutation type/ mutation	Found by panel?	Reason not found
<i>CACNA1A</i>	Missense/ Gly405Arg	Yes	-
<i>CACNA1A</i>	Missense/ p.Arg1345Gln	Yes	-
<i>CACNA1A</i>	Missense/ p.Arg1433Trp	Yes	-
<i>CACNA1A</i>	Splicing/ c.3989+1G>A	Yes	-
<i>CACNA1A</i>	CNV/ Deletion of exon 27	No	Large scale deletions not identified
<i>KCNA1</i>	Missense/ p.Cys185Trp	Yes	-
<i>KCNA1</i>	Missense/ p.Thr226Arg	Yes	-
<i>KCNA1</i>	Missense/ p,Ile229Thr	Yes	-
<i>KCNA1</i>	Missense/ p.Ile1407Met	Yes	-
<i>KCNK18</i>	Deletion/ p. Phe139Trpfs*24	Yes	-
<i>PRRT2</i>	Deletion/ p.Ser172Argfs*3	No	<i>PRRT2</i> region not covered
<i>PRRT2</i>	Missense/ p.Pro216Leu	No	<i>PRRT2</i> region not covered
<i>PRRT2</i>	Insertion/ p.Arg217Pfs*8	No	<i>PRRT2</i> region not covered
<i>PRRT2</i>	Insertion/ p.Cys332insAsp	Yes	-
<i>PRRT2</i>	Missense/ p.Gly305Trp	Yes	-
<i>PRRT2</i>	CNV/ Whole gene deletion	No	Large scale deletions not identified

Table 4.5 – The positive controls included on the brain channel panel and details of if, and why they were not identified

4.2.2. False Positive Calls

The filtering process left 27 variants from the 79 patient samples. All of these were sequenced using Sanger sequencing, despite some having low quality/ depth scores, as these calls were not filtered out. 15 were confirmed, thus 12 of the 27 were not real variants, and so could be classed as false positives. However, if a standard quality filter of ≥ 70 and a depth filter of 5 had been used, only one would have remained, therefore, for the purpose of this analysis, the panel produced one false positive call. This meant that, using standard quality and depth filters, the specificity of the brain channel panel is 0.94. Furthermore, all true variants had a quality score of 99 (out of 100), and so a quality cut off that was more stringent than 70 could have been used to produce no false negatives, whilst still keeping all true variants.

4.2.3. Patient Results

There were 15 real heterozygous variants found by the brain channel panel (14 distinct variants) in 15 patients that were rare and affected the amino acid sequence. Patients in whom no variants (after filtering) were identified are listed in Appendix 3. The variants found are listed, along with Polyphen-2 and SIFT predictions, as well as population frequency information, in Table 4.6. Sanger sequencing chromatograms are shown with the visualisation of the mutation using a genome browser for a selection of the mutations found in Figure 4.2. Four mutations (patients 4.1, 4.2, 4.6, and 4.16) have previously been reported to be pathogenic, three in *CACNA1A* and one in *PRRT2*, and all are presenting with the expected phenotype, and so are undoubtedly causative. Interestingly however, c.904G>A p.(Asp302Asn) was previously reported to cause a non-episodic, progressive ataxia, whereas here, it is causing EA2. There were three further variations identified in *CACNA1A*, all in patients with an expected EA phenotype. Two are nonsense changes which will result in a premature stop codon and either a truncated protein or nonsense mediated decay, thus these are both likely to be pathogenic. The remaining mutation, c.4202G>A p.(Gly1401Glu) is more ambiguous, but as it is absent from all three control databases, is predicted to be pathogenic and is causing an expected phenotype, again it is likely to be pathogenic.

One unreported variant, c.917C>T p.(Ser306Phe), was found in *KCNA1* in patient 4.7. This was again absent from the three control databases and predicted to be pathogenic. Furthermore, it is next to two pathogenic amino acid positions, as c.913C>T p.(Leu305Phe) and c.919C>T p.(Arg307Cys) both cause EA1 (Poujois et al. ; Graves et al. 2010). These factors all strongly indicate that this variant could be disease-causing, however, the phenotype, PKD, is novel for *KCNA1*. This could therefore be a new clinical presentation for the gene.

Two variations were found in *KCNK18*. The first in patient 4.8 is c.361insT p.(Tyr121Leufs*44), a frameshift resulting in a stop codon after 44 amino acids. This is present in EVS, but at an extremely low level; it has only been seen in one of the 6500 controls (MAF = 0.00008). However, there is a higher frequency within the other population databases as MAF = 0.003 in both ExAC and 1000genomes. Again, the presentation is novel for the gene, as the patient has PKD. It is unclear whether this mutation is contributing to the disease. The second, c.328T>C p.(Cys110Arg), was found in three patients with a mix of phenotypes, although none previously associated with *KCNK18* (patients 4.10, 4.11 and 4.12). This variation was present in EVS, 1000genomes and ExAC (MAF = 0.006, 0.0037 and 0.0069 respectively). Functional investigation has previously shown that the variant results in a complete loss of

channel current, however, in the study it was used as a control variation that was not present in affected patients (Andres-Enguix et al. 2012). Thus it is likely that it is benign, nevertheless it is interesting that it was found in three patients here, a higher number than would be expected by chance given the low population frequency. In an additional side-project in which 44 patients with FHM were screened for mutations in the *KCNK18* gene, variations were found in two patients. The first had the mutation initially described when the gene was linked to migraine, c.414_415delCT, p.(Phe139Trpfs*24), for which MAF = 0.0003 and 0.0006 in EVS and ExAC respectively. In the second c.218A>C p.(Glu73Ala) was identified, a variant that has MAF = 0.002 in 1000genomes, absent from EVS, and has MAF = 0.0009 in ExAC. Given the ambiguity surrounding the pathogenicity of *KCNK18* mutations, the clinical relevance of these variations is, again, unclear.

One mutation was found in each of *CACNB4* and *SLC2A1* (c.52G>C p.(Gly18Arg) and c.1238T>A p.(Leu413Gln) respectively), both with an EA phenotype. Both of these variations were absent from control databases, and pathogenicity predictions were mixed. Patient 4.13, harbouring the *CACNB4* variation, presented in her thirties with right-sided facial weakness, dysarthria torticollis. She subsequently had several daily attacks; the severity appeared to be related to her menstrual cycle. She underwent several genetic and functional investigations and was negative for EA1 and 2, FHM1, PP and SCA6, and additionally had normal EEG, EMG, and McManis testing. There was a family history of headaches, but hers seemed to be unrelated to her attacks. The patient was diagnosed with hemiplegic migraine. To date, only one family has previously been reported to have a mutation in this gene, resulting in long attacks of ataxia (Escayg et al. 2000), therefore if this mutation was disease causing, it would be an important finding, as it would be a novel phenotypic presentation and only the second ever reported *CACNB4* case. As this mutation is assumed to be de novo, genetic analysis of the gene in her parents will give a good indication of the pathogenicity of the change, and this sequencing will be carried out when parental DNA is available.

SLC2A1 mutations cause GLUT1 DS, and EA can be a feature of, and in one case the sole presentation of, the syndrome (Ohshiro-Sasaki et al. 2014). Therefore, it is probable that the mutation in patient 4.12, who presented with a complex episodic ataxia, is responsible for their phenotype.

The last variation discovered by this brain panel was c.919G>A p.(Glu307Lys) in *PNKD* (patient 4.15). This variation is present at a low frequency in the control populations (MAFs: EVS = 0.00054, 1000genomes = 0, ExAC = 0.001) and the *in silico*

predictions contradict each other, thus it is unclear whether the mutation is pathogenic. The phenotype is FHM, a completely novel phenotype for the gene; however, mutations in the PKD gene, *PRRT2* can cause FHM. Additionally, a C-terminal frameshift PNKD mutation, c.1022delC p.(Pro341Argfs*3) was identified in a patient with an FHM-like presentation in Chapter 3 of this thesis. This mutation is in the same region as p.(Glu307Lys) (and separate from all reported PNKD mutations at the N-terminal), so could be having a similar effect as p.(Glu307Lys), thus resulting in a similar clinical presentation. Further functional characterisation is needed to confirm this speculation.

For all of the unpublished variations discussed above, pathogenicity is only speculated upon, and thus either functional data or segregating family members would be required to prove the mutation's impact.

Patient	Gene	Mutation	Previously reported? (reference)	PolyPhen – 2 prediction	SIFT prediction	Phenotype	MAF EVS/ 1000 genomes/ ExAC	Atypical phenotype?	Probably pathogenic?
4.1	CACNA1A	p.Asp302Asn	Yes (Bürk et al. 2014)	Pr D (1)	D (0)	EA2	0/ 0/ 0	No	Yes
4.2	CACNA1A	p.Thr666Met	Yes (Ophoff et al. 1996)	Pr D (1)	D (0)	FHM	0/ 0/ 0	No	Yes
4.3	CACNA1A	p.Arg1352*	No	-	-	EA2	0/ 0/ 0	No	Yes
4.4	CACNA1A	p.Gly1401Glu	No	Pr D (1)	D (0)	EA2	0/ 0/ 0	No	Yes
4.5	CACNA1A	p.Lys1937*	No	-	-	EA	0/ 0/ 0	No	Yes
4.6	CACNA1A	c.3992+1G>A	Yes (Ophoff et al. 1996)	-	-	EA2	0/ 0/ 0	No	Yes
4.7	KCNA1	p.Ser306Phe	No	Pr D (1)	D (0)	PKD	0/ 0/ 0	Yes	Yes
4.8	KCNK18	p.Tyr121Leu fs*44	No	-	-	PKD	0.00008/ 0.003/ 0.003	Yes	Unclear
4.9	KCNK18	p.Cys110Arg	Yes – although pathogenicity is unclear (Andres-Enguix et al. 2012)	Pr D (1)	D (0.01)	EA	0.006/ 0.002/ 0.007	Yes	No
4.10						Complex EA		Yes	
4.11						PNKD		Yes	
4.12	SLC2A1	p.Gly18Arg	No	B (0.036)	T (0.11)	Complex EA	0/ 0/ 0	Yes	Yes
4.13	CACNB4	p.Leu413Gln	No	Pr D (1)	T (0.3)	HM	0/ 0/ 0	Yes	Yes
4.14	PRRT2	p.Arg240*	Yes (Lee et al. 2012)	-	-	PKD	0/ 0/ 0	No	Yes
4.15	PNKD	p.Glu307Lys	No	Po D(0.85)	T (0.25)	EA	0.00054/ 0/ 0.001	Yes	Unclear

Table 4.6 – Possible pathogenic mutations identified by the brain channel panel. Pr D=probably damaging, Po D=possibly damaging, D=damaging, B=benign, T=tolerated

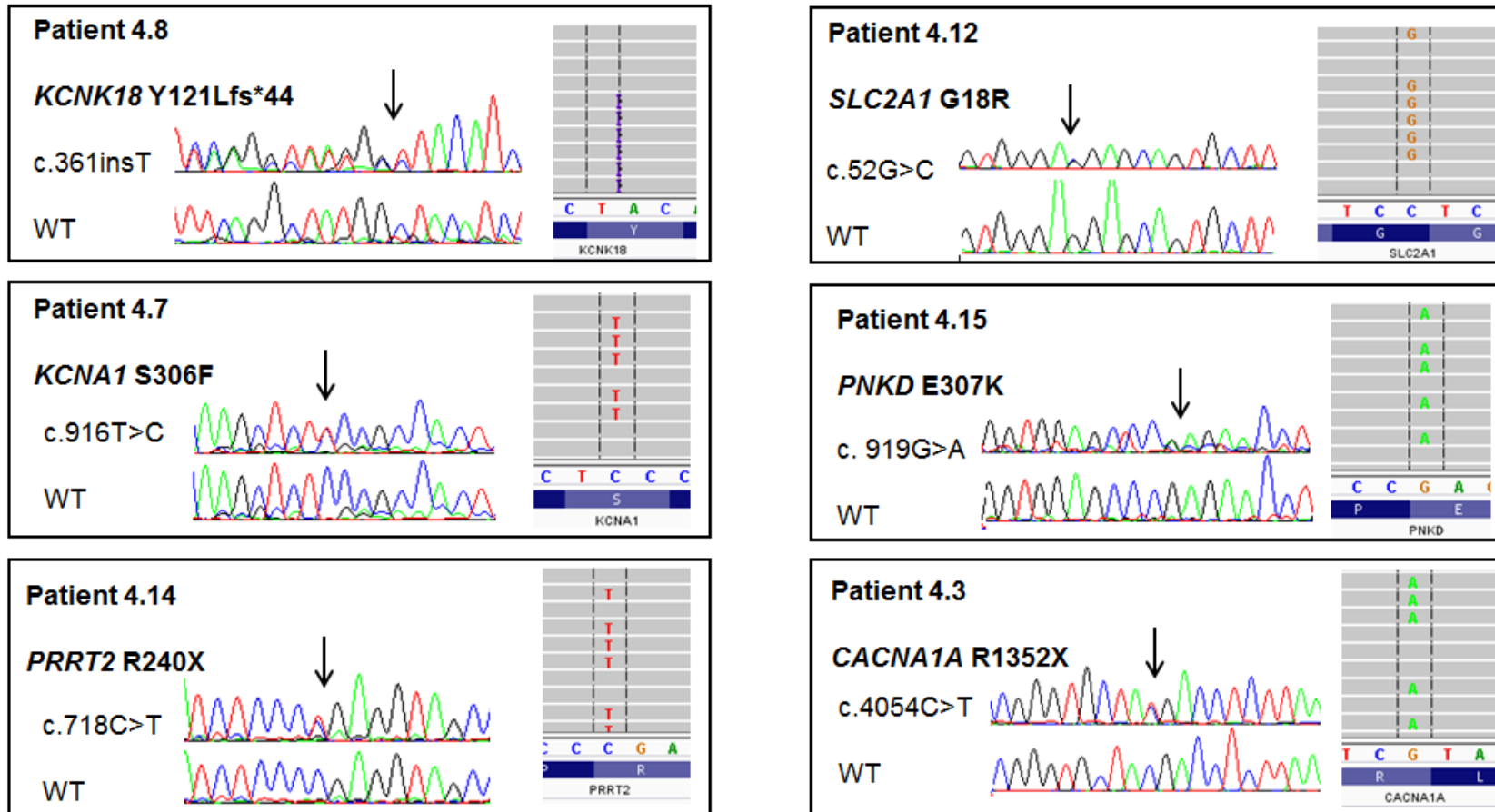


Figure 4.2 – Chromatograms and genome browser visualisations of a selection of mutations (described in terms of the protein change) found by the brain channel panel. CACNA1A is on the reverse strand and therefore the genome browser shows the reverse complement of the mutation. The genome browser used was IGV (www.broadinstitute.org/igv/)

4.2.4. Clinical Benefit

The brain channel panel identified definite or possible pathogenic mutations in 12 patients, which is 15% of the cohort. Of these patients, five had an 'atypical phenotype' i.e. the mutation found would not have been identified by routine diagnostic Sanger sequencing because the gene would not have been screened. This is 6% of the cohort and 42% of the mutations found. Therefore, the brain panel has notable clinical benefit over the equivalent Sanger sequencing in terms of mutation identification.

4.2.5. Coverage

Taking an average of every sample, the overall percentage of the bases in target exons covered by at least 20x is 81%, a much lower figure than the 97% predicted in the panel design. This percentage includes the three exons that could not have amplicons designed against them (*CACNA1A* exon 36, 37, and 38); if these are excluded the figure rises to 82%. Excluding these three exons, of the 95 target exons, only 48 had 100% coverage at 20x (51%), although 69 exons (73%) had at least 90% coverage. Only one exon (*CACNB4* exon one) was not sequenced at all (therefore failed) for all samples, however eight (8%) failed in at least 20 samples. The percentage coverage distribution over the exons of each gene is shown in Figure 4.3 and the exact percentages for each exon can be found in Appendix 1.

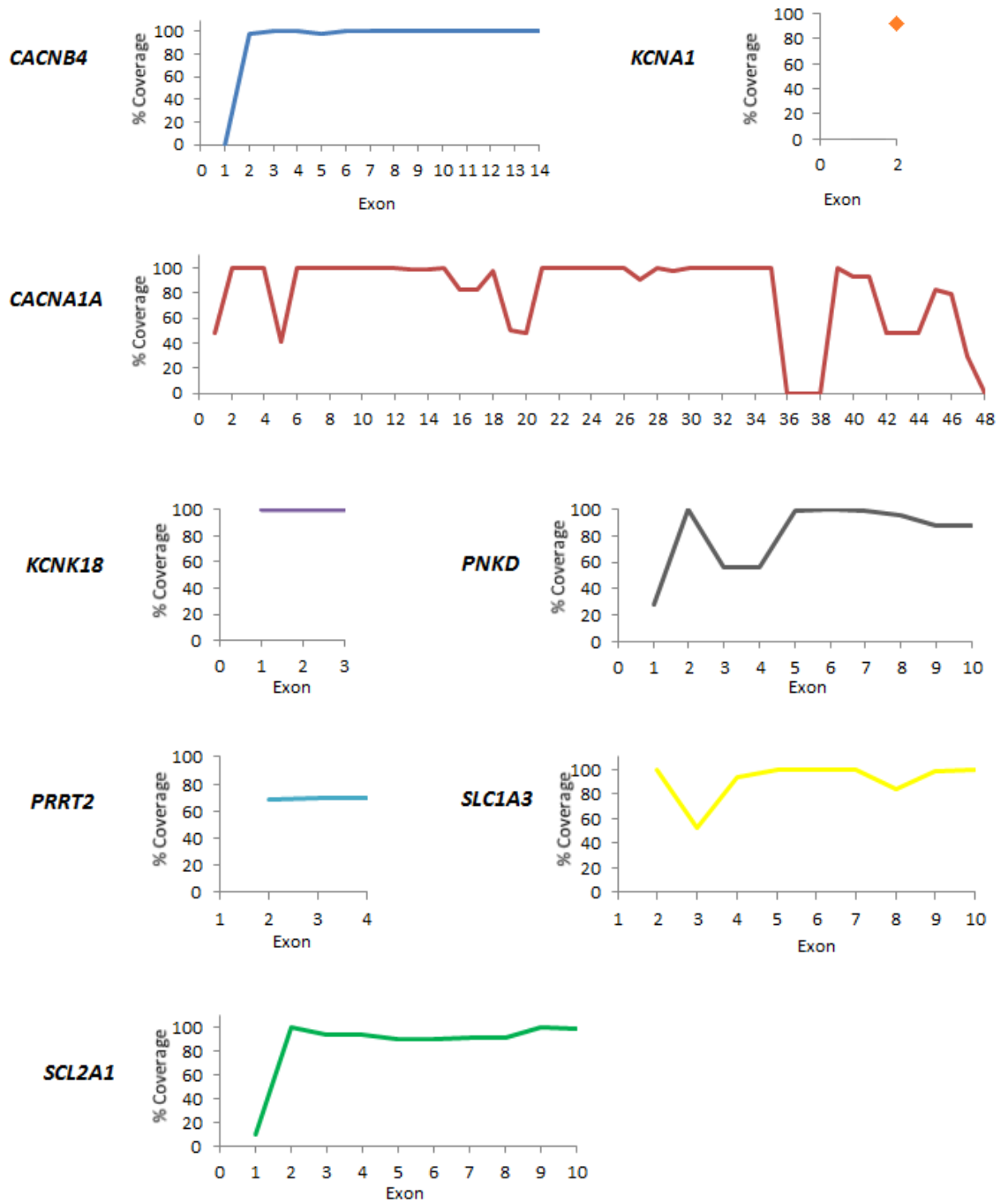


Figure 4.3 – The average percentage coverage for each exon of each gene included in the brain channel panel

4.3. Muscle Channel Panel Results

The muscle panel was run on the patients and controls discussed above. The positive controls and false positive rates were again used to determine the sensitivity and specificity of the panels. The 10 known single *CLCN1* mutations were included in these calculations as positive controls. The mutations found in both of the test patient cohorts were analysed in terms of pathogenicity and thus the clinical benefit of the panel was determined. This was compared with clinical mutation discovery likelihood groupings. Finally, again the target exon coverage was determined.

4.3.1. Positive Controls

Of the 18 positive controls run on muscle panel, 15 were identified, which amounts to 83% (Table 4.7). The three mutations were missed for the same reasons as for the brain panel; they were in regions not covered well, or because the analysis pipeline did not detect CNVs. The control mutations were not spread ideally throughout the four genes (six in *SCN4A*, 10 in *CLCN1*, one in each *KCNJ2* and *CACNA1S*) reflecting the relative frequencies of mutations in these genes. Of the nine additional *CLCN1* known mutations from the second patient cohort, eight were detected. The ninth was a splice site 21bp into the intron and thus was too far from the exon to be included by the analysis pipeline. This is a problem that would have to be rectified in future panels. Therefore, in total, 85% of known mutations were identified by the muscle panel, giving a sensitivity of 0.85.

Gene	Mutation type/ mutation	Found by panel?	Reason not found
SCN4A	Missense/ p.Arg222Gln	No	Low depth coverage
SCN4A	Missense/ p.Thr704Met	Yes	-
SCN4A	Missense/ p.Arg1135His	Yes	-
SCN4A	Missense/ p.Val1293Ile	Yes	-
SCN4A	Missense/ p.Gly1306Val	Yes	-
SCN4A	Missense/ p.Met1592Val	Yes	-
KCNJ2	Missense/ p.Arg312Cys	Yes	-
CACNA1S	Missense/ p.Arg1239His	Yes	-
CLCN1	Splicing/ c.180+3A>T	No	Coverage gap over the exon end
CLCN1	Missense/ p.Gln154Arg	Yes	-
CLCN1	Deletion/ p.Glu232del	Yes	-
CLCN1	Missense/ p.Gly285Glu	Yes	-
CLCN1	Missense/ p.Val327Ile	Yes	-
CLCN1	Missense/ p.Pro480Ser	Yes	-
CLCN1	Deletion/ p.Ser656Asnfs*138	Yes	-
CLCN1	Missense/ P774T	Yes	-
CLCN1	Insertion/ p.A943fs	Yes	-
CLCN1	CNV /Duplication of exons 8-14	No	Large duplications not identified

Table 4.7 – The positive controls included on the muscle channel panel and details of if, and why they were not identified

4.3.2. False Positive Calls

Filtering of variants from the 68 genetically undiagnosed patients (without quality/ depth filtering) resulted in 37 changes remaining. Sanger sequencing validation was performed on all, and 17 were not real, leaving 20 real variants. Of the 17 'false positives', filtering with a depth filter of 5 and a quality filter of ≥ 70 would have left 3 variations that would have appeared to be real. Two of these had a depth of 13 and were in the same sample (a sample containing six false calls in total, all in SCN4A) and thus it was unsurprising they were not real despite their quality scores (98 and 99). The third however had high depth and quality so it was unexpected that it was an artefact.

In total, for the purpose of this analysis the muscle panel produced three false positive calls, giving a specificity score of 0.87. Again, all of the 20 real variants had a quality score of 99, and so a more stringent quality filter could have been used.

4.3.3. Patient Results – Genetically Undiagnosed Patient Cohort

From the 68 patients in this cohort, 20 rare or novel variations (19 distinct) were found in 18 patients, as shown in Table 4.8. Patients in whom no variants (after filtering) were identified are listed in Appendix 3. Again, chromatograms and genome browser visualisations for a selection of the mutations found are shown in Figure 4.4. Seven of these had been previously reported in the literature as pathogenic mutations. Five of the seven had phenotypes consistent with the mutation, two, however, did not. The first is patient 4.17, a patient with myotonia congenita, caused by mutations in *CLCN1*; their mutation was in *SCN4A* (c.3917G>C p.(Gly1306Ala)). This is likely to be a misdiagnosis, as features of MC can overlap with PMC and SMC. The patient also has a novel variant in *CACNA1S* (c.G2055G>C p.(Lys685Asn)) that was present in only one of the 65,000 control genomes; however, as this gene does not cause any type of myotonia, it is likely that this is unrelated to the phenotype. This variant highlights the danger of classing a variant as pathogenic based on population frequency alone. The second of the patients with a published mutation that is inconsistent with the initial clinical diagnosis is patient 4.33, who has HypoPP, but a mutation in *KCNJ2*, the gene for Andersen-Tawil Syndrome (ATS). Periodic paralysis is one of a triad of features (also including cardiac and skeletal abnormalities) caused by *KCNJ2* mutations, and while patients do not always present with all three, they will usually exhibit signs of at least two features. It is possible that further retrospective investigation will uncover further ATS symptoms in this patient. One further variation in *SCN4A* (c.2341G>A p.(Val781Ile)) was initially reported to be pathogenic, but subsequent functional investigation found that it was likely to be benign (Baquero et al. 1995; Green et al. 1997) thus it is unlikely to account for patient 4.27's myotonia.

A further three variations in *SCN4A* (c.748C>G p.(Leu250Val), c.4087A>T p.(Ile1363Phe), c.4109T>A (p.Met1370Lys), patients 4.24, 4.29 and 4.30 respectively) affect the same codons as published pathogenic mutations, but result in different amino acids (Okuda et al. 2001; Miller et al. 2004; Stunnenberg et al. 2010). All of these substitutions are predicted to be damaging by both Polyphen-2 and SIFT, are absent from all three control databases and are associated with patients with correlating phenotypes. Therefore, they are likely to all be pathogenic mutations.

Three of the variations found in four patients, c.355G>A p.(Val119Ile) and c.403A>C p.(Met135Leu), both in *SCN4A* (patients 4.22 and 4.23) and c.2440G>A p.(Ala814Thr) in *CACNA1S* (patients 4.19 and 4.20) are present within control populations at low levels and so are probably benign polymorphisms and not disease-causing in these patients. Additionally, c.2253G>C p.(Glu751Asn), found in *CACNA1S* in patient 4.18 was not present in the patient's unaffected mother and thus did not segregate and is probably benign.

The remaining four variations found by the panel are more ambiguous. The *CLCN1* variation, c.412G>A p.(Val138Ile) found in patient 4.32 is adjacent to two known causative mutations (c.409T>G p.(Tyr137Asn), c.411C>G (p.Try137*)), close to several others, and not present either EVS or 1000genomes, nevertheless in ExAC MAF = 0.00031. It is predicted to be benign by both prediction programs. Furthermore the patient had a clear history of episodes of paralysis associated with low potassium, which would be highly unexpected for a *CLCN1* variation. Taking these factors into account, it seems probable that this variation is not pathogenic, although functional characterisation would be required to prove this conclusion.

Also found in *CLCN1* was the splice site alteration c.774+1G>A in patient 4.19. This patient has a dominant PMC pedigree, and the variation was also seen in her affected daughter. Mutations in *CLCN1* can cause either dominant or recessive MC, however a mutation which affects splicing would usually cause loss of function and therefore be recessive. Consequently, it would be unexpected for this particular variation to cause the dominant pedigree exhibited. Unfortunately, it would be difficult to explore the variation functionally, as the mutant protein cannot be expressed *in vitro* without determining the effect of the splice site disruption on the RNA and so the cDNA. To do this, a muscle biopsy would be needed from the patient (the channel is not expressed in the blood), which is not possible in this family.

The two remaining variations are both in *CACNA1S*. They are c.665T>A p.(Met222Lys) and c.2957G>A p.(Arg986His), identified in patients 4.16 and 4.21. Aside from one reported mutation (Ke et al. 2009), all known disease mutations in the gene neutralise a charged amino acid and cause a gating pore leak into the cell; neither of these mutations would have that consequence as they are both in the S5-S6 linker region of the channel (Met222 in DI and Arg986 in DIII). However, they are both located in the functionally important channel pore. p.(Met222Lys) is absent from controls, appears to be highly conserved and predicted to be pathogenic, all factors that would indicate its pathogenicity. p.(Arg986His) has a MAF of 0.0006 in EVS and 0.0001 in ExAC and is predicted to be benign. Alignment of p.(Met222Lys) with both

CACNA1F and *CACNA1A* reveals mutation hotspots; the equivalent amino acids to positions 218, 223 and 226 (*CACNA1S*) harbour EA2 causing mutations while equivalent to positions 214 and 220 (*CACNA1F*) harbour congenital night blindness mutations (cardiondb.org/Paralogue_Annotation/). Similarly, the equivalent amino acid to R988 in *CACNA1F* harbours another congenital night blindness mutation. As discussed in section 2.2.1.2 of the introduction chapter, EA2 mutations are usually loss of function, as are the X-chromosomal *CACNA1F* mutations. Therefore, it is possible that these mutations could represent a new loss of function mechanism for HypoPP. If this is the case, it would be an important finding. Clearly, functional work is needed to determine the effect of this variant, if any, on the channel. However, this would need to be performed *in vivo* to establish any Ryr1 compensation.

Patient	Gene	Mutation	Previously reported? (ref)	PolyPhen-2 prediction	SIFT prediction	Phenotype	Likelihood rating	MAF in EVS/ 1000g/ ExAC	Atypical phenotype?	Probably pathogenic?
4.16	CACNA1S	p.Met222Lys	No	Pr D (0.999)	D (0)	HypoPP	Very probable	0/ 0/ 0	No	Unclear
4.17	CACNA1S	p.Lys685Asn	No	Pr D (0.991)	T (0.16)	Myotonia Congenita	Probable	0/ 0/ 0.000009	Yes	No
	SCN4A	p.Gly1306Ala	Yes, causing PMC (McClatchey et al. 1992)	Po D (0.54)	D (0)			0/ 0/ 0.000009	Yes	Yes
4.18	CACNA1S	p.Glu751Asn	No	B (0.05)	T (0.1)	HypoPP	Low probability	0/ 0/ 0	No	No (does not segregate)
4.19	CACNA1S	p.Ala814Thr	No	B (0.008)	D (0.02)	PMC	Probable	0.003/ 0.001/ 0.002	Yes	No
	CLCN1	c.774+1G>A	No	-	-			0/ 0/ 0.00002	Yes	Unclear
4.20	CACNA1S	p.Ala814Thr	No	B (0.008)	D (0.02)	PP	Low probability	0.003/ 0.001/ 0.002	No	No
4.21	CACNA1S	p.Arg986His	No	B (0.001)	T (0.09)	HypoPP	Very probable	0.0006/ 0/ 0.0001	No	Unclear
4.22	SCN4A	p.Val119Ile	No	B (0)	T (0.241)	HyperPP	Low probability	0.006/ 0.0014/ 0.003	No	No
4.23	SCN4A	p.Met135Leu	No	B (0.032)	D (0.01)	PP	Low probability	0.002/ 0.0005/ 0.0008	No	No
4.24	SCN4A	p.Leu250Val	No, Leu250Pro causes myotonia	Pr D (1)	D (0)	Myotonia	Possible	0/ 0/ 0	No	Yes

4.25	SCN4A	p.Val445Met	Yes, causing MC (Rosenfeld et al. 1997)	Pr D (1)	D (0.02)	Myotonia	Very probable	0/ 0/ 0	No	Yes
4.26	SCN4A4	p.Arg675Gln	Yes, causing NormoPP (Vicart et al. 2004)	Pr D (0.999)	D (0)	HyperPP	Very probable	0/ 0/ 0.00002	No	Yes
4.27	SCN4A	p.Val781Ile	Yes (Baquero et al. 1995), but subsequently proved to be benign (Green et al. 1997)	Po D (0.891)	T (0.006)	Myotonia	Low probability	0.009/ 0.01/ 0.01	No	No
4.28	SCN4A	p.Val1293Ile	Yes, causing PMC (Koch et al. 1995)	Po D (0.767)	D (0)	Myotonia	Very Probable	0/ 0/ 0	No	Yes
4.29	SCN4A	p.Ile1363Phe	No, Ile1363Thr causes PMC	Pr D (0.999)	D (0)	SCM/ PMC	Very probable	0/ 0/ 0	No	Yes
4.30	SCN4A	p.Met1370Lys	No, M130V causes HyperPP	Pr D (0.995)	D (0)	PMC	Very probable	0/ 0/ 0	No	Yes
4.31	CLCN1	p.Phe306Leu	Yes, causes MC (Fialho et al. 2007)	Pr D (0.996)	T (0.08)	PMC	Very probable	0/ 0/ 0	No	Yes
4.32	CLCN1	p.Val138Ile	No	B (0.01)	T (0.09)	HypoPP	Very probable	0/ 0/ 0.0003	Yes	Unclear
4.33	KCNJ2	p.Arg67Gln	Yes, causing ATS (Haruna et al. 2007)	Pr D (1)	D (0)	HypoPP	Probable	0/ 0	Yes	Yes

Table 4.8 – Possible pathogenic mutations identified by the muscle channel panel. Pr D=probably damaging, Po D= possibly damaging, D= damaging, B=benign, T=tolerated

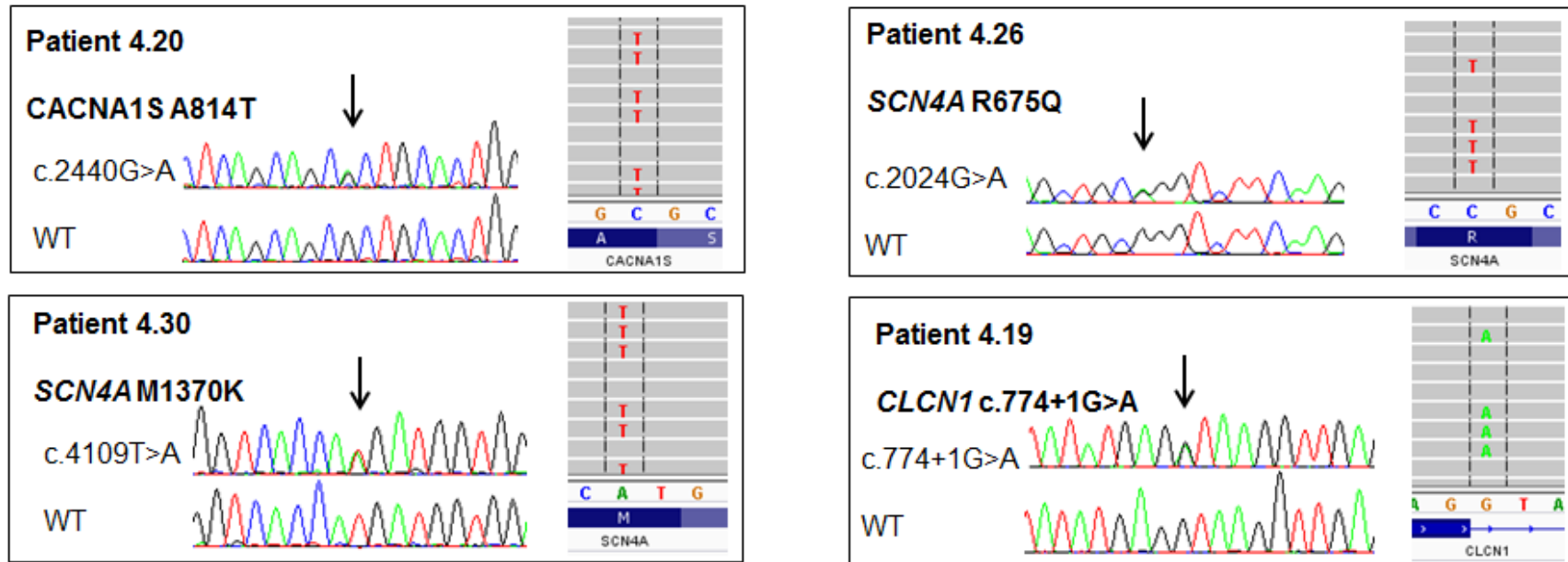


Figure 4.4 – Chromatograms and genome browser visualisations of a selection of mutations (described in terms of the protein change) found by the muscle channel panel. CACNA1S is on the reverse strand and therefore the genome browser shows the reverse complement of the mutation. The genome browser used was IGV (www.broadinstitute.org/igv/)

4.3.4. Patient Results – Single Recessive *CLCN1* Mutation Patients

With the aim of identifying a second mutation, nine patients who had a single known recessive *CLCN1* mutation were run on the panel. No further mutations were found in any of the nine patients. There are a number of possible explanations for this. The patients could have *CLCN1* compound heterozygosity, with the second mutation being unidentifiable by this panel; it could be a deep intronic mutation, a CNV or a mutation in an area with poor sequencing coverage. The patients could have a second mutation in a gene not targeted by the panel, for example *DMPK*; a recent report described co-occurrence of mutations in these two genes causing myotonia (Kassardjian and Milone 2014). Lastly, as some mutations in *CLCN1* have been reported to cause either a dominant or a recessive inheritance pattern, the single *CLCN1* already identified could be solely responsible for the channelopathy (Kubisch et al. 1998).

4.3.5. Clinical Benefit

This muscle panel identified possible or probably pathogenic mutations in 13 previously genetically undiagnosed patients, which is 19% of the cohort. Four of those mutations caused atypical phenotypes, although three retrospectively would fit the diagnosis, and fourth may not be pathogenic. Using the diagnostic algorithm given in Figure 1.4b (Rayan and Hanna 2010), four mutations deemed possibly or probably pathogenic would not have been identified by traditional Sanger sequencing (p.(Met222Lys) and p.(Arg986His) in *CACNA1S*, p.(Val138Ile) in *CLCN1* and c.200G>A p.(Arg67Gln) in *KCNJ2*) as only selected exons are screened in *CACNA1S*, *CLCN1* would not be screened for PP, and *KCNJ2* is only considered for patients who are diagnosed as having ATS. Furthermore, only two of the five *SCN4A* mutations would have been found initially, although the rest would have been discovered later on in the diagnostic process. Therefore, this panel offers substantial clinical benefit over traditional diagnostic sequencing techniques.

4.3.6. Clinical ‘Likelihood’ Ratings

The genetically undiagnosed samples were given a clinical ‘likelihood’ score of finding a mutation based on their phenotype. The 68 samples were distributed fairly evenly between the four groups (low probability, possible, probable, and very probable). Of the 13 patients for whom a mutation was found, nine (70%) were from the ‘very probable’ group. This is 60% of the ‘very probable’ group. Three were ‘probable’, one ‘possible’ and none were from the ‘low probability’ group. This shows that clinical likelihood scores were accurate, and that the more clear the phenotype, the higher the chance of genetic diagnosis.

4.3.7. Coverage

One sample on the muscle channel panel failed and is not included in any of the coverage analysis. Excluding that sample, the overall percentage of the bases in target exons covered by at least 20x is 86%; higher than the 81% of the brain panel, but still much lower than the predicted 99.5%. Of the 92 target exons, 37 had 100% coverage in the remaining 94 samples (this is only 40%), however 65 had coverage at 20x of over 90%. At 70% this is very similar to the 73% equivalent for the brain panel. Four exons failed completely, these are *CACNA1S* exons 20, 23 and 29 and *SCN4A* exon five. Graphs of the percentage coverage distribution for each of the four genes can be found in Figure 4.5, and, similarly to the brain panel, the exact percentages coverage for each exon are shown in Appendix 2.

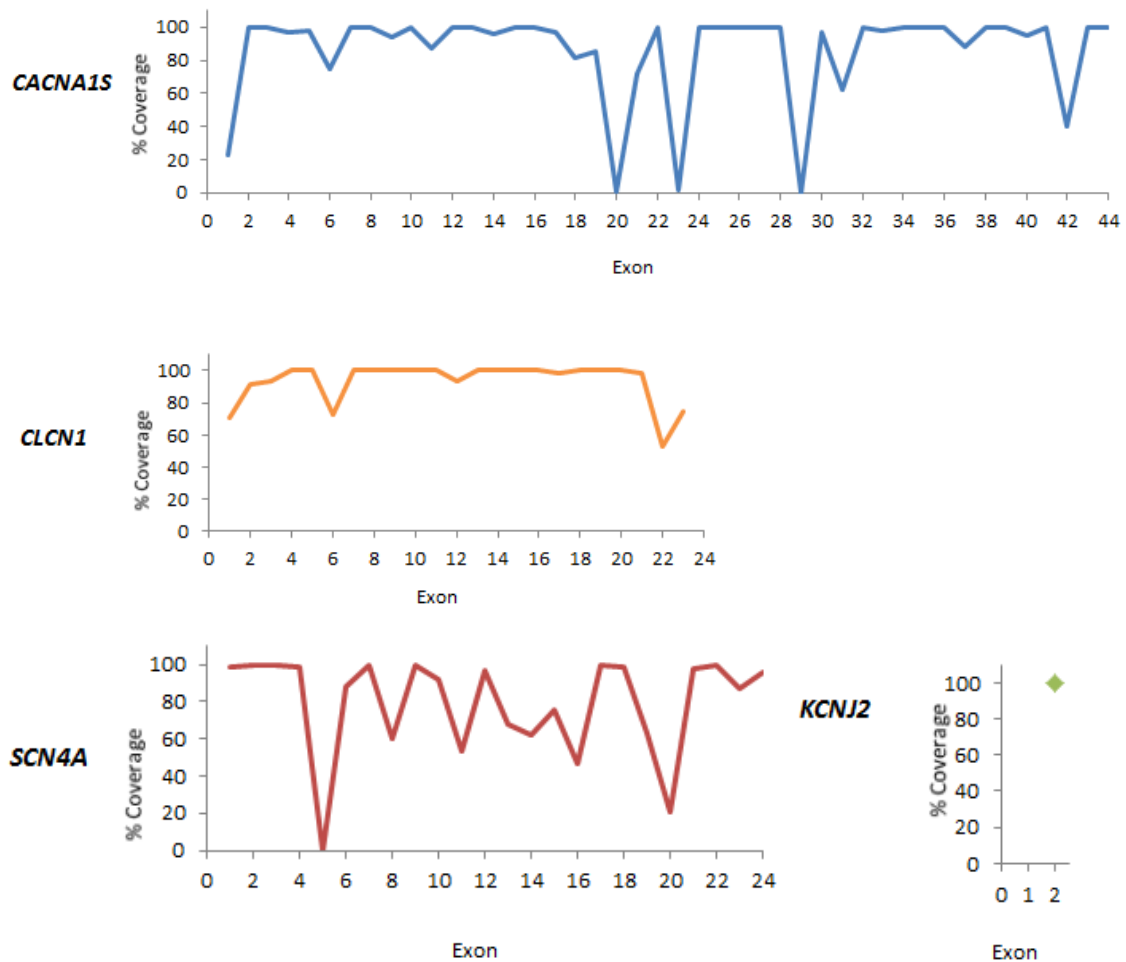


Figure 4.5 – The average percentage coverage for each exon of each gene included in the muscle channel panel

5. Discussion

In this chapter, the use of next-generation sequencing technology was trialled as an alternative to Sanger sequencing for genetic diagnosis of the channelopathies. Two panels, the brain channel panel and the muscle channel panel, were designed and used to sequence target genes for a group of undiagnosed samples and controls. The clinical benefit (defined here in terms of mutations that would not have been found without this technology) to the patients was investigated.

The brain channel panel identified 10 probable pathogenic and two possible pathogenic variants in a cohort of genetically undiagnosed mixed neuronal channelopathy patients, accounting for 15% of the cohort. This number is probably not a true reflection of the rate of neuronal channelopathy mutations in EA/ FHM/ PxD patients as many of those included would have been pre-screened for the main known genes. Unfortunately, the exact extent of pre-screening in this cohort is unknown. Importantly five of the twelve (42%) presented with an atypical phenotype, and thus the mutations would not have been identified by traditional diagnostic Sanger sequencing. This demonstrates the huge genetic and phenotypic overlap amongst this group of diseases, as well as the considerable clinical benefit of using panel sequencing technology for their diagnosis. In particular, a novel *CACNB4* mutation and phenotype identified in a patient who had been extensively investigated highlighted the necessity for screening the rarer genes in these patients.

The muscle channel panel uncovered nine probable and four possible pathogenic variants, accounting for 19% of a cohort of genetically undiagnosed muscle channelopathy patients. Again, this number is lower than expected, probably due to extensive pre-screening, but again the exact extent of which is unclear. Four of the patients (31%) had an atypical phenotype, although, retrospectively three did correlate with the mutation, and probably would have been found in the diagnostic Sanger sequencing process, and the remaining one may not be pathogenic. Therefore, while the clinical benefit of the muscle panel is evident, there is less phenotypic and genetic overlap between the skeletal muscle channelopathies in comparison to the neuronal channelopathies, and so the benefit is less distinct than that of the neuronal panel.

The clinical benefit for both groups of channelopathy patients has therefore been established, and it is evident that, in these groups of diseases at least, next-generation sequencing is advantageous in terms of finding unexpected mutations. There are other additional benefits. For a large cohort of patients, and for large genes

or many genes, panel sequencing is both cheaper and faster than the equivalent Sanger sequencing. The exact time and cost benefit is hard to estimate, however, as it is dependent on the phenotype, the genes to be screened and the result (i.e. if a causative mutation is found straight away, or if many genes are investigated). Additionally, NGS reagent and running costs are continually falling. There are two other major benefits of this technology to discuss. The first is that it removes diagnostic bias. If a clinician has misdiagnosed a patient, traditional Sanger sequencing will mean that the causative mutation may never be found, as the gene responsible will not be considered, this bias is removed with diagnostic channelopathy panels. The second is that it allows for new findings and thus greater understanding into the disease mechanisms. For example, if functional studies prove that the two novel *CACNA1S* variations are disease causing, they will represent a new disease mechanism for HypoPP, which could in turn result in new understanding of the channel function and new pharmacological targets. The regions of the gene that these mutations were found in are not routinely sequenced diagnostically, as it is deemed not cost or time effective, however in panel sequencing investigating new regions does not take any longer, and cost increases are minimal. Additionally, the brain channel identified probable pathogenic mutations in patients with unexpected phenotypes in *SLC2A1*, *PNKD*, *KCNA1* and *CACNB4*, all which would have been missed by Sanger sequencing investigation. Therefore, the phenotypic spectrum for all of these genes was expanded.

Despite the advantages NGS diagnostic panels, there are also disadvantages. The biggest of these is coverage. The level of coverage required to provide reliable results has been set at 20x. This threshold has been chosen because 20 concordant readings are likely to be a true representation of the sequence. If the threshold is lower, there is chance the results could be artificial and therefore confidence decreases. A coverage requirement over 20x would not increase the confidence by much, but would add to the time and cost of the sequencing. For the brain panel, 81% was covered at 20x, and for the muscle panel 86%. This shortfall is represented by only 79% of non-CNV control mutations being identified, and thus brain and muscle panels demonstrated sensitivity rates of 0.69 and 0.89 respectively. In both cases, the design coverage was much better than the experimental coverage. This is because designing primers is never 100% accurate, they are predicated to work by bioinformatic tools, but until the PCR is carried out it is unknown whether they will or not.

The coverage figures are far too low for diagnostic testing, as while it will be able to provide positive results, the panels will not be able to confirm that samples are negative for mutations in the genes tested. To increase the sensitivity of the panels, the

areas of the panels with low coverage could be re-designed. Larger target areas could be used so avoid the regions which previously failed. This could be done with the help of Illumina's technical support. Additionally, fewer patients could be sequenced at once; this would mean the remaining patients would get higher depth of sequencing, and so regions with low coverage may be improved. This would not help regions without any coverage, so these could be sequenced manually to fill in 'gaps'. Lastly, the problems could have been due to poor sample quality, contamination or incorrect following of the procedure. Therefore to improve this, more care could be taken to ensure high quality samples are used and no pre- and post- PCR contamination occurs. Additionally, advice could be sort from Illumina to ensure the protocol is executed exactly, and any parts of particular vulnerability are explained.

Another problem with the panels is that they provide a greater number of inconclusive results, when variations are found that are difficult to interpret. This was seen repeatedly in the results of these panels. Whilst the novel variants can be speculated upon, without additional lengthy and costly functional work, which is not usually possible for a genetic diagnostic service, diagnostic conclusions cannot be drawn. Lastly, although infrequent when thorough quality and depth filters are used, false positive calls were present in both brain and muscle panels, giving specificity rates of 0.94 and 0.87 respectively. Consequently, any variations found by these panels will still always have to be confirmed by Sanger sequencing.

An additional disadvantage is the limited number of genes analysed. In order to genetically diagnose patients who were negative on these panels (shown in appendix 3), more genes will need to be screened, for example the FHM genes that were not included, SCA genes or the genes from the other panel (muscle panel genes for brain patients or vice versa). This will incur more time and expense. Furthermore, as new genes are discovered, or the phenotypes of known genes broadened to include these clinical presentations, more genes will have to be added to the panels to accommodate them. Again, for these reasons, these panels are useful for patients positive for the genes screened but less so for those who are negative.

The panels here sequenced relatively small numbers of genes. The technology could also be used to sequence diseases with a much larger number of genes implicated. In that case, the main benefit would shift from unexpected findings to the improvement in cost and time in sequencing all of the genes. This application of panel sequencing will be investigated in the following chapter.

Chapter 5: Panel Sequencing in a Large Cohort of Patients with Rhabdomyolysis and Exercise Intolerance

1. Introduction

Rhabdomyolysis (RM) is the breakdown of damaged skeletal muscle tissue and subsequent release of potentially toxic molecules into the blood stream, resulting in muscle pain, nausea, kidney damage and, in extreme cases, fatal kidney failure. Episode triggers can include alcohol or drug abuse, muscle injury or extreme exertion, however there can also be underlying genetic causes (Figure 1.9). In these cases, triggers can be understood and so avoided. Genetic diagnosis of recurrent RM and resulting prevention of dangerous episodes can therefore be life-saving (Scalco et al. 2015). Exercise intolerance is a condition related to, and often co-occurring with recurrent RM, and thus it is frequent that the two are considered together.

There are a number of genetic causes for RM and exercise intolerance. Firstly, there are two main energy-producing pathways that, when disrupted, can lead to RM; the glycolysis pathway and the fatty acid oxidation pathway. Enzymatic reduction by recessive loss of function mutations in each can result in insufficient energy production during exercise and, consequently, muscle damage and a RM episode. Muscular dystrophies can also involve RM and exercise intolerance, although usually as a secondary feature; only a comparatively small number of the muscular dystrophies have been known to present with these symptoms (Scalco et al. 2015). Importantly, VGIC channel dysfunction can also be responsible for RM and exercise intolerance in cases of malignant hyperthermia (due to *RYR1* and *CACNA1S* mutations), and in two cases, as a result of an *SCN4A* mutation (Lee and Chahin ; Bendahhou et al. 2000). Usually MHS patients display no symptoms until RM is triggered by anaesthesia, extreme exercise heat or infection (Capacchione and Muldoon 2009). Lastly, there are

several 'miscellaneous' individual genes in which mutations can present with exercise intolerance and RM.

Genetic diagnosis of recurrent RM and exercise intolerance is highly complex. Careful clinical phenotyping, muscle biopsy examination and biochemical assays can provide vital insights; however identifying the causative mutation(s) is still not straightforward. There are many, often large, genes implicated, frequently with heterogeneous and overlapping presentations. Inheritance is usually recessive, although in some cases can be dominant or X-linked, and penetrance can be incomplete. Furthermore, there are several reported genetic risk factors with common frequency in the population, and it is unclear what their impact is. The many genes currently thought to be involved in recurrent RM and exercise intolerance are comprehensively reviewed in the introduction of this thesis (section 3). To date, the majority of the literature genetically investigating these patients has focussed on case reports, or single gene screening in small homogenous cohorts. There has been no large, multigene study, and thus the overall genetic landscape surrounding these conditions is currently uncertain. Therefore, although it is known that channelopathies are implicated, their contribution is unclear.

2. Chapter Aims

The previous chapter saw the trialling of next-generation sequencing panels for genetic diagnosis of the neuronal and skeletal muscle channelopathies. These panels were largely successful, with improved clinical benefit, cost and time taken in comparison to traditional Sanger sequencing genetic diagnosis. However, the classic channelopathies are relatively easy to diagnose genetically, as pedigrees usually follow a fully penetrant, autosomal-dominant, Mendelian inheritance pattern. Furthermore, there are few known genes implicated.

In this chapter, NGS panels will be used to investigate a different set of patients with possible VGIC dysfunction. The underlying genetic causes for patients with RM and/ or exercise intolerance in a large cohort of patients will be examined, and the contribution of channelopathies determined. It is hypothesised that, since *RYR1* mutations are a large factor in recurrent RM, levels of mutations in *CACNA1S* and *SCN4A* may be underestimated as they are often not routinely investigated. This analysis will present a more difficult task due to the large number of genes implicated and the sometimes non-Mendelian nature of the genetic background. Additionally,

multiple panels will need to be run to accommodate the large number of patients. Initially, Truseq Custom Amplicon technology will be used to design a bespoke panel. However, as shown in chapter four, this sequencing method has large problems with incomplete coverage. Therefore, if this does not produce high quality results, a non-customised, standard sequencing panel, TruSight One will be used instead for the remaining samples. The two methods will then be compared. Additionally, the data produced will to be used to determine whether any previously reported genetic risk factors are more common in this cohort than in the general population by comparison of MAFs with EVS, ExAC, 1000genomes and an in-house control dataset. Due to the much larger scale of this project, the sensitivity, specificity and control tests performed in the previous chapter will not be carried out for the RM panels.

3. Methods

3.1. Patients

Patients with recurrent RM or exercise intolerance were recruited internally, nationally, and internationally for this study. In total, a cohort of 224 patients was collected and tested on the panels. Unfortunately, many patients' DNA samples were sent without clinical information, and when referring clinicians were contacted, the information was still not provided. It is therefore possible that some of the patients did not fit the criteria specified (recurrent episodes of rhabdomyolysis and/or exercise intolerance). Clinical data, where available, was compiled by Dr Renata Scalco.

3.2. Panels

Two types of NGS panel were used to screen the candidate genes in for this cohort. Each of the panels uses different chemistry, has a different method of library preparation and is sequenced on a different sequencing machine.

3.2.1. TruSeq Custom Amplicon Panel Design, Library Preparation and Sequencing

The TSCA was designed using Illumina's design studio software (<http://designstudio.illumina.com/>) as described in the methods section of results chapter two. Details of the design are given in the results section 4.1.1 of this chapter. 95 patients were run on the panel; 250ng of DNA from each underwent library preparation and sequencing as described in section 4 of the materials and methods chapter.

3.2.2. TruSight One Library Preparation and Sequencing

TruSight One panels are sequencing panels consisting of 4813 genes with known clinical phenotypes; the genes are listed at <http://www.illumina.com/products/trusight-one-sequencing-panel>. The libraries of 72 patients can be sequenced simultaneously using 2 x 36 TruSight One kits, following the protocol described in section 4.2 of the materials and methods chapter. The quality of the libraries was assessed with the bioanalyzer after the first PCR (before pooling) and before sequencing. 10pm of the resultant libraries were loaded onto the Illumina HiSeq 2500 for sequencing. 50ng of DNA was used for each patient. This process was repeated three times, and thus 216 patients were analysed with TruSight One panels. Although all 4813 genes were analysed, only the 46 genes chosen (discussed in section 4.2.1. of this chapter) were examined in the patients.

3.2.3. Primary Data Analysis and Coverage Determination

Primary data analysis was carried out for all panels by Dr Alan Pittman, as described in section 4.4 of the materials and methods chapter. Percentage coverage at 20x of target exons was determined as described in section 4.6 of the same chapter with the help of Dr Joshua Hersheson.

3.3. Variant Filtering

Synonymous and non-coding variants that did not affect possible splice sites were first filtered out, leaving only changes that are likely to affect amino acid sequence. As a recessive inheritance pattern was predicted for the majority of genes included, variants with a MAF ≥ 0.1 were removed using 1000genomes and the exome variant server (both are discussed in section 4.2.2. of the introduction chapter). When other inheritance patterns were assumed for specific genes, more rigorous filtering was applied, and this is detailed in the relevant section of the results. For TSCA panel variants, a depth filter of 70 and a quality filter of 5 were used. For TruSight One panel variants, a depth filter of 5 was used.

3.4. Variant Confirmation

Variants remaining after the filtering process were confirmed using Sanger sequencing if they were deemed possibly disease causing, including variants previously reported as pathogenic, homozygous or possible compound heterozygous variants. Confirmation was performed using the protocols described in section 2 of the materials and methods chapter.

3.5. Known Polymorphism Analysis

The MAF of the common polymorphisms investigated was determined from patients sequenced using TruSight One. The number of alternate alleles was divided by the total number of alleles (408). The in-house control dataset was produced from WES of healthy controls and compiled by Jack Humphrey.

3.6. Enolase Activity Assay

Snap frozen muscle was prepared as 1% homogenate in potassium phosphate and dithiothreitol. The enolase-assisted conversion from NAD to NADH was followed by measuring the decrease in fluorescence at excitation 340 nm emission 460 nm Tecan Infinite M200Pro plate reader set to 30°C. For every one mole of 2-phosphoglycerate converted by enolase, 1 mole of NADH is reduced. The reaction buffer consisted of Imidazole pH 7.4 Containing ADP NADH magnesium sulphate, potassium chloride, pyruvate kinase and Lactate dehydrogenase. The reaction is started by the addition of 2-phosphoglycerate. This assay was performed by Dr Ralph Wigely at Great Ormond Street Hospital.

3.7. Western Blot

Western blots were performed as described in section 3.4 of the materials and methods chapter. Blots were incubated with antibodies against β -dystroglycan, (Leica Biosystems, dilution 1/350) and caveolin-3 (BD Biosciences BD610421, dilution 1/350). The staining of myosin heavy chain with Coomassie blue on the post-blotted gel and the intensity of the β -dystroglycan band were used as controls for protein loading and quality of the transfer. Bands were visualised with SuperSignal West Pico Chemiluminescent Substrate detection (Life Technology) using AlphaInnotech FluorChemR Q platform and AlphaViewR software v3.0. Densitometric analysis was undertaken using ImageJ v1.47 software (with data normalised to the intensity of the myosin heavy chain band on the Coomassie blue stained post-blotted gel) and expressed as a percentage of the control sample. The caveolin-3 western blot was performed at the NHS Muscle Immunoanalysis Unit in Newcastle by Julie Marsh and, Rita Barresi.

4. Results

4.1. TruSeq Custom Amplicon Rhabdomyolysis Panel

4.1.1. Panel Design

The original gene list for the custom RM panel was assembled by Dr Robert Pitceathly, the clinical fellow who initiated the project and recruited the majority of referring clinicians. The details of the genes and panel design are shown in Tables 5.1 and 5.2. The same target design strategy was used as for the channel panels: genomic coordinates for the coding exons plus or minus 25bp were input into design studio and if this approach could not produce amplicon designs the coordinates given were readjusted until design was possible. 60 out of 690 exons could not have amplicons designed against them, and a further 29 had coverage gaps, resulting in predicted amplicon coverage of only 91.8%. This is lower than both of the channel panel designs (97.4% and 99.5%).

Gene	N° Target Exons	N° Amplicons	Gene	N° Target Exons	N° Amplicons
<i>GYS1</i>	16	18	<i>CPT2</i>	5	13
<i>GAA</i>	21	16	<i>ACADVL</i>	21	24
<i>PHKG2</i>	10	13	<i>HADHA</i>	20	22
<i>PYGM</i>	20	29	<i>HADHB</i>	16	15
<i>PFKM</i>	25	28	<i>ETFPA</i>	12	13
<i>PGAM2</i>	3	6	<i>ETFB</i>	5	8
<i>LDHA</i>	8	5	<i>ETFDH</i>	12	12
<i>ALDOA</i>	10	13	<i>SLC52A2</i>	4	11
<i>ENO3</i>	12	15	<i>SLC52A1</i>	4	9
<i>PGM1</i>	11	12	<i>SLC52A3</i>	4	11
<i>GYG1</i>	8	13	<i>TSFM</i>	7	9
<i>PRKAG2</i>	16	16	<i>ISCU</i>	5	7
<i>PGK1</i>	11	16	<i>ATP2A1</i>	22	29
<i>SIL1</i>	9	10	<i>SLC22A5</i>	11	10
<i>PHKA2</i>	33	36	<i>CYB5B</i>	5	5
<i>PHKB</i>	31	33	<i>FKBP1A</i>	4	4
<i>PHKG1</i>	10	14	<i>MEF2C</i>	11	26
<i>CAV3</i>	2	4	<i>PPARGC1A</i>	13	20
<i>RYR1</i>	106	136	<i>PPARA</i>	8	10
<i>HSPA1B</i>	1	13	<i>LPIN1</i>	22	28
<i>CCL2</i>	3	1	<i>CHKB</i>	11	166
<i>CCR2</i>	2	8	<i>ACE</i>	25	35
<i>MYLK</i>	34	36	<i>ACTN3</i>	21	28
<i>SLC2A2</i>	11	13	<i>SLC37A4</i>	9	15

Table 5.1 – Genes, exons and amplicons included in the TSCA rhabdomyolysis panel

Total number of target exons	690
Number of exons missed	40
Number exons with coverage gaps	29
Number of target bases	119,918
Number of bases missed	9811
% of target covered	91.8%
Total number of amplicons	877

Table 5.2 – The final TSCA rhabdomyolysis panel design metrics

4.1.2. Failed samples

Of the 95 samples, 40 (42%) completely failed and produced no sequencing results. The reason for this was unknown. Illumina were contacted but were unable to provide a solution.

4.1.3. Coverage

Excluding failed samples, the 20x coverage for the TSCA RM panel was 83%. This was a similar figure to the 81% and 86% seen for the channel panels, but as the number of target exons rises, so does the number of exons not sequenced. More than 100 exons were missed by this panel.

4.1.4. Decision to Change Sequencing Method

The initial TSCA panel did not work successfully. Almost half of the samples completely failed and Illumina were not able to provide an explanation or solution. Furthermore, the low level of coverage meant that even in samples that were sequenced, mutations could be missed. Therefore the decision was taken to use a different panel instead; the Illumina TruSight One. This is a standard product and thus likely to have better coverage and sequencing quality than the TSCA RM panel. If no obvious causative mutation had been identified by TSCA, and enough DNA was available, samples run on the TSCA RM panel (both successful and failed samples) were repeated on the TruSight One panel.

4.2. TruSight One Panel

The TruSight One sequencing panel sequences 4813 genes with known clinical phenotype using enrichment probes targeting these regions. For gene analysis of RM and exercise intolerance, only sequencing data from the clinically relevant genes was analysed.

4.2.1. Gene Selection

The list of genes to be analysed was reassessed, as the TSCA list did not include some important RM and exercise intolerance genes. Only genes fitting the inclusion criteria below were included:

- If the gene is known to cause RM
- If the gene is known to cause exercise intolerance
- If the gene causes a glycogen storage disorder with some skeletal muscle features

- If the gene product is known to form a complex with others that cause RM and/or exercise intolerance
- If the gene has a known risk factor locus for RM or exercise intolerance

The 46 genes that met these criteria are shown in Table 5.3, along with their inclusion justification.

Gene/ protein	Inclusion justification (disease/ muscle features/ other reasons)	Causes RM?
GYS1/ Muscle glycogen synthase-1	GSD0B: cardiomyopathy and exercise intolerance	No
GAA/ Acid alpha-1,4-glucosidase	Pompe's: muscular hypotonia	No
PHKG2/ Hepatic phosphorylase kinase, gamma 2	GSDIXc: cases of muscle weakness after extreme exertion	No
PHKG1/ Muscle phosphorylase kinase, gamma 2	None: muscle equivalent of PHKG2, genes in same complex cause exercise intolerance and RM	No
PYGM/ Muscle glycogen phosphorylase	McArdle's: exercise intolerance, muscle cramps, myalgia	Yes
PFKM/ Muscle phosphofructokinase	Tarui's: exercise intolerance, muscle cramps, myalgia	Yes
PGAM2/ Muscle phosphoglycerate mutase	GSDX: exercise intolerance and cramps	Yes
LDHA/ Lactate dehydrogenase	GSDXI: exercise intolerance and cramps	Yes
ALDOA/ Fructose-1,6-bisphosphate aldolase A	GSDXII: myopathy can be associated with symptoms	Yes
ENO3/ Beta-enolase	GSDXIII: exercise intolerance and myalgia	Yes
PGM1/ Phosphoglucomutase	GSDXIV: exercise intolerance	Yes
GYG1/ Glycogenin-1	GSDXV: myopathy with slowly progressive weakness	No
PGK1/ Phosphoglycerate kinase 1	Phosphoglycerate kinase 1 deficiency: Myopathy	Yes
SIL1/ Nucleotide exchange factor SIL1	Marinesco-Sjogren syndrome: weakness	Yes
PHKA2/ Hepatic phosphorylase kinase alpha 2	GSDIXa: genes in same complex cause exercise intolerance and RM	No

PHKB/ Phosphorylase kinase, beta	GSDIXb: mild muscle signs	No
CAV3/ Caveolin-3	Rippling muscle disease: exercise intolerance, myalgia and weakness	Yes (one case)
RYR1/ Ryanodine receptor 1	MHS1: muscle rigidity	Yes
CCL2/ Monocyte chemotactic protein-1	Polymorphism is risk factor associated with exercise induced muscle damage	No
CCR2/ Monocyte chemoattractant protein-1	Polymorphism is risk factor associated with exercise induced muscle damage	No
CPT2/ Carnitine palmitoyltransferase II	CPT2 deficiency: exercise intolerance	Yes
ACADVL/ Very long-chain acyl-CoA dehydrogenase	VLCAD deficiency: exercise intolerance	Yes
HADHA/ Mitochondrial trifunctional protein, alpha subunit	Trifunctional protein deficiency: skeletal myopathy	Yes
HADHB/ Mitochondrial trifunctional protein, beta subunit	Trifunctional protein deficiency: skeletal myopathy	Yes
ETFA/ Electron transfer flavoprotein, alpha	MADD, Glutaric aciduria type IIA: exercise intolerance and myalgia	Yes
ETFB/ Electron transfer flavoprotein, beta	MADD, Glutaric aciduria type IIB: exercise intolerance and myalgia	Yes
ETFDH/ Electron transfer flavoprotein dehydrogenase	MADD, Glutaric aciduria type IIC: exercise intolerance and myalgia	Yes
TSM/ Elongation factor Ts, mitochondrial	Combined oxidative phosphorylation deficiency 3: weakness	Yes
ISCU/ Iron-sulphur cluster scaffold protein	Myopathy with lactic acidosis: exercise intolerance, muscle tenderness and cramping	Yes
LPIN1/ Phosphatidate phosphatase LPIN1	Acute recurrent myoglobinuria	Yes
ACE/ Angiotensin I-converting enzyme	Polymorphism is risk factor associated with exercise induced increase in CK	No
MYLK/ Myosin light chain kinase	Polymorphism is risk factor associated with exercise induced muscle damage and MR	Yes
ACTN3/ Alpha actinin 3	Polymorphism is risk factor associated with exertional MR	Yes

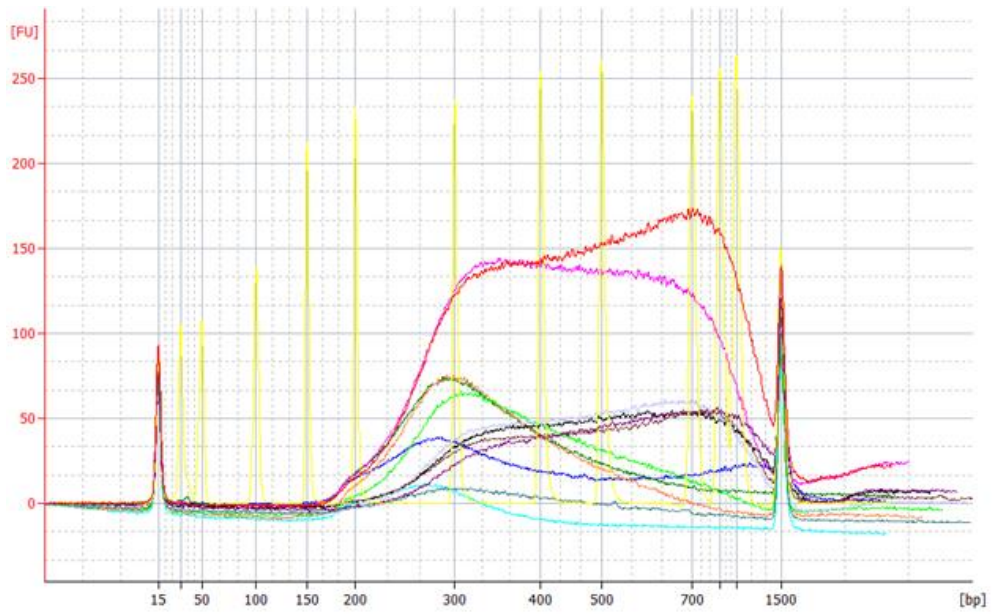
ANO5/ anoctamin-5	Miyoshi muscular dystrophy type 3: exercise intolerance, severe myalgia and weakness	Yes
CKM/ Muscle creatine kinase	Polymorphism is risk factor associated with exertional RM and raised CK	Yes
CACNA1S/ Ca _v 1.1 alpha subunit	MHS5: muscle rigidity	Yes
PHKA1/ Muscle phosphorylase kinase alpha 1	GSDIXd: exercise intolerance and myalgia	Yes
FKRP/ Fukutin-related protein	LGMD2I: exercise induced RM and myalgia can be presenting features	Yes
DMD/ Dystrophin	Becker's muscular dystrophy: exercise intolerance, cramps and RM can be presenting features	Yes
SGCA/ Alpha sarcoglycan	LGMD2D: can present as RM triggered by infection	Yes
SGCB/ Beta sarcoglycan	LGMD2E: can present as RM triggered by infection	Yes
DYSF/ Dysferlin	LGMD2B: in one case, kidney failure as a result of RM has been the presentation	Yes
IL6/ Interleukin 6	Polymorphism is risk factor associated with exertional RM and raised CK	Yes
TNF/ Tumour necrosis factor alpha	Polymorphism is risk factor associated with raised CK following extreme exercise	No
IGF-2/ Insulin-like growth factor 2	Polymorphism is risk factor associated with muscle damage following extreme exercise	No
SCN4A/ Na _v 1.4 alpha subunit	Two case reports of recurrent RM and weakness (one fixed, one episodic)	Yes

Table 5.3 – Genes included in the revised gene list and so analysed on the TruSight One rhabdomyolysis panel, and the justification for their inclusion

4.2.2. Library Quality

The quality of libraries was assessed using the bioanalyzer at two steps in the library preparation; after the first PCR (before pooling) and before loading onto the sequencer. This was to ensure that DNA fragments were of the right size (between 300bp-1kb). Each of the runs had good quality fragments; Figure 5.1 shows an example of the bioanalyzer readout from the first of the three TruSight One runs.

a)



b)

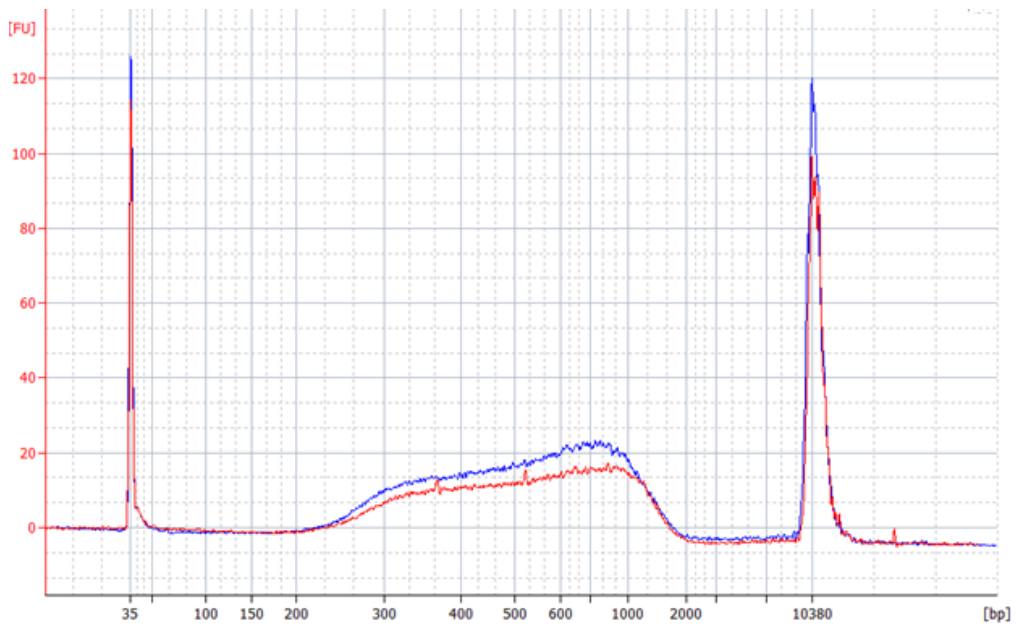


Figure 5.1 – The TruSight One library fragments as shown on the bioanalyzer (a) after the first PCR step (a random selection of samples, yellow = ladder) and (b) before loading onto the sequencer. FU = fluorescence units, bp= base pairs

4.2.3. Coverage

The 20x average coverage of the new target genes by the TruSight One panel is 93.7%. This is 10% higher than that of the TSCA panel, and so will provide a much more thorough level of sequencing. However, 6.3% of target exons are still missed, and this will mean that some mutations are not identified.

4.3. Patient Results

Combining the results from the three TruSight One panels with the few positive results from the initial TSCA panel produced sequencing data on 224 patients. The variants were filtered as described in section 3.3; all remaining variants found can be found in Appendix 4. The pathogenicity of the remaining variants was assessed based on a recessive inheritance model for all genes except *RYR1*, *CACNA1S*, *SCN4A*, *CAV3* and any X chromosome genes.

Genes in which possible or definite pathogenic mutations were identified are discussed below, and the findings of the panel overall are summarised in section 4.3.5.

4.3.1. Channelopathy Genes

A large proportion of patients in whom possible or definite mutations were found, had their mutations in the channelopathy genes assessed (*RYR1*, *CACNA1S*, and *SCN4A*). These are discussed below.

4.3.1.1. *RYR1* Results

Recessive or dominant mutations in the 106-exon-long ryanodine receptor encoding gene, *RYR1*, are known to cause a range of congenital myopathies. Additionally, dominant mutations can result in malignant hyperthermia susceptibility (MHS), a potentially fatal condition in which RM episodes can be triggered previously healthy individuals by factors such as exertion, illness or anaesthesia.

In this cohort, 37 distinct variations were identified in 43 patients. Pathogenicity determination of *RYR1* mutations is particularly challenging for several reasons. The gene is exceptionally large, with 5038 amino acids, and so it is not unusual for rare or even private benign variations to occur. Additionally, patients are phenotypically heterogeneous, and mutations can be either dominant or recessive. There are often conflicting reports of whether a mutation is pathogenic in the literature. Lastly, MHS is not fully penetrant and many genetic carriers may not trigger RM episodes, thus variations may be more frequent in the population than for other diseases. The

European Malignant Hyperthermia Group (EMHG) have recognised these problems, and have collated a database in which mutations that have been functionally characterised as causing MHS are listed, and is a useful resource for determining pathogenicity. The *RYR1* variations found here (with the exception of three that are recognised as polymorphisms - c.4024A>G p.(Ser1342Gly), c.6178G>T p.(Gly2060Cys), and c.11266C>G p.(Gln3756Glu)) are shown in Table 5.4, along with population frequency data, previous pathogenicity reports and whether the variation is in, or near other mutations in the EMHG database. Fortunately, clinical data was available for the majority of these patients. The table identifies whether the patient's presentation correlates with MHS (i.e. RM triggered by exercise, infection or anaesthesia).

Two of the mutations found by the RM panel, c.6617C>T p.(Thr2206Met) (Patient 5.119) and c.7300G>A p.(Gly2434Arg) (Patients 5.177, 5.18, 5.139) were present in the EMHG database, and thus can be considered definitely pathogenic. One further mutation, c.13513G>C p.(Asp4505His) has been shown in functional studies to be pathogenic and was seen in two patients, 5.3 and 5.30. Patient 5.30, however, had additional pathogenic *ANO5* mutations, which are more consistent with the patient's presentation (see section 4.3.3.1).

c.10747G>C p.(Glu3583Gln) has MAF=0.01, and was seen in five patients here. It was reported to be pathogenic in a poster in a family with hereditary myotonia in 1975, but has not been reported since (Torbergson 1975). Due to its high population frequency and inconsistent presentation, it is likely to be benign.

Two of the patients received alternative diagnoses, 5.90 was subsequently found to have Duchene's MD, and 5.99 had a pathogenic *CAV3* mutation confirmed by western blot analysis (section 4.3.4.2). Therefore, both of these *RYR1* variations are not considered to be disease causing, although they could contribute to the patients' phenotypes.

Due to the large number of *RYR1* variations identified, the remaining 33 cannot be discussed separately. *RYR1* mutations are thought to account for 50-70% of MHS, and thus it is likely that many of found by this screening are disease-causing. Here, mutations are considered to be pathogenic if they have MAF \leq 0.001 and correlate with the patient phenotype, or if they have been convincingly reported to be disease-causing. If these limits do not apply, they are considered to be possibly pathogenic. This resulted in 23 patients with pathogenic and 13 with possibly pathogenic variations. However, diagnostic IVCT or HCCT testing would be required to confirm these assertions.

Patient	Mutation	Mutation information	MAF EVS/ 1000g/ ExAC	Ref	EMHG – in database or +/- 10aa	Phenotype fits with MHS?	Likely to be pathogenic?
5.179 (also in SCN4A results)	p.Leu32Phe	Mixed pathogenicity predictions	0.0009/ 0.001/ 0.0003	None	p.Cys35Arg	Yes, exercise- induced RM	Yes
5.170 (also in CACNA1S results)	p.Glu508Gln	Predicted to be damaging	0/ 0/ 0	None	No	Yes, exercise- induced RM	Yes
5.105	p.Ile637Phe	Predicted to be damaging	0/ 0/ 0	None	No	Unknown	Possibly
5.209	p.Asn759Asp	Predicted to be damaging	0.0002/ 0.0014/ 0.0003	None	No	Unknown	Possibly
5.176	p.Arg817Gln	Mixed pathogenicity predictions	0/ 0/ 0.0001	None	No	Yes, exercise- induced RM	Yes
5.90	p.Glu818Ala	Mixed pathogenicity predictions	0/ 0/ 0	None	No	No, later found to have	No
	p.Ala1708Ser	Predicted to be benign	0/ 0/ 0	None	No	Duchene's MD	
5.100	p.Asp849Asn	Mixed pathogenicity predictions	0.0004/ 0.0005/ 0.0002	None	No	Unknown	Possibly
	p.Pro1632Ser	Predicted to be pathogenic	0.0057/ 0.01/ 0.003	None	No		

5.43	p.R896Q	Predicted to be damaging	0.0001/ 0/ 0.0003	None	No	Unknown	Possibly
5.174	p.Ala933Thr	Seen in African men with MHS and exertional RM	0.0013/ 0/ 0.001	(Sambuughin et al. 2009)	No	Yes, exercise- and infection induced RM	Yes
	p.Ala1352Gly	Reported as MHS mutation, but also seen in non-MHS patients	0.0037/ 0.01/ 0.002	(Levano et al. 2009)	No		
5.13	p.Ala941Val	Mixed pathogenicity predictions	0/ 0/ 0.0004	None	No	No, no RM	Possibly
5.194 (also in <i>CACNA1S</i> and <i>DYSF</i> results)	p.Arg1109Lys	Predicted to be tolerated	0.0068/ 0.01/ 0.002	None	No	Yes, exercise- and infection induced RM	Possibly
	p.Thr2787Ser	Seen in a large MHS pedigree, but two variants segregated, unclear which is pathogenic.	0.01/ 0.01/ 0.003	Guis et al. 2004)	No		
5.115	p.Ala1352Gly	Reported as MHS mutation, but also seen in non-MHS patients	0.0037/ 0.01/ 0.002	(Levano et al. 2009)	No	Yes, infection induced RM	Yes
	p.Thr2787Ser	Seen in a large MHS pedigree, but two variants segregated, unclear which is pathogenic.	0.01/ 0.01/ 0.003	Guis et al. 2004)	No		
5.92	p.Ala1372Val	Predicted to be tolerated	0.0001/ 0/	None	No	Yes, exercise-	Yes

			0.00009			induced RM	
5.175	p.Gly1497Arg	Predicted to be damaging	0/ 0/ 0.00004	None	No	No, no RM	Possibly
5.154	p.Asp1856Asn hom	Mixed pathogenicity predictions	0/ 0/ 0	None	No	No, fixed weakness	Possibly
5.136	p.Glu1878Asp	Mixed pathogenicity predictions	0.0052/ 0.0041/ 0.0014	None	No	Unknown	Possibly
	p.Asp2943Asn	Predicted to be damaging	0.0042/ 0.0023/ 0.0009	None	No		
	p.His3647Gln	Predicted to be damaging (seems to be co – inherited with p.Asp2943Asn)	0.0042/ 0.0023/ 0.001	None	No		
5.119 (also in SCN4A results)	p.Thr2206Met	Reported as pathogenic, in database	0/ 0/ 0.00003	(Manning et al. 1998)	In database	Yes, RM with unknown trigger	Yes
5.24	p.Arg2224Cys	Mixed pathogenicity predictions	0/ 0/ 0.0002	None	No	Yes, exercise triggered RM	Yes
5.177 (also in CACNA1S results)	p.Gly2434Arg	Reported as pathogenic, in database	0/ 0/ 0.00002	(Keating et al. 1994)	In database	Yes, exercise triggered RM	Yes
5.18	p.Gly2434Arg	Reported as pathogenic, in	0/ 0/ 0.00002	Keating et al.	In database	Yes, exercise-	Yes

		database		1994)		and infection induced RM	
5.139	p.Gly2434Arg	Reported as pathogenic, in database	0/ 0	Keating et al. 1994)	In database	Unknown	Yes
5.178	p.Ser2685Phe	Predicted to be damaging, but also in unaffected mother	0/ 0/ 0.000008	None	No	Yes, exercise triggered RM	Yes
5.160 (also in <i>DYSF</i> results)	p.Thr2787Ser	Seen in a large MHS pedigree, but two variants segregated, unclear which is pathogenic.	0.01/ 0.01/ 0.003	Guis et al. 2004)	No	Unknown	Possibly
5.173	p.Thr2787Ser	Seen in a large MHS pedigree, but two variants segregated, unclear which is pathogenic.	0.01/ 0.01/ 0.003	Guis et al. 2004)	No	Yes, exercise- and infection induced RM	Possibly
5.99 (also in <i>CAV3</i> results)	p.Asp2943Asn	Predicted to be damaging	0.0042/ 0.0023/ 0.0009	None	No	No, no RM, <i>CAV3</i> mutation	No
	p.His3647Gln	Predicted to be damaging (seems to be co – inherited with p.Asp2943Asn)	0.0042/ 0.0023/ 0.001	None	No		
5.202	p.Val3088Met	Predicted to be damaging	0.0004/ 0.0009/ 0.0006	None	No	Yes, exercise-induced RM	Yes

5.131	p.Arg3366His	Reported as pathogenic with p.Tyr3933Cys probably co-inherited	0.0008/ 0.007/ 0.0009	(Duarte et al. 2011)	No	Unknown	Yes
	p.Tyr3933Cys	Reported as pathogenic in an MHS pedigree	0.0008/ 0.007/ 0.0009	(Gillies et al. 2008)	No		
5.65	p.Thr3425Met	Predicted to be damaging	0.0002/ 0/ 0.0002	None	No	Unknown	Possibly
5.37	p.Arg3539His	Reported to be pathogenic	0.0018/ 0.0005/ 0.0018	(Klein et al. 2012)	No	Yes, exercise-induced RM	Yes
5.64 (also in SCN4A results)	p.Arg3539His	Reported to be pathogenic	0.0018/ 0.0005/ 0.0018	(Klein et al. 2012)	No	Yes, exercise-induced RM	Yes
5.111	p.Arg3550Trp	Predicted to be pathogenic	0/ 0/ 0.0002	None	No	Yes, infection induced RM	Yes
5.12 (also in SCN4A results)	p.Glu3583Gln	Reported as possibly pathogenic in a poster	0.01/ 0.01/ 0.01	(Torbergsen 1975)	No	Yes, exercise-induced RM	Yes
	p.Val4547Met	Mixed pathogenicity predictions	0/ 0/ 0	None	No		
5.28	p.Glu3583Gln	Reported as possibly pathogenic in a poster	0.01/ 0.01/ 0.01	(Torbergsen 1975)	No	No, no RM	No

5.101	p.Glu3583Gln	Reported as possibly pathogenic in a poster	0.01/ 0.01/ 0.01	(Torbergesen 1975)	No	Unknown	No
5.183	p.Glu3583Gln	Reported as possibly pathogenic in a poster	0.01/ 0.01/ 0.01	(Torbergesen 1975)	No	Unknown	No
5.221	p.Glu3583Gln	Reported as possibly pathogenic in a poster	0.01/ 0.01/ 0.01	(Torbergesen 1975)	No	Unknown	No
5.109 (also in <i>DYSF</i> and <i>SCN4A</i> results)	p.His3981Tyr c.12861_12869dup9	Reported as pathogenic Known pathogenic mutation in the African population (not found by this panel)	0.004/ 0.01/ 0.001 0/ 0/ 0	(Wilmshurst et al. 2010) (Sambuughin et al. 2009)	No No	Yes, exercise-induced RM	Yes (mutation not found by this panel)
5.93	p.Gly4344Glu	Predicted to be damaging	0/ 0/ 0	None	No	Yes, RM although trigger unknown	Yes
5.3	p.Asp4505His	Causes MHS, shown with functional studies	0.003/ 0.003/ 0.006	(Groom et al. 2011)	No	Yes, infection-induced RM	Yes
5.30 (also in <i>ANO5</i> results)	p.Asp4505His	Causes MHS, shown with functional studies	0.003/ 0.003/ 0.006	(Groom et al. 2011)	No	No, no RM, and cardiomyopathy	No
5.89	p.D4878N	Mixed pathogenicity predictions	0/ 0/ 0	None	No	Yes, fever-induced RM	Yes

5.104	c.5671_5673 del	In-frame deletion	0.0005/ 0/ 0.0008	None	No	Yes, exercise- induced RM	Yes
5.159	c.5671_5673 del	In-frame deletion	0.0005/ 0/ 0.0008	None	No	No, no RM	Possibly

Table 5.4 – Rare variations found in RYR1. EMHG is the European malignant hyperthermia group, who have a database of proven pathogenic MHS mutations in Europe. Variations are heterozygous unless stated otherwise

Subsequent to this panel sequencing, patient 5.109 was found elsewhere to have an additional *RYR1* mutation, c.12861_12869dup9. This mutation has been widely reported to cause MHS in the African population, with a recent study finding the insertion present in almost a third of MHS families (Sambuughin et al. 2009; Dlamini et al. 2013). Manual inspection of the genomic region using the IGV genome browser showed that the region was not covered by the NGS here, and thus the mutation was not identified in this patient. It is possible that the mutation was also present in other patients, and this possibility will have to be investigated in the future.

4.3.1.2. CACNA1S Results

As well as HypoPP, mutations in *CACNA1S* are also a rare cause of MHS5, thought to account for about 1% of MHS patients. However, whilst the pathomechanism of HypoPP mutations is largely understood, little is known about how MHS5 mutations cause disease. The gene is, again, large and variable, and consequently variations are difficult to interpret. Due to the autosomal dominant inheritance pattern of MHS and the low incidence of MHS-causing *CACNA1S* mutations, only variations with MAF of ≥ 0.01 were considered. 14 heterozygous such variations were identified in 15 patients (one variation was seen twice) and are shown in Table 5.5.

One of the variations, c.4060A>T p.(Thr1354Ser), has previously been reported to be pathogenic in a large Italian pedigree. The variation segregated in 10 family members; it was present in those deemed MHS and MHE (malignant hyperthermia equivocal) and absent MHN (malignant hyperthermia negative) subjects, determined by IVCT. Furthermore, in myotubes, it caused faster activation and increased caffeine sensitivity (Pirone et al. 2010). However, more recently, p.(Thr1354Ser) has been re-classed as a variant of unknown significance due to its frequency in the population (EVS data shows it is present in 0.7% of people, which is roughly 1/150; prevalence of MHS is thought to be 1/2000 (Rosenberg et al. 2007)). Therefore it is unclear of the clinical significance of this variation in these patients, and if possible IVTC should be carried out to determine their MH status.

Patient	Mutation	Mutation information	MAF EVS/ 1000g/ ExAC	Reference
5.56 (also in <i>PFKM</i> and <i>PHKA1</i> results)	p.Lys88Glu	Conflicting pathogenicity predictions	0.0002/ 0/ 0.0003	
5.161	p.Ala102Thr	Novel, predicted to be tolerated	0/ 0/ 0.00007	
5.171	p.Lys132Met	Predicted to be tolerated	0.00008/ 0/ 0.0016	
5.180	p.Gly264Ser	Novel, conflicting pathogenicity predictions	0/ 0/ 0.00002	
5.201	p.Arg422His	Novel, predicted to be damaging	0/ 0/ 0.00008	
5.78	p.Arg462His	Predicted to be tolerated	0.00008/ 0/ 0.00008	
5.205 (also in <i>SGCA</i> results)	p.Arg498His	Novel, predicted to be damaging	0/ 0/ 0.0002	
5.204	p.Met635Val	Predicted to be damaging	0.0003/ 0/ 0.0004	
5.122	p.Val991Leu	Novel, predicted to be damaging	0/ 0/ 0	
5.177 (also in <i>RYR1</i> results)	p.Gly1210Arg	Conflicting pathogenicity predictions	0.0009/ 0/ 0.0005	
5.194 (also in <i>RYR1</i> and <i>DYSF</i> results)	p.Ala1271Thr	Predicted to be damaging	0.0072/ 0.0027/ 0.0017	
5.110, 5.127	p.Thr1354Ser	Mixed reports (see text)	0.0037/ 0.0009/ 0.002	(Pirone et al. 2010), (Gonsalves et al. 2013)
5.20	c.4242-1G>T	Novel, splice site mutation	0/ 0/ 0	
5.170 (also in <i>RYR1</i> results)	p.Asn1775Ser	Novel, predicted to be tolerated	0/ 0/ 0	

Table 5.5 – Rare heterozygous mutations found in *CACNA1S*

The remaining 13 variants found are equally difficult to interpret. Five of the patients also have results in other genes. One of those, 5.56, has been re-diagnosed since inclusion in the study as not having RM or exercise intolerance and thus unlikely to have mutation, demonstrating that rare variations are not necessarily disease causing. Patient 5.205 has a homozygous *SCGA* mutation that has been previously reported as pathogenic. The other three all have additional *RYR1* variations, two of which are deemed pathogenic, therefore if the patients did have MHS, an IVCT would not determine which gene was the cause without additional segregation studies. However, for the remaining nine *CACNA1S* variations found, especially the three novel that are not seen in population frequency databases, IVCT could give a good indication of their pathogenicity.

4.3.1.3. *SCN4A* Results

Mutations in *SCN4A* are known to cause a range of classic skeletal muscle channelopathy phenotypes including HypoPP, HyperPP, PMC and SCM. There has, however, been one case report of a patient with a known HyperPP mutation, c.4774A>G p.(Met1592Val), presenting with recurrent episodes of RM and fixed progressive weakness (Lee and Chahin), and a further AD family with PP and MHS segregating with two *SCN4A* mutations on the same allele (Bendahhou et al. 2000). Additionally, linkage studies of MHS families has led to the gene being suggested as a disease locus (Moslehi et al. 1998). As mutations in the gene are traditionally dominant, a filter of MAF ≥ 0.01 was used.

14 variations (12 distinct) were identified in 12 patients (two patients had the same two variations), shown in Table 5.6. None of the variations found have been reported in the literature. c.92G>T p.(Arg31Leu) and c.241G>C p.(Glu81Gln) were both found in two patients. Given this and their MAF similarity, it is likely they are co-inherited and found on the same allele.

One of the variations, c.968C>T p.(Thr323Met) was seen in patient 5.142, in whom likely pathogenic compound heterozygous *PYGM* mutations were found. This *SCN4A* mutation therefore is almost certainly benign. Additionally, five patients also had *RYR1* mutations that can be considered as pathogenic. The remaining six changes are extremely difficult to interpret, as *SCN4A* is a large and variable gene, and as none have been reported previously. Therefore, without functional investigations or segregation studies they must all remain variants of unknown significance and further conclusions cannot be drawn.

Patient	Mutation	Mutation information	MAF EVS/ 10009/ ExAC
5.57/ 5.61	p.Arg31Leu	Predicted to be benign	0.005/ 0.004/ 0.002
	p.Glu81Gln	Predicted to be damaging	0.005/ 0.004/ 0.002
5.163	p.Pro73Leu	Predicted to be damaging	0.0004/ 0.0009/ 0.00009
5.142 (also in <i>PYGM</i> results)	p.Thr323Met	Conflicting pathogenicity predictions	0.007/ 0.002/ 0.009
5.64 (also in <i>RYR1</i> results)	p.His599Arg	Conflicting pathogenicity predictions	0.003/ 0.0009/ 0.003
5.196	p.Thr603Arg	Novel, predicted to be damaging	0/ 0/ 0.000008
5.12 (also in <i>RYR1</i> results)	p.Val662Ile	Novel, conflicting pathogenicity predictions	0/ 0/ 0.00003
5.179 (also in <i>RYR1</i> results)	p.Pro882Gln	Predicted to be benign	0.003/ 0.004/ 0.001
5.119 (also in <i>RYR1</i> results)	p.Gly902Ser	Predicted to be benign	0.00008/ 0/ 0.0002
5.109 (also in <i>RYR1</i> and <i>DYSF</i> results)	p.Asn1503Ser	Predicted to be damaging	0.0005/ 0.0009/ 0.0002
5.186	p.Pro1571Ser	Novel, predicted to be damaging	0/ 0/ 0.00008
5.75	p.Val1644Met	Novel, predicted to be damaging	0/ 0/ 0.000008

Table 5.6 – Rare heterozygous mutations found in *SCN4A*

4.3.2. Glycogen Storage Disorder Genes

4.3.2.1. *PYGM* Results

Mutations in the *PYGM* gene cause McArdle's disease, also known as GSDV. This is the most common of the glycogen storage disorders, and patients' symptoms usually include RM and exercise intolerance, as well as characteristic 'second wind' phenomenon. Three of the patients in this study were found to have recessive *PYGM* mutations, as shown in Table 5.7.

Patient	Mutation	Mutation information	MAF EVS/ 1000g/ ExAC	Reference
5.142 (also in SCN4A results)	p.Met1? p.Ile571Ser	Disrupts start codon, published pathogenic Novel, in mutation hotspot	0/ 0/ 0.000008 0/ 0/ 0	(Tsuji no et al. 1994)
5.167	p.Arg50* hom	Most common mutation, present in at least 40% of confirmed GDSV patients	0.002/0.001/ 0.001	(Tsuji no et al. 1993)
5.218	p.Arg50* c.772+1G>T	(see above) Novel, splicing mutation	0.002/0.001/ 0.001 0/ 0/ 0	(Tsuji no et al. 1993)

Table 5.7 – Recessive mutations found in PYGM. Mutations are heterozygous unless stated otherwise

Of the three patients, two had compound heterozygous mutations and one had a homozygous mutation. c.148C>T p.(Arg50*) is the most common PYGM mutation and so there is no doubt that it is disease-causing when homozygous in patient 5.167. Interestingly, patient 3.167 has not had rhabdomyolysis episodes, however does experience exercise intolerance. McArdle's disease has been confirmed by muscle biopsy.

Each of the compound heterozygotes contained one known pathogenic mutation and one novel mutation. Both of these, however, are likely to be disease-causing as c.1702T>G p.(Ile571Ser) (harboured by patient 5.142) is in a mutation hotspot, with reported McArdle's mutations c.1709G>A p.(Arg570Gln), c.1708C>T p.(Arg70Trp), c.1722T>G p.(Tyr574*), c.1723A>G p.(Lys757Glu) and c.1726C>T (Arg576*) all within five amino acids. The phenotype of this patient is unknown. Patient 5.218 harbours the novel change c.772+1G>T predicted to disrupt splicing. This patient has an interesting case history; she is a 24 year old Brazilian woman who was unaffected with any muscle symptoms until performing a caesarean section delivery, after which she presented with compartment syndrome and a rhabdomyolysis event. Her muscle biopsy showed a vacuolar myopathy with increased glycogen content, consistent with McArdle's disease. Half (3/6) of the disease mutations seen in this cohort were p.Arg50*, reflecting the frequency that has been reported in the literature (Andreu et al. 2007).

4.3.2.2. PFKM Results

Tarui's disease or GSDVII is caused by mutations in the *PFKM* gene, encoding muscle phosphofructokinase. This screening produced two homozygous mutations in the gene, shown in Table 5.8.

Patient	Mutation	Mutation information	MAF EVS/ 1000 genomes	Reference
5.140	p.Tyr635His hom	Well conserved and predicted to be damaging	0/ 0/ 0	
5.56 (also in <i>PKHA1</i> and <i>CACNA1S</i> results)	p.Arg696His hom	Reported as pathogenic but with little evidence	0.012/ 0.01/ 0.01	(Raben et al. 1995)

Table 5.8 – Recessive mutations found in *PFKM*

Patient 5.140 harbours the novel homozygous change c.1903T>C p.(Tyr635His). This variation is not in population frequency databases, is at a conserved amino acid position and is predicted to be pathogenic by both Polyphen2 and SIFT, thus is likely to be disease causing, however, clinical data for the patient is unavailable.

c.2087G>A p.(Arg696His), found in patient 5.56, was reported to be pathogenic in 1995. In the study it was found as part of a compound heterozygous mutation in *PFKM*. Functional characterisation was carried out in the form of a yeast assay, which did not show the mutation was damaging. However, it was deemed pathogenic because it correlated with the patient phenotype and was not present in 30 controls (Raben et al. 1995). Due to this paper the mutation is included in the Human Gene Mutation Database (<http://www.hgmd.cf.ac.uk/>), a curated catalogue of disease causing mutations. The patient in question was a boy submitted to the study because of muscle pain and exercise intolerance, but since has been re-diagnosed with isolated knee pain and has been excluded, despite having a homozygous 'pathogenic' mutation. This suggests, along with the weakness of the initial evidence, and the high frequency (1%) in the population that the variation is actually a polymorphism. This finding highlights the importance of the re-evaluation of published mutation reports, as they can contain incorrect information.

4.3.2.3. *PHKA1* Results

Mutations in the X-chromosomal *PHKA1* gene are known to be responsible for GSDIXd, although only seven have been reported to date. Due to the X-linked nature of the disease, mutations are likely to be in men (as men only have one copy of the X chromosome). Furthermore, as the mutations in men are essentially dominant, only variations with a MAF ≥ 0.01 will be considered. Two such variations were identified in three male patients, as shown in Table 5.9. Neither had been previously reported. c.1468A>G p.(Asn490Asp), found in patient 5.56, was not seen in any frequency databases. However, this patient, as discussed in the previous section, has been re-diagnosed since submission into the study and is unlikely to harbour a RM or exercise intolerance causing mutation. This shows that, while absence from population frequency databases can be an indication of pathogenicity, they should still be treated with caution. The other variation, c.2462G>A p.(Arg821His), seen in patients 5.96 and 5.164, is present in EVS/ 1000genomes at a low level and is present in 130 hemizygous individuals in the ExAC browser and so is unlikely to be pathogenic, although biochemical analysis could be used to investigate the change further.

Patient	Mutation	Mutation information	MAF EVS/ 1000 genomes	Reference
5.56 (also in <i>PFKM</i> and <i>CACNA1S</i> results)	p.Asn490Asp	Predicted to be tolerated	0/ 0/ 0	
5.96/ 5.164	p.Arg821His	Predicted to be tolerated	0.003/ 0.003/ 0.004	

Table 5.9 – Possible pathogenic mutations found in *PHKA1*

4.3.2.4. *ENO3* Results

GSDXIII is a rare disorder caused by mutations in *ENO3*; to date mutations have only been reported in three families. A novel homozygous mutation was identified in patient 5.70 that had not been seen in EVS, 1000genomes or ExAC; c.1010G>A, p.(Cys357Tyr). Pathogenicity predictions for the variation are conflicting. Patient 5.70 has had four episodes of rhabdomyolysis with unknown trigger and has exercise intolerance, a phenotype consistent with GSDXIII. Based on the findings of this project, enolase enzymatic activity of the patient was assessed and found to be 33% that of simultaneous controls (normal activity of other metabolic enzymes confirmed sample integrity). Additionally there was a significant lag in the reaction running to completion, as shown in Figure 5.2 (36 minutes in this patient, compared to 18 minutes in controls).

These results strongly indicate that the mutation found was disease-causing in this patient, and so represents only the fourth ever GSDXIII case.

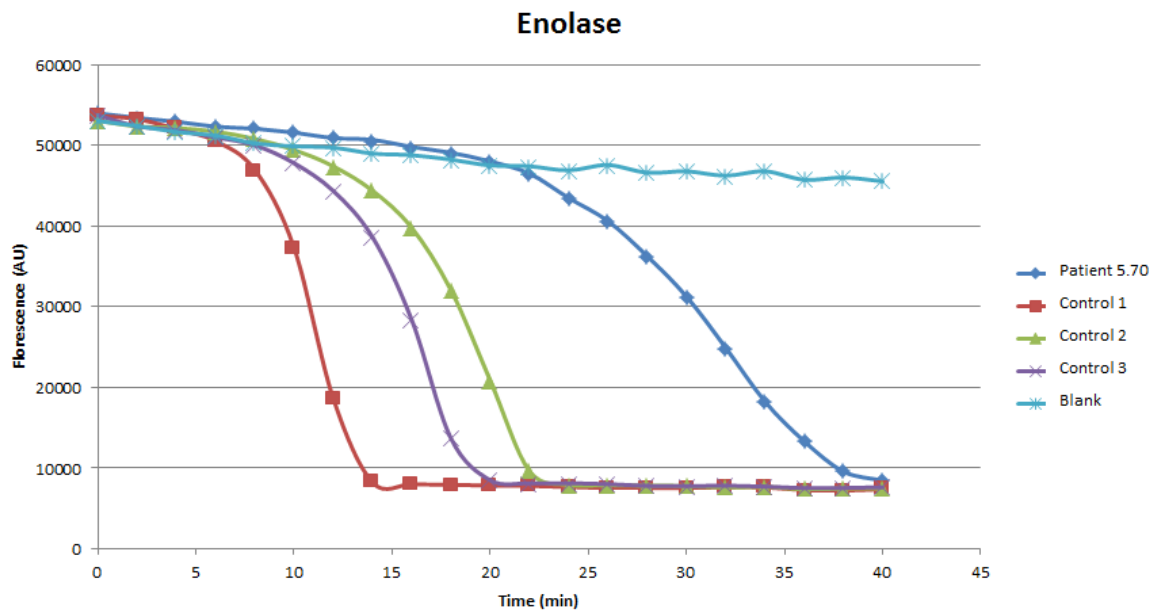


Figure 5.2 – Enolase activity assay, showing that there is a significant lag of reaction completion comparing the sample of patient 5.70 and controls. The assay was performed by Dr Ralph Wigley at Great Ormond Street Hospital

4.3.2.5. GYG1 Results

GYG1 mutations cause GSDXV, a rare glycogen storage disease. To date only eight patients have been reported with mutations in the gene, one with cardiomyopathy and muscle weakness and seven with slowly progressive myopathy and no cardiac involvement (Moslemi et al. 2010; Malfatti et al. 2014). Neither exercise intolerance nor RM have been reported in connection with the gene.

In this cohort one patient (patient 5.26) was found to have a homozygous mutation in the gene; c.487delG, p.(Asp163Thrfs*5). This mutation has been reported in both of the above studies, once as part of a compound heterozygote and once as a homozygote. It has been shown to result in nonsense-mediated decay and thus the patient will have a complete absence of glycogenin-1 enzymatic activity (Malfatti et al. 2014).

Patient 5.26 is an 84 year old woman with a life-long history of progressive muscle weakness, initially misdiagnosed with muscular dystrophy. Her weakness caused her to have a serious car accident, and subsequently a glycogen storage disorder was diagnosed. She does not describe exercise intolerance, however was encouraged not to exercise much due to muscle pain. She has had several episodes of

dark urine, but it is unclear if these were RM episodes as it was thought they were urinary tract infections, and no CK level was taken. Therefore it is possible that this could be the first time that *GYG1* mutations are responsible for RM. The finding also demonstrates that glycogen storage disorders can be mistaken for muscular dystrophy, and so should be considered as a differential diagnosis for patients with progressive muscle weakness.

4.3.3. Fatty Acid Metabolism Genes

4.3.3.1. *CPT2* Results

CPTII deficiency, the most common of the fatty acid metabolism disorders, results from recessive mutations in the *CPT2* gene. Here, panel screening identified compound heterozygous or homozygous variations in four patients, shown in Table 5.10.

Patient	Mutation	Mutation information	MAF EVS/ 1000g/ ExAC	Reference
5.7	p.Gln304His	Predicted to be benign, not well conserved	0.0005/ 0.0005/ 0.0001	
	p.Val507Ile	Predicted to be benign, not well conserved	0.0005/ 0.0005/ 0.0002	
5.63 (also in <i>ANO5</i> results)	p.Ala101Val	Predicted to be benign, not well conserved	0.005/ 0.003/ 0.002	
	p.Phe352Cys	Mixed pathogenicity reports in the literature	0.007/ 0.06/ 0.02	(Isackson et al. 2006; Yao et al. 2008)
5.152/ 5.153	p.Ser113Leu hom	Most common mutation, common in 60% confirmed <i>CPTII</i> deficiency patients	0.001/ 0.001/ 0.001	(Taroni et al. 1993)

Table 5.10 – Recessive mutations found in *CPT2*. Mutations are heterozygous unless stated otherwise

Two of the patients, 5.152 and 5.153 were homozygous for c.338C>T p.(Ser113Leu), by far the most common mutation in *CPT2* (Thuillier et al. 2003), and so the cause of their disease has been determined, although clinical information has not been provided for either patient. The two patients with compound heterozygous *CPT2* variations are more ambiguous. The first, patient 5.7, has two variants that are present in the

population, but are very rare with MAF = 0.0005 or 0.0001 depending on the database. They are both poorly conserved and predicted to be benign. Furthermore, their MAF similarities suggest they may be on the same allele and thus are co-inherited; this would infer the patient still had one normal copy of the *CPT2* gene. These factors together suggest they are benign. The second patient, 5.63, has two variants which are more frequent in the population, with c.1055T>G p.(Phe352Cys) being in 6% in 1000 genomes and reported in up to 20% of the Japanese population (Wataya et al. 1998). However, the variation has been reported elsewhere as pathogenic and functional studies has shown that it causes reduction of CPTII activity (Isackson et al. 2006; Yao et al. 2008). Therefore, it is currently unclear whether this combination of variations is disease causing, benign, or contributing to a wider genetic picture, as the patient in question also harbours two *ANO5* variations of unknown significance and a heterozygous *PYGM* splicing mutation. The variations found may be not deleterious to result in isolation, but have a cumulative effect. Clinical information could be used to unravel the genetic information, however unfortunately none was provided by the referring clinician.

4.3.3.2. HADHB Results

Recessive mutations in both *HADHA* and *HADHB* result in deficiency of the mitochondrial trifunctional protein, and the residual level of enzyme remaining governs the severity of the condition. Patient 5.158 was found to harbour two compound heterozygous mutations in *HADHB*. The first of the mutations, c.1289T>C p.(Phe430Ser) had previously been reported causing a severe new-born phenotype, and together with a mutation on the other allele resulted in only 4% enzymatic activity (Das et al. 2006). The second mutation, c.397A>G p.(Thr133Ala) is unreported, but affects the same amino acid as a known pathogenic mutation, c.397A>C p.(Thr133Pro) (Spiekerkoetter et al. 2003). This mutation was present in a myopathy patient with 17% residual activity. Therefore the two mutations together are likely to cause a non-severe phenotype; however, regrettably, once again a lack of phenotypic description means that this assertion cannot be confirmed.

4.3.3.3. ACADVL Results

VLCAD (Very long-chain acyl-CoA dehydrogenase) deficiency is a disorder caused by recessive mutations in the *ACADVL* gene; over 100 mutations have been reported in the gene to date. The panels identified homozygous or compound heterozygous mutations in three of the patients tested, detailed in Table 5.11.

Patient	Mutation	Mutation information	MAF EVS/ 1000g/ ExAC	Reference
5.16	p.Arg469Gln hom	Reported as pathogenic	0/ 0/ 0	(Andresen et al. 1999)
5.113	p.Arg366His	Reported as pathogenic	0/ 0.0005/ 0.00002	(Andresen et al. 1999)
	p.Arg469Gln	Reported as pathogenic	0/ 0/ 0	(Andresen et al. 1999)
5.217	p.Phe376Ser	Well conserved and predicted to be damaging	0/ 0/ 0.000008	
	c.1752-1G>A	Splice site mutation	0/ 0/ 0	

Table 5.11 – Recessive mutations found in ACADVL. Mutations are heterozygous unless stated otherwise

c.1406G>A p.(Arg469Gln) appeared as both a homozygous mutation and as part of a compound heterozygous mutation. It is a mutation that has been well correlated with a disease-related reduction in VLCAD levels, as has c.1097G>A p.(Arg366His) (Andresen et al. 1999). Additionally, patient 5.16 displays the typical VLCAD deficiency phenotypic features, and has had reduced enzyme levels shown biochemically. Therefore it can confidently be assumed that they are the disease causing mutations in both patients 5.16 and 5.113; however VLCAD levels should be assessed in patient 5.113 for confirmation.

Both of the variations found in patient 5.217 are novel and have not before been reported to cause disease. However, they are both largely absent from control populations (c.1127T>C p.(Phe376Ser) was seen in one out of more than 65,000 control genomes) and predicted to have functional consequences; c.1752-1G>A is predicted to affect splicing and p.(Phe376Ser) is predicted by both Polyphen2 and SIFT to be damaging. Additionally, the patient's phenotype is consistent with VLCAD deficiency, and, based on the findings of this project, the patient's VLCAD levels were assessed biochemically and found to be deficient. Therefore, it is highly likely that both variations are pathogenic.

4.3.4. Muscular Dystrophy Genes

4.3.4.1. ANO5 Results

ANO5 gene mutations are known to cause Miyoshi muscular dystrophy type 3 and limb-girdle dystrophy type 2L; however RM and exercise intolerance can be the presenting features for patients. This study identified homozygous or compound heterozygous variations in four patients, as shown in Table 5.12.

Patient	Mutation	Mutation information	MAF EVS/ 1000g/ ExAC	Reference
5.30 (also in <i>RYR1</i> results)	p.Asn64Leufs*15 hom	Published, common muscular dystrophy mutation	0.002/ 0/ 0.001	(Hicks et al. 2011)
5.200	p.Ile300Asnfs*35 p.His334Ilefs*17	Novel, leads to premature stop codon Novel, leads to premature stop codon	0/ 0/ 0 0/ 0/	
5.19	p.Asn64Leufs*15 p.Gly231Val	Published, common muscular dystrophy mutation Published as pathogenic	0.002/ 0/ 0.001 0.0008/ 0.0005/ 0.001	(Hicks et al. 2011) (Bolduc et al. 2010)
5.63 (also in <i>CPT2</i> results)	p.Val87Ile p.Gly227Ala	Predicted to be possibly damaging and tolerated Predicted to be benign and tolerated	0.003/ 0.003/ 0.001 0.003/ 0.002/ 0.0009	

Table 5.12 – Recessive mutations found in ANO5. Mutations are heterozygous unless stated otherwise

The mutations found in two of the patients, 5.30 and 5.19 seem to be undoubtedly pathogenic, as both the mutations found have been reported to be disease-causing. c.191dupA p.(Asn64Leufs*15), especially, has been reported widely and is a relatively

common mutation in *ANO5*; one study identified it in one third of their cohort (Hicks et al. 2011). Patient 5.30, however, was also found to have a known MHS mutation in *RYR1*, p.(Asp4505His). Functional studies have proved that this mutation to be pathogenic (Groom et al. 2011). The patient does not have episodes of RM, but instead exercise intolerance and cardiomyopathy. This is more consistent with an MD than an MHS diagnosis, thus it is likely that the *ANO5* mutations are underlying the patient's condition. However the *RYR1* mutation could be contributing to the phenotype or the patient could have additional underlying MHS. This case demonstrates the genetic complexity that can underpin these disorders.

Patient 5.19 also has an interesting clinical history. She is a 75 year old lady with debilitating exertional myalgia. She has been extensively investigated, with no previous success as she had no evidence of dystrophy on her muscle biopsy. This panel has therefore provided a long-needed diagnosis for the patient.

Patient 5.200 has two novel compound heterozygous frameshift mutations which both result in premature stop codons, c.898_899insA p.(Ile300Asnfs*35) and c.1000delC p.(His334Ilefs*17). This is likely to result in nonsense mediated decay, as has been reported for similar mutations in the gene (Bolduc et al. 2010). The mutations are on different alleles, therefore it is highly likely that this combination of mutations is pathogenic, as the patient will have a complete lack of the *ANO5* protein. No clinical information is available for the patient.

The mutations of the last patient, patient 5.63, are more difficult to interpret. Both variations seen have not been predicted to be pathogenic by either Polyphen2 or SIFT. Furthermore, their population frequency similarities suggest they could be present on the same allele and so co-inherited. This patient also has compound heterozygous *CPT2* mutations of unknown significance, no clinical information, and is discussed further in section 4.3.3.1.

4.3.4.2. SGCA Results

Mutations in *SGCA* cause limb-girdle muscular dystrophy type 2D, one of the sarcoglycanopathies. In rare cases, RM can be a presenting feature of this disorder (Ceravolo et al. 2014). This study identified one patient, patient 5.205 with a homozygous mutation in the gene, c.850C>T, p.(Arg284Cys). This mutation is very rare, only being present in the population at rates of 0.00007 and 0.000008 (EVS and ExAC respectively), and has previously been reported to be disease-causing (Angelini et al. 1998). In the initial report the homozygous mutation was present in a pair of siblings; the index case with muscular dystrophy and her asymptomatic brother

(although his CK was raised). Interestingly, although they had the same mutation, western blot analysis showed that she had 10% residual enzyme, while he had 25%, presumably accounting for the variation in their severity. This mutation is therefore highly likely to be pathogenic in this patient, although unfortunately clinical details are not available to confirm the diagnosis.

4.3.4.3. *DYSF* Results

Miyoshi muscular dystrophy and limb-girdle muscular dystrophy type 2B are caused by mutations in the *DYSF* gene, encoding the protein dysferlin. To date, there has only been one reported case of a patient with *DYSF* mutations presenting with RM, and none of exercise intolerance, and so it is likely that it will be a rare cause of disease in this cohort (Moody and Mancias 2013). However, it is a variable gene, making coding changes difficult to interpret, and more than 350 *DYSF* mutations have been reported. The variability was reflected in this study, as rare homozygous or compound heterozygous variations were identified in 14 patients, shown in Table 5.13, several of which have been reported as being disease causing previously. Some of these, however, are relatively common in the population and when the literature is examined do not appear to be likely to be pathogenic. Of the 14 patients in whom variations were found, four have possible pathogenic mutations in other genes and only one is highly probable having pathogenic *DYSF* mutations. This is the novel homozygous change c.3708delA, p.(Asn1237Thrfs*25) found in patient 5.150, which is likely to result nonsense mediated decay and thus complete absence of the dysferlin protein. Again, unfortunately the clinical details of the patient are unavailable. A further six patients have possible pathogenic mutations, and western blot analysis of dysferlin levels would be required to confirm the effects of the variations found. These results again highlight the importance of being discerning when reading published mutation reports.

Patient	Mutation	Mutation information	MAF EVS/ 1000g/ ExAC	Disease Causing?	Reference
5.40	p.Leu189Val	Conflicting reports in literature; reported in patient with reduced dysferlin on WB, but also seen described as polymorphism	0.02/ 0.002/ 0.008	Possibly	(van der Kooi et al. 2007; Krahn et al. 2009)
	p.Gln1784Lys	Novel, conflicting pathogenicity predictions	0/ 0/ 0		
5.88/ 5.89 (also in RYR1 results)	p.Arg1331Leu	Seen frequently in literature, probably polymorphism	0.02/ 0.02/ 0.02	Probably not	(Cagliani et al. 2003; Nguyen et al. 2005; Rosales et al. 2010)
	p.Tyr1494His	Seen in patient with 3 potential <i>DYSF</i> mutations	0.0005/ 0/ 0.0005		
5.108	p.Glu140Asp	Novel, Predicted to be benign	0/ 0/ 0	Possibly	(Nguyen et al. 2007)
	p.Glu457Lys	Reported in compound het with nonsense mutation	0.02/ 0.008/ 0.02		
5.109 (also in RYR1 and SCN4A results)	p.Arg1022Gln	Reported in patient without another mutation, and elsewhere as unclear pathogenicity	0.02/ 0.01/ 0.02	Probably not	(Cagliani et al. 2003; Krahn et al. 2009)
	p.Thr1662Met	Seen with other pathogenic mutation -	0.00008/ 0/ 0.0001		

		probably pathogenic			
5.125	p.Leu189Val	Conflicting reports in literature; reported in patient with reduced dysferlin on WB, but also seen described as polymorphism	0.02/ 0.002/ 0.008	Possibly	(van der Kooi et al. 2007; Krahn et al. 2009)
	p.Ser1353Tyr	Novel, predicted to be damaging	0/ 0/ 0		
5.144	p.Glu541Gly	Novel, predicted to be benign	0/ 0.0002/ 0.00006	Possibly	
	p.Ile1607Thr	Found in patient with negative dysferlin WB staining (poster abstract only)	0.001/ 0.001/ 0.003		(Looi et al. 2010)
5.150 (also in <i>DMD</i> results)	p.(Asn1237Thrfs*25) hom	Likely to result in nonsense mediated decay and thus complete protein deficiency	0/ 0/ 0	Yes	
5.169/ 5.192	p.Arg1022Gln	Reported in patient without another mutation, and elsewhere as unclear pathogenicity	0.02/ 0.01/ 0.02	Probably not	(Cagliani et al. 2003; Krahn et al. 2009)
	p.Arg1331Leu	Seen frequently in literature, probably polymorphism	0.02/ 0.02/ 0.02		(Cagliani et al. 2003; Nguyen et al. 2005; Rosales et al. 2010)
5.185	p. Arg1022Gln	Reported in patient without another mutation, and elsewhere as unclear pathogenicity	0.02/ 0.01/ 0.02	Possibly	(Cagliani et al. 2003; Krahn et al. 2009)

	p. Ile1325Val	Possibly on same allele as V398M as similar frequency	0.0046/ 0.0023/ 0.001		
	p.Val398Met	Possibly on same allele as I1325V as similar frequency	0.0048/ 0.0023/ 0.001		
5.194 (also in <i>RYR1</i> and <i>CACNA1S</i> results)	p.Pro233Leu	Novel, conflicting pathogenicity predictions	0.00046/ 0/ 0.0001	Probably not	(Cagliani et al. 2003; Nguyen et al. 2005; Rosales et al. 2010)
	p.Arg1331Leu	Seen frequently in literature, probably polymorphism	0.02/ 0.02/ 0.02		
5.26 (also seen in <i>GYG1</i> results)	p.Val705Met	Predicted to be benign	0/ 0.0005/ 0.0002	Probably not	
	p.Met968Leu	Predicted to be benign	0.0018/ 0.0014/ 0.0015		
5.35	p.Glu1471Lys	Novel, predicted to be pathogenic	0/ 0/ 0.0003	Possibly	
	p.Ile2047Val	Novel, conflicting pathogenicity predictions	0.0002/ 0.0014/ 0.0004		

Table 5.13 – Recessive mutations found in *DSYF*. Mutations are heterozygous unless stated otherwise

4.3.4.4. DMD Results

Similarly to *DYSF*, *DMD*, the gene encoding dystrophin, is large and variable. The gene is found on the X chromosome, almost 3000 mutations have been reported to date, and the vast majority of mutations result in a truncated or absent protein. Mutations cause Duchene or Becker muscular dystrophy, or X-linked dilated cardiomyopathy. Due to the X-linked nature of the diseases, the large amount of variability and the huge bias against missense mutations, variations in the gene were only considered if they were in men or homozygous in women and either a) previously reported as being deleterious, b) not present in either EVS or 1000 genomes or c) likely to result in a truncated or absent protein. Mutations that fit these criteria were present in four patients and are shown in Table 5.14.

Patient	Mutation	Mutation information	MAF EVS/ 1000g/ ExAC	Reference
5.143	c.31+1G>T hemizygous	Reported to cause cardiomyopathy	0/ 0/ 0	(Milasin et al. 1996)
5.160 (also in RYR1 results)	p.Asn1672Lys p.Glu2910Val p.Asn2912Asn	Initially reported as pathogenic but since deemed too common Both E2910V and N2912D initially reported as pathogenic but since deemed too common, probably co-inherited	0.02/ 0.02/ 0.008 0.03/ 0.04/ 0.02 0.03/ 0.04/ 0.02	(Feng et al. 2002; Andreasen et al. 2013) (Lenk et al. 1994; Piton et al. 2013)
5.116	p.Glu2910Val p.Asn2912Asn	Both E2910V and N2912D initially reported as pathogenic but since deemed too common, probably co-inherited	0.03/ 0.04/ 0.02 0.03/ 0.04/ 0.02	(Lenk et al. 1994; Piton et al. 2013)
5.150 (also in <i>DYSF</i> results)	p.Thr1948Ser hemizygous	Novel, conflicting pathogenicity predictions	0/ 0/ 0.00001	

Table 5.14 – Mutations, that fit the described criteria, found in *DMD*

Three of the mutations (c.5016T>A p.(Asn1672Lys), c.8729A>T p.(Glu2910Val) and c.8734A>G p.(Asn2912Asn) were initially reported as responsible for X-linked dilated cardiomyopathy, but since the availability of large amounts of exome data have been deemed too frequent to be disease-causing (Andreasen et al. 2013; Piton et al. 2013). Therefore, they are unlikely to be pathogenic in these patients. c.5842A<T p.(Thr1948Ser), identified in patient 5.150, is novel and not present in population databases. However, the patient also has a homozygous frameshift *DYSF* variation; so again, this DMD variant is probably not disease-causing. The one remaining patient, 5.143, has an undisputed published splice site mutation, c.31+1G>T, reported to again cause X-linked dilated cardiomyopathy (Milasin et al. 1996). This, traditionally, does not have any skeletal involvement, thus this is a new presentation of the mutation; however, the clinical data for the patient is again unavailable. It is worth noting that, as 65% of known disease-causing mutations are large-scale deletions (Monaco et al. 1988) and so would not have been identified by this sequencing panel, *DMD* mutations may have been missed in this cohort. Further MLPA or CGH analysis would be required to investigate if this is the case.

4.3.5. Miscellaneous Genes

4.3.5.1. *LPIN1* Results

In one patient, 5.199, a novel homozygous 1bp insertion resulting in a premature stop codon, c.2269dupA, p.(Ser757Lys)fs*12, was identified in the *LPIN1* gene. This is likely to cause nonsense mediated decay of the mRNA, and thus result in a complete deficiency of the phosphatidic acid phosphatase 1 enzyme. A clinical picture has not been provided for the patient to corroborate this assertion.

LPIN1 mutations are thought to be a common cause of unexplained RM episodes, and in one study mutations in the gene were found in 59% of the cohort (Michot et al. 2010). Therefore, it is surprising that more *LPIN1* mutations were not identified in our cohort. In the study, however, 47% of the mutations identified were the same large in-frame intronic deletion, c.2295-866_2410-30del, p.)Glu766_Ser838del) which removed exons 18 and 19 from the resultant protein. This mutation is too large to be identified by this panel technology, and so it is likely that it could have been present in some of the samples tested here. Furthermore, four patients (patients 735, 5.57, 71303, 76161) had one novel mutation in the gene that were not seen in control populations, and a further one patient, patient 67035, had a known recessive pathogenic mutation. It is a possibility that some of these patients also harbour the

deletion. CNV analysis or LPIN biochemical enzymatic activity is needed to confirm these suspicions.

4.3.5.2. CAV3 Results

Caveolin-3 is the muscle specific form of the caveolin protein, encoded by the *CAV3* gene. Caveolin-3 is thought to be a principal component of caveolea (literally ‘little caves’), which are small invaginations on the cell surface, compartmentalising the plasma membrane (Minetti et al. 1998). Additionally, caveolin-3 is important for the regulation of sarcolemmal stability, signalling pathways and vesicular transport (Hayashi et al. 2004). The term ‘caveolinopathy’ refers to the broad spectrum of disorders known to be associated with autosomal dominant or recessive mutations in the *CAV3* gene. This spectrum consists of five main phenotypes; LGMD1C, hyperCKemia, rippling muscle disease (RMD), hypertrophic cardiomyopathy and distal myopathy, although other, rarer, clinical presentations have been reported including only one case of RM (McNally et al. 1998).

Two heterozygous mutations were identified in five patients in this cohort, shown in Table 5.15. One had been previously reported, and both are present in population databases. One further LGMD-causing mutation, c.166G>A p.(Gly56Ser), was found in three patients (5.222, 5.216, and 5.174), but this mutation is thought to be recessive, and genetic and functional investigations have shown that one copy is unlikely to be pathogenic (McNally et al. 1998; de Paula et al. 2001; Brauers et al. 2010).

Patient	Mutation	Mutation information	MAF EVS/ 1000g/. ExAC	Reference
5.102, 5.25	p.Val14Ile	Predicted to be benign, at same amino acid as previously reported mutation (Val14Leu)	0.001/ 0.001/ 0.0005	(Cronk et al. 2007)
5.99 (also seen in <i>RYR1</i> results), 5.68, 5.31	p.Thr78Met	Widely reported to be pathogenic	0.004/ 0.002/ 0.003	(Vatta et al. 2006)

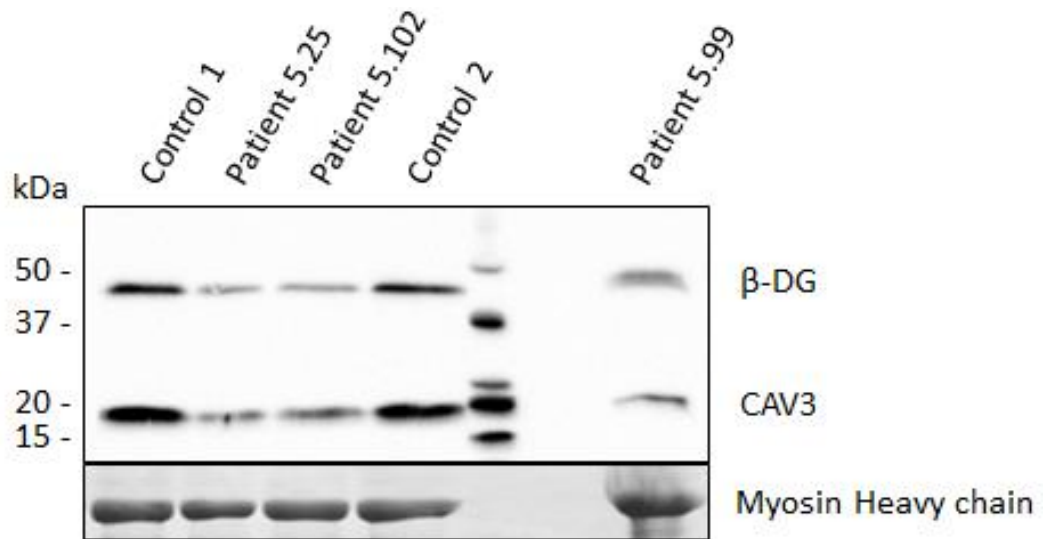
Table 5.15 –Heterozygous mutations found in *CAV3*

Both of these mutations were considered to be potentially disease-causing in our five patients. c.233C>T p.(Thr78Met) has been frequently reported cause a range a

caveolinopathies including hyperCKemia, RMD, distal myopathy, cardiomyopathy, sudden infant death syndrome and LGMD (Vatta et al. 2006; Cronk et al. 2007; Traverso et al. 2008). One study claimed that p.(Thr78Met) was a polymorphic variant in southern Italy (Spadafora et al. 2012), however expression of the mutant in HEK cells resulted in 5-fold increase in sodium current, implying a functional consequence (Cronk et al. 2007) The same study showed a similar finding for c.40G>C p.(Val14Leu), a mutation that disrupts the same amino acid c.40G>A p.(Val14Ile), seen twice in this cohort. To investigate the effect of the mutation, levels of the caveolin-3 in three patients (2 x p.(Val14Ile), 1 x p.(Thr78Met)) were assessed using a western blot; they were found to be reduced by more than 50% compared to controls (Figure 5.3). This suggests that the mutations are disease-causing. Interestingly, β -dystroglycan, used as a loading control, also had reduced levels in samples. β -dystroglycan, is a known interactor of caveolin-3 (Sharma et al. 2010). The significance of this reduction is unknown; however myosin heavy chain was also used to as a protein loading control, ensuring the effect is not due to uneven protein loading. The western blot was performed by Julie Marsh and, Rita Barresi at the NHS Muscle Immunoanalysis Unit in Newcastle.

As there has only been one reported case of caveolin-3- related RM in the literature, the relative frequency of *CAV3* mutations was an intriguing and exciting finding. Therefore, the clinical features of these five patients were thoroughly examined and are summarised in Table 5.16. Two of the patients had recurrent RM, three had muscle rippling, and all five had myalgia. Interestingly, the father patient 5.31 had LGMD, and also carried the mutation, highlighting the phenotypic variability of the change. These results suggest that *CAV3* mutations are a more common cause of recurrent RM than previously thought.

a)



b)

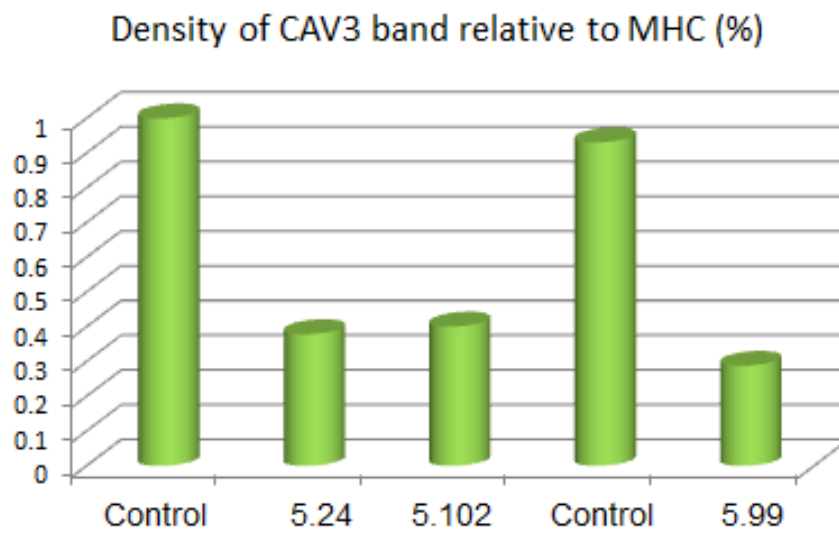


Figure 5.3 – Levels of caveolin-3 and β -dystroglycan in three patients with CAV3 mutations. Myosin heavy chain is used as a protein loading control. The western blots were performed by Julie Marsh and, Rita Barresi at the NHS Muscle Immunoanalysis Unit in Newcastle

Patient	5.102	5.25	5.68	5.99	5.31
Mutation	p.Val14Ile	p.Val14Ile	p.Thr78Met	p.Thr78Met	p.Thr78Met
Ethnicity + gender	African, M	Afro-Caribbean, F	Spanish, M	Unknown, M	Greek Cypriot, M
Age of onset	20s	30s	30s: first	Childhood	Childhood
Presenting symptom	Severe fatigue, malaise and widespread muscle pain	Calf pain	Aching following physical activity	Myalgia Muscle cramps	Muscle weakness
RM	Recurrent	No	3 episodes	No	No
Rippling	Yes	Yes	NA	No	Yes
Myalgia	Widespread muscle pain	Widespread muscle pain	Following exertion	Following prolonged exertion	Discomfort following prolonged physical exertion
Fixed weakness	Upper limbs	Proximal lower limbs	No	No	Handgrip - mild
Muscle atrophy	NA	Thigh	No	No	No
Exercise intolerance	NA	Yes	Yes	Yes (Mild)	Yes
Fatigue	Yes	Yes	No	No	Yes
Basal CK	500	300 - 600	126	600 - 800	142
Highest CK	28,000	Unknown ('raised')	5,000	4,000	Unknown
Family history	Negative	Negative	Negative	Negative	Father: LGMD
Additional features	Mild sensory deficit to light touch	NA	NA	Early hypoglycaemic seizures	NA

Table 5.16 –Clinical features of the five patients with CAV3 mutations. Compiled by Renata Scalco

4.3.6. Overall

Overall, the panel identified pathogenic mutations in 47 patients (21.0% of the cohort) and possible pathogenic mutations in a further 38 patients (16.9% of the cohort), summarised in Table 5.17. If a patient had a possible pathogenic mutation and a pathogenic mutation in different genes, only the pathogenic mutation is counted. If they had two possibly pathogenic mutations they are included in the lists for both genes in bold.

Gene	Patients - pathogenic mutations	Total	Patients – possible pathogenic mutations	Total
<i>RYR1</i>	5.179, 5.170, 5.176, 5.174, 5.115, 5.92, 5.119, 5.24, 5.177, 5.18, 5.139, 5.178, 5.202, 5.131, 5.37, 5.64, 5.111, 5.12, 5.109, 5.93, 5.3, 5.89, 5.104	23	5.105, 5.209, 5.100, 5.43, 5.13, 5.194 , 5.175, 5.154, 5.136, 5.160, 5.173, 5.65, 5.159	13
<i>CACNA1S</i>		0	5.20, 5.78, 5.110, 5.127, 5.122, 5.161, 5.171, 5.180, 5.201, 5.204, 5.202	11
<i>SCN4A</i>		0	5.57, 5.61, 5.163, 5.196, 5.186, 5.75	6
<i>PYGM</i>	5.142, 5.167, 5.218	3		0
<i>PFKM</i>	5.140	1		0
<i>ENO3</i>	5.70	1		0
<i>GYG1</i>	5.26	1		0
<i>CPT2</i>	5.152, 5.153	2	5.63	1
<i>HADHB</i>	5.158	1		0
<i>ACADVL</i>	5.16, 5.113, 5.217	3		0
<i>ANO5</i>	5.30, 5.200, 5.19	3	5.63	1
<i>SGCA</i>	5.205	1		0
<i>DYSF</i>	5.150	1	5.40, 5.108, 5.125, 5.144, 5.185, 5.35, 5.194	7
<i>DMD</i>	5.143	1		0
<i>LPIN</i>	5.199	1		0
<i>CAV3</i>	5.102, 5.25, 5.99, 5.68, 5.31	5		0

Table 5.17 – Patients in whom pathogenic and possibly pathogenic mutations were found by the rhabdomyolysis panel

4.4. Polymorphism Analysis - Previously Reported Risk Factors

It is well documented that there are direct genetic causes for recurrent RM and exercise intolerance. However, it is also thought that some common CNVs and polymorphisms are risk factors, and thus make someone harbouring them more susceptible to an RM episode under certain conditions such as physical exertion (Deuster et al. 2013). To date 18 polymorphisms or CNVs have been reported to contribute to RM, exercise intolerance or raised CK (Table 1.12). The majority of these are in intronic or in the UTR, thus only two were covered by the TruSight one panel. The MAF of each of the two in this cohort was compared to the population and in-house frequency databases to determine if they were present at a higher level in the disease group.

4.4.1. *ACTN3* p.(Arg577*) - rs1815739

ACTN3 encodes α -actinin-3, a structural skeletal muscle protein with additional roles in signalling and metabolic functions (Norman et al. 2014). c.1729C>T p.(Arg577*) is a common polymorphism (rs1815739) (described here as R577X, where X is a stop codon) in the *ACTN3* gene, and results in the loss of the protein, therefore XX homozygotes possess no α -actinin-3 within their skeletal muscles. This loss is largely compensated by the homologous α -actinin-2 (North et al. 1999). However, it has long been noted that there is a lower percentage of elite athletes with the XX genotype than in the general population; therefore, it is likely that the protein has a function in exercise (Yang et al. 2003), a finding that has been emulated in many sporting communities of different ethnicities (Guth and Roth 2013).

The MAF of the polymorphism varies depending on population, with the lowest incidence occurring in Africa, and the frequency of XX individuals increasing with distance from Africa. Incidence of the XX genotype is highest in America (Guth and Roth 2013). Reports of the population percentage harbouring the XX genotype varies, but is thought to be around 18% in white European populations and 25% in Asian populations (Yang et al. 2003).

In recent years, the polymorphism has been associated with recurrent RM, with one study finding that XX people were almost three times more likely to have recurrent RM than RR individuals (Deuster et al. 2013). However, the control group used contained proportionally four times more individuals of African descent (who are more likely to be RR) than the cases, which would have perhaps skewed the results. Another study showed that the XX genotype resulted in a lower baseline CK, although the

authors failed to find a significant relationship with post-exercise CK and myoglobin levels (Clarkson et al. 2005).

Here, the X allele had a MAF of 0.49, with 28% of the cohort harbouring the XX genotype (in-house control data not available). This figure is higher than EVS (MAF = 0.36, XX = 15%) and ExAC (MAF = 0.46, XX = 13%) databases, however regional 1000genomes data showed that MAF=0.53 in America. Therefore, without knowing the exact ethnic distribution of the cohort examined, and matching it to a similar control group, it is difficult to carry out statistical analysis and draw meaningful conclusions for this polymorphism. However, as there are not many Americans in the cohort, it does appear that the frequency of the XX genotype is increased amongst the recurrent RM and exercise-intolerance patients in this study.

4.4.2. *MYLK* p.(Pro21His) - rs28497577

Myosin light chain kinase, encoded by *MYLK*, phosphorylates the regulatory light chain of myosin, and thus is an important factor in skeletal muscle contraction (Szczesna et al. 2002). Although less is known about its relationship with exercise than *ATCN3*, Clarkson et al demonstrated that the homozygous c.62C>A p.(Pro21His) variation (rs28497577) correlated with higher baseline strength and higher CK and myoglobin levels in the blood after exercise (Clarkson et al. 2005). However, the variation is relatively rare, and so only six homozygotes were included in the study, reducing the power of their findings, and in a subsequent study, no association was identified between the polymorphism and recurrent RM (Deuster et al. 2013).

In this cohort the p.(Pro21His) MAF was 0.11, which was higher than the in-house MAF (0.07), but less than both 1000genomes (0.16), EVS (0.18) and the ExAC browser (0.13). Additionally, the percentage of homozygotes here was 3.4%, which is at similar level to in house (2.7%), 1000genomes (3.8%), EVS (5.5%) and ExAC (2.4%). Therefore, this study did not find an association between *MYLK* p.(Pro21His) and recurrent RM or exercise intolerance.

5. Discussion

This chapter investigated the use of large NGS panels for genetic diagnosis of recurrent rhabdomyolysis and the related condition exercise intolerance. These are difficult conditions for which to determine a genetic cause, as there are a large number of genes known to be associated, phenotype and severity are highly heterogeneous,

and a range of inheritance patterns can be responsible. Furthermore, underlying genetic factors can result in susceptibility and so be non-Mendelian, and RM episodes can be the result of entirely non-genetic influences. However, RM events can be fatal, and so genetic diagnosis is extremely important as it can aid trigger avoidance.

Despite these difficulties, overall, the RM panel was a success. A cohort of 224 patients was screened for mutations in 46 clinically relevant genes. Pathogenic mutations were identified in 21% of the cohort, with a further 17% harbouring possible pathogenic mutations, giving a total potential genetic diagnosis rate of 38%. Given that the majority of patients with these conditions were probably pre-screened for the commonest genes, this is a commendable hit-rate. Furthermore, upon undertaking this study, it was expected that roughly 30 – 50 patients would be received for sequencing; the large group of patients referred highlights the requirement for and importance of this technology.

This chapter set out to investigate the genetic landscape underlying recurrent RM and exercise intolerance, with a focus on determining the contribution of the ion channel genes (*RYR1*, *CACNA1S* and *SCN4A*). The gene with the highest number of pathogenic mutations found was the VGCC-like ryanodine receptor gene *RYR1*, accounting for half of the pathogenic mutations found (24/47). There were no pathogenic mutations found in the other two channelopathy genes investigated, although two patients had a *CACNA1S* variation, p.(Thr1354Ser), which was previously reported to cause MHS, but has since been classed as a polymorphism. In fact *CACNA1S* and *SCN4A* had the highest number of possible pathogenic mutations (14 and nine respectively), however, this is probably due to the AD inheritance pattern associated with them; heterozygous mutations were considered, whereas only homozygous or compound heterozygous mutations were considered for most of the other genes. It is hoped that these patients will be investigated neurophysiology to determine the significance of the variations found in this cohort. Nevertheless, despite only being due to *RYR1* mutations, the VGIC channel genes still had substantial contribution to the overall mutation rate.

The gene with the second highest number of pathogenic mutations was *CAV3*, with five patients, each harbouring one of two different mutations (p.(Val14Ile) and p.(Thr78Met)). Western blot analysis showed that the mutations resulted in reduced levels of caveolin-3 and β -dystroglycan, a protein with which it interacts (Figure 5.3). This is suggestive that the mutations are damaging, however, the significance of the β -dystroglycan reduction is unclear. Two of the patients had RM episodes and, as there has been only one case of *CAV3*-related RM in the literature (McNally et al. 1998), this

is an important finding, and shows that *CAV3* mutations may be a more common cause of RM than previously thought.

The remaining mutations were spread fairly evenly amongst the expected RM genes including *PYGM*, *PFKM*, *CPT2*, *HADHB*, *ACADVL* and *LPIN1*. Surprisingly, given the rare incidence of MD genes presenting with RM, six pathogenic mutations were found in four different MD genes (*ANO5*, *DMD*, *DYSF* and *SGCA*). However, limited clinical information means that it cannot be certain that these patients were not misdiagnosed or wrongly referred.

One particularly interesting finding was a homozygous *GYG1* mutation in patient 5.26, causing GSDXV, in an elderly patient who was initially diagnosed with MD. Only eight patients have ever been reported with the condition, and none have had RM episodes or exercise intolerance. This patient did have some episodes of dark urine, but it was unclear whether they were RM events. Additionally, she was encouraged not to exercise so cannot say if she has exercise intolerance. However, she represents an interesting clinical story, and demonstrates the need to consider the GDSs as a differential diagnosis for MD. A further notable discovery was a homozygous *ENO3* mutation in a patient with rhabdomyolysis episodes and exercise intolerance (patient 5.70), as only three families have been described in the literature with mutations in the gene. Furthermore, the mutation was novel and proven to be pathogenic biochemically (Figure 5.2).

Two different panels were used in this project. Initially, a custom-designed TSCA panel was used, the same technology as in chapter four of this thesis. However, coverage was poor (83% at 20x), and almost half of the samples unaccountably failed. The decision was then made to continue to the study with the TruSight One panel instead. This is a standard, non-customisable product which sequences 4813 genes with clinical phenotypes (genes present in the OMIM database <http://www.omim.org/>). This panel provided better coverage (93.4%) than the TSCA panel. There are two reasons for this. The first is that the panel is a standard product and as such had been optimised by Illumina to give the best coverage of the target genes. The second is that the TruSight one uses a capture method instead of an amplicon method. This means that the target sequences are already present and are enriched by hybridisation to become a higher proportion of the DNA present. However, in an amplicon procedure, only the target sequences are amplified, and so it relies on correct primer binding and successful DNA amplification for the target sequences to be present.

Despite having higher coverage, the 6.3% coverage shortfall was exposed in the *RYR1* results, as one of the most common MHS mutations was not covered and was missed in one patient, being subsequently identified in another institute. This region will have to be addressed in future rhabdomyolysis panels. Nonetheless, no samples failed and the sequencing was much more thorough, thus overall the decision to change technology was the right one, especially as the panels are similarly priced. Furthermore, if new genes are found to be linked to RM or exercise intolerance, as long as they are in OMIM, they will have been sequenced and can be investigated for these patients. This is not the case with TSCA sequencing, and it is unfeasible to keep redesigning the panel and resequencing patients that have already been sequenced.

Despite the panel's success, and aside from the technical problems, there were additional difficulties drawing conclusions from the data produced. There were several reasons for this. The first one was a lack of clinical information. Many of the referring clinicians neglected to provide a thorough clinical picture of the patients that were sent for RM panel sequencing. This made interpreting the variants found difficult, as it could not be determined whether the phenotype correlated with the genetic findings. Furthermore, it meant that knowledge was lost regarding expanding the phenotypes connected to the genes, as undoubtedly, some of the patients with mutations would have had novel clinical features. Another difficulty with data interpretation was the high number of rare variants; each of the 224 patients had roughly four-eight variants after filtering (shown in Appendix 4). This was due to the large number of genes analysed. With the previous panels, there was usually just one variant to focus on for each patient, however, here it was not always simple to interpret so many variants and to decide which, if any were disease-causing. Additionally, the complexity of the genetic basis of recurrent RM added to the difficulty. Many patients had published RM risk factors and deducing their contribution was challenging. Furthermore, many mutations are not fully penetrant, and individuals with a genetic predisposition to recurrent RM may never trigger episodes, making population frequency data of variations hard to interpret. Lastly, there are often conflicting reports in the literature pertaining to whether a mutation is pathogenic, thus it is not easy deducing the reliability of a report and each must be carefully examined and not just taken at face-value. These factors mean that biochemical and immunohistochemical assays are still important in determining pathogenicity, but they can at least be guided by the genetic results.

A patient that exemplifies many of these issues and the complexity of the data interpretation is patient 5.56. This patient had a homozygous *PFKM* mutation that been reported to be pathogenic, a novel *PHKA1* mutation and a rare *CACANA1S* mutation.

Initially, limited clinical information resulted in difficulty knowing which of the mutations found were disease-causing, and evaluation of the original report of the *PFKM* mutation resulted in the conclusion that there was limited evidence that it was a pathogenic change. However, eventually it was determined that the patient had been misdiagnosed; they actually only had isolated knee pain, and was unlikely to have a mutation in any of the genes.

The panel sequencing provided a large amount of data that was not fully utilised in this study. The stringent variation analysis used, in which only mutations consistent with known inheritance patterns were considered, left a large amount of data that was discounted and which could have potentially provided novel findings. Rare variants in genes within the same pathway could have had a cumulative effect within a patient and caused disease, however such analysis was beyond the time constraints of this thesis. Furthermore, only 46 of the 4813 genes were examined, the rest were discounted at the beginning of the analysis process, therefore there is a wealth of information that is untouched. For some of the patients, it is possible that analysis of other MD or myopathy genes will reveal pathogenic mutations; however, once again, time constraints did not allow this. Another use for the data generated could be a case-control study to investigate novel polymorphisms that have a higher frequency in this population than in the general public. New genes could possibly even be found with a burden analysis (comparison of the amount of rare variants in a gene in the disease population compared to a control population). However, as seen for p.(Arg577*) analysis, this is impossible without knowledge of the ethnic distribution of the cohort to match with a control group, which is currently unavailable with the limited clinical information given. Additionally, it is likely that the cohort is not clinically homogenous enough or big enough for this sort of analysis to be successful.

Two common polymorphisms that have previously been associated with recurrent RM were investigated in this cohort, *MYLK* p.(Pro21His) and *ACTN3* p.(Arg577*). There was no association found with p.(Pro21His). p.(Arg577*) levels did seem higher in this cohort than in control groups, but was still within the normal range for some ethnicities, and statistical analysis was impossible without a matched control group.

This chapter successfully employed large-scale panel NGS in a cohort of recurrent rhabdomyolysis and exercise intolerance patients, although the large number of genes analysed amplified the continual problem of assigning pathogenicity to variations, and so while genetic tests are informative, they should still be accompanied by biochemical assays and immunohistochemistry to confirm genetic findings. The new

TruSight One panel, had better coverage than TSCA, however it is possibly still too low for implementation into a diagnostic laboratory, and this must be resolved before this sort of technology is viable diagnostically. The results of this chapter promote the question of whether the TruSight One panel should also be used for the channelopathies, as once the initial causative genes have been analysed, if they are negative further genes can then be easily investigated. The benefit of this method in the diagnosis of channelopathies will have to be determined by comparing the prices of both panels (as the channel TSCA panels are much smaller than the RM panel, they are also much cheaper), and by determining the hit-rate in a cohort of none pre-screened channelopathy patients. This will help establish whether TruSight One should be used in the first instance, after an initial TSCA screen or not at all (i.e. if they undergo WES instead)

A future solution to this problem could be to use a custom enrichment of the standard TruSight One panel (<http://www.illumina.com/products/nextera-rapid-capture-custom-enrichment-kit.html>). This product contains the standard probes of the TruSight One panel, yet allows the user to select regions to be enriched at a higher level, and so increased coverage is gained for these areas. Additionally, the user can add in new regions if new genes of interest need to be included. This product would therefore solve the previous problems of low coverage and of user-designed custom probes not working successfully.

Chapter 6: Whole Exome Sequencing in Two Genetically Unexplained Possible Channelopathy Families

1. Introduction

There are estimated to be roughly 6000 monogenic disorders, however, to date the genetic cause of fewer than half have been established (Rabbani et al. 2014). Nonetheless, gene discovery in these conditions is highly important for understanding the disease mechanism and possible therapies. Additionally, it is important on an individual level, as patient genetic diagnosis informs treatment, helps with genetic counselling and can provide peace of mind for those affected. The development of next-generation sequencing (NGS), has led to vast advances in the field of gene discovery, as huge amounts of genetic data are provided quickly, at a relatively low cost and without the need for selecting candidate genes. This can take the form of whole-genome sequencing (WGS), but more commonly, whole-exome sequencing (WES) is used in gene discovery as the exome (protein-coding regions) accounts for less than 2% of the genome yet is predicted to harbour 85% of disease-causing mutations (Choi et al. 2009). Since the first such publication in 2009 (Ng et al. 2009) more than 150 articles have been published detailing gene discovery using WES, a figure which is growing exponentially (Rabbani et al. 2012).

Despite the decreased size of the exome in comparison to the genome, gene discovery using WES is not straightforward. The average exome contains about 23,000 variations, of which about 10,000 will affect protein structure, and 50-100 that would cause disease in a homozygous state (Schouten et al. 2002). Variants can be filtered by population frequency and gene, but nevertheless additional information in the form of family members or linkage data are usually required. Strategies that can be used for gene discovery are shown in Figure 1.11.

Estimates of the percentage of channelopathy patients without a genetic diagnosis vary, but is thought to be about 20% for the skeletal muscle channelopathies, about 33% for episodic ataxia, (Tomlinson et al. 2009) and 60% for paroxysmal dyskinesia based on chapter three. Therefore, there is still much to be understood regarding the genetic causes of the channelopathies, and it is likely that there are further causative genes to be discovered.

2. Aims

Next-generation sequencing (NGS) techniques have been used in the previous two chapters in the form of targeted sequencing panels. Firstly, this was with smaller custom-designed panels, and later with larger off-the-shelf panels. These panels facilitated the use of NGS to screen known candidate genes, improving efficiency over traditional Sanger sequencing and investigating phenotypic overlap between causative genes.

In this chapter NGS, will instead be used in the attempt to discover novel genetic causes for known possible channelopathy phenotypes. Whole-exome sequencing will be employed in two separate projects, each using different gene discovery strategies:

Project One – In a large dominant pedigree (Family A) with paroxysmal exercise-induced dyskinesia (PED), WES will be undertaken on one family member initially, and a candidate gene approach employed. If this is not fruitful, further family members will then also undergo WES. If possible, functional studies will be used to investigate mutations found.

Project Two – In a pedigree with a complex myopathy (Family B), WES will be performed on three affected family members simultaneously, and a shared-variant approach will be used to filter candidate genes. Several non-channelopathy genes have already been excluded and so it is possible that this family could represent a novel channelopathy phenotype.

3. Methods

3.1. Whole Exome Sequencing and Primary Data Analysis

WES and primary data analysis were carried out as described in section 4.3 of the materials and methods chapter. The TruSeq 62mb capture (Illumina) was used on patients A.I.2 and B.IV.5. Sequencing was performed on the HiSeq 2000. The Nextera focused 37mb capture (also Illumina) was used on patients B.IV.8 and B.IV.9. Sequencing was performed on the HiSeq 2500. The different methods reflect the change in the WES technology and protocol used in our department.

3.2. Sequencing of *KCNA1*

The whole of the coding region of *KCNA1* (one large exon) was amplified and sequenced in three fragments using the protocol given in section 2.1 and 2.2 of the materials and methods chapter, and using primers designed against the longest transcript for the gene in Ensembl (<http://www.ensembl.org/index.html>): KCNA1-001 – ENST00000382545. The Primer sequences are given in Table 6.1.

Gene	Primer	Sequence (5' – 3')
<i>KCNA1</i>	1F	CTGGTCCCTGGCTGCTTC
	1R	AGATGACGATGGAGATGAGG
	2F	GAGAGCTCGGGGCCCGCCAG
	2R	AAAGATGAGCAGCCCTAGCT
	3F	GGCCTCCAGATCCTGGGCCA
	3R	TTAAACATCGGTCAGTAGCT

Table 6.1 - Primer sequences used to screen *KCNA1*

3.3. Expression of Wild type and Mutant *KCNA1* RNA in Oocytes

The *Xenopus* oocyte expression vector pGEMHE containing the human *KCNA1* gene was present in the department, containing the c.677C>G p.(Thr226Arg) mutation. The vector contains the untranslated regions of a *Xenopus* β -globin gene for *Xenopus* oocyte expression, as well as a NheI restriction site for linearization and a T7 promotor site for RNA transcription, both used in the RNA preparation process.

The vector was transformed into bacteria, and mutagenesis was performed twice, firstly to create a wild type *KCNA1* vector, and secondly to introduce the c.893G>C, p.(Arg298Thr) mutation. This was carried out in accordance with sections

3.1 and 3.2 of the materials and methods chapter. The sequences of the mutagenesis primers designed for this purpose are given in Table 6.2.

Mutation	Primer	Sequence (5' – 3')
c.677G>C p.Arg226Thr (to revert to WT)	F	ACCCCTTCTTCATCGTGGAAACGCTGTGTATCATC
	R	GATGATACACAGCGTTTCCACGATGAAGAAGGGGT
c.893G>C, p.Arg298Thr	F	CAGGGTCATCCGCTTGGTAACGGTTTTTAGAATC
	R	GATTCTAAAAACCGTTACCAAGCGGATGACCCTG

Table 6.2 – Mutagenesis primer sequences used to create the wild type and p.(Arg298Thr) *KCNA1* vector

3.4. Electrophysiological Investigation of Wild Type and mutant *KCNA1*

Mutant (c.893G>C, p.(Arg298Thr)) and wild type (WT) *KCNA1* RNA was produced as described in section 5.1 of the materials and methods chapter, using an NheI restriction enzyme (NEB) in the following conditions: 4µg DNA, 13µl 10x buffer 2 (NEB), 3µl 10x BSA, 1µl NheI in a total volume of 30µl at 37°C for 2 hours. The RNA was injected into *Xenopus* oocytes as described in section 5.2 of the materials and methods chapter. Oocytes were initially injected with 0.05µl of either WT or mutant (MT) RNA. Next, oocytes were co-injected with WT and MT in varying ratios (see Table 6.3). 2µl aliquots of the ratios were created according to Table 6.3 and at stored at -80°C. The ratios of WT and MT were varied by keeping the volume of WT constant. 0.05µl of the WT and MT RNA mixtures were injected into oocytes.

WT:MT	Volume WT RNA (µl)	Volume MT RNA	Volume H ₂ O (µl)
1:0	1	0	1
4:1	1	0.25	0.75
2:1	1	0.5	0.5
1:1	1	1	0
0:1	0	1	1

Table 6.3 – The volumes of WT RNA, mutant RNA and water used to create varying WT:MT ratios, whilst keeping the amount of WT constant.

3.5. Two-Electrode Voltage-Clamp (TEVC) Protocols

TEVC was used to measure currents as described in section 5.3 of the materials and methods chapter. The protocols used in this chapter are as below

1) Ionic currents were measured in response to 90ms voltage steps from the holding potential of -90 mV to test potentials of -100mV to +45mV in 5mV increments.

2) Steady-state currents were measured in response to 300ms voltage steps from the holding potential of -90 mV to test potentials of -125 mV to + 100mV in 5mV increments.

3.6. Analysis

TEVC data analysis was completed using Clampfit (from pCLAMP 9.2™, Axon instruments), Excel 2010 (Microsoft Office) and OriginPro 9.0 (OriginLab). For quantification of steady-state currents, the mean current between 397 and 401ms (representing tail currents) was plotted against the test voltage and fitted to a Boltzmann charge –voltage curve: $f(V) = I_{max}/(1 + e^{(V_{mid}-V_c)/V_c}) + C$.

4. Results

4.1. Project One – Whole Exome Sequencing in a Large Paroxysmal Exercise-Induced Dyskinesia Pedigree

4.1.1. Clinical Presentation and Family Tree of Family A

Family A presented with classical PED. Typically in this disorder patients experience exercise induced episodes of dystonia and or dyskinesia, however, a more detailed clinical description was not able to be obtained for the family.

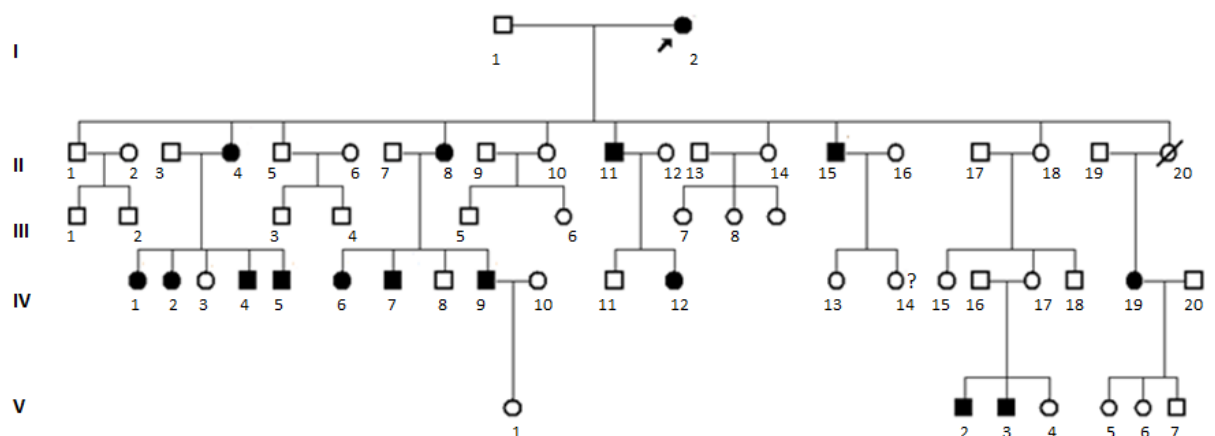


Figure 6.1 – Family tree of family A. Black individuals are affected, white unaffected and ? possibly affected. The proband is indicated by the arrow

4.1.2. Index Case Whole Exome Sequencing

The family was non-consanguineous and appeared to exhibit an autosomal dominant inheritance pattern; therefore it was assumed that a single heterozygous mutation was responsible. Initially, WES was performed on the index case in this pedigree (patient A.I.2). This patient had previously been screened for mutations in the three paroxysmal dyskinesia genes (*PRRT2*, *SLC2A1* and *PNKD*) and was found to be negative. The WES metrics are shown in Table 6.4.

Total Reads	Mean Target coverage	% Target covered at 2x	% Target covered at 10x	Total number variations
50363860	32.5x	66.1%	54.8%	22562

Table 6.4 – WES metrics for patient A.I.2

As shown in the Table, only 66% of the target regions (the protein-coding areas of the genome) were covered by the sequencing at 2x. However, roughly 22,500 variants were found. As only one member of this family had undergone WES, and as the sequencing was incomplete, the strategy employed was to first look for mutations in candidate genes. If this was negative, WES would be performed on further family members (WES strategy is shown in Figure 6.2). The genes considered were the known neuronal channelopathy genes; *KCNA1*, *CANCA1A*, *SLC1A3*, *CACNB4* and *KCNK18*.

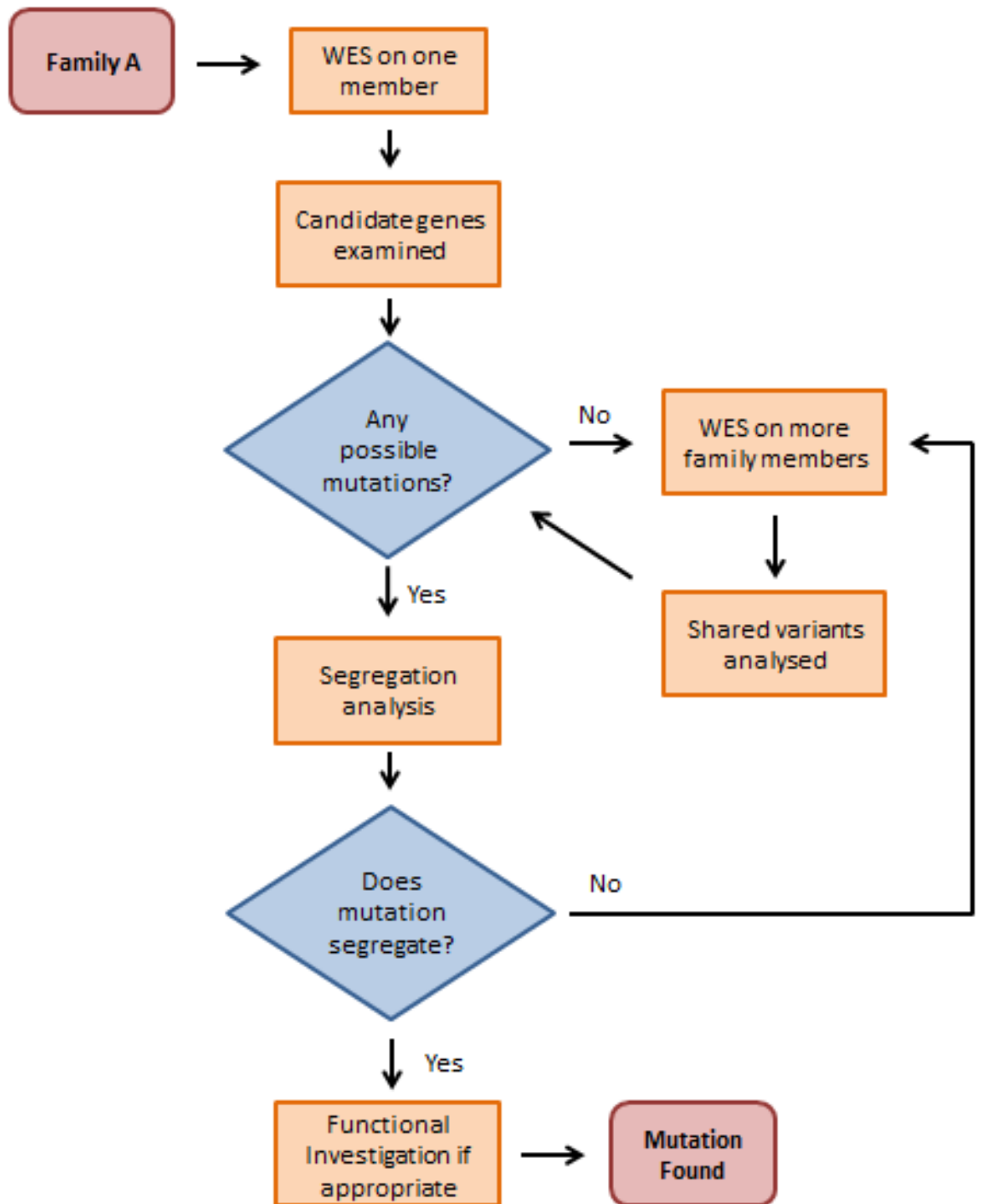


Figure 6.2 – Flow diagram to show the candidate gene strategy employed for mutation discovery in family A

4.1.3. Candidate Gene Screening Result

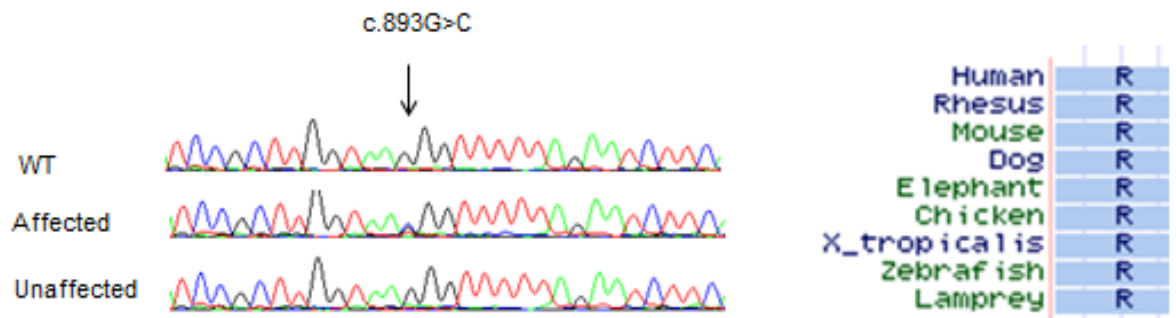
The only candidate gene that harboured a nonsynonymous change was *KCNA1*; c.893G>C, p.(Arg298Thr). This was absent from over 65,000 control subjects in 1000genomes, EVS and ExAC, found at a highly conserved amino acid and predicted to be pathogenic by both Polyphen-2 and SIFT. This variation was a good candidate, and so segregation analysis was performed on 12 family members including 10 affected, one unaffected and one possibly affected (family member A.IV.14). The variation segregated perfectly in the family, excluding the 'possibly affected member', which is likely to be a phenocopy (Figure 6.3).

KCNA1 encodes the VGKC alpha subunit K_v1.1; either four K_v1.1 subunits form homotetramer, or they assemble with other alpha K_v1 family subunits to form a heterotetramer (see section 1.3.4 of the introduction chapter). *KCNA1* mutations are known for causing the neuronal channelopathy, EA1 (see section 2.2.1.1 of the introduction chapter) and usually follow an autosomal dominant inheritance pattern, although one de novo change has been reported (Demos et al. 2009). EA1 patients classically present in the first two decades of life with brief attacks of ataxia and myokymia, sometimes associated with seizures, although there have been reports of mutations in patients with only myokymia. Mutations in the gene have not before been reported as responsible for a paroxysmal dyskinesia presentation, although some choreic and 'jerking muscle contractions' have been seen as part of a wider EA phenotype (Shi et al. 2013). Therefore, if this mutation is disease-causing in this family, it would represent a completely new phenotype for the gene.

4.1.4. Screening of *KCNA1* in a Cohort of 190 Mixed Channelopathy Patients

The single coding exon of *KCNA1* was screened in 190 patients with mixed neuronal channelopathy phenotypes. The only further rare nonsynonymous variation identified was the same variation, p.(Arg298Thr) in patient 6.1, initially classed as EA, but with unavailable clinical information.

a)



b)

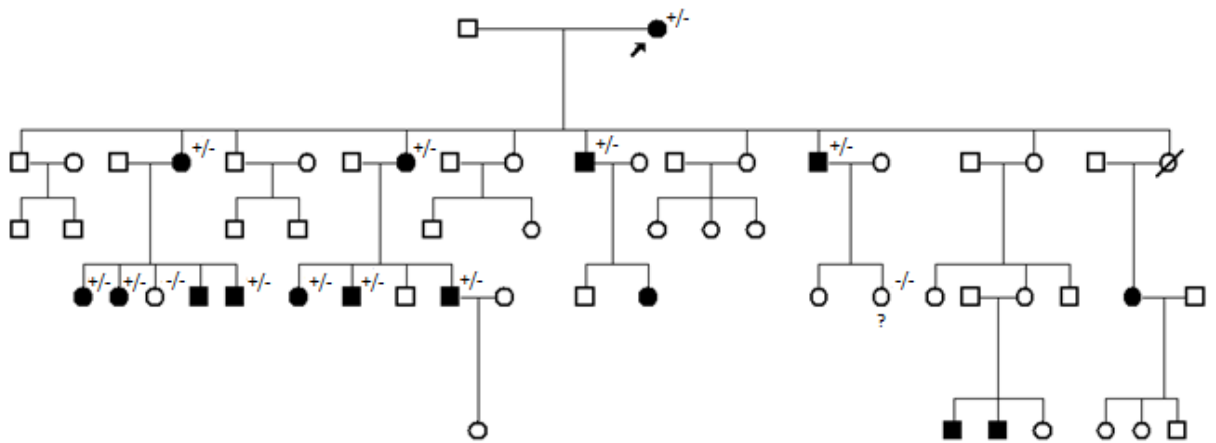


Figure 6.3 – (a) The chromatogram of the *KCNA1* mutation found in family A and the conservation of the amino acid (taken from the UCSC genome browser (<https://genome-euro.ucsc.edu>)) (b) Segregation of the mutation in Family A. Black individuals are affected, white unaffected and ? possibly affected. +/- indicates patient is heterozygous for the c.893G>C p.(Arg298Thr) *KCNA1* variation and -/- indicates the individual is homozygous for the WT allele

4.1.5. Hypothesis – A Gating Pore Current?

The p.(Arg298Thr) mutation found in this family is located in the S4 voltage sensor of the K_v1.1 alpha subunit. As discussed previously in section 2.1.2.2 of the introduction chapter, the voltage sensor comprises a number of positively charged amino acids called “gating currents” which confer voltage dependence to the channel. p.(Arg298Thr) affects the highly conserved third arginine of the voltage sensor, known as R3.

Normally, the positively charged amino acids form an electrostatic interaction with surrounding negative amino acids within the S1-S3 segments of the voltage sensing domain (VSD). Mutations which neutralise the positively charged gating charges have been previously shown to cause disruption to these interactions and allow an alternative and aberrant ionic leak through the VSD of the channel at certain membrane potentials, known as a gating pore current (Figure 6.4). To date, gating pore current mutations associated with human disease have been found in only four channels; S4 mutations in Ca_v1 and 1 Na_v1.4 cause HypoPP (Matthews et al. 2009), S4 mutations in K_v7.2 have been associated with benign familial neonatal seizures (Miceli et al. 2008) and, more recently S4 Na_v1.5 mutations have been reported to cause atypical cardiac impairment (Moreau et al. 2015).

Gating pore currents have never before been associated with *KCNA1* mutations. Moreover, a recent study modelled the highly homologous Kv1.2, channel and found that neutralising the same arginine resulted in a gating pore current (Jensen et al. 2012). Therefore, we hypothesise that this is the first example of a *KNCA1* gating pore current mutation, a theory which could account for the novel phenotypic features seen in this family. Oocyte expression studies will be required to assess this hypothesis.

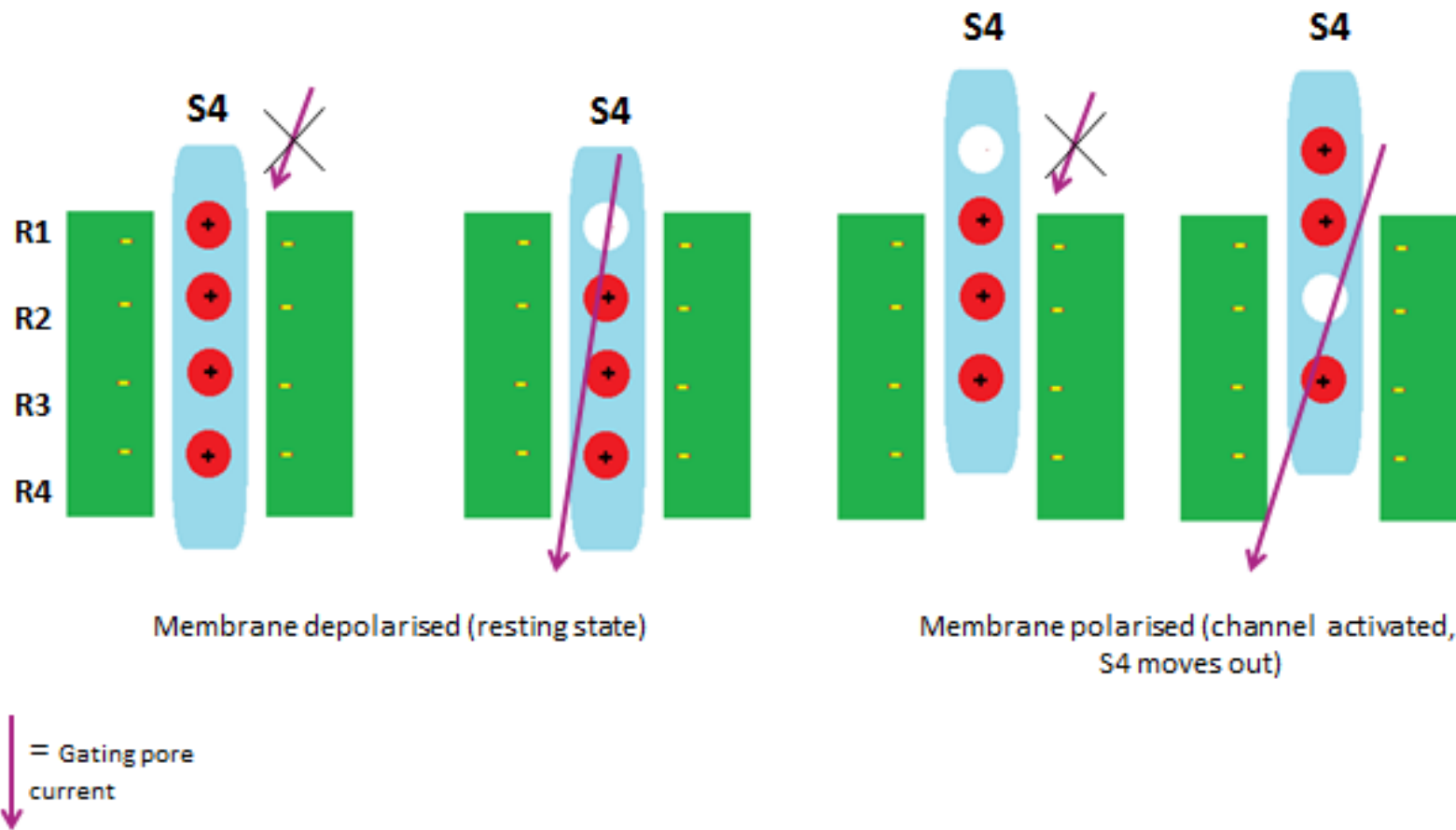


Figure 6.4 – Schematic to show how neutralisation of an S4 arginine (shown by red circles) can result in a gating pore current. The four arginines are named R1-R4. The second and third picture show a R1 mutation, which only creates a gating pore current at depolarised states. The fourth picture shows a R3 mutation which creates a gating pore current when the cell is polarised and the S4 moves out

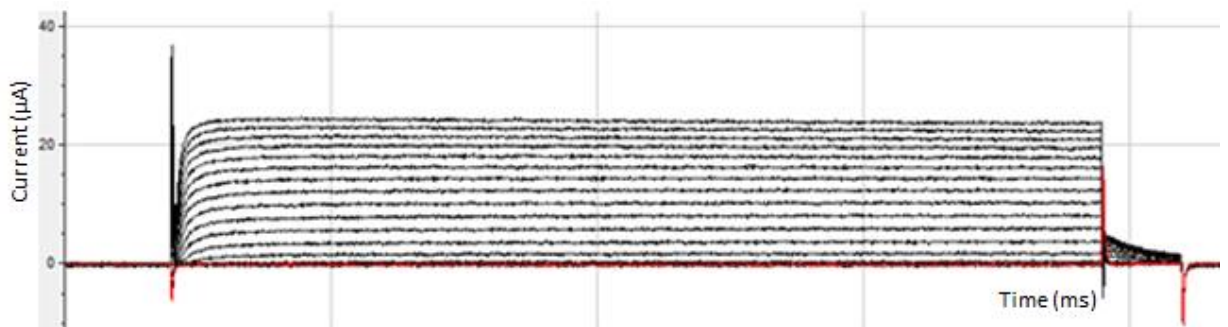
4.1.6. Two-Electrode Voltage-Clamp

The hypothesis that *KCNA1* p.(Arg298Thr) produced a gating pore current was tested by measuring biophysical properties of WT or mutant channels using TEVC. The experimental premise was that the alpha currents (currents produced by the main pore of the channel) could be blocked using dendrotoxin (DTX), and remaining currents detected could be attributed to the gating pore current. This method has been used previously to detect gating pore currents in *Xenopus* oocytes for VGSCs (Siobhan Durran, unpublished work).

4.1.7. Crude Currents Test

Initially, the presence of alpha $K_v1.1$ currents was crudely tested for using protocol one. Oocytes were injected with either WT or MT RNA. This test does not fully mimic the heterozygous state of the mutation. Figure 6.5 shows currents measured in response to protocol one. p.(Arg298Thr) homotetrameric channels did not produce any alpha currents alone, whereas WT homotetrameric channels did (Figure 6.5 (b) and (a) respectively), suggesting that p.(Arg298Thr) does not produce functional channels.

a)



b)



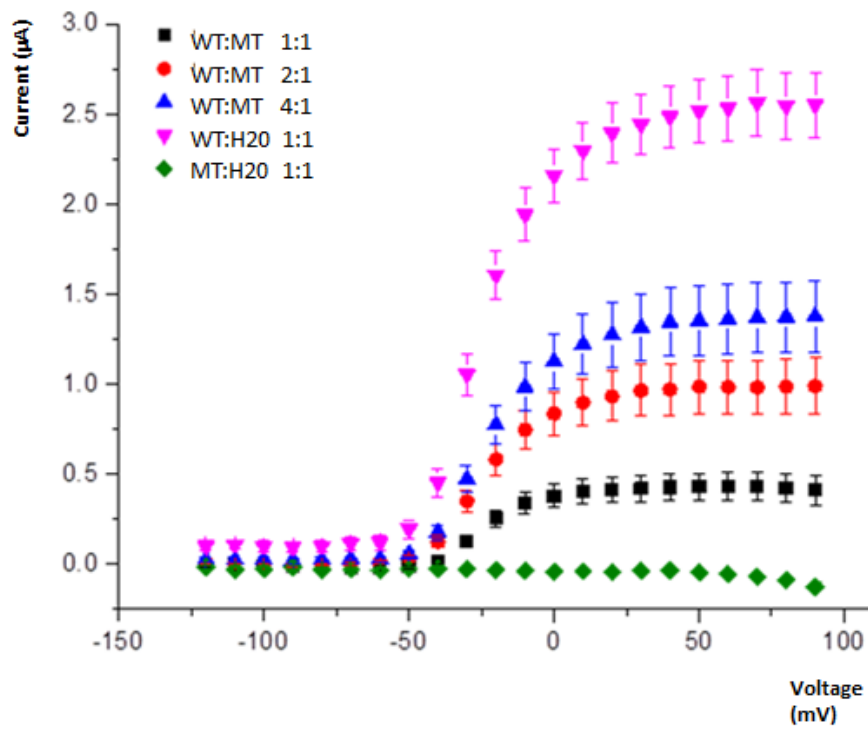
Figure 6.5 – Currents produced in response to protocol one by homotetrameric (a) WT and (b) p.(Arg298Thr) (MT) $K_v1.1$ channels

4.1.8. Quantification of Steady-State Currents at Different WT:MT Ratios

Since the p.(Arg298Thr) mutation is heterozygous, the channels are likely to assemble as heterotetramers as well as homotetramers. Thus to more accurately mimic the heterozygous state oocytes were co-injected with WT and MT KCNA1 RNA in a 1:1 ratio. Additionally, they were co-injected at 2:1 and 4:1 ratios to investigate the effect of the mutant subunit on the WT subunit. The volume of WT injected remained constant throughout (for details of the composition in each case, refer to Table 6.3).

Steady-state currents were measured using protocol two and calculated as described in section 3.7 of this chapter. Figure 6.6 shows the currents for each of the ratios, as well as WT and MT each at 1:1 with water. The WT control (WT:H₂O) expressing cells show currents which were activated around -50mV and levelled off around +50mV with a peak current of 2.5. In the presence of MT RNA, currents demonstrated roughly the same voltage dependence. However, the peak currents decreased when the ratio of MT RNA was increased. WT:MT 1:4 expressing cells produced currents which were about 60% that of the WT control. Therefore, the results indicate that the more mutant subunit present, the fewer currents produced.

a)



b)

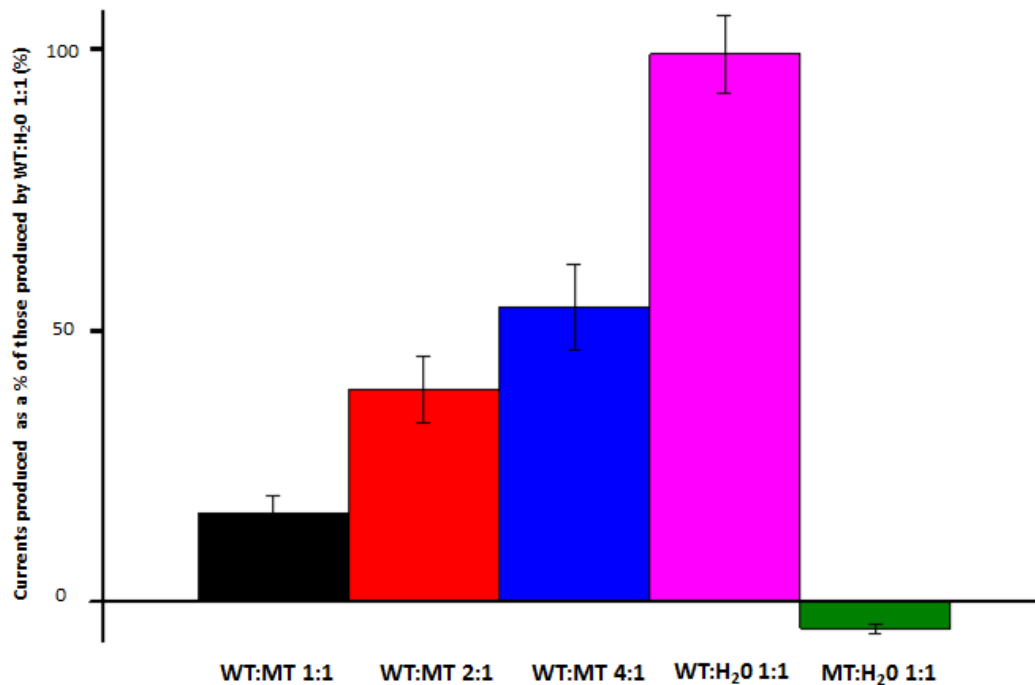


Figure 6.6 - (a) Mean currents produced by the varying subunit ratios between 378 and 401ms fitted to a Boltzmann voltage-charge curve. (b) Largest current produced by each subunit ratio, as a percentage of that of WT:H₂O 1:1. N numbers are as follows: WT:MT 1:1 = 30, WT:MT 2:1 = 27, WT:MT 4:1 = 24, WT:H₂O 1:1 = 20, MT:H₂O 1:1 = 12. Error bars represent SEM

4.1.9. Pathology of p.(Arg298Thr) Mutation Discussion

The complete absence of currents produced by homomeric K_v1.1 mutant channels suggests that p.(Arg298Thr) subunits alone cannot produce functional channels and thus it is unlikely that this mutation does produce a gating pore current. However, the homomeric channels would not be the main consequence of the heterozygous mutation identified in this family, and thus the mutant channel must be co-expressed with the wild type for a true representation of the effect of the mutation.

When expressed at a WT:MT ratio of 1:1 to mimic the heterozygous state, currents were produced were about a fifth of the current size produced by WT with water. This result confirms that the mutant K_v1.1 subunit is being expressed by the cell, and suggests that it is having a dominant-negative impact on the WT, as the actual number of WT subunits remained constant. As the number of mutant subunits is reduced (2:1 and 4:1 ratios), the current size increases, corroborating this suggestion. Therefore, it appears that the mutant subunit is binding to the wild type, and preventing it from becoming a functional channel.

The channel is a tetramer, and therefore the ratios of each K_v1.1 channel composition (4 WT, 3 WT+1MT, 2WT+2MT, 3MT+1WT, 4MT) should be 1:4:6:4:1 respectively (see Figure 6.7). If the mutant was having a complete dominant-negative effect and only channels composed of 4 WT subunits were functional, the current size for the heterozygous state would only be about 6% of WT alone. Alternatively, if both 4WT and 3WT+1MT could produce functional channels, the current would be about 31% of WT alone. At about 20%, the actual figure is between the two, so the composition of current-producing channels is not completely clear. This discrepancy could be due to the cell expressing WT subunits more efficiently than MT subunits, and thus in reality, there may not be a true 1:1 ratio within the cell.

This biophysical study of the p.(Arg298Thr) mutant shows that mutation affects channel functioning and is indeed pathogenic. However the pathomechanism responsible for the disease in the described family is not a gating pore current as hypothesised but in fact a dominant-negative mechanism. This mechanism has been shown before in typical EA1 mutations, and so this work does not explain the novel phenotype exhibited. However it could be due to other unidentified co-inherited genetic modifiers (Zuberi et al. 1999), or without further clinical information, it cannot be certain that this family were not misdiagnosed.

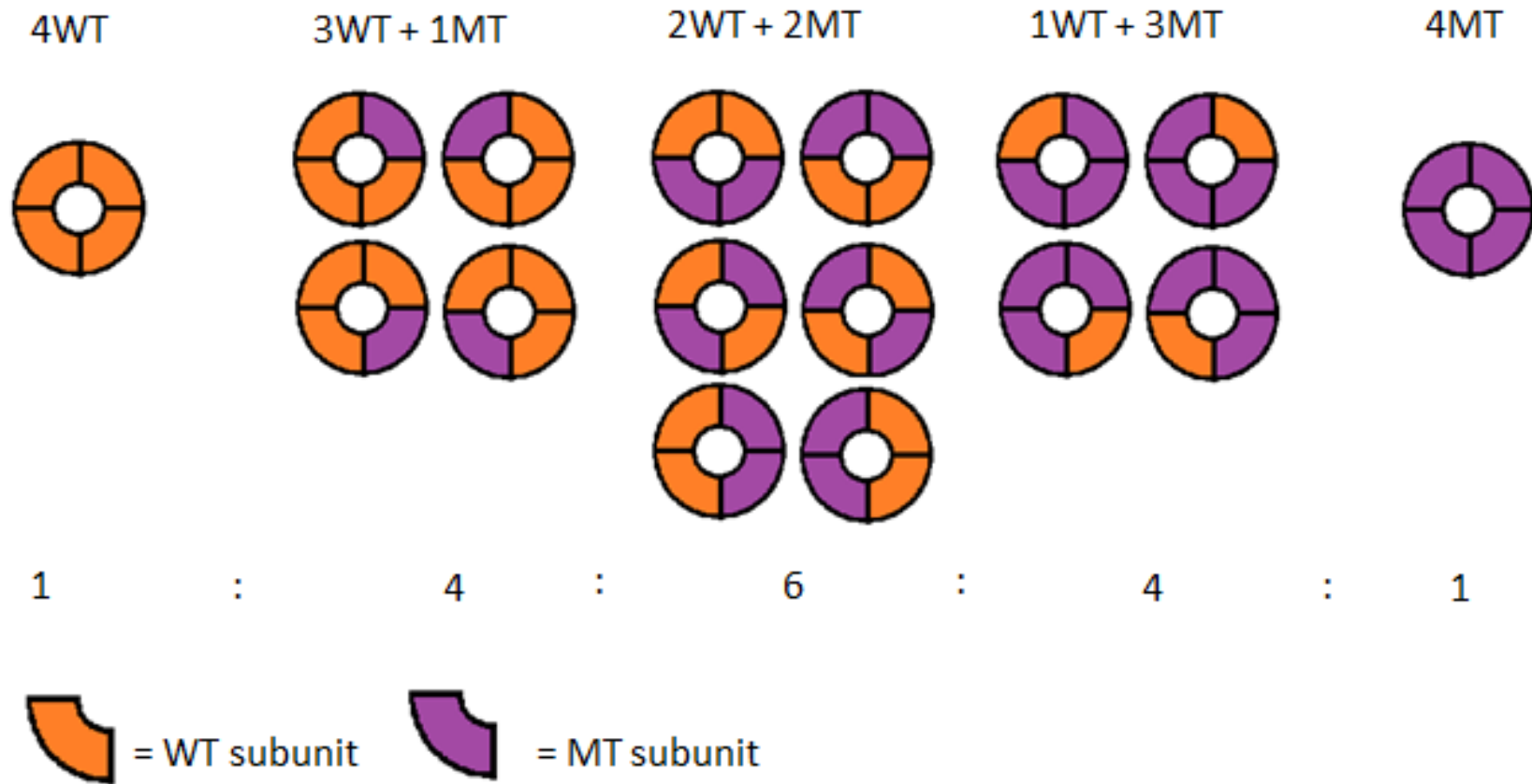


Figure 6.7 – The ratios of each of the five types of $K_v1.1$ channel containing the different numbers of mutant and wild type KCNA1 subunits when they are expressed in a cell in equal amount (to mimic the heterozygous state)

4.2. Project Two - Exome Sequencing in a Complex Myopathy Family

4.2.1. Clinical Presentation and Family Tree of Family B

Family B is a large pedigree with a distal myopathy, shown in Figure 6.8. Patient B.IV.5 (indicated by the arrow) first presented in his thirties with weakness and pain in his shoulders, aching in his neck and mild weakness in his hands. Examination revealed generalised thinning of his muscles. Over the last decade his weakness had progressed, with the result that he can no longer climb stairs and walks with two sticks. He was diagnosed with nemaline myopathy following the presence of nemaline rods on a muscle biopsy. Genetic investigations of *ACTA1*, *CRYAB*, *MYOT*, *ZASP*, *MYH7* and *DES* have all proved negative. He does not have any cardiac involvement. Both of his sons have visual problems due to cone dystrophy, but it is thought to be unrelated.

The brother of the proband (patient B.IV.6) has a milder myopathy with similar features, and showed rimmed vacuoles on his muscle biopsy suggesting possibly genetic IBM. Both of the parents appear to be unaffected, although their father (B.III.2) has thin calves, and so could be displaying a milder phenotype of the myopathy. A son of their half-sister (B.V.1) may also be affected.

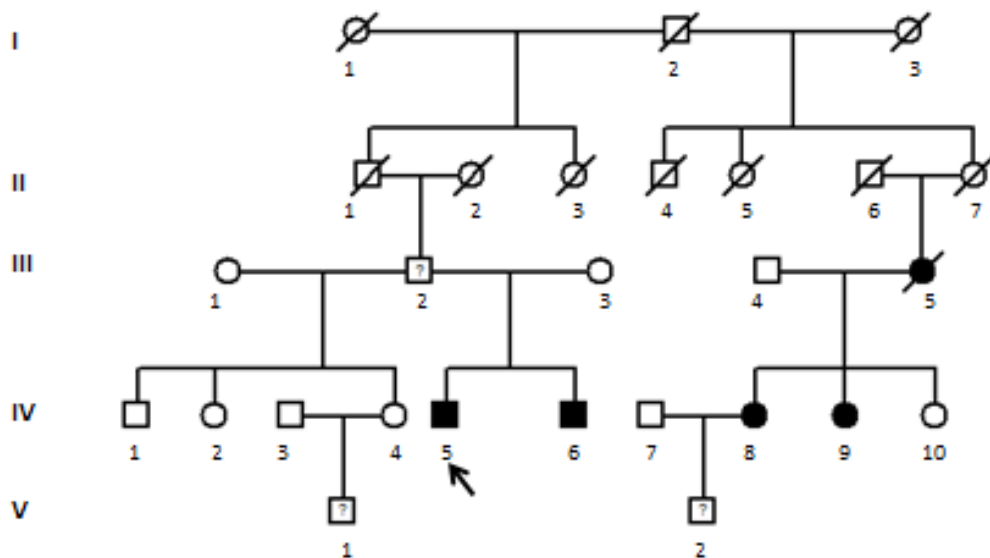


Figure 6.8 – Family tree of family B. Black individuals are affected, white unaffected and ? possibly affected. Individuals with a line through are deceased. The proband is indicated by the arrow

The second cousin of the father, patient B.III.5 also has a distal myopathy; again, progressive leg weakness left her with trouble climbing stairs. A pace-maker was inserted due to cardiac arrhythmias. Two of her daughters (patients B.IV.8 and B.IV.9) have a similar skeletal muscle presentation and pace-makers. Muscle biopsies of patients B.III.5 and B.IV.8 showed inclusions with positive staining for desmin, dystrophin and vimentin. This family was written up as one of the first with desmin-aggregation myopathy (Helliwell et al. 1994), but DNA sequencing revealed no desmin mutation.

Due to the similarity of the neuromuscular disorders, it is thought that there is a single autosomal dominant genetic cause underlying the myopathy in all family members. As several non-channelopathy genes have been ruled out, it was thought that this family could possibly represent a novel clinical manifestation of a channelopathy mutation, as there have been rare reports of progressive weakness due to *SCN4A* mutations (Lee and Chahin), and myopathy and weakness is a recognised phenotype of *RYR1* mutations (Zhang et al. 1993).

4.2.2. Whole Exome Sequencing of Three Family Members

WES was performed on three affected members of this family: individuals (patients B.IV.5, B.IV.8 and B.IV.9). The sequencing metrics for each of the three are shown in Table 6.5.

Patient	Total Reads	Mean Target coverage	% Target covered at 2x	% Target covered at 10x	Total number variations
B.IV.8	72734706	43.9x	98.9%	94.5%	23430
B.IV.9	64475040	39.9x	99.0%	93.6%	23260
B.IV.5	120227945	86.2x	94.6%	90.7%	22039

Table 6.5 – WES metrics for patients B.IV.8, B.IV.9 and B.IV.5

The WES coverage for all three of these samples is at the level expected for good sequencing. They are all much higher than for patient A.I.2, which only had 54.8% of the target covered by 10 or more reads. The family was non-consanguineous and appeared to exhibit an autosomal dominant inheritance pattern, and so again, a single rare heterozygous variation was likely to be the disease-causing mutation. A shared variant strategy was employed for mutation discovery, shown in Figure 6.9, as there are several degrees of separation between the two sides of the family and so there should not be many shared variants.

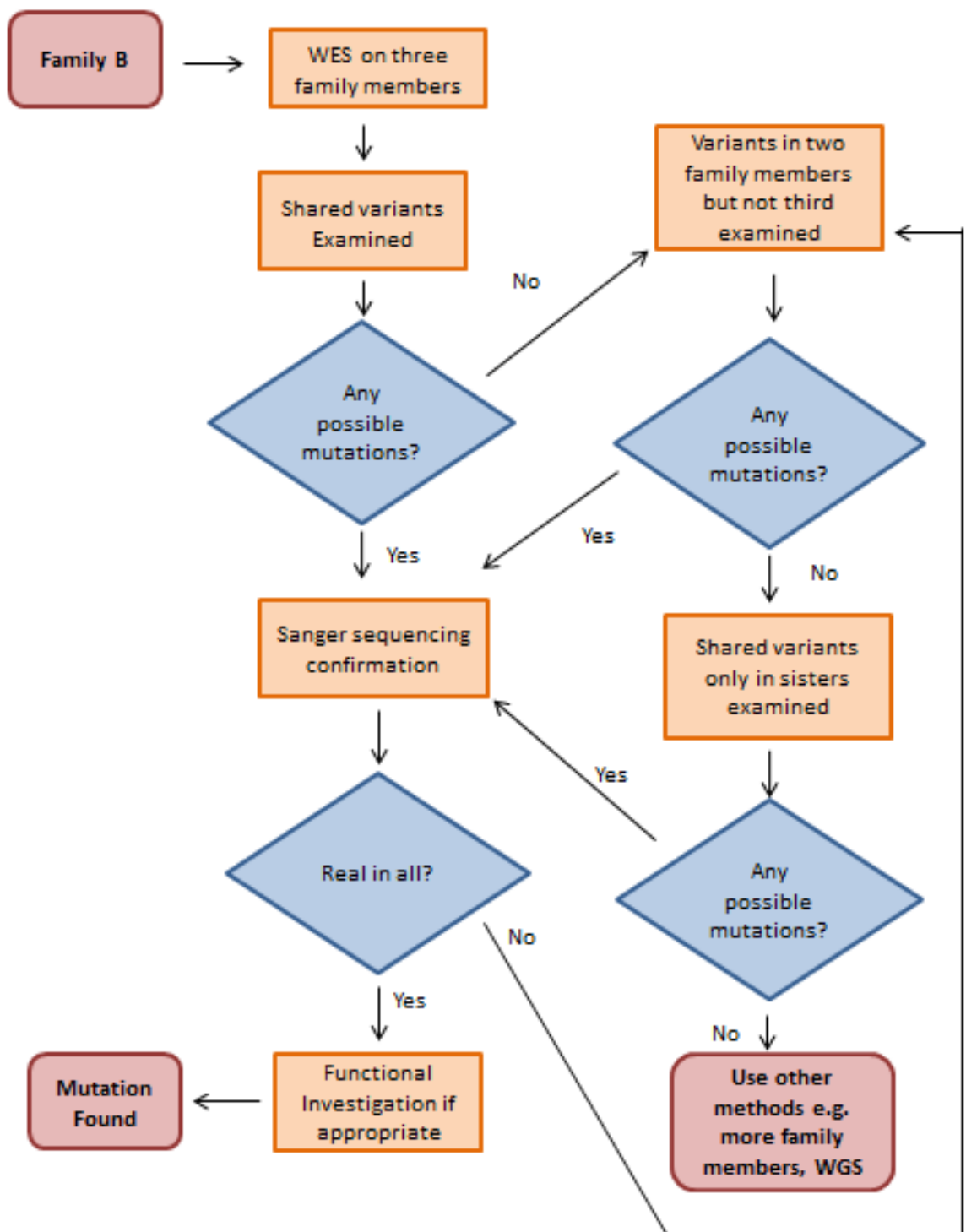


Figure 6.9 – Flow diagram to show shared variant strategy employed for mutation discovery in family B

4.2.3. Shared Variants Between all Three Members

Initially, the strategy was to investigate rare variants that were shared between the three individuals. There were 11137 variants shared by the three. When variants that were synonymous, homozygous, with a SegDup ≥ 0.96 or a MAF ≥ 0.01 (using EVS and 1000genomes) were excluded, 131 variants remained. Finally, resultant variants were filtered using in-house control and artefact lists, again using a MAF ≥ 0.01 . This left four variants, shown in Table 6.6. None were in channel genes.

Gene	Variation	MAF EVS/ 1000g	Gene function
<i>NADK</i>	p.Glu90dup	0/ 0	Catalyses the synthesis of NADP from NAD and ATP
<i>ACTRT2</i>	p.Lys55del	0/ 0	Unknown, actin-related protein
<i>PRAMEF11</i>	p.Glu144Gly	0/0	Unknown
<i>C5orf15</i>	p.Ile92Arg	0.0005/ 0.0009	Interacts with keratinocytes

Table 6.6 – Shared variants between patients B.IV.5, B.IV.8 and B.IV.9 after filtering was applied

On closer inspection of *NADK*, the in-frame insertion of a Glutamine falls in a string of nine Glutamines, and other Glu insertions within the string are present in dbSNP (rs71578334, MAF unknown). This suggests that either the variation is a sequencing error (as can often be the case in long stretches of repeats), or has been mislabelled and thus not flagged as a SNP. This variation was therefore excluded. Similarly, the deletion in *ACTRT2* is the same change with an alternate name as rs4013154, MAF=0.15 and the *PRAMEF11* variation does not appear to have been labelled correctly, as the dbSNP number (rs2994114) was connected to a variation with a MAF of 0.3, so both were excluded. The final variation in *C5orf15* (rs149845423) is present in 63 individuals in the ExAC database and interacts with keratinocytes. Both of these factors suggest it is not the cause of the neuromuscular disease in this family.

Therefore, in this family the strategy of identifying only shared variations was not successful in identifying the causative mutation. There could be several reasons for this. The first is that the two sides of the family may not actually have the same neuromuscular disorder, and the phenotypic similarity could be due to coincidence. Alternatively, the mutation could be intronic or intergenic and so not captured by WES. Lastly, the mutation could be in an area that is not covered in one or all of the samples.

4.2.4. Shared Variants between Two Family Members

The next step in the analysis was to assume that the mutation was missed in one sample; if it was in two samples but not covered by the third, this filtering used above would have excluded it. If two of the samples are compared, variants that are in those two but not in the third will either be a) not present or b) not covered. Visualisation of the sequence using a BAM file on a genome browser for promising variants can determine which of the two scenarios is true.

This strategy is most likely to be successful using the two samples with the highest coverage as they are the least likely to have missed a mutation. However, as these samples are the sisters, it would produce a large amount of variants. Therefore first each sister was compared with patient B.IV.5 in the hope that one of them was missing the causative variant.

4.2.4.1. Patients B.IV.5 and B.IV.8

Patients B.IV.5 and B.IV.8 shared 1648 variants that were not present in patient B.IV.9. However, when these were filtered using the above criteria, no variants remained. Therefore there was no potentially pathogenic variant missed by the sequencing in patient B.IV.9.

4.2.4.2. Patients B.IV.5 and B.IV.9

Patients B.IV.5 and B.IV.9 shared 1519 variants that were not present in patient B.IV.8; the number was reduced to three when filtered. These were visually examined in the BAM file of patient B.IV.8 to determine if sequencing may have missed them, and the results are shown in Table 6.7. All of the 3 variants were in areas covered well by the WES and so can be excluded. Therefore there was no potentially pathogenic variant missed by the sequencing in patient B.IV.8.

Gene	Variation	MAF EVS/ 1000 genomes	Gene function	Area Covered?
<i>ARHGAP29</i>	p.Arg798Gln	0.003/ 0.0018	GTPase activator	Yes – variant not present
<i>FCRL3</i>	p.Gly296Arg	0.002/ 0	Immunoglobulin receptor	Yes – variant not present
<i>TMEM186</i>	p.Met1?	0.004/ 0.002	TM protein, unknown	Yes – variant not present

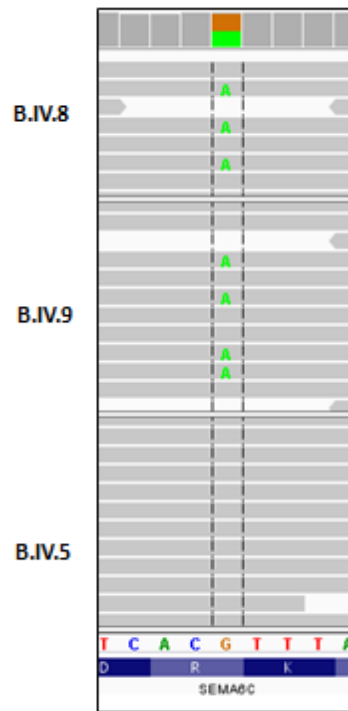
Table 6.7 – Shared variants between patients B.IV.5 and B.IV.9 but not B.IV.8 after filtering was applied

4.2.4.3. Patients B.IV.8 and B.IV.9

As there did not seem to be a pathogenic mutation that was missed in the sequencing of either of the sisters, variants that were present in them and not in patient B.IV.5 were next examined. There were 7245 such variations, when filtered this was reduced to 183. For each, the coverage in patient B.IV.5 was examined using IGV genome browser, and if the area was covered sufficiently and the variant was not present, it was excluded, leaving 69. Three were on the X-chromosome, and these were considered unlikely to cause a disease in this family. The 66 remaining variants are shown in Table 6.8 (For example of variants that were not covered, or covered and not present see Figure 6.10).

The genes were then annotated, where possible, with protein function information from the OMIM (online Mendelian inheritance in man) and GeneCards websites (<http://omim.org/>), (<http://www.genecards.org>). Genes were ranked as relevant, not relevant, and possibly relevant, (to the patient phenotype) and variants in gene that were not considered relevant (for example proteins involved in mucus or skin production) were excluded. 35 variations remained (shown in bold) in 21 genes. Three of these had been classed as relevant and were explored further (shown in red). There was one channel gene on the list, *CLCN3*, however, this gene is preferentially expressed in the brain and retina and so is unlikely to be associated with a myopathy (Borsani et al. 1995).

a)



b)

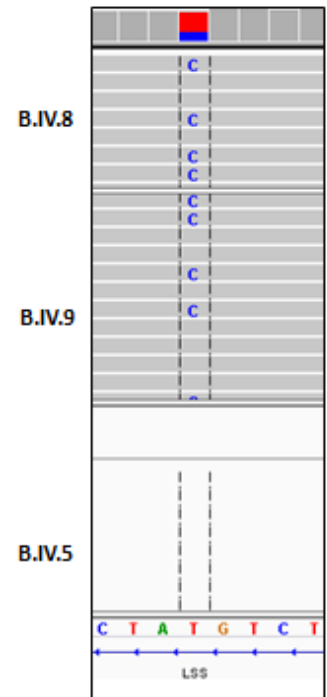


Figure 6.10 – Visualisations of the difference between (a) a variant that was covered but not present and (b) a variant that was not covered. Taken from the genome browser IGV

Gene	Variation	Gene function	Relevant?
<i>PRAMEF1</i>	p.Pro464Leu	Reproductive development	No
TCEB3	p.Pro15Ser	Transcription elongation factor	Possibly
ACTN2	p.Pro32Leuf*12	Actin-binding, cardiomyopathy gene	Yes
HEATR7B1	p.Lys1457Arg	Unknown	Possibly
<i>COL6A5</i>	c.7922+1G>A	Collagen protein	No
RP3-368B9.1	p.Val66Leu, p.Trp72*, p.Met101Thr, p.His121Tyr, p.Asn167Thr, p.The185Ile	Long non-coding RNA	Possibly
AC118759.1	p.Ile29Thr, p.Ans93Ser, p.Pro95Leu, p.Ser123Leu, p.Ala152Thr, p.Ser159Pro, p.Ser175Pro, p.Thr183Met, p.Thr187Ile	Unknown	Possibly
<i>MUC3A</i>	p.Thr370Ser, p.Ile374Met, p.The379Ala, p.Thr381His	Intestinal	No
<i>TRBV11-1</i>	p.Pro62Leu	T cell receptor	No
<i>CYP11B1</i>	p.Thr198Lys	Aldosterone synthase	No
<i>EPPK1</i>	p.Ala1237Val	Epidermal antigen	No
<i>MUC2</i>	p.Pro258Leu	Intestinal	No
RP1-239B22.1	p.Leu449Thrfs*9	Long non-coding RNA	Possibly
<i>OR4C5</i>	p.Val307Gly, p.Asn304Ser, p.Phe278Leu	Olfactory receptor	No
<i>KRTAP5-11</i>	p.Pro159Ser, p.Lys158Arg	Keratin-associated protein	No
C12orf5	p.Leu217Phe	Glycolysis pathway	Yes
GALNT9	p. Gln59Argfs*3	Glycosylation	Possibly
<i>ANKLE2</i>	p.Arg634Gln	Causes scurvy	No
TRAJ56	Unknown	Unknown	Possibly
ACTR10	c.871-1->AG	Actin-related protein	Yes
<i>PNMA1</i>	p.Val193Gly	Induces anti-neuronal antibody	No
<i>IGHV3-11</i>	p.Gly74Ser	Immunoglobulin protein	No
<i>IGHV5-51</i>	p.Gly54Ser	Immunoglobulin protein	No
<i>IGHV4-59</i>	p.Asp117His	Immunoglobulin protein	No

<i>IGHV3-64</i>	p.Ala43Ser	Immunoglobulin protein	No
<i>GOLGA6L2</i>	p.Arg716Lys	Causes speech disorder	No
<i>RP11-178D12.1</i>	p.Ser88*	Long non-coding RNA	Possibly
<i>TNFRSF17</i>	Unknown	Tumour necrosis factor	No
<i>LINC00273</i>	p.Ala360Thr	Long non-coding RNA	Possibly
<i>RP11-830F9.6</i>	p.Arg270Trp	Long non-coding RNA	Possibly
<i>AC004148.1</i>	p.Lys154Argfs*1	Unknown	Possibly
<i>KRTAP29-1</i>	p.Pro173Glnfs*109	Keratin-associated protein	No
<i>C19orf45</i>	p.Asp155Asn	Unknown	Possibly
<i>ZNF585A</i>	p.Ser592Ala	Transcription regulation	Possibly
<i>ZNF296</i>	p.Arg150His	Causes leukaemia	No
<i>AP001468.1</i>	p.His35Arg	Cholesterol synthesis	No
<i>IGLC3</i>	Unknown	Immunoglobulin protein	No
<i>FSIP2</i>	p.Ser554insAsp	Sperm Protein	No
<i>CLCN3</i>	p.Lys187_Lys190del	Brain/ retinal chloride channel	No
<i>AKD1</i>	p.Ser331insAlaThr	Nucleoside phosphates kinase	Possibly
<i>FAM189A2</i>	p.Cys20insSerCys	Unknown, expressed highly in muscle	Yes
<i>NOX4</i>	p.Glu3insGlu	Renal oxygen sensor	No
<i>DHX37</i>	p.Glu160del	Regulates RNA secondary structure	Possibly
<i>TNFRSF17</i>	Unknown	Tumour necrosis factor receptor	No
<i>FAM187A</i>	p.Gly14insSer	Unknown	Possibly
<i>CARD10</i>	p.Glu262insGluLys	Caspase recruitment	Possibly

Table 6.8 – Variations found in patients B.IV.8 and B.IV.9 that are in regions not covered by WES in patient B.IV.5. Genes likely be relevant are in red, and genes that are possibly relevant in bold (based on what is known of gene function). Variants that were sequenced by Sanger sequencing are shown in blue

Firstly, *ACTN2* encodes alpha-actinin 2, an actin binding protein that has multiple roles within the cell. There has been one report of a heterozygous mutation causing a cardiomyopathy, and thus this gene seemed promising (Mohapatra et al. 2003). However, on closer expectation, the gene transcript used to annotate the variation was a disused one and consequently the variation was not annotated with the correct population frequency data (MAF = 0.44, rs11355106). The variation was not pursued any further. Secondly, *C12orf5* was considered relevant as the enzyme it encodes, TIGAR, regulates glycolysis. Disruption of glycolysis can result in myopathy, as discussed chapter 5. However, unfortunately again this variation (rs75781974) was not annotated correctly, and in fact has MAF = 0.27, consequently it was excluded. The third of the relevant genes, *ACTR10*, is an actin-related protein. However, similarly, the exome was annotated with a disused transcript, and the variation is not close to any exons in any of the currently used transcripts and so was again discarded.

Due to this high rate of mis-annotation, the remaining 32 possibly relevant variations were investigated and excluded if the MAF \geq 0.01 or the transcript was disused. Only three of the 32 variations were not excluded (shown in blue) in the genes *TCEB3*, *HEATR7B1* and *C19orf45*. Primers for these variants were ordered to check for their presence in patient B.IV.5. None were present in the patient.

4.2.5. Analysis of only the Sisters

As considering all three family members together did not solve the family, the next part of the analysis was to assume that coincidentally, the two parts of the family had different neuromuscular diseases. Based on this assumption, only the WES results of the two sisters, patients B.IV.8 and B.IV.9 were analysed together. They shared 18382 variants, when filtering was applied this was reduced to 214. One of the remaining changes was a splice site mutation in *DES* that has previously been reported to be pathogenic.

4.2.5.1. Desmin

The *DES* gene encodes an intermediate filament (IF) protein, desmin. Specialised IF proteins are differentially expressed in many cell types including neurofilament proteins in neurones, keratins in epithelial cells and glial fibrillary acidic proteins in astrocytes (Clemen et al. 2013). Desmin is the most abundant IF protein in all muscle types and forms a scaffold across myofibrils, connecting parts of the muscle including z-disks, sarcolemma and cell organelles (Kouloumenta et al. 2007). Mutations in desmin can be autosomal recessive, autosomal dominant or de novo and can result in a range of disorders known as desminopathies including LGMD2R, cardiomyopathy, myofibrillar

myopathy and Scapulo-peroneal syndrome (OMIM# 615325, 604765, 601419, 181400 respectively).

The heterozygous mutation that was identified in patients B.IV.8 and B.IV.9 is c.735+1G>A, a highly-conserved splice site mutation 1bp upstream of the end of exon three. This mutation has been reported twice before, initially in a review without an associated phenotype (Goldfarb et al. 2004), and more recently in a patient with a cardiomyopathy (Gudkova et al. 2013). In the former of these articles, the authors provided a table of splice site mutations which all had the same consequence of removing exon three and resulting in the in-frame fusions of exon two and four. This 32 amino acid deletion disrupted the structure of desmin and prevented the protein from forming its filamentous network (Goldfarb et al. 2004). *DES* was previously screened in all three family members and no mutations were found. However, there can therefore be little doubt that this mutation in these sisters is pathogenic given the previously published evidence and the presence of desmin accumulation in their biopsies. The variation was Sanger sequenced in all three family members and, as expected, was present in patients B.IV.8 and B.IV.9 but not B.IV.5 (Figure 6.11). The mutation must have been missed by previous Sanger sequencing.

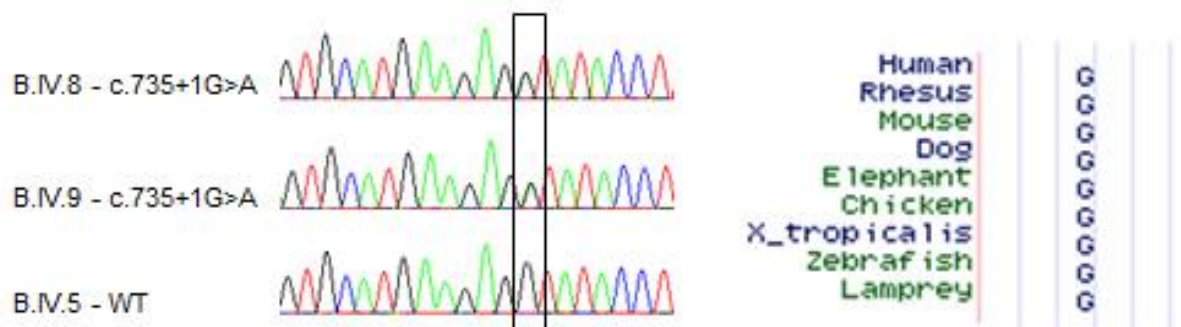


Figure 6.11 – Chromatograms in three family members and nucleotide conservation for the *DES* mutation c.735+1G>A. Nucleotide conservation is taken from the UCSC genome browser (<https://genome-euro.ucsc.edu>)

4.2.6. Analysis of only RW

The pathogenic *DES* mutation identified in half of the family but absent from the other half suggests that there are two different myopathy mutations within the family that are coincidentally causing similar phenotypes. Therefore the WES results for patient B.IV.5 were analysed in isolation in an attempt to uncover the genetic basis of his disease.

Filtering using the above criteria, as well as a depth filter of 5, revealed 302 variations, which was too many to investigate individually. There were no obvious

known genes, and no relevant pathogenic previously reported mutations. There was one VGIC gene, *CACNA1E*, however this is again predominantly expressed in brain regions and unlikely to be associated with myopathy (Williams et al. 1994). Therefore, more family members from this side of the family would be needed to elucidate the genetic cause of disease in this family.

5. Discussion

In this chapter, whole-exome sequencing was undertaken to genetically diagnose two families with unexplained hereditary diseases.

The first was a large kindred with paroxysmal exercise-induced dyskinesia (Family A, Figure 6.1). The paroxysmal dyskinesia genes had already been screened and were negative. For this family, a candidate gene approach was used and consequently, only the proband was sequenced initially. The candidate gene list used was the genes known to be associated with the paroxysmal dyskinesias. This approach yielded one variation; p.(Arg298Thr) in *KCNA1*, (the gene for EA1) which segregated in the other 11 family members that has a definitive affected/ unaffected status and for who DNA was available for. Functional work went on to show that this mutation was pathogenic. The success of this approach in this family was due to a combination of the large number of family members and of fortune.

WES on only one family member and then examining candidate genes will only provide convincing results if either a known pathogenic mutation is found, the gene exactly matches the clinical presentation, or if there are enough family members to carry out segregation studies. As, in this case, a known pathogenic mutation was not identified, and the patient phenotype was not previously associated with gene, had so many family members not been available, the initial pathogenicity of the mutation would have been questionable. This is because none of the other variations were investigated and ruled out. However, a variation is highly unlikely to segregate in so many family members, and so strong evidence is provided that this is the true causative mutation.

There was also a large deal of luck involved. Had the list of candidate genes not provided a promising variant, there would have been too many variations left to use the exome of just one family member to discern pathogenic from non-pathogenic, as seen in the analysis of patient B.IV.5's WES results. Furthermore, only 55% of the target exonic regions were covered by the sequencing, and thus it was fortuitous that the variation was covered at all. However, given the number of family members that were

available, a variation in a non-candidate gene would have likely been identified by WES of more affected individuals; however this would have increased the cost and time of the study.

As seen frequently in the previous chapter, lack of clinical information again proved problematic in this family. An initial diagnosis of classical PED was given, however, further clinic details were not provided, and the family were not able to be re-assessed in light of the genetic diagnosis. It is therefore a possibility that the family were misdiagnosed, especially as a further EA patient was identified with the same mutation. A thorough phenotypic evaluation of this family would be needed to be certain of and to characterise the novel phenotype.

Family B was a family with a complex myopathy (Figure 10.8). In this family, the unusual phenotype and list of previously excluded genes suggested that a candidate-gene approach would not be successful, and instead a shared variant approach was used instead. Three family members underwent WES. It was thought that it would be particularly powerful as the affected family members were several degrees of separation from each other, and therefore would not share many rare variants. This was true; they shared only four, but, on closer inspection, none appeared to be the causative variant. Next, variants were examined that were shared in two of the three but could have been missed in the third. This was again, unfruitful. Lastly, only the two sisters were analysed, and a previously reported *DES* splicing mutation was found which causes myopathy due to a truncated desmin protein. This was present in both sisters but not patient B.IV.5. The mutation was missed when the patients were previously screened diagnostically. Further investigation was needed to uncover the genetic basis of the neuromuscular disease in other side of the family, however initial investigation suggests a channelopathy is not the cause of this patient's myopathy.

This project highlighted two major problems with WES. The first is that of mis-annotation. Many of the variants left by the filtering processes remained because they had been mislabelled in the primary analysis. They were either too common but without associated frequency annotation, sequencing artefacts, or associated with disused transcripts. This problem was especially prominent when variants present in patient B.IV.9 and B.IV.8 but not in B.IV.5 were examined, this is likely to be because the sisters were sequenced with a different exome capture method to patient B.IV.5. A different capture was used because of the times that the sequencing took place. There was a delay in obtaining DNA samples from B.IV.9 and B.IV.8, and thus the sequencing occurred later than that of B.IV.5. Advances in the field are fast-paced and in that time the department has changed its protocol to use a more update capture for

its exome sequencing. This has different target regions, resulting in a slightly different sequencing profile in B.IV.5. Additionally, the in-house analysis pipeline would have also been updated in the time and variations may have been annotated differently, further complicating the problem.

The second issue that was that, although appearing to share a myopathy phenotype, the two sides of the family did not actually have the same disease. This was an unfortunate coincidence, as if only the sisters had been analysed from the start, the solution could have been found much quicker. This will not be a common problem, as these disorders are very rare; however, it is something to be considered when finding a solution in this type of family is proving problematic. There were phenotypic differences in the two sides of the family, including presence or lack of cardiac involvement and biopsy differences, which could have perhaps suggested different diseases, however, such conclusions are easiest to make with hindsight.

The project did, however, identify a mutation that was missed by diagnostic Sanger sequencing. The mutation may have been missed because it is a splice site change and so just outside of the exon. Sanger sequencing is supposed to be the gold standard, however this finding demonstrates that WES can provide more thorough sequencing than Sanger.

This chapter has shown that WES can be used to identify the genetic basis of a disease for previously undiagnosed families. However, it has also shown that this process is not always straightforward, and some of the limitations have been highlighted. Two different strategies were used here to uncover pathogenic variants; a candidate-gene approach and a shared-variant approach; the work here has shown that luck, as well as study design, is important for mutation discovery in WES.

Chapter 7: General

Conclusions

The aim of this thesis was to improve the understanding of the genetic basis of neuronal and skeletal muscle paroxysmal conditions. We also aimed to investigate the methods that can be used for their discovery with a view to improving the diagnostic process. The channelopathies are a group of rare, often debilitating diseases caused by voltage-gated ion channel dysfunction.

1. Chapter Three

Chapter three investigated the paroxysmal dyskinesias, a group of rare paroxysmal movement disorders that, although not actually caused by VGIC dysfunction, share characteristics with the neuronal channelopathies such as episodic attacks interspersed with periods of normal function. Additionally, they have overlapping symptomatic features such as migraine and hemiplegia. They were therefore included in this study. Each of the three PxDs, (PKD, PED and PNKD) has a known causal gene (*PRRT2*, *SLC2A1* and *PNKD* respectively), but no large-cohort screening study has ever been performed across all three. Here, the three genes were screened in a mixed paroxysmal dyskinesia cohort of 159 patients to determine the mutational frequency and the phenotypic overlap amongst the genes. Mutations were identified in all three genes, and a genetic diagnosis was provided to 39% of the cohort (62 patients). 10% of these did not have a mutation in the expected gene, confirming that genetic heterogeneity is more common than previously thought (a recent review found that this figure was 2% in published cases (Erro et al. 2014)) and highlighting the need to assess all three genes when genetically diagnosing these patients. One particularly interesting patient with myotonia-like characteristics and positive McManis test (suggesting a skeletal muscle channelopathy) had a mutation in *SLC2A1*. There are many channelopathy-gene negative patients with similar test results; if this mutation is pathogenic, it could lead to the genetic diagnosis of some of those patients.

The genes were also screened in a smaller cohort of 55 well-defined patients with other episodic disorders, including episodic ataxia, familial hemiplegic migraine

and benign infantile seizures. Mutations were identified seven individuals, three with EA, one with FHM and three had infantile seizures. Additionally, in the department a patient with FHM was found to have a novel C-terminal deletion in *PNKD* (all current known mutations in the gene are N-terminal) Therefore, for all three of these genes, novel mutations have been found and the phenotypic spectrum of gene mutation has been expanded. An additional 192 poorly characterised patients with episodic features were included in the study; however, no mutations were identified in this cohort.

PRRT2 mutations are thought to cause disease through haploinsufficiency, and a recent study has shown that exon-two nonsense mutations result in nonsense mediated decay. Some of our novel mutations did not fit this theory, as they were in exon three and did not result in a premature stop codon. To investigate whether NMD decay was occurring, mRNA was extracted from patient fibroblasts and reverted into cDNA by reverse transcription. cDNA sequencing showed the mutations were present, and thus excluded the possibility of NMD. Therefore, this work established that haploinsufficiency is not the disease mechanism in these mutations; however, they could still be causing loss of *PRRT2* function, perhaps by interrupting protein interactions or membrane docking.

A similar experiment was performed to determine whether the novel *PNKD* deletion resulted in NMD. Again the mutation was found to be present in the cDNA, showing existence of a truncated protein. This possibly disrupts a C-terminal enzymatic domain, and could represent an entirely new disease mechanism, perhaps accounting for the novel phenotype. This work suggests that *PNKD* mutations should be considered for genetically undiagnosed FHM patients.

Lastly, the current knowledge of the etiology behind the PxDs was consolidated to produce a suggested underlying mechanism (Figure 3.11), whereby *PRRT2* and *PNKD* regulate vesicle release at the synaptic junction and their dysfunction results in excessive neurotransmitter discharge. This mechanism is largely speculative and additional functional characterisation is required to establish its validity.

In chapter three, the genetic overlap surrounding the neuronal channelopathies was highlighted, and the inefficiencies of using Sanger sequencing as a method of genetic diagnosis demonstrated. The complex sequencing algorithm used for diagnosing the skeletal muscle channelopathies suggests that the same is also true for this group of diseases. Therefore, it was thought that next-generation sequencing could provide a more efficient method of genetic diagnosis for the channelopathies, as well as improve the diagnostic rate with novel findings.

2. Chapter Four

Chapter four saw the design and implementation of two NGS channel panels using Illumina's TruSeq Custom Amplicon technology; one that simultaneously sequenced neuronal channelopathy genes (the brain channel panel) and one that sequenced the skeletal muscle channelopathy genes (the muscle channel panel). Each was trialled on a mix of 95 positive controls and patients.

The brain channel panel found probable pathogenic mutations in 10 patients, and further possible pathogenic mutations in two, giving an overall mutation rate of 15%. It was noted that this was lower than expected, probably because many of the patients in the department had been pre-screened for these genes in the diagnostic process and thus the undiagnosed patients remaining are more likely not have mutations in the expected genes. Of the mutations found, five patients had an atypical phenotype in relation to their genetic diagnosis (four of which were probably pathogenic). Therefore, 6% of the cohort and 42% of the mutations were in unexpected genes and would have been missed in a Sanger sequencing genetic investigation. This clinical benefit shows the importance of this technology for the neuronal channelopathies.

The muscle channel panel identified 13 possible or probable pathogenic mutations, which is 19% of the cohort. There was less phenotypic overlap than for the neuronal channelopathies; four appeared to cause atypical phenotypes, but three retrospectively did fit to the diagnosis and the fourth may not be disease-causing. All but one of the probable pathogenic mutations would have been found in the Sanger sequencing diagnostic process (a *KCNJ2* mutation would have been missed), however, the complexity of the diagnostic algorithm would mean that several would not have been found initially, and so the panel still offers a clinical benefit over the previous method.

Whilst both panels demonstrated their advantages clearly, they both had the same problems; low sensitivity (the ability to identify positive control mutations) and low coverage. The sensitivities were 0.69 and 0.85 for the brain and muscle panels respectively. The positive controls that were missed were either CNVs or in areas with low coverage as the brain channel panel coverage was 81% and the muscle 86%. The low coverage would mean that they are not yet suitable for application into a diagnostic laboratory as they could produce false negative results. Therefore, this is an issue that needs to be resolved before their implementation diagnostically.

The classic channelopathies are a group of diseases clearly well suited to NGS panel technology as they are large, phenotypically heterogeneous genes, and varying presentations can make clinical diagnosis difficult. Additionally, the small numbers of genes involved and highly penetrant, autosomal dominant inheritance pattern makes the results relatively easy to interpret. The next chapter, focused on using the same technology on a much larger scale; for the genetic diagnosis of patients with recurrent rhabdomyolysis and/ or exercise intolerance.

3. Chapter Five

Recurrent RM is a potentially fatal condition, with episodes involving muscle breakdown and release of toxic cellular components into the bloodstream. The underlying genetic causes are varied and widespread, following a range of inheritance patterns and often have reduced penetrance. Additionally, non-Mendelian genetic risk factors are known to increase the likelihood of episodes in individuals who harbour them. These factors can make genetic diagnosis problematic. Currently, many patients with recurrent RM, or the related condition, exercise intolerance are screened for single genes sequentially and investigated extensively biochemically and immunohistochemically without a genetic diagnosis being determined. Chapter five aimed to sequence the 46 known associated genes simultaneously in a large cohort of 224 patients with recurrent RM or exercise intolerance to investigate the feasibility of using NGS panel technology for diagnosis in these conditions. Whilst not classed as a classic channelopathy, VGIC dysfunction is known to be an important genetic cause of recurrent RM, as mutations in both *RYR1*, a VGCC-related protein, and *CACNA1S* cause the condition malignant hyperthermia susceptibility. Additionally, *SCN4A* mutations have, in rare cases been known to cause RM. Therefore, this project attempted to uncover the contribution of VGIC channel genes to genetic landscape of recurrent RM and exercise intolerance.

The RM panel identified probable pathogenic mutations in 46 patients; this is 21% of the cohort. Additionally, possible pathogenic mutations were identified in 40 patients (17% of the cohort). Therefore, it produced a potential hit rate of 38%. This high frequency, along with the high number of patients recruited for the study show the importance and benefit of NGS panel technology for the conditions, and demonstrates that it should be put into clinical practice. Again, pre-screening of patients probably resulted in a lower mutation detection rate than if genetically un-investigated patients had been sequenced. VGIC genes accounted for half of the patients with probable

pathogenic mutations; however, these were all *RYR1* mutations as none were found in *CACNA1S* or *SCCN4A*. The other possible and probable pathogenic mutations were spread out amongst 13 genes, consequently 30 of the genes analysed had no hits at all. From this panel it can be concluded that VGIC dysfunction does have a substantial contribution to recurrent RM and exercise intolerance, however, only in the form of *RYR1* mutations.

Unfortunately, there were, again, some technical problems. Initially, a customised TSCA panel was used; however, a high sample failure rate and low coverage meant that this was not continued. Consequently, a standard TruSight One product was used instead. This allowed for inclusion of new genes. Additionally, no samples failed and the level of coverage was much higher, despite some gaps still being evident. Therefore, it was concluded that the TruSight One panel was preferable to the TSCA.

Another difficulty arising from the RM panel was the sheer amount of data produced. After filtering, each sample still had roughly four-eight rare variants (see Appendix 4), and discerning the pathogenic from the benign was challenging. Additionally, time constraints meant that a wealth of information, both in the 46 genes chosen, and the other almost 5000 genes that were sequenced, was not analysed. This is something, that to make the most of the data, will have to be addressed.

4. Chapter Six

Chapter six continued to use NGS, but progressed to whole-exome sequencing. Two genetically undiagnosed families with possible ion channel dysfunction were investigated using different WES strategies. This chapter aimed to examine the benefit of using WES in potential channelopathy families in general, as well as provide a solution for the two specific families analysed.

Family A was a large pedigree with PED that had previously been screened for the PxD genes. A candidate gene strategy was employed, whereby WES was performed on one family member, and then candidate genes were examined. If nothing was found WES would be performed on further individuals. Fortunately, this approach did find a mutation, c.893G>C, p.(Arg298Thr) in *KCNA1*. This mutation segregated in the large family, was predicted to be pathogenic and was absent from over 65,000 controls. It was thought that the novel phenotype might be due to the first *KCNA1* gating-pore mutation, but functional work demonstrated that, while it did appear to be

pathogenic, this was not the case. Therefore it is not clear why this mutation is causing PED in family A, as further screening of *KCNA1* also found the same mutation in an additional EA patient.

Family A showed that a candidate gene approach, with good fortune, can be successful. Therefore it is a good strategy if time is not a constraint as it saves the cost of sequencing multiple family members; however, it will take much longer if nothing is found in the first instance. This family did have a channelopathy, and the clear presentation of such was probably what made the candidate gene screening successful, as it limited the potential candidate genes. In hindsight, however, they could have been investigated using the brain channel panel.

Family B had a different presentation; there were two sides of the family, each with distal myopathy. They had previously been screened for many candidate genes. There have been reports of such families having *RYR1* mutations, and even one report of a related *SCN4A* mutation, so it was thought that it was possible WES could reveal a known channel or novel channel mutation. A shared variant strategy was used as the two sides of the family had several degrees of separation and so would share few variants; however, no shared potential mutations were found. Subsequently, the WES results of the two sisters were analysed alone and a known pathogenic mutation was found in *DES*, the gene encoding desmin, which was not present in their affected cousin. They had previously been screened for desmin mutations, as their muscle biopsy showed desmin aggregations, however the mutation had been missed. The other side of the family remained unresolved.

Family B raised a number of points to address. The first was that, although this large family appeared to have a common muscle condition, they did not. Coincidentally, they had similar presentations, although in retrospect there were differences in cardiac involvement and on muscle biopsies. This shows the need for careful phenotypic analysis, for exercising caution when assigning affected/ unaffected status and for being flexible in WES data analysis. The second point is that, although Sanger sequencing is classed as the gold standard, mutations can be missed, and as such, Sanger results cannot always be relied upon. The strategy employed probably would have been successful had the family shared the same mutation, and thus it can be concluded that WES can be a successful way of investigating potential channelopathy families as long as further options are explored.

5. Overall

One of the main themes of this thesis was to genetically investigate the channelopathies and thus expand the knowledge of their genetic underpinnings. Accordingly, this thesis has expanded the phenotypic spectrum of many of the neuronal channelopathy genes and highlighted the overlap that exists between them. Following this, they should perhaps be viewed as a spectrum of symptoms, and not a group of separate diseases as they were presented in the introduction of this thesis, and routinely in the literature. Of course, in a diagnostic setting, classification must be given to a patient's symptoms in order for effective treatment, but when it comes to investigating the genetic causes, these strict classifications are not always helpful and can hinder progress, as has been seen in chapters three, four and six. This point is demonstrated in Table 7.1, where Table 1.6 from the introduction has been adapted to include data from the this project and other publications to present a less black and white picture of the neuronal channelopathies. This observation demonstrates the necessity of the use of NGS when investigating these, and similar heterogeneous groups of diseases.

Gene	Associated Phenotypes
<i>KCNA1</i>	EA1, PED, PKD , myokymia, epilepsy
<i>CACNA1A</i>	EA2, FHM, SCA6, head tremor, epilepsy, dyskinesia , alternating hemiplegia
<i>ATP1A2</i>	FHM, migraine with seizures
<i>SCN1A</i>	FHM, epilepsy, Dravet syndrome
<i>KCNK18</i>	PKD , FHM, Migraine with aura
<i>PNKD</i>	PNKD, PKD, FHM
<i>SLC2A1</i>	GLUT1 DS 1, PED, Seizures, alternating hemiplegia, EA, myotonia
<i>PRRT2</i>	PKD, FHM, EA , PED
<i>CACNB4</i>	EA5, HM

Table 7.1 – A revised summary of the genes involved in neuronal channelopathies, novel findings from this thesis are highlighted in bold

Whilst this technology is clearly also beneficial for the skeletal muscle channelopathies, there is less clinical overlap and thus the genetic causes are more

predictable. This was demonstrated by the likelihood scores used in the muscle panel; many more mutations were found patients deemed very probable to harbour a channelopathy than patients deemed not likely. Consequently, from this thesis it can be concluded that the implementation of the muscle channel panel is not as important as the implementation if the brain channel panel.

The role of ion channel dysfunction in recurrent RM was also examined under the scope of genetically investigating the channelopathies. It was thought that the contribution of classic VGIC genes (*CACAN1S* and *SCN4A*) could be underestimated, as they are often not routinely investigated in patients with RM. The results showed that while *RYR1* mutations contributed substantially the overall genetic diagnosis, *CACAN1S* and *SCN4A* mutations have not yet been shown to be important factors, although many variations of unknown clinical significance were identified that should be investigated further.

The second theme of this thesis was an assessment of the progression of the different sequencing technologies and their viability for genetic diagnosis of the channelopathies. Sanger sequencing was used initially in chapter three to screen three genes in a large cohort. Next, small NGS panels were used for parallel sequencing of a small number of genes in chapter four. In chapter five, two different larger NGS panels were utilised to examine much larger group of genes and patients. Lastly, in chapter six, WES was used to investigate single families.

Each of these sequencing methods has their advantages and disadvantages. Sanger sequencing is thorough and should not provide false negative or positive results. It is necessary for confirming variations found by NGS. Furthermore, data is easy to interpret and does not require primary analysis. However, at the scale at which it was carried out here (14 exons in over 300 patients), it was expensive and time-consuming. Using a panel instead would have been quicker and possibly cheaper for this task.

Small panel sequencing, on the other hand, allowed for investigation of genetic and phenotypic overlap, and meant that genetic investigations were not impinged by diagnostic bias. It was faster and cheaper than Sanger sequencing. However, as the number of genes increased, the analysis became more difficult. More rare variants were found, and discerning the benign from the damaging was challenging. Also technical problems resulted in gaps in coverage and false negatives and positives.

TruSight One provided a solution to the coverage problem experienced with TSCA. The large number of genes sequenced meant a complex condition such as recurrent rhabdomyolysis, which has many possible genetic causes, could be examined. Additionally, it has the benefit that if the clinical diagnosis changes or known genes are newly linked to a condition and so there is a requirement to examine other clinically relevant genes, they have been sequenced and the data will be readily available. The disadvantages of this approach are that some coverage gaps still exist, there is surplus data to analyse which may be wasted, and again, difficulty interpreting the results, especially when multiple plausible pathogenic variations are found.

WES is an excellent tool for gene discovery and can lead to completely novel findings, however, this relies on large families, accurate clinical information, good fortune, and functional investigations are still required to prove novel findings. If enough family members are not available, again, large numbers of rare variants are impossible to interpret, and attempting to do so can be a time consuming and often unfruitful task. Differences in capture and annotation methods can result in false positive results and wasted analysis. Finally, as it is often assumed that the mutation will be present in the exome, much time can be wasted if this does not turn out to be the case.

Based on the advantages and disadvantages of each approach, when designing a diagnostic study it is important to carefully consider which technology is most appropriate. Factors such as cohort size, availability of clinical data and number of genes to be examined must be taken into account. There is a balance between having the necessary data to examine the genes of interest, whilst not producing so much data that much is unusable and wasted. In general it appears that the fewer genes to be investigated, the larger number of patients it is feasible to analyse.

This thesis also represents the improvement in technology that has occurred over the four years that it has taken to complete. Initially, Sanger sequencing was the only method available. Subsequently, NGS became more accessible and the introduction of the Illumina HiSeq and MiSeq into the department meant that some WES and TSCA could be performed. The work in this thesis represents some of first ever panel sequencing projects employed within the department. Initially, however, WES was slow and expensive and TSCA had technical problems which reduced its reliability. Technology has improved at an astounding rate and in recent years WES has become cheaper, faster and of higher quality, and standard panel sequencing, such as TruSight One has eliminated the design problems of TSCA. These trends are set to continue, with high-throughput sequencing becoming ever cheaper, and WGS more easily available. Undoubtedly, there will soon be little financial or time benefit to

performing any other sequencing than WES or WGS when examining more than a few genes. A cost analysis of the NGS technologies used in this thesis is difficult as the different kits were bought and the different sequencing methods carried at different points during the project, and as prices were changing so rapidly, they are not comparable. Additionally, as mentioned above, the price of sequencing is falling so fast that the prices quoted here will already be out of date. However, as a rough guide, the TSCA was about £100 per sample, the TruSight One was about £160 per sample and the whole exome sequencing was about £500 per sample. These prices include the cost of reagents, kits and running of the machines.

Providing a genetic diagnosis to patients is vital. It can help guide treatment, and in the case of recurrent RM can help avoid triggers of potentially fatal events. It can inform genetic counselling so and aid people in decisions regarding having children. It can assist ensuring patients are entitled to any disability aids or benefits. Lastly, it gives patients peace of mind and helps them to cope with their disease. Furthermore, discovering the genetic basis of a disease can also aid scientific discovery; it furthers the understanding of the disease and provides knowledge of the pathway that is affected. Consequently, it can result in novel therapeutic targets.

These factors therefore highlight the importance of the work in this thesis for channelopathy patients and for the channelopathy field in general. NGS technology is rapidly progressing and, if applied to channelopathy research and diagnosis, will hopefully change the field for the better and improve the lives of patients affected with these often debilitating diseases.

Appendices

Appendix 1 – Target and Designed Amplicon Coordinates and Target Coverage of Brain Channel Panel

Target	Start Coordinate	End Coordinate	Length	Amplicon number	Coverage	Score
cacna1a ex36	19:13340865	19:13341021	157	0	0	0
cacna1a ex37	19:13339501	19:13339599	99	0	0	0
cacna1a ex38	19:13338247	19:13338360	114	0	0	0
cacna1a ex20	19:13397289	19:13397807	519	3	82	83
cacna1a ex19	19:13409340	19:13410205	866	5	94	87
cacn4b ex1	2:152955461	2:152955526	66	1	100	87
cacn4b ex10	2:152717222	2:152717339	118	1	100	95
cacn4b ex11	2:152711736	2:152711893	158	1	100	87
cacn4b ex12	2:152709959	2:152710060	102	1	100	95
cacn4b ex13	2:152698410	2:152698606	197	2	100	83
cacn4b ex14	2:152695628	2:152695902	275	3	100	88
cacn4b ex2	2:152954843	2:152954929	87	1	100	74
cacn4b ex3	2:152739762	2:152739888	127	1	100	95
cacn4b ex4	2:152737312	2:152737439	128	1	100	95
cacn4b ex5	2:152732935	2:152733074	140	1	100	80
cacn4b ex6	2:152728928	2:152729010	83	1	100	74
cacn4b ex8+ cacn4b ex7	2:152727044	2:152727376	333	3	100	90
cacn4b ex9	2:152725688	2:152725752	65	1	100	95
cacna1a ex1	19:13616739	19:13617047	309	3	100	83
cacna1a ex10	19:13441055	19:13441153	99	1	100	95
cacna1a ex11	19:13427920	19:13428144	225	2	100	84
cacna1a ex12	19:13423480	19:13423602	123	1	100	80
cacna1a ex14+ cacna1a ex13	19:13418925	19:13419346	422	3	100	92
cacna1a ex15	19:13418594	19:13418672	79	1	100	74
cacna1a ex17 + cacna1a ex16	19:13414350	19:13414701	352	3	100	87
cacna1a ex18	19:13411354	19:13411484	131	1	100	95
cacna1a ex2	19:13565918	19:13566031	114	1	100	95
cacna1a ex21	19:13395878	19:13396025	148	1	100	95
cacna1a ex22	19:13394078	19:13394217	140	1	100	95
cacna1a ex23	19:13387881	19:13387945	65	1	100	95
cacna1a ex24	19:13386660	19:13386775	116	1	100	74
cacna1a ex25	19:13373545	19:13373650	106	1	100	74
cacna1a ex26	19:13372259	19:13372428	170	1	100	74
cacna1a ex27	19:13370374	19:13370520	147	1	100	95

cacna1a ex28	19:13368161	19:13368370	210	2	100	74
cacna1a ex29	19:13365903	19:13366082	180	1	100	74
cacna1a ex3	19:13563686	19:13563836	151	1	100	95
cacna1a ex30	19:13363797	19:13363923	127	1	100	74
cacna1a ex31	19:13355991	19:13356085	95	1	100	95
cacna1a ex32	19:13346426	19:13346548	123	1	100	95
cacna1a ex33) + cacna1a ex34	19:13345732	19:13346091	360	3	100	87
cacna1a ex35	19:13342514	19:13342679	166	1	100	95
cacna1a ex39	19:13335477	19:13335594	118	1	100	95
cacna1a ex4	19:13482500	19:13482597	98	1	100	80
cacna1a ex41 + cacna1a ex40	19:13325045	19:13325427	383	3	100	89
cacna1a ex44 + cacna1a ex43 + cacna1a ex42	19:13322915	19:13323559	645	4	100	87
cacna1a ex45	19:13321430	19:13321469	40	1	100	95
cacna1a ex46	19:13320121	19:13320320	200	1	100	87
cacna1a ex47	19:13319565	19:13319830	266	2	100	87
cacna1a ex48	19:13318114	19:13318882	769	5	100	87
cacna1a ex5	19:13476122	19:13476295	174	1	100	80
cacna1a ex6	19:13470414	19:13470626	213	2	100	83
cacna1a ex7	19:13446616	19:13446729	114	1	100	95
cacna1a ex8	19:13445189	19:13445311	123	1	100	87
cacna1a ex9	19:13443681	19:13443743	63	1	100	95
KCNA1 ex2	12:5020519	12:5022091	1573	10	100	88
kcnk18 ex1	10:11895700 0	10:11895723 4	235	2	100	81
kcnk18 ex2	10:11896066 3	10:11896080 5	143	1	100	95
kcnk18 ex3	10:11896898 6	10:11896995 2	967	6	100	87
pnkd ex1	2:219135217	2:219135310	94	1	100	87
pnkd ex10 + pnkd ex9	2:219209176	2:219209708	533	4	100	87
pnkd ex2	2:219136101	2:219136277	177	1	100	95
pnkd ex4 + pnkd ex3	2:219204502	2:219204867	366	3	100	80
pnkd ex5	2:219205449	2:219205511	63	1	100	74
pnkd ex6	2:219206256	2:219206357	102	1	100	74
pnkd ex7	2:219206702	2:219206871	170	1	100	84
pnkd ex8	2:219208222	2:219208313	92	1	100	74
prrt2 ex2	16:29824369	16:29825268	900	5	100	85
prrt2 ex3 + prrt2 ex4	16:29825651	16:29825960	310	2	100	87
slc1a3 ex10	5:36686161	5:36686376	216	2	100	87
slc1a3 ex2	5:36608524	5:36608727	204	1	100	95
slc1a3 ex3	5:36629544	5:36629697	154	2	100	91
slc1a3 ex4	5:36671126	5:36671342	217	2	100	84
slc1a3 ex5	5:36674148	5:36674196	49	1	100	95
slc1a3 ex6	5:36676991	5:36677291	301	3	100	87
slc1a3 ex7	5:36679724	5:36679967	244	2	100	91
slc1a3 ex8	5:36680494	5:36680696	203	2	100	95

slc1a3 ex9	5:36683962	5:36684107	146	1	100	95
slc2a1 ex1	1:43424304	1:43424323	20	1	100	87
slc2a1 ex10	1:43392711	1:43392916	206	2	100	83
slc2a1 ex2	1:43408894	1:43408995	102	1	100	95
slc2a1 ex4 + slc2a1 ex3	1:43396295	1:43396880	586	4	100	89
slc2a1 ex6+ slc2a1 ex5	1:43395262	1:43395714	453	3	100	84
slc2a1 ex8 + slc2a1 ex7	1:43394600	1:43394989	390	3	100	83
slc2a1 ex9	1:43393269	1:43393483	215	2	100	87

Brain channel panel design details

Ampl -icon	Start coordinate	End coordinate	Length	Ampl -icon	Start coordinate	End coordinate	Length
1	12:5020398	12:5020624	227	78	19:13414557	19:13414814	258
2	12:5020552	12:5020777	226	79	19:13418804	19:13419034	231
3	12:5020710	12:5020945	236	80	19:13418980	19:13419206	227
4	12:5020898	12:5021128	231	81	19:13419152	19:13419407	256
5	12:5021074	12:5021301	228	82	19:13322794	19:13323032	239
6	12:5021244	12:5021485	242	83	19:13322984	19:13323208	225
7	12:5021428	12:5021663	236	84	1:43392608	1:43392882	275
8	12:5021612	12:5021850	239	85	1:43392828	1:43393090	263
9	12:5021798	12:5022022	225	86	1:43393150	1:43393389	240
10	12:5021968	12:5022223	256	87	1:43393342	1:43393597	256
11	10:118956877	10:11895712 1	245	88	1:43408863	1:43409097	235
12	10:118957069	10:11895733 2	264	89	1:43424267	1:43424501	235
13	10:118960634	10:11896087 4	241	90	1:43394485	1:43394721	237
14	10:118968861	10:11896908 9	229	91	1:43394667	1:43394922	256
15	10:118969037	10:11896927 3	237	92	1:43394871	1:43395134	264
16	10:118969223	10:11896945 7	235	93	1:43395137	1:43395380	244
17	10:118969405	10:11896964 0	236	94	1:43395327	1:43395600	274
18	10:118969583	10:11896981 3	231	95	1:43395551	1:43395796	246
19	10:118969757	10:11896999 0	234	96	1:43396174	1:43396399	226
20	19:13317993	19:13318219	227	97	1:43396346	1:43396579	234
21	19:13318145	19:13318407	263	98	1:43396530	1:43396760	231
22	19:13318359	19:13318604	246	99	1:43396706	1:43396979	274
23	19:13318533	19:13318764	232	100	2:152695505	2:152695729	225
24	19:13318713	19:13318968	256	101	2:152695663	2:152695916	254
25	19:13319444	19:13319681	238	102	2:152695863	2:152696088	226
26	19:13319630	19:13319883	254	103	2:152698289	2:152698520	232
27	19:13320090	19:13320362	273	104	2:152698473	2:152698739	267
28	19:13321403	19:13321642	240	105	2:152709918	2:152710144	227
29	19:13335448	19:13335691	244	106	2:152711705	2:152711940	236
30	19:13342479	19:13342706	228	107	2:152717193	2:152717463	271
31	19:13346399	19:13346645	247	108	2:152725637	2:152725865	229
32	19:13355964	19:13356222	259	109	2:152728897	2:152729131	235
33	19:13363754	19:13363989	236	110	2:152732884	2:152733124	241
34	19:13365872	19:13366130	259	111	2:152737283	2:152737525	243
35	19:13368038	19:13368262	225	112	2:152739733	2:152739977	245
36	19:13368208	19:13368462	255	113	2:152954818	2:152955075	258
37	19:13370347	19:13370577	231	114	2:152955428	2:152955694	267
38	19:13372232	19:13372499	268	115	2:152726919	2:152727147	229

39	19:13373516	19:13373769	254	116	2:152727093	2:152727328	236
40	19:13386631	19:13386888	258	117	2:152727275	2:152727532	258
41	19:13387852	19:13388076	225	118	2:219136072	2:219136342	271
42	19:13394045	19:13394311	267	119	2:219205420	2:219205649	230
43	19:13395829	19:13396079	251	120	2:219206229	2:219206485	257
44	19:13397162	19:13397386	225	121	2:219206671	2:219206917	247
45	19:13397310	19:13397536	227	122	2:219208195	2:219208463	269
46	19:13397490	19:13397715	226	123	2:219204377	2:219204605	229
47	19:13409391	19:13409632	242	124	2:219204557	2:219204788	232
48	19:13409565	19:13409800	236	125	2:219204739	2:219204984	246
49	19:13409749	19:13409976	228	126	2:219209053	2:219209280	228
50	19:13409929	19:13410175	247	127	2:219209223	2:219209447	225
51	19:13410121	19:13410361	241	128	2:219209397	2:219209638	242
52	19:13411327	19:13411591	265	129	2:219209585	2:219209823	239
53	19:13418561	19:13418791	231	130	2:219135122	2:219135347	226
54	19:13423451	19:13423681	231	131	5:36608495	5:36608762	268
55	19:13427793	19:13428026	234	132	5:36629421	5:36629647	227
56	19:13427975	19:13428211	237	133	5:36629595	5:36629857	263
57	19:13441028	19:13441254	227	134	5:36671001	5:36671235	235
58	19:13443648	19:13443898	251	135	5:36671179	5:36671431	253
59	19:13445152	19:13445377	226	136	5:36674115	5:36674349	235
60	19:13446587	19:13446831	245	137	5:36676864	5:36677090	227
61	19:13470291	19:13470530	240	138	5:36677016	5:36677247	232
62	19:13470483	19:13470723	241	139	5:36677198	5:36677442	245
63	19:13476093	19:13476335	243	140	5:36679599	5:36679863	265
64	19:13482471	19:13482697	227	141	5:36679811	5:36680068	258
65	19:13563657	19:13563931	275	142	5:36680369	5:36680627	259
66	19:13565887	19:13566129	243	143	5:36680579	5:36680840	262
67	19:13616632	19:13616857	226	144	5:36683933	5:36684201	269
68	19:13616796	19:13617048	253	145	5:36686034	5:36686262	229
69	19:13616996	19:13617259	264	146	5:36686212	5:36686455	244
70	19:13324922	19:13325147	226	147	16:29824248	16:29824473	226
71	19:13325096	19:13325322	227	148	16:29824400	16:29824662	263
72	19:13325272	19:13325510	239	149	16:29824612	16:29824851	240
73	19:13345611	19:13345852	242	150	16:29824802	16:29825074	273
74	19:13345803	19:13346028	226	151	16:29825022	16:29825293	272
75	19:13345975	19:13346232	258	152	16:29825528	16:29825792	265
76	19:13414221	19:13414445	225	153	16:29825746	16:29825991	246
77	19:13414379	19:13414612	234	154	19:13323162	19:13323416	255
				155	19:13323366	19:13323619	254

Brain channel panel designed amplicon coordinates

Exon	Average coverage	Exon	Average coverage
cacn4b ex1	0	cacna1a ex33+ ex34	1
cacn4b ex2	0.97872	cacna1a ex35	1
cacn4b ex3	1	cacna1a ex36	not designed
cacn4b ex4	1	cacna1a ex37	not designed
cacn4b ex5	0.97727	cacna1a ex38	not designed
cacn4b ex6	1	cacna1a ex39	1
cacn4b ex7+ ex8	1	cacna1a ex40+ ex41	0.935223372
cacn4b ex9	1	cacna1a ex42+ ex43+ ex44	0.480606968
cacn4b ex10	1	cacna1a ex45	0.829787234
cacn4b ex11	1	cacna1a ex46	0.795466649
cacn4b ex12	1	cacna1a ex47	0.295303074
cacn4b ex13	1	cacna1a ex48	0.006344193
cacn4b ex14	1	kcnk18 ex2	0.913803511
cacna1a ex1	0.4846	kcnk18 ex1	1
cacna1a ex2	1	kcnk18 ex2	1
cacna1a ex3	1	kcnk18 ex3	1
cacna1a ex4	1	pnkd ex1	0.281743245
cacna1a ex5	0.41711	pnkd ex2	1
cacna1a ex6	1	pnkd ex3+ ex4	0.569046862
cacna1a ex7	1	pnkd ex5	0.991420723
cacna1a ex8	1	pnkd ex6	1
cacna1a ex9	1	pnkd ex7	0.996789628
cacna1a ex10	1	pnkd ex8	0.957446809
cacna1a ex11	1	pnkd ex9+ ex10	0.884198638
cacna1a ex12	1	prrt2 ex2	0.682483798
cacna1a ex13+ ex14	0.98764	prrt2 ex3+ ex4	0.697307649
cacna1a ex15	1	slc1a3 ex2	1
cacna1a ex16+ ex17	0.83118	slc1a3 ex3	0.518495436
cacna1a ex18	0.97136	slc1a3 ex4	0.935973191
cacna1a ex19	0.50572	slc1a3 ex5	1
cacna1a ex20	0.48065	slc1a3 ex6	1
cacna1a ex21	1	slc1a3 ex7	1
cacna1a ex22	1	slc1a3 ex8	0.833157894
cacna1a ex23	1	slc1a3 ex9	0.983272191
cacna1a ex24	1	slc1a3 ex10	1
cacna1a ex25	1	slc2a1 ex1	0.106382979
cacna1a ex26	1	slc2a1 ex2	1
cacna1a ex27	0.90236	slc2a1 ex3+ ex4	0.936388468
cacna1a ex28	1	slc2a1 ex5+ ex6	0.902913926
cacna1a ex29	0.97997	slc2a1 ex7+ ex8	0.920390745
cacna1a ex30	1	slc2a1 ex9	1
cacna1a ex31	1	slc2a1 ex10	0.993876489
cacna1a ex32	1		

Average coverage of brain channel panel exons

Appendix 2 – Target and Designed Amplicon Coordinates and Target Coverage of Muscle Channel Panel

Target	Start coordinate	End coordinate	Length	Amplicon number	Coverage	Score
scn4a ex24	17:62015897	17:62019387	3491	23	100	70
scn4a ex23	17:62020160	17:62020488	329	3	100	73
scn4a ex22	17:62021080	17:62021237	158	1	100	60
scn4a ex18	17:62024379	17:62024555	177	1	100	60
scn4a ex17	17:62025225	17:62025449	225	2	100	70
scn4a ex16	17:62025945	17:62026151	207	2	100	60
scn4a ex15	17:62026728	17:62026914	187	2	100	70
scn4a ex14	17:62028761	17:62029290	530	4	100	70
scn4a ex13	17:62034495	17:62034907	413	3	100	73
scn4a ex12	17:62036599	17:62036826	228	2	100	60
scn4a ex11	17:62038527	17:62038819	293	2	100	80
scn4a ex10	17:62041006	17:62041212	207	1	100	96
scn4a ex9	17:62041802	17:62042065	264	2	100	88
scn4a ex5	17:62048496	17:62048640	145	1	100	80
kcnj2 ex1	17:68165652	17:68165870	219	2	100	70
kcnj2 ex2	17:68170943	17:68176245	5303	34	100	78
clcn1 ex1	7:143013195	7:143013512	318	2	100	60
clcn1 ex2	7:143016822	7:143016994	173	1	100	96
clcn1 ex3	7:143017732	7:143017915	184	2	100	77
clcn1 ex4	7:143018432	7:143018512	81	1	100	80
clcn1 ex5	7:143018782	7:143018968	187	1	100	80
clcn1 ex7	7:143021482	7:143021611	130	1	100	80
clcn1 ex17	7:143042589	7:143042882	294	3	100	60
clcn1 ex18	7:143043207	7:143043370	164	1	100	80
clcn1 ex23	7:143048666	7:143049125	460	3	100	73
cacna1s ex41	1:201010607	1:201010743	137	1	100	96
cacna1s ex40	1:201012383	1:201012688	306	3	100	66
cacna1s ex39	1:201013430	1:201013611	182	1	100	80
cacna1s ex36	1:201017685	1:201017838	154	1	100	60
cacna1s ex35	1:201018106	1:201018253	148	1	100	80
cacna1s ex34	1:201019490	1:201019670	181	1	100	80
cacna1s ex33	1:201020086	1:201020298	213	2	100	80
cacna1s ex32	1:201021659	1:201021803	145	1	100	96
cacna1s ex29	1:201023607	1:201023715	109	1	100	80
cacna1s ex28	1:201027510	1:201027645	136	1	100	80
cacna1s ex27	1:201028312	1:201028453	142	1	100	60
cacna1s ex26	1:201029760	1:201029970	211	2	100	96
cacna1s ex25	1:201030369	1:201030624	256	2	100	70
cacna1s ex24	1:201031046	1:201031245	200	2	100	60
cacna1s ex23	1:201031564	1:201031668	105	1	100	80

cacna1s ex20	1:201035989	1:201036148	160	1	100	96
cacna1s ex17	1:201039374	1:201039559	186	2	100	70
cacna1s ex16	1:201041857	1:201041978	122	1	100	80
cacna1s ex15	1:201042651	1:201042797	147	1	100	96
cacna1s ex14	1:201043608	1:201043775	168	1	100	60
cacna1s ex13	1:201044597	1:201044770	174	1	100	80
cacna1s ex12	1:201046023	1:201046283	261	2	100	78
cacna1s ex11	1:201046982	1:201047260	279	2	100	70
cacna1s ex10	1:201052264	1:201052477	214	2	100	78
cacna1s ex9	1:201054052	1:201054176	125	1	100	80
cacna1s ex8	1:201054529	1:201054736	208	2	100	70
cacna1s ex7	1:201056928	1:201057084	157	1	100	80
cacna1s ex6	1:201058360	1:201058619	260	2	100	88
cacna1s ex3	1:201062984	1:201063176	193	1	100	80
cacna1s ex2	1:201079266	1:201079424	159	1	100	80
cacna1s ex1	1:201081290	1:201081724	435	3	100	66
scn4a ex6	17:62045330	17:62045745	416	2	84	80
clcn1 ex6	7:143020376	7:143020505	130	1	100	96
scn4a ex21 + scn4a ex20 + scn4a ex19	17:62022007	17:62023026	1020	6	100	70
scn4a ex8 + scn4a ex7	17:62043436	17:62043930	495	4	100	65
scn4a ex4 + scn4a ex3 + scn4a ex2 + scn4a ex1	17:62049057	17:62050306	1250	8	100	69
clcn1 ex8 + clcn1 ex9 + clcn1 ex10	7:143027840	7:143028771	932	6	100	78
clcn1 ex13 + clcn1 ex14	7:143036320	7:143036740	421	3	100	85
clcn1 ex15 + clcn1 ex16	7:143038996	7:143039624	629	4	100	88
clcn1 ex19 + clcn1 ex20	7:143043676	7:143044068	393	3	100	90
cacna1s ex44 + cacna1s ex43 + cacna1s ex42	1:201008617	1:201009867	1251	8	100	75
cacna1s ex38 + cacna1s ex37	1:201016217	1:201016780	564	4	100	70
cacna1s ex31 + cacna1s ex30	1:201022311	1:201022742	432	4	100	70
cacna1s ex22 + cacna1s ex21	1:201034941	1:201035470	530	4	100	69
cacna1s ex19 + cacna1s ex18	1:201038239	1:201038756	518	4	100	70
cacna1s ex5 + cacna1s ex4	1:201060742	1:201061269	528	4	100	79
clcn1 ex11 + clcn1 ex12	7:143029487	7:143030010	524	3	96	66
clcn1 ex21 + clcn1 ex22	7:143047439	7:143047790	352	2	83	70

Muscle channel panel design details

Ampli-con	Start coordinate	End coordinate	Length	Ampli-con	Start coordinate	End coordinate	Length
1	1:201008490	1:201008714	225	108	17:62036476	17:62036702	227
2	1:201008638	1:201008881	244	109	17:62036652	17:62036895	244
3	1:201008828	1:201009059	232	110	17:62038402	17:62038627	226
4	1:201009014	1:201009260	247	111	17:62038576	17:62038845	270
5	1:201009208	1:201009441	234	112	17:62040979	17:62041247	269
6	1:201009388	1:201009612	225	113	17:62041677	17:62041902	226
7	1:201009560	1:201009786	227	114	17:62041847	17:62042110	264
8	1:201009740	1:201009998	259	115	17:62048467	17:62048706	240
9	1:201016108	1:201016333	226	116	17:68165531	17:68165773	243
10	1:201016282	1:201016506	225	117	17:68165721	17:68165945	225
11	1:201016456	1:201016689	234	118	17:68170858	17:68171097	240
12	1:201016636	1:201016861	226	119	17:68171016	17:68171240	225
13	1:201022182	1:201022407	226	120	17:68171162	17:68171386	225
14	1:201022334	1:201022558	225	121	17:68171306	17:68171531	226
15	1:201022504	1:201022736	233	122	17:68171474	17:68171701	228
16	1:201022682	1:201022924	243	123	17:68171618	17:68171845	228
17	1:201034834	1:201035058	225	124	17:68171766	17:68171990	225
18	1:201034984	1:201035214	231	125	17:68171904	17:68172128	225
19	1:201035164	1:201035390	227	126	17:68172048	17:68172272	225
20	1:201035338	1:201035591	254	127	17:68172188	17:68172412	225
21	1:201038114	1:201038338	225	128	17:68172332	17:68172556	225
22	1:201038290	1:201038528	239	129	17:68172480	17:68172704	225
23	1:201038470	1:201038721	252	130	17:68172620	17:68172845	226
24	1:201038672	1:201038934	263	131	7:143027713	7:143027937	225
25	1:201060617	1:201060842	226	132	7:143027863	7:143028103	241
26	1:201060775	1:201061004	230	133	7:143028049	7:143028276	228
27	1:201060957	1:201061188	232	134	7:143028225	7:143028450	226
28	1:201061133	1:201061387	255	135	7:143028405	7:143028638	234
29	1:201010578	1:201010820	243	136	7:143028579	7:143028830	252
30	1:201012256	1:201012486	231	137	7:143036195	7:143036428	234
31	1:201012438	1:201012669	232	138	7:143036375	7:143036607	233
32	1:201012622	1:201012864	243	139	7:143036553	7:143036814	262
33	1:201013401	1:201013650	250	140	7:143038867	7:143039097	231
34	1:201017660	1:201017887	228	141	7:143039045	7:143039277	233
35	1:201018077	1:201018351	275	142	7:143039223	7:143039454	232
36	1:201019463	1:201019699	237	143	7:143039403	7:143039664	262
37	1:201019961	1:201020205	245	144	7:143043549	7:143043776	228
38	1:201020155	1:201020415	261	145	7:143043701	7:143043972	272
39	1:201021632	1:201021900	269	146	7:143043921	7:143044174	254
40	1:201023574	1:201023804	231	147	7:143029376	7:143029606	231
41	1:201027483	1:201027742	260	148	7:143029554	7:143029787	234
42	1:201028277	1:201028511	235	149	7:143029736	7:143029988	253
43	1:201029633	1:201029866	234	150	7:143047312	7:143047538	227
44	1:201029813	1:201030072	260	151	7:143047478	7:143047729	252

45	1:201030248	1:201030472	225	152	7:143013074	7:143013345	272
46	1:201030420	1:201030675	256	153	7:143013294	7:143013555	262
47	1:201030919	1:201031148	230	154	7:143016777	7:143017041	265
48	1:201031101	1:201031326	226	155	7:143017605	7:143017852	248
49	1:201031535	1:201031798	264	156	7:143017805	7:143018069	265
50	1:201035960	1:201036230	271	157	7:143018403	7:143018657	255
51	1:201039247	1:201039480	234	158	7:143018753	7:143019025	273
52	1:201039431	1:201039682	252	159	7:143021447	7:143021701	255
53	1:201041832	1:201042058	227	160	7:143042462	7:143042686	225
54	1:201042622	1:201042851	230	161	7:143042624	7:143042859	236
55	1:201043577	1:201043840	264	162	7:143042812	7:143043051	240
56	1:201044562	1:201044814	253	163	7:143043182	7:143043435	254
57	1:201045902	1:201046151	250	164	7:143048541	7:143048770	230
58	1:201046102	1:201046359	258	165	7:143048723	7:143048968	246
59	1:201046855	1:201047113	259	166	7:143048919	7:143049183	265
60	1:201047063	1:201047314	252	167	7:143020337	7:143020605	269
61	1:201052139	1:201052368	230	168	1:201058233	1:201058477	245
62	1:201052319	1:201052551	233	169	1:201058427	1:201058685	259
63	1:201054021	1:201054271	251	170	1:201062955	1:201063211	257
64	1:201054404	1:201054629	226	171	1:201079237	1:201079495	259
65	1:201054582	1:201054849	268	172	1:201081165	1:201081393	229
66	1:201056899	1:201057125	227	173	1:201081345	1:201081571	227
67	17:62015772	17:62016003	232	174	1:201081525	1:201081763	239
68	17:62015924	17:62016149	226	175	17:68172760	17:68172985	226
69	17:62016078	17:62016303	226	176	17:68172916	17:68173141	226
70	17:62016222	17:62016448	227	177	17:68173056	17:68173281	226
71	17:62016374	17:62016600	227	178	17:68173198	17:68173423	226
72	17:62016516	17:62016741	226	179	17:68173348	17:68173572	225
73	17:62016658	17:62016885	228	180	17:62021886	17:62022120	235
74	17:62016806	17:62017031	226	181	17:62022066	17:62022299	234
75	17:62016954	17:62017178	225	182	17:62022246	17:62022480	235
76	17:62017092	17:62017318	227	183	17:62022430	17:62022654	225
77	17:62017242	17:62017468	227	184	17:62022602	17:62022848	247
78	17:62017390	17:62017614	225	185	17:62022798	17:62023058	261
79	17:62017550	17:62017775	226	186	17:62043311	17:62043548	238
80	17:62017698	17:62017923	226	187	17:62043491	17:62043718	228
81	17:62017872	17:62018096	225	188	17:62043661	17:62043893	233
82	17:62018046	17:62018277	232	189	17:62043843	17:62044069	227
83	17:62018232	17:62018456	225	190	17:62048932	17:62049156	225
84	17:62018404	17:62018628	225	191	17:62049086	17:62049313	228
85	17:62018578	17:62018802	225	192	17:62049264	17:62049490	227
86	17:62018742	17:62018969	228	193	17:62049440	17:62049665	226
87	17:62018918	17:62019142	225	194	17:62049616	17:62049843	228
88	17:62019092	17:62019321	230	195	17:62049790	17:62050022	233
89	17:62019268	17:62019523	256	196	17:62049970	17:62050201	232

90	17:62020035	17:62020264	230	197	17:62050154	17:62050410	257
91	17:62020213	17:62020453	241	198	17:68173516	17:68173742	227
92	17:62020403	17:62020640	238	199	17:68173684	17:68173909	226
93	17:62021053	17:62021301	249	200	17:68173834	17:68174065	232
94	17:62024352	17:62024624	273	201	17:68174010	17:68174247	238
95	17:62025102	17:62025332	231	202	17:68174186	17:68174460	275
96	17:62025282	17:62025541	260	203	17:68174404	17:68174652	249
97	17:62025820	17:62026072	253	204	17:68174598	17:68174830	233
98	17:62026024	17:62026267	244	205	17:68174758	17:68174983	226
99	17:62026601	17:62026826	226	206	17:68174904	17:68175137	234
100	17:62026781	17:62027041	261	207	17:68175076	17:68175315	240
101	17:62028636	17:62028861	226	208	17:68175262	17:68175487	226
102	17:62028808	17:62029033	226	209	17:68175428	17:68175652	225
103	17:62028972	17:62029214	243	210	17:68175596	17:68175858	263
104	17:62029166	17:62029436	271	211	17:68175794	17:68176027	234
105	17:62034366	17:62034590	225	212	17:68175970	17:68176244	275
106	17:62034542	17:62034774	233	213	17:68176188	17:68176422	235
107	17:62034726	17:62034978	253	214	17:62045397	17:62045622	226
				215	17:62045573	17:62045832	260

Muscle channel panel designed amplicon coordinates

Exon	Average coverage	Exon	Average coverage
cacn4b ex1	0	cacna1a ex33+ ex34	1
cacn4b ex2	0.97872	cacna1a ex35	1
cacn4b ex3	1	cacna1a ex36	not designed
cacn4b ex4	1	cacna1a ex37	not designed
cacn4b ex5	0.97727	cacna1a ex38	not designed
cacn4b ex6	1	cacna1a ex39	1
cacn4b ex7+ ex8	1	cacna1a ex40+ ex41	0.935223372
cacn4b ex9	1	cacna1a ex42+ ex43+ ex44	0.480606968
cacn4b ex10	1	cacna1a ex45	0.829787234
cacn4b ex11	1	cacna1a ex46	0.795466649
cacn4b ex12	1	cacna1a ex47	0.295303074
cacn4b ex13	1	cacna1a ex48	0.006344193
cacn4b ex14	1	kcnk1 ex2	0.913803511
cacna1a ex1	0.4846	kcnk18 ex1	1
cacna1a ex2	1	kcnk18 ex2	1
cacna1a ex3	1	kcnk18 ex3	1
cacna1a ex4	1	pnkd ex1	0.281743245
cacna1a ex5	0.41711	pnkd ex2	1
cacna1a ex6	1	pnkd ex3+ ex4	0.569046862
cacna1a ex7	1	pnkd ex5	0.991420723
cacna1a ex8	1	pnkd ex6	1
cacna1a ex9	1	pnkd ex7	0.996789628
cacna1a ex10	1	pnkd ex8	0.957446809
cacna1a ex11	1	pnkd ex9+ ex10	0.884198638
cacna1a ex12	1	prrt2 ex2	0.682483798
cacna1a ex13+ ex14	0.98764	prrt2 ex3+ ex4	0.697307649
cacna1a ex15	1	slc1a3 ex2	1
cacna1a ex16+ ex17	0.83118	slc1a3 ex3	0.518495436
cacna1a ex18	0.97136	slc1a3 ex4	0.935973191
cacna1a ex19	0.50572	slc1a3 ex5	1
cacna1a ex20	0.48065	slc1a3 ex6	1
cacna1a ex21	1	slc1a3 ex7	1
cacna1a ex22	1	slc1a3 ex8	0.833157894
cacna1a ex23	1	slc1a3 ex9	0.983272191
cacna1a ex24	1	slc1a3 ex10	1
cacna1a ex25	1	slc2a1 ex1	0.106382979
cacna1a ex26	1	slc2a1 ex2	1
cacna1a ex27	0.90236	slc2a1 ex3+ ex4	0.936388468
cacna1a ex28	1	slc2a1 ex5+ ex6	0.902913926
cacna1a ex29	0.97997	slc2a1 ex7+ ex8	0.920390745
cacna1a ex30	1	slc2a1 ex9	1
cacna1a ex31	1	slc2a1 ex10	0.993876489
cacna1a ex32	1		

Average coverage of muscle channel panel exons

Appendix 3 – Negative Patients included on the Brain and Muscle Channel Panels

Patient	Phenotype	Patient	Phenotype
4.34	EA	4.65	FHM.
4.35	EA	4.66	FHM
4.36	EA	4.67	FHM
4.37	EA2	4.68	Epilepsy/ PKD
4.38	EA2	4.69	EA2
4.39	EA2	4.7	FHM
4.4	EA2	4.71	Alternating hemiplegia
4.41	EA1	4.72	PRRT2
4.42	EA1	4.73	EA2
4.43	EA1	4.74	EA
4.44	EA1	4.75	Late onset EA2
4.45	EA2	4.76	EA2
4.46	FHM	4.77	EA
4.47	HM	4.78	EA2/ odd phenotype
4.48	EA2	4.79	EA1/EA2
4.49	FHM	4.8	Late onset EA2
4.5	EA2	4.81	EA2/ exercise triggered
4.51	EA1	4.82	PRRT2
4.52	Late onset EA2	4.83	EA1/EA2
4.53	EA2	4.84	EA2
4.54	FHM	4.85	PKD
4.55	EA2	4.86	PKD
4.56	EA	4.87	PKD
4.57	EA1	4.88	HM, progressive ataxia
4.58	HM	4.89	PKD
4.59	EA2	4.9	PKD
4.6	EA2	4.91	PKD
4.61	SCA6	4.92	PKD
4.62	EA2	4.93	PKD
4.63	EA1	4.94	PKD
4.64	EA2	4.95	PKD

Negative patients included in the brain channel panel

Patient	Phenotype	Likelihood	Patient	Phenotype	Likelihood
4.96	Hyper PP	Very Probable	4.122	PMC/MC	Possible
4.97	PMC	Probable	4.123	PP	Possible
4.98	PMC	Very Probable	4.124	Myotonia	Possible
4.99	HypoPP	Very Probable	4.125	PP	Low
4.100	PMC	Very Probable	4.126	PMC	Possible
4.101	PP	Low	4.127	PMC	Possible
4.102	PMC	Very Probable	4.128	PMC	Possible
4.103	MC	Very Probable	4.129	PP	Possible
4.104	PP	Very Probable	4.130	Severe PP	Probable
4.105	PP	Probable	4.131	PP	Low
4.106	ATS	Probable	4.132	PP	Low
4.107	PP	Probable	4.133	PP	Low
4.108	PP	Probable	4.134	PP	Low
4.109	PMC	Probable	4.135	PP	Probable
4.110	PP	Probable	4.136	PP	Low
4.111	FHM/PP	Low	4.137	PP	Low
4.112	ATS	Low	4.138	PP	Low
4.113	PMC	Low	4.139	PP	Low
4.114	PP	Probable	4.140	PP	Low
4.115	PP	Low	4.141	PP	Low
4.116	PP	Possible	4.142	PP	Low
4.117	PP/EA	Possible	4.143	PP	Probable
4.118	SCM	Possible	4.144	PP	Very Probable
4.119	PP/ATS	Possible	4.145	Myotonia	Probable
4.120	PP	Possible	4.146	HypoPP	Very Probable
4.121	MC	Possible			

Negative patients included in the muscle channel panel

Appendix 4 –Variants Identified by the Rhabdomyolysis Panel

Patient	Gene	Protein change (unless c.)	Het/hom	Rs number	EVS	1000g	Discussed in results?
5.1	CPT2	F352C	het	rs2229291	0.007	0.060	
5.1	PGM1	V519I	het	rs6676290	0.050	0.050	
5.2	DMD	S666L	hom	rs34563188	0.006	0.01	
5.2	DMD	T409S	hom	rs34155804	0.013	0.01	
5.2	DYSF	I865V	het	rs34671418	0.043	0.03	
5.2	DYSF	R1053Q	het	rs34211915	0.024	0.01	
5.2	GAA	P451R	het	rs7215458	0.002	0.002	
5.2	IGF2	R159H	het	rs61732764	0.011	0.01	
5.2	PYGM	N596S	het	rs150622626	0.001	0.000	
5.3	ACADVL	E534K	het	rs2230180	0.010	0.003	
5.3	ACE	Y244C	het	rs3730025	0.011	0.010	
5.3	DYSF	S290N	het				
5.3	HADHA	Q358K	het	rs2229420	0.023	0.020	
5.3	PGM1	C52Y	het	rs140738630	0.000	0.004	
5.3	PGM1	V519I	het	rs6676290	0.050	0.050	
5.3	RYR1	D4500H	het	rs150396398	0.003	0.003	Yes
5.4	PHKB	Y770C	het	rs16945474	0.080	0.060	
5.4	IGF2	R159H	het	rs61732764	0.011	0.01	
5.4	IL6	V168M	het	rs2069842	0.025	0.02	
5.5	RYR1	P1787L	het	rs34934920	0.017	0.010	
5.5	RYR1	G2060C	het	rs35364374	0.051	0.030	
5.6	PGM1	V519I	het	rs6676290	0.050	0.050	
5.7	ACE	A183T	het	rs12720754	0.002	0.002	
5.7	CPT2	Q304H	het	rs141553491	0.001	0.001	Yes
5.7	CPT2	V507I	het	rs142600166	0.001	0.001	Yes
5.7	LPIN1	P610S	het	rs4669781	0.039	0.020	
5.8	ACADVL	R615Q	het	rs148584617	0.003	0.001	
5.9	LPIN1	I541V	het	rs148499322	0.002	0.001	
5.10	ACADVL	G43D	het	rs2230178	0.011	0.070	
5.10	SGCA	R374C	het	rs35495899	0.006	0.01	
5.11	ACE	G354R	het	rs142350301	0.006	0.010	
5.11	ETFB	c.13_14insCTG TGG	het	rs61361626		0.060	
5.11	HADHA	Q358K	het	rs2229420	0.023	0.020	
5.11	MYLK	K903R	het				
5.11	PGAM2	A104T	het	rs150570281	0.001	0.001	
5.11	PHKB	Y770C	het	rs16945474	0.080	0.060	
5.12	CACNA1S	A69G	het	rs12406479	0.039	0.020	
5.12	DYSF	R499C	het	rs185119682		0.0005	
5.12	FKRP	R143S	het	rs148206382	0.004	0.0046	
5.12	GAA	D91N	het	rs1800299	0.023	0.020	
5.12	MYLK	G439R	het	rs190877071		0.001	
5.12	RYR1	V4542M	het				Yes
5.12	RYR1	E3578Q	het	rs55876273	0.013	0.010	Yes

5.12	SCN4A	V662I	het				Yes
5.13	ACADVL	L17F	het	rs2230179	0.022	0.020	
5.13	ACE	S32P	het	rs4317	0.052	0.050	
5.13	ACE	S49G	het	rs4318	0.054	0.050	
5.13	ACTN3	R902C	het	rs71457732	0.007	0.010	
5.13	ANO5	R58W	het	rs201725369	0.000	0.001	
5.13	LPIN1	P610S	het	rs4669781	0.039	0.020	
5.13	PGAM2	I114S	het	rs61756062	0.021	0.030	
5.13	RYR1	A941V	het				Yes
5.14	DMD	N797K	hom	rs72468681	0.006	0.01	
5.15	nothing						
5.16	ACADVL	R469Q	hom				Yes
5.16	CPT2	M342T	het	rs144658100	0.001		
5.17	ETFA	T171I	het	rs1801591	0.062	0.050	
5.17	GAA	E689K	hom	rs1800309	0.030	0.090	
5.17	GAA	T739S	het				
5.17	MYLK	R845C	het	rs3732485	0.006	0.030	
5.17	MYLK	R544W	het				
5.17	PHKB	N273D	het				
5.17	PHKB	Y770C	het	rs16945474	0.080	0.060	
5.18	PYGM	G205S	het	rs119103251	0.000	0.001	
5.18	RYR1	G2434R	het	rs121918593			Yes
5.19	FKRP	A114G	het	rs143793528	0.008	0.01	
5.19	LPIN1	P610S	het	rs4669781	0.039	0.020	
5.19	MYLK	V836L	het				
5.19	ANO5	c.191_192insA	het				Yes
5.19	ANO5	G231V	het	rs137854523	0.001	0.001	Yes
5.19	PHKB	Y770C	het	rs16945474	0.080	0.060	
5.20	CACNA1S	c.4242-1G>T	het				Yes
5.20	PHKB	Q657K	het	rs34667348	0.004	0.002	
5.21	ACADVL	E534K	het	rs2230180	0.010	0.003	
5.21	ACE	R442H	het	rs35865660	0.006	0.001	
5.21	ACE	T1187M	het	rs12709442	0.003		
5.21	ACE	R1286S	het	rs4364	0.029	0.030	
5.21	ACE	R1290Q	het	rs12720745	0.006	0.001	
5.21	DYSF	R1127H	het	rs59915619	0.007	0.01	
5.21	HADHA	Q358K	het	rs2229420	0.023	0.020	
5.21	HADHB	K255R	het	rs57969630	0.007	0.010	
5.21	PGM1	V519I	het	rs6676290	0.050	0.050	
5.21	PHKB	Y770C	het	rs16945474	0.080	0.060	
5.21	SIL1	K132Q	het	rs61745568	0.026	0.020	
5.22	ACE	R487H	het	rs37643090 7	0.000		
5.22	CKM	T166M	het	rs17357122	0.006	0.004	
5.22	PFKM	Q518K	het	rs145040928	0.002	0.002	
5.23	GAA	D91N	het	rs1800299	0.023	0.020	
5.23	LPIN1	P610S	het	rs4669781	0.039	0.020	
5.23	MYLK	R845C	het	rs3732485	0.006	0.030	
5.23	RYR1	P1787L	het	rs34934920	0.017	0.010	
5.23	RYR1	G2060C	het	rs35364374	0.051	0.030	
5.23	SIL1	L7V	het	rs11555154	0.060	0.050	
5.24	DYSF	G128E	het	rs34997054	0.003	0.0018	

5.24	RYR1	R2224C	het	rs199870223	.	.	Yes
5.25	ACE	R1286S	hom	rs4364	0.029	0.030	
5.25	CAV3	V14I	het	rs121909281	0.001	0.001	Yes
5.25	MYLK	T1085A	het	rs75370906	0.065	0.050	
5.25	PGM1	V519I	het	rs6676290	0.050	0.050	
5.26	DYSF	V736M	het	rs182450244		0.0005	
5.26	DYSF	M999L	het	rs144636654	0.002	0.0014	
5.26	ETFB	P52L	het	rs79338777	0.061	0.070	
5.26	GYG1	c.487delG	hom				Yes
5.26	LPIN1	P610S	het	rs4669781	0.039	0.020	
5.26	SIL1	L7V	het	rs11555154	0.060	0.050	
5.27	CACNA1S	G258D	het	rs35534614	0.008	0.010	
5.27	DYSF	A201E	het	rs34999029	0.010	0.01	
5.27	ETFA	T171I	het	rs1801591	0.062	0.050	
5.27	GYS1	M416V	het	rs5447	0.007	0.030	
5.27	LDHA	A147S	het	rs116841148	0.002	0.001	
5.28	RYR1	E3578Q	het	rs55876273	0.013	0.010	Yes
5.29	ISCU	A4P	het				
5.30	ANO5	c.191_192insA	hom				Yes
5.30	CKM	E83G	het	rs11559024	0.010	0.010	
5.30	ETFB	P52L	het	rs79338777	0.061	0.070	
5.30	RYR1	D4500H	het	rs150396398	0.003	0.003	Yes
5.31	CAV3	T78M	het	rs72546668	0.004	0.002	Yes
5.31	MYLK	T1085A	het	rs75370906	0.065	0.050	
5.31	MYLK	R506G	het	rs77323602	0.005	0.010	
5.31	MYLK	K173E	het				
5.31	PYGM	R410H	het				
5.32	GAA	V816I	hom	rs1800314	0.054	0.080	
5.32	GAA	T927I	het	rs1800315	0.047	0.040	
5.32	SIL1	L7V	het	rs11555154	0.060	0.050	
5.33	ENO3	V128F	het	.	.	.	
5.33	PHKA2	E38Q	hom,	rs17313469	0.024	0.020	
5.34	ETFB	P52L	hom	rs79338777	0.061	0.070	
5.35	DYSF	E1471K	het				
5.35	DYSF	I2047V	het	rs150834671	0.000	0.0014	Yes
5.35	ETFA	T171I	het	rs1801591	0.062	0.050	Yes
5.35	MYLK	R845C	het	rs3732485	0.006	0.030	
5.35	SGCA	T27M	het				
5.37	CACNA1S	A69G	het	rs12406479	0.039	0.020	
5.37	RYR1	G2060C	het	rs35364374	0.051	0.030	
5.37	RYR1	R3534H	het	rs143987857	0.002	0.001	Yes
5.38	ACE	Y244C	het	rs3730025	0.011	0.010	
5.38	MYLK	P443S	het	rs35156360	0.015	0.010	
5.38	PHKB	Q657K	het	rs34667348	0.004	0.002	
5.38	PYGM	R816H	het	rs139230055	0.000		
5.39	ACADVL	P65L	het	rs28934585	0.034	0.030	
5.39	FKRP	A114G	het	rs143793528	0.008	0.01	
5.39	GAA	V816I	het	rs1800314	0.054	0.080	
5.39	GAA	T927I	het	rs1800315	0.047	0.040	
5.39	HADHA	Q358K	het	rs2229420	0.023	0.020	
5.40	ACADVL	L17F	het	rs2230179	0.022	0.020	

5.40	ACE	A261S	het	rs4303	0.032	0.030	
5.40	ANO5	L785R	het	rs146136277	0.004	0.003	
5.40	DYSF	L180V	het	rs13407355	0.023	0.02	Yes
5.40	DYSF	Q1784K	het				Yes
5.40	ETFB	c.13_14insCTG TGG	het	rs61361626			
5.40	MYLK	A701T	het	rs142835596	0.007	0.003	
5.40	PHKG2	G86S	het	rs143983247	0.004	0.002	
5.41	ACE	R482C	het		0.000	0.001	
5.41	MYLK	P443S	het	rs35156360	0.015	0.010	
5.42	PYGM	G205S	het	rs119103251	0.000	0.001	
5.44	ACE	Y244C	het	rs3730025	0.011	0.010	
5.44	CPT2	V2A	het				
5.44	PFKM	Q518K	het	rs145040928	0.002	0.002	
5.44	PHKG1	W20R	het	rs148807750	0.001	0.001	
5.46	ANO5	S796L	het	rs61910685	0.009	0.003	
5.46	DMD	T1245I	het	rs1800269	0.008	0.01	
5.46	ETFB	T31M	het		0.000		
5.46	RYR1	G2060C	het	rs35364374	0.051	0.030	
5.47	ACE	G590S	het				
5.47	ETFB	P52L	het	rs79338777	0.061	0.070	
5.48	ANO5	S796L	het	rs61910685	0.009	0.003	
5.48	IL6	D162V	het	rs2069860	0.006	0.0018	
5.48	LPIN1	R801*	het	rs119480073			
5.49	ACE	D1249N	het				
5.49	DYSF	R1362L	het	rs61742872	0.025	0.02	
5.49	GAA	L264F	het				
5.49	GAA	G44V	het				
5.49	MYLK	K1114E	het				
5.49	PFKM	R767H	het	rs41291971	0.012	0.010	
5.50	ACE	A261S	het	rs4303	0.032	0.030	
5.50	ACE	R324W	het	rs35141294	0.009	0.010	
5.50	ACE	D592G	het	rs12709426	0.017	0.020	
5.50	ACE	S32P	het	rs4317	0.052	0.050	
5.50	ACE	S49G	het	rs4318	0.054	0.050	
5.50	ACTN3	V529M	het				
5.50	ANO5	L785R	het	rs146136277	0.004	0.003	
5.50	CACNA1S	R683C	het	rs35708442	0.010	0.010	
5.50	DMD	A573V	hom	rs5972599	0.005	0.01	
5.50	ETFB	c.13_14insCTG TGG	het	rs61361626			
5.50	GAA	W804R	het				
5.50	IGF2	R159H	het	rs61732764	0.011	0.01	
5.50	IL6	P32S	het	rs2069830	0.026	0.02	
5.50	IL6	V168M	het	rs2069842	0.025	0.02	
5.50	PGM1	V519I	het	rs6676290	0.050	0.050	
5.50	PYGM	T395M	het	rs71581787	0.018	0.020	
5.51	DYSF	E488K	het	rs61740288	0.018	0.01	
5.52	DMD	H2921R	het	rs1800279	0.021	0.01	
5.52	ETFB	P52L	hom	rs79338777	0.061	0.070	
5.53	ACADVL	L17F	het	rs2230179	0.022	0.020	

5.53	ACE	R1286S	het	rs4364	0.029	0.030	
5.53	DMD	T409S	hom	rs34155804	0.013	0.01	
5.53	DYSF	I1356V	het	rs145401010	0.005	0.0023	
5.53	IGF2	R159H	het	rs61732764	0.011	0.01	
5.53	MYLK	T1085A	het	rs75370906	0.065	0.050	
5.53	PHKB	E820V	het	rs9934849	0.005	0.003	
5.54	LPIN1	P610S	het	rs4669781	0.039	0.020	
5.55	DYSF	E488K	het	rs61740288	0.018	0.01	
5.55	PHKB	Y770C	het	rs16945474	0.080	0.060	
5.56	CACNA1S	K88E	het	rs140330831	0.000		Yes
5.56	CKM	T166M	het	rs17357122	0.006	0.004	
5.56	PFKM	R767H	hom	rs41291971	0.012	0.010	Yes
5.56	PHKA1	N490D	hom				Yes
5.57	DMD	N1672K	het	rs16990264	0.025	0.02	
5.57	DMD	F1388V	het	rs28715870	0.033	0.02	
5.57	DMD	D518E	het	rs61733587	0.013	0.01	
5.57	DYSF	L220V	het	rs13407355	0.023	0.02	
5.57	IL6	P32S	het	rs2069830	0.026	0.02	
5.57	LPIN1	A34T	het				
5.57	PHKB	Y770C	het	rs16945474	0.080	0.060	
5.57	SCN4A	R31L	het	rs112142736	0.005	0.0037	Yes
5.57	SCN4A	E81Q	het	rs111926172	0.005	0.0037	Yes
5.58	ETFB	P52L	het	rs79338777	0.061	0.070	
5.58	SIL1	L7V	het	rs11555154	0.060	0.050	
5.59	ACE	I798V	het	rs117647476	0.003	0.001	
5.59	CACNA1S	A69G	het	rs12406479	0.039	0.020	
5.59	DMD	R2155W	het	rs1800273	0.027	0.01	
5.59	ETFB	P52L	het	rs79338777	0.061	0.070	
5.59	RYR1	G2060C	het	rs35364374	0.051	0.030	
5.59	SIL1	L7V	het	rs11555154	0.060	0.050	
5.60	ACE	Y244C	het	rs3730025	0.011	0.010	
5.60	ANO5	E185Q	het	rs140381407	0.000		
5.60	ETFA	T171I	het	rs1801591	0.062	0.050	
5.60	FKRP	R143S	het	rs148206382	0.004	0.0046	
5.61	ACADVL	L17F	het	rs2230179	0.022	0.020	
5.61	ACE	S32P	het	rs4317	0.052	0.050	
5.61	ACE	S49G	het	rs4318	0.054	0.050	
5.61	ACE	P1102T	het	rs145349565	0.004	0.002	
5.61	DMD	T715S	hom	rs16998350	0.005	0.0036	
5.61	DYSF	I865V	het	rs34671418	0.043	0.03	
5.61	DYSF	R1126C	het	rs141536854	0.006	0.0037	
5.61	SCN4A	R31L	het	rs112142736	0.005	0.0037	Yes
5.61	SCN4A	E81Q	het	rs111926172	0.005	0.0037	Yes
5.62	ACE	R1286S	het	rs4364	0.029	0.030	
5.62	ANO5	E202K	het	rs115750596	0.012	0.010	
5.62	ANO5	N882K	het	rs34969327	0.013	0.010	
5.62	DMD	F1388V	het	rs28715870	0.033	0.02	
5.62	DMD	D518E	het	rs61733587	0.013	0.01	
5.62	DYSF	R1362L	het	rs61742872	0.025	0.02	

5.62	ETFB	c.13_14insCTG TGG	het	rs61361626			
5.62	GAA	T927I	het	rs1800315	0.047	0.040	
5.62	IL6	V168M	het	rs2069842	0.025	0.02	
5.62	MYLK	T1085A	het	rs75370906	0.065	0.050	
5.62	PFKM	G847R	het				
5.62	PHKB	Y770C	het	rs16945474	0.080	0.060	
5.62	SIL1	D63E	het	rs115591710	0.004	0.004	
5.63	ACADVL	P65L	het	rs28934585	0.034	0.030	
5.63	ANO5	V87I	het	rs34994927	0.003	0.003	Yes
5.63	ANO5	G227A	het	rs140903276	0.003	0.002	Yes
5.63	CPT2	A101V	het	rs75939866	0.005	0.003	
5.63	CPT2	F352C	het	rs2229291	0.007	0.060	Yes
5.63	DMD	R1324C	het	rs143184877	0.003	0.0012	Yes
5.63	DYSF	L220V	het	rs13407355	0.023	0.02	
5.63	FKRP	V79M	het	rs104894683	0.004	0.0041	
5.63	GAA	T927I	het	rs1800315	0.047	0.040	
5.63	GAA	V816I	het	rs1800314	0.054	0.080	
5.63	GYG1	G157D	het	rs75445811	0.002	0.002	
5.63	HADHA	N615D	het	rs61731155	0.004	0.003	
5.63	HADHA	Q358K	het	rs2229420	0.023	0.020	
5.63	IL6	V168M	het	rs2069842	0.025	0.02	
5.63	PHKB	Y770C	het	rs16945474	0.080	0.060	
5.63	PYGM	R414G	het	rs11231866	0.061	0.040	
5.63	RYR1	S1342G	hom	rs34694816	0.037	0.050	
5.64	CACNA1S	G258D	het	rs35534614	0.008	0.010	
5.64	DYSF	E488K	het	rs61740288	0.018	0.01	
5.64	IGF2	M53V	het				
5.64	RYR1	G2060C	het	rs35364374	0.051	0.030	
5.64	RYR1	R3534H	het	rs143987857	0.002	0.001	Yes
5.64	SCN4A	H599R	het	rs187401185	0.003	0.0009	Yes
5.65	CACNA1S	A69G	het	rs12406479	0.039	0.020	
5.65	GYS1	A125S	het				
5.65	PFKM	R767H	het	rs41291971	0.012	0.010	
5.65	RYR1	T3425M	het	rs150977342	0.000		Yes
5.66	ETFA	T171I	het	rs1801591	0.062	0.050	
5.67	CACNA1S	A69G	het	rs12406479	0.039	0.020	
5.67	GAA	V816I	het	rs1800314	0.054	0.080	
5.68	CAV3	T78M	het	rs72546668	0.004	0.002	Yes
5.68	ETFA	T171I	het	rs1801591	0.062	0.050	
5.68	MYLK	V892M	het				
5.68	PGAM2	R62W	het				
5.69	GAA	E689K	het	rs1800309	0.030	0.090	
5.69	PHKB	Q657K	het	rs34667348	0.004	0.002	
5.69	RYR1	G2060C	het	rs35364374	0.051	0.030	
5.70	ACE	c.55_56insCGC TGCL	het				
5.70	CCR2	M249K	het	rs200491743	0.001		
5.70	ENO3	C357Y	hom				5.70
5.70	FKRP	P75Q	het				
5.70	MYLK	R845C	het	rs3732485	0.006	0.030	
5.71	ACE	G128A	het				

5.72	ANO5	N18S	het				
5.72	DYSF	R1362L	het	rs61742872	0.025	0.02	
5.72	GAA	D91N	het	rs1800299	0.023	0.020	
5.73	ETFA	T171I	het	rs1801591	0.062	0.050	
5.74	ACADVL	P219L	het				
5.74	ACE	R953Q	het	rs143507892	0.000		
5.74	GAA	T927I	het	rs1800315	0.029	0.040	
5.74	PGAM2	L182P	het				
5.74	PGAM2	I114S	het	rs61756062	0.021	0.030	
5.75	ACE	A261S	het	rs4303	0.032	0.030	
5.75	ACE	D592G	het	rs12709426	0.017	0.020	
5.75	ACE	S49G	het	rs4318	0.054	0.050	
5.75	MYLK	T1085A	het	rs75370906	0.065	0.050	
5.75	PFKM	Q518K	het	rs145040928	0.002	0.002	
5.75	SCN4A	V1644M	het				Yes
5.76	ENO3	Q298K	het				
5.76	LPIN1	V494M	het	rs33997857	0.016	0.010	
5.76	PHKB	Y770C	het	rs16945474	0.080	0.060	
5.77	GYS1	Y551H	het				
5.77	LPIN1	P610S	het	rs4669781	0.039	0.020	
5.77	RYR1	c.12610-2A>C	het				
5.78	CACNA1S	R462H	het	rs146696298	0.000		Yes
5.78	CACNA1S	A69G	het	rs12406479	0.039	0.020	
5.78	DYSF	R1053Q	het	rs34211915	0.024	0.01	
5.79	PYGM	A193S	het	rs77656150	0.003	0.002	
5.79	RYR1	G2060C	het	rs35364374	0.051	0.030	
5.80	ACE	Y244C	het	rs3730025	0.011	0.010	
5.80	DMD	H2921R	hom	rs1800279	0.021	0.01	
5.81	ANO5	A98P	het				
5.81	CACNA1S	A69G	het	rs12406479	0.039	0.020	
5.81	CPT2	A470T	het				
5.81	DMD	R2155W	het	rs1800273	0.027	0.01	
5.81	FKRP	R143S	het	rs148206382	0.004	0.0046	
5.81	RYR1	G2060C	het	rs35364374	0.051	0.030	
5.81	RYR1	P1787L	het	rs34934920	0.017	0.010	
5.82	ACADVL	A10V	het	rs78514016		0.004	
5.82	DMD	Q1411R	het				
5.82	DMD	N797K	het	rs72468681	0.006	0.01	
5.82	GAA	V816I	het	rs1800314	0.054	0.080	
5.83	DMD	R2155W	het	rs1800273	0.027	0.01	
5.83	ETFA	T171I	het	rs1801591	0.062	0.050	
5.84	nothing						
5.85	DMD	N797K	hom	rs72468681	0.006	0.01	
5.85	ETFB	P52L	het	rs79338777	0.061	0.070	
5.85	GAA	L769F	het		0.000		
5.85	LDHA	D285V	het	rs147520495	0.000		
5.86	CKM	L127V	het	rs17875653	0.002	0.003	
5.86	LPIN1	V494M	het	rs33997857	0.016	0.010	
5.87	DMD	H2921R	het	rs1800279	0.021	0.01	
5.87	DMD	I2152F	het				

5.87	DYSF	R1362L	het	rs61742872	0.025	0.02	
5.87	MYLK	W656C	het	rs138172035	0.002	0.001	
5.87	SIL1	L7V	het	rs11555154	0.060	0.050	
5.88	CACNA1S	A69G	het	rs12406479	0.039	0.020	
5.88	DYSF	R1331L	het	rs61742872	0.025	0.02	Yes
5.88	DYSF	Y1494H	het	rs150139276	0.000		Yes
5.88	ETFA	T171I	het	rs1801591	0.062	0.050	
5.89	ACE	A261S	het	rs4303	0.032	0.030	
5.89	ACE	D592G	het	rs12709426	0.017	0.020	
5.89	ACE	S32P	het	rs4317	0.052	0.050	
5.89	ACE	S49G	het	rs4318	0.054	0.050	
5.89	ACTN3	G835V	het		0.000		
5.89	DYSF	R1331L	het	rs61742872	0.025	0.02	Yes
5.89	DYSF	Y1494H	het	rs150139276	0.000		Yes
5.89	GAA	A704T	het				
5.89	HADHA	Q358K	het	rs2229420	0.023	0.020	
5.89	HADHB	K255R	het	rs57969630	0.007	0.010	
5.89	LPIN1	T145M	het	rs201744351	0.000		
5.89	PGAM2	W78*	het	rs10250779	0.003	0.002	
5.89	RYR1	D4873N	het				Yes
5.90	ACE	c.55_56insCGC TGC	het				
5.90	ACE	E78*	het				
5.90	ACE	A261S	het	rs4303	0.032	0.030	
5.90	ACTN3	A294S	het	rs193169026	0.003	0.002	
5.90	ETFB	c.13_14insCTG TGG	het	rs61361626			
5.90	MYLK	T1085A	het	rs75370906	0.065	0.050	
5.90	RYR1	E818A	het				Yes
5.90	RYR1	A1708S	het				Yes
5.91	ACTN3	R244C	het				
5.91	ENO3	A76P	het	rs143945974	0.000	0.010	
5.91	ETFA	T171I	het	rs1801591	0.062	0.050	
5.91	ETFB	P52L	het	rs79338777	0.061	0.070	
5.91	FKRP	V79M	het	rs104894683	0.004	0.0041	
5.91	GAA	A704T	het				
5.91	LPIN1	P610S	het	rs4669781	0.039	0.020	
5.91	PGAM2	I114S	het	rs61756062	0.021	0.030	
5.91	PHKG1	R355C	het	rs149458708	0.001	0.001	
5.91	PYGM	D629Y	het	rs137986928	0.000	0.000	
5.91	RYR1	S1342G	het	rs34694816	0.037	0.050	
5.92	ACE	H417R	het				
5.92	LPIN1	V494M	het	rs33997857	0.016	0.010	
5.92	PHKB	V999L	het				
5.92	RYR1	A1372V	het		0.000		Yes
5.93	CACNA1S	G258D	het	rs35534614	0.008	0.010	
5.93	IL6	D162V	het	rs13306435	0.007	0.03	
5.93	RYR1	G4339E	het				Yes
5.93	SIL1	L7V	het	rs11555154	0.060	0.050	
5.94	ACTN3	E170A	het				
5.94	ACTN3	A460S	het	rs201812719	0.000		
5.95	nothing						

5.96	ACE	Y244C	het	rs3730025	0.011	0.010	
5.96	ETFA	T171I	het	rs1801591	0.062	0.050	
5.96	GYG1	D102H	het	rs143137713	0.001	0.001	
5.96	MYLK	P336L	het	rs35912339	0.001	0.001	
5.96	PHKA1	R821H	hom	rs139803629	0.003	0.003	Yes
5.96	PHKB	Y167C	het	rs151155518	0.004	0.002	
5.97	DYSF	E488K	het	rs61740288	0.018	0.01	
5.97	GAA	I257T	het				
5.98	ETFB	P52L	het	rs79338777	0.061	0.070	
5.98	RYR1	G2060C	het	rs35364374	0.051	0.030	
5.98	SIL1	T123I	het	rs115800498	0.006	0.002	
5.99	ACADVL	P65L	het	rs28934585	0.034	0.030	
5.99	ACE	P1102T	het	rs145349565	0.004	0.002	
5.99	CAV3	T78M	het	rs72546668	0.004	0.002	Yes
5.99	CCR2	G355E	het	rs3918387	0.005	0.002	
5.99	ETFB	R265H	het	rs141917423	0.001	0.003	
5.99	ETFB	c.13_14insCTG TGG	het	rs61361626			
5.99	ISCU	S29A	het				
5.99	LPIN1	c.1110_1114TC	het				
5.99	PGM1	V519I	het	rs6676290	0.050	0.050	
5.99	RYR1	S1342G	het	rs34694816	0.037	0.050	
5.99	RYR1	D2943N	het	rs79294840	0.004	0.002	Yes
5.99	RYR1	H3642Q	het	rs114351116	0.004	0.002	Yes
5.100	ACE	R1286S	hom	rs4364	0.029	0.030	
5.100	DYSF	L220V	het	rs13407355	0.023	0.02	
5.100	FKRP	V79M	het	rs104894683	0.004	0.0041	
5.100	GYS1	M416V	het	rs5447	0.007	0.030	
5.100	IGF2	E150K	het	rs150866176	0.000	0.0005	
5.100	PGAM2	E128K	het		0.000		
5.100	RYR1	D849N	het	rs200893443	0.000	0.001	Yes
5.100	RYR1	S1342G	het	rs34694816	0.037	0.050	
5.100	RYR1	P1632S	het	rs76537615	0.006	0.010	Yes
5.100	SIL1	K132Q	het	rs61745568	0.026	0.020	
5.101	ACE	K155E	het				
5.101	ACE	M312V	het		0.000		
5.101	ENO3	c.788_789insAT C	het				
5.101	ETFB	P52L	het	rs79338777	0.061	0.070	
5.101	GAA	V222M	het		0.000		
5.101	GAA	V816I	het	rs1800314	0.054	0.080	
5.101	RYR1	E3578Q	het	rs55876273	0.013	0.010	Yes
5.101	RYR1	Q3751E	het	rs4802584	0.012	0.030	
5.102	ACE	R1286S	het	rs4364	0.029	0.030	
5.102	CAV3	V14I	het	rs121909281	0.001	0.001	Yes
5.102	GAA	T927I	het	rs1800315	0.047	0.040	
5.102	GAA	V816I	het	rs1800314	0.029	0.080	
5.102	LPIN1	c.369_369del	het	rs149564563		0.010	
5.102	MYLK	T1085A	het	rs75370906	0.065	0.050	
5.102	PGM1	V519I	het	rs6676290	0.050	0.050	
5.102	PHKB	Y770C	het	rs16945474	0.080	0.060	
5.103	DYSF	I865V	het	rs34671418	0.043	0.03	

5.103	DYSF	R1053Q	het	rs34211915	0.024	0.01	
5.103	GAA	E689K	het	rs1800309	0.030	0.090	
5.103	MYLK	P443S	het	rs35156360	0.015	0.010	
5.103	SIL1	T123I	het	rs115800498	0.006	0.002	
5.104	CCR2	T94I	het				
5.104	MYLK	R845C	het	rs3732485	0.006	0.030	
5.104	RYR1	c.5671_5673del	het				Yes
5.104	RYR1	Q3751E	het	rs4802584	0.012	0.030	
5.105	ETFB	P52L	het	rs79338777	0.061	0.070	
5.105	MYLK	P443S	het	rs35156360	0.015	0.010	
5.105	RYR1	I637F	het				Yes
5.106	ETFA	T171I	het	rs1801591	0.062	0.050	
5.106	SGCB	L277M	het				
5.107	CPT2	R219W	het		0.000		
5.107	GAA	E689K	het	rs1800309	0.030	0.090	
5.107	MYLK	R845C	het	rs3732485	0.006	0.030	
5.107	PFKM	Q518K	het	rs145040928	0.002	0.002	
5.107	RYR1	Q3751E	het	rs4802584	0.012	0.030	
5.108	ACE	R508Q	het				
5.108	CKM	T166M	het	rs17357122	0.006	0.004	
5.108	DYSF	E140D	het				Yes
5.108	DYSF	E457K	het	rs61740288	0.018	0.01	Yes
5.108	ETFB	P52L	het	rs79338777	0.061	0.070	
5.108	PGAM2	I114S	het	rs61756062	0.021	0.030	
5.108	PHKB	N173S	het	rs139738333	0.002	0.001	
5.109	ACE	S32P	het	rs4317	0.052	0.050	
5.109	ACE	S49G	het	rs4318	0.054	0.050	
5.109	ACE	R1290Q	het	rs12720745	0.006	0.001	
5.109	ACTN3	R242*	het		0.000		
5.109	DYSF	V429M	het	rs144202114	0.005	0.0023	
5.109	DYSF	R1022Q	het	rs34211915	0.024	0.01	Yes
5.109	DYSF	T1662M	het	rs143059463	0.000		Yes
5.109	ENO3	V332I	het	rs61735456	0.010	0.010	
5.109	LPIN1	P610S	het	rs4669781	0.039	0.020	
5.109	RYR1	S1342G	het	rs34694816	0.037	0.050	
5.109	RYR1	H3976Y	het	rs148772854	0.004	0.010	Yes
5.109	SCN4A	N1503S	het	rs114900922	0.000	0.0009	Yes
5.109	SIL1	L7V	het	rs11555154	0.060	0.050	
5.110	ACE	Y244C	het	rs3730025	0.011	0.010	
5.110	CACNA1S	T1354S	het	rs145910245	0.004	0.001	Yes
5.110	IL6	D162V	het	rs2069860	0.006	0.0018	
5.111	ETFB	c.13_14insCTG TGG	het	rs55874945			
5.111	ETFB	P52L	het	rs79338777	0.061	0.070	
5.111	PHKB	M185I	het	rs56257827	0.011	0.010	
5.111	RYR1	R3545W	het				Yes
5.112	ACE	R953Q	het	rs143507892	0.000		
5.112	PHKB	M185I	het	rs56257827	0.011	0.010	
5.112	SIL1	K132Q	het	rs61745568	0.026	0.020	
5.113	ACADVL	R366H	het	rs112406105		0.001	Yes
5.113	ACADVL	R469Q	het				Yes

5.113	DYSF	E488K	het	rs61740288	0.018	0.01	
5.113	ETFA	T171I	het	rs1801591	0.062	0.050	
5.113	ETFB	P52L	het	rs79338777	0.061	0.070	
5.113	PFKM	R767H	het	rs41291971	0.012	0.010	
5.113	RYR1	G2060C	het	rs35364374	0.051	0.030	
5.113	SIL1	L7V	het	rs11555154	0.060	0.050	
5.114	GAA	T927I	het	rs1800315	0.047	0.040	
5.114	GAA	V816I	het	rs1800314	0.054	0.080	
5.114	PGAM2	D53V	het				
5.114	PYGM	R293W	het				
5.114	RYR1	G2060C	het	rs35364374	0.051	0.030	
5.115	ACE	A261S	het	rs4303	0.032	0.030	
5.115	ACE	R324W	het	rs35141294	0.009	0.010	
5.115	DMD	F1388V	het	rs28715870	0.033	0.02	
5.115	DMD	R943S	het				
5.115	GAA	N290D	het	.	.	.	
5.115	HADHB	A189T	het	rs143683481	0.000	.	
5.115	IGF2	R159H	hom	rs61732764	0.011	0.01	
5.115	PHKB	M185I	het	rs56257827	0.011	0.010	
5.115	RYR1	S1342G	het	rs34694816	0.037	0.050	
5.115	RYR1	A1352G	het	rs112105381	0.004	0.010	Yes
5.115	RYR1	T2787S	het	rs35180584	0.010	0.010	Yes
5.116	DMD	N2912D	hom	rs1800278	0.032	0.04	Yes
5.116	DMD	E2910V	hom	rs41305353	0.030	0.04	Yes
5.116	DYSF	V405L	het	rs150724610	0.008	0.0023	
5.116	ETFA	T171I	het	rs1801591	0.062	0.050	
5.116	PHKA2	I693V	hom	rs143732206	0.008	0.004	
5.116	PHKB	P865A	het	rs142281844	0.001	.	
5.117	ACTN3	T215I	het	.	.	.	
5.117	ETFB	P52L	het	rs79338777	0.061	0.070	
5.117	GAA	E689K	het	rs1800309	0.030	0.090	
5.117	PYGM	R414G	het	rs11231866	0.061	0.040	
5.118	CACNA1S	S606N	het	rs142356235	0.009	0.010	
5.119	GAA	E689K	het	rs1800309	0.030	0.090	
5.119	RYR1	T2206M	het	rs118192177	.	.	Yes
5.119	SCN4A	G902S	het	rs200517944	0.000		Yes
5.120	ISCU	A4P	het	.	.	.	
5.120	PHKA2	V1082M	hom	rs142123423	0.000	.	
5.120	RYR1	G2060C	het	rs35364374	0.051	0.030	
5.121	ETFA	T171I	het	rs1801591	0.062	0.050	
5.121	PHKB	M185I	het	rs56257827	0.011	0.010	
5.121	PYGM	A193S	het	rs77656150	0.003	0.002	
5.122	CACNA1S	V991L	het				Yes
5.122	MYLK	P443S	het	rs35156360	0.015	0.010	
5.123	IL6	D162V	het	rs13306435	0.007	0.03	
5.123	MYLK	P1043A	het	.	.	.	
5.123	PHKB	Y770C	het	rs16945474	0.080	0.060	
5.124	CPT2	S122F	het	rs192275019	.	0.002	
5.124	DMD	A699G	hom	rs202008454		0.0012	
5.124	GAA	E689K	hom	rs1800309	0.030	0.090	
5.124	GAA	T739S	het	.	.	.	

5.124	MYLK	A128T	het	rs147840022	0.000	.	
5.124	PYGM	A193S	het	rs77656150	0.003	0.002	
5.125	ANO5	N882K	het	rs34969327	0.013	0.010	
5.125	DYSF	L189V	het	rs13407355	0.023	0.02	Yes
5.125	DYSF	S1353Y	het				Yes
5.125	FKRP	I274M	het	rs77138370	0.000	0.01	
5.125	GAA	V816I	het	rs1800314	0.054	0.080	
5.125	MYLK	R1450Q	het	rs41366751	0.005	0.010	
5.125	PGM1	V519I	het	rs6676290	0.050	0.050	
5.125	PYGM	R414G	het	rs11231866	0.061	0.040	
5.125	RYR1	S1342G	hom	rs34694816	0.037	0.050	
5.126	ANO5	E185Q	het	rs140381407	0.000		
5.126	ETFB	P52L	het	rs79338777	0.061	0.070	
5.126	MYLK	V1213M	het	rs368390254	0.000	.	
5.127	CACNA1S	T1354S	het	rs145910245	0.004	0.001	Yes
5.127	ETFB	P52L	hom	rs79338777	0.061	0.070	
5.127	GAA	D91N	het	rs1800299	0.023	0.020	
5.127	RYR1	P1787L	het	rs34934920	0.017	0.010	
5.127	RYR1	G2060C	het	rs35364374	0.051	0.030	
5.128	RYR1	G2060C	het	rs35364374	0.051	0.030	
5.128	RYR1	P1787L	het	rs34934920	0.017	0.010	
5.129	ACE	Y244C	het	rs3730025	0.011	0.010	
5.129	DMD	H2921R	het	rs1800279	0.021	0.01	
5.130	PHKB	Q657*	het	rs34667348	.	.	
5.131	PFKM	Q518K	het	rs145040928	0.002	0.002	
5.131	PGM1	E90V	het	rs200881174	0.001	.	
5.131	RYR1	R3366H	het	rs137932199	0.001	0.004	Yes
5.131	RYR1	Y3928C	het	rs147136339	0.001	0.004	Yes
5.131	RYR1	G2060C	?	rs35364374	0.051	0.030	
5.132	ANO5	S796L	het	rs61910685	0.009	0.003	
5.132	ETFA	T171I	het	rs1801591	0.062	0.050	
5.132	GAA	V816I	het	rs1800314	0.054	0.080	
5.133	ANO5	G231V	het	rs137854523	0.001	0.001	
5.133	ETFB	P52L	het	rs79338777	0.061	0.070	
5.133	GAA	E689K	het	rs1800309	0.030	0.090	
5.134	GAA	R819W	het	rs61736895	.	.	
5.134	PYGM	A193S	het	rs77656150	0.003	0.002	
5.134	RYR1	Q3751E	het	rs4802584	0.012	0.030	
5.135	ACE	A261S	het	rs4303	0.032	0.030	
5.135	ACE	R324W	het	rs35141294	0.009	0.010	
5.135	ACE	D592G	het	rs12709426	0.017	0.020	
5.135	CACNA1S	R683C	het	rs35708442	0.010	0.010	
5.135	DMD	A573V	hom	rs5972599	0.005	0.01	
5.135	ETFB	c.13_14insCTG TGG	het	rs61361626	.	.	
5.135	IGF2	R159H	het	rs61732764	0.011	0.01	
5.135	IL6	P32S	het	rs2069830	0.026	0.02	
5.135	IL6	V168M	het	rs2069842	0.025	0.02	
5.135	PGM1	V519I	het	rs6676290	0.050	0.050	
5.135	PYGM	T395M	het	rs71581787	0.018	0.020	
5.136	ACE	R1286S	het	rs4364	0.029	0.030	

5.136	ACE	A261S	het	rs4303	0.032	0.030	
5.136	ACE	D592G	het	rs12709426	0.017	0.020	
5.136	ANO5	T206A	het	rs78266558	0.009	0.020	
5.136	CPT2	A101V	het	rs75939866	0.005	0.003	
5.136	DYSF	L220V	het	rs13407355	0.023	0.02	
5.136	GYS1	Q360H	het	.	.	.	
5.136	HADHA	Q358K	het	rs2229420	0.023	0.020	
5.136	MYLK	R845C	het	rs3732485	0.006	0.030	
5.136	PGM1	V519I	het	rs6676290	0.050	0.050	
5.136	PYGM	R414G	het	rs11231866	0.061	0.040	
5.136	RYR1	E1878D	het	rs114203198	0.005	0.004	Yes
5.136	RYR1	D2943N	het	rs79294840	0.004	0.002	Yes
5.136	RYR1	H3642Q	het	rs114351116	0.004	0.002	Yes
5.137	ACADVL	R615Q	het	rs148584617	0.003	0.001	
5.137	ETFA	T171I	het	rs1801591	0.062	0.050	
5.137	ETFB	P52L	het	rs79338777	0.061	0.070	
5.137	PHKA2	I693V	hom	rs143732206	0.008	0.004	
5.138	ACADVL	E534K	het	rs2230180	0.010	0.003	
5.138	ANO5	G227A	het	rs140903276	0.003	0.002	
5.138	CACNA1S	R683C	het	rs35708442	0.010	0.010	
5.138	DMD	N2912D	het	rs1800278	0.032	0.04	
5.138	DMD	E2910V	het	rs41305353	0.030	0.04	
5.138	DMD	F1388V	het	rs28715870	0.033	0.02	
5.138	DYSF	L220V	het	rs13407355	0.023	0.02	
5.138	GAA	T927I	het	rs1800315	0.047	0.040	
5.138	GAA	S306L	het	rs138097673	0.003	0.003	
5.138	GAA	V816I	het	rs1800314	0.054	0.080	
5.138	GYG1	H151L	het	rs35054019	0.011	0.010	
5.138	IL6	V168M	het	rs2069842	0.025	0.02	
5.138	LPIN1	P610S	het	rs4669781	0.039	0.020	
5.138	MYLK	M1236V	het	rs113124819	0.001	0.002	
5.138	PHKB	Y770C	het	rs16945474	0.080	0.060	
5.139	ETFB	P52L	het	rs79338777	0.061	0.070	
5.139	GAA	E689K	het	rs1800309	0.030	0.090	
5.139	PGAM2	I114S	het	rs61756062	0.021	0.030	
5.139	RYR1	G2434R	het	rs121918593			Yes
5.140	MYLK	E1194G	het	.	.	.	
5.140	PFKM	Y706H	hom	.	.	.	Yes
5.141	GYG1	A16T	het	rs200947378	.	.	
5.141	PHKA2	E38Q	hom	rs17313469	0.024	0.020	
5.142	DYSF	P1760Q	het	rs145272777	0.000		
5.142	GAA	D91N	het	rs1800299	0.023	0.020	
5.142	PGAM2	I114S	het	rs61756062	0.021	0.030	
5.142	PYGM	M1V	het	.	.	.	Yes
5.142	PYGM	I571S	het	.	.	.	Yes
5.142	SCN4A	T323M	het	rs80338952	0.007	0.0018	Yes
5.143	DMD	c.31+1G>T	hom				Yes
5.143	DYSF	G128E	het	rs34997054	0.003	0.0018	
5.143	GYG1	N256T	het	rs142869401	0.001	0.001	
5.143	LDHA	R157H	het	rs368815124	0.000	.	

5.143	RYR1	S1342G	het	rs34694816	0.037	0.050	
5.144	ACTN3	R357C	het	rs200574979	0.000	.	
5.144	CPT2	F352C	het	rs2229291	0.007	0.060	
5.144	DYSF	E541G	het				Yes
5.144	DYSF	I1607T	het	rs146384562	0.001	0.0014	Yes
5.144	GAA	E689K	het	rs1800309	0.030	0.090	
5.144	PGAM2	I114S	het	rs61756062	0.021	0.030	
5.144	PYGM	T395M	het	rs71581787	0.018	0.020	
5.145	RYR1	G2060C	het	rs35364374	0.051	0.030	
5.146	ACTN3	R902C	het	rs71457732	0.007	0.010	
5.147	LPIN1	N376D	het	.	.	.	
5.147	RYR1	G2060C	het	rs35364374	0.051	0.030	
5.148	GYS1	M416V	het	rs5447	0.007	0.030	
5.149	ACADVL	V283A	het	rs113994167	0.001	.	
5.149	MYLK	T1085A	het	rs75370906	0.065	0.050	
5.150	DMD	T1948S	hom				
5.150	DYSF	c.3708delA	hom				Yes
5.150	LPIN1	V494M	het	rs33997857	0.016	0.010	
5.150	PHKB	Y770C	het	rs16945474	0.080	0.060	
5.151	ANO5	A205S	het				
5.151	SIL1	Q80K	het	.	0.000	.	
5.152	CPT2	S113L	hom	rs17355168	0.001	0.001	Yes
5.152	GAA	D91N	het	rs1800299	0.023	0.020	
5.152	MYLK	H1081L	het	.	.	.	
5.153	CPT2	S113L	hom	rs17355168	0.001	0.001	Yes
5.153	GAA	E689K	het	rs1800309	0.030	0.090	
5.154	ACTN3	R457W	het	rs200842599	0.000	.	
5.154	DYSF	R1072C	het	rs144598063	0.000		
5.154	PYGM	R194Q	het	rs115259855	.	.	
5.154	RYR1	D1856N	hom	.	.	.	Yes
5.155	LPIN1	L164M	het	.	.	.	
5.156	ACADVL	G43D	het	rs2230178	0.011	0.070	
5.156	ACE	A319S	het	rs34126458	0.000	0.001	
5.156	CPT2	D421N	het	.	.	.	
5.156	GYS1	Y600C	het	.	.	.	
5.156	LPIN1	P610S	het	rs4669781	0.039	0.020	
5.157	ETFB	P52L	het	rs79338777	0.061	0.070	
5.157	GAA	E689K	het	rs1800309	0.030	0.090	
5.157	GAA	V816I	het	rs1800314	0.054	0.080	
5.158	ANO5	c.191_192insA	het				
5.158	FKRP	R143S	het	rs148206382	0.004	0.0046	
5.158	HADHB	T133A	het	.	0.000	.	Yes
5.158	HADHB	F430S	het	.	0.000	.	Yes
5.158	PHKB	Y770C	het	rs16945474	0.080	0.060	
5.159	MYLK	R845C	het	rs3732485	0.006	0.030	
5.159	PGAM2	I114S	het	rs61756062	0.021	0.030	
5.159	RYR1	E1888del	het	.	0.000	.	Yes
5.159	SIL1	R92W	het	rs149242794	0.000	.	
5.160	ACE	A261S	het	rs4303	0.032	0.030	
5.160	ACE	D592G	het	rs12709426	0.017	0.020	
5.160	ANO5	N882K	het	rs34969327	0.013	0.010	

5.160	DMD	N2912D	hom	rs1800278	0.032	0.04	
5.160	DMD	E2910V	hom	rs41305353	0.030	0.04	
5.160	DMD	N1672K	hom	rs16990264	0.025	0.02	
5.160	DMD	F1388V	hom	rs28715870	0.033	0.02	
5.160	GYS1	M416V	het	rs5447	0.007	0.030	
5.160	IL6	P31T	het	rs142759801	0.009	0.0032	
5.160	PGAM2	W78*	het	rs10250779	0.003	0.002	
5.160	PHKB	Y770C	het	rs16945474	0.080	0.060	
5.160	PHKB	V762I	het	rs56010117	0.001	0.001	
5.160	PYGM	R414G	hom	rs11231866	0.061	0.040	
5.160	RYR1	S1342G	hom	rs34694816	0.037	0.050	
5.160	RYR1	T2787S	het	rs35180584	0.010	0.010	Yes
5.160	SGCA	T39A	het	rs145774501			
5.161	CACNA1S	A102T	het				Yes
5.161	LPIN1	P610S	het	rs4669781	0.039	0.020	
5.162	ACE	R1279Q	het	rs200754517	0.005	.	
5.163	ACADVL	P65L	het	rs28934585	0.034	0.030	
5.163	CACNA1S	R683C	het	rs35708442	0.010	0.010	
5.163	DMD	N2912D	het	rs1800278	0.032	0.04	
5.163	DMD	E2910V	het	rs41305353	0.030	0.04	
5.163	ETFA	I276L	het	rs141200145	0.001	0.001	
5.163	ETFB	P52L	het	rs79338777	0.061	0.070	
5.163	SCN4A	P73L	het	rs75086141	0.000	0.0009	Yes
5.164	ACE	Q574*	het				
5.164	CACNA1S	A69G	het	rs12406479	0.039	0.020	
5.164	DYSF	A201E	het	rs34999029	0.010	0.01	
5.164	ETFB	P52L	het	rs79338777	0.061	0.070	
5.164	PGAM2	I160V	het				
5.164	PHKA1	R821H	hom	rs139803629	0.003	0.003	Yes
5.164	PHKG1	R138S	hom				
5.164	PYGM	R50*	het	rs116987552	0.002	0.001	
5.165	PFKM	R767H	het	rs41291971	0.012	0.010	
5.166	ACADVL	P65L	het	rs28934585	0.034	0.030	
5.166	SIL1	Q80R	het	rs35581768	0.008	0.010	
5.167	GAA	D91N	het	rs1800299	0.023	0.020	
5.167	PYGM	R50*	hom	rs116987552	0.002	0.001	Yes
5.168	DMD	H2921R	hom	rs1800279	0.021	0.01	
5.168	PHKA2	I693V	hom (hom)	rs143732206	0.008	0.004	
5.169	CCR2	G273S	het	rs201184651	0.000	0.001	
5.169	DYSF	I865V	het	rs34671418	0.043	0.03	
5.169	DYSF	R102Q	het	rs34211915	0.024	0.01	Yes
5.169	DYSF	R1331L	het	rs61742872	0.025	0.02	Yes
5.169	IL6	D162V	het	rs13306435	0.007	0.03	
5.170	ACE	I1081V	het	.	.	.	
5.170	ACTN3	R357C	het	rs200574979	0.000	.	
5.170	ANO5	E202K	het	rs115750596	0.012	0.010	
5.170	CACNA1S	N1775S	het				
5.170	PYGM	P635L	het	.	0.000	.	

5.170	RYR1	E508Q	het	.	.	.	Yes
5.171	CACNA1S	L132M	het	rs377030324	0.000		Yes
5.171	DYSF	A201E	het	rs34999029	0.010	0.01	
5.171	GAA	V816I	het	rs1800314	0.054	0.080	
5.172	nothing						
5.173	ANO5	T267S	het	rs138144479	0.007	0.004	
5.173	CACNA1S	R683C	het	rs35708442	0.010	0.010	
5.173	DYSF	L220V	het	rs13407355	0.023	0.02	
5.173	DYSF	I865V	het	rs34671418	0.043	0.03	
5.173	HADHA	Q358K	het	rs2229420	0.023	0.020	
5.173	RYR1	S1342G	het	rs34694816	0.037	0.050	
5.173	RYR1	T2787S	het	rs35180584	0.010	0.010	Yes
5.174	ACE	R1286S	het	rs4364	0.029	0.030	
5.174	ANO5	T267S	het	rs138144479	0.007	0.004	
5.174	CAV3	G56S	het	rs72546667	0.037	0.030	Yes
5.174	ETFB	c.13_14insCTG TGG	hom	rs61361626			
5.174	IGF2	R159H	het	rs61732764	0.011	0.01	
5.174	IL6	P32S	het	rs2069830	0.026	0.02	
5.174	PYGM	T395M	het	rs71581787	0.018	0.020	
5.174	RYR1	A933T	het	rs148623597	0.001		Yes
5.174	RYR1	S1342G	hom	rs34694816	0.037	0.050	
5.174	RYR1	A1352G	het	rs112105381	0.004	0.010	Yes
5.174	SIL1	K132Q	het	rs61745568	0.026	0.020	
5.175	RYR1	G1497R	het		0.000		Yes
5.176	PHKA2	E38Q	hom	rs17313469	0.024	0.020	
5.176	RYR1	R817Q	het				Yes
5.177	CACNA1S	G1210R	het	rs148870919	0.001		Yes
5.177	RYR1	G2434R	het	rs121918593	.	.	Yes
5.178	DMD	H2921R	hom	rs1800279	0.021	0.01	
5.178	ETFA	T171I	het	rs1801591	0.062	0.050	
5.178	LPIN1	V494M	het	rs33997857	0.016	0.010	
5.178	RYR1	S2685F	het	.	.	.	Yes
5.179	ACADVL	P65L	het	rs28934585	0.034	0.030	
5.179	ACADVL	I356V	het	rs150140386	0.004	0.003	
5.179	ACE	c.55_56insCGC TGC	het				
5.179	ANO5	T267S	het	rs138144479	0.007	0.004	
5.179	DMD	F1388V	hom	rs28715870	0.033	0.02	
5.179	DMD	D518E	hom	rs61733587	0.013	0.01	
5.179	DYSF	A641G	het		0.000		
5.179	ETFB	c.13_14insCTG TGG	het	rs61361626			
5.179	HADHA	Q358K	het	rs2229420	0.023	0.020	
5.179	HADHB	K255R	het	rs57969630	0.007	0.010	
5.179	IGF2	R159H	het	rs61732764	0.011	0.01	
5.179	IL6	P32S	het	rs2069830	0.026	0.02	
5.179	MYLK	T1763I	het	rs142220417	0.002	0.002	
5.179	RYR1	L32F	het	rs138630815	0.001	0.002	Yes
5.179	SCN4A	P882Q	het	rs111858905	0.003	0.0041	Yes
5.180	CACNA1S	G264S	het				Yes

5.180	CACNA1S	A69G	het	rs12406479	0.039	0.020	
5.180	DMD	M2466L	het				
5.180	DYSF	R1454C	het		0.000		
5.180	ETFA	T171I	het	rs1801591	0.062	0.050	
5.180	PGK1	N295H	het	.	.	.	
5.180	PHKA1	C697R	het				
5.180	PHKA1	D687N	het				
5.180	PHKA1	A672P	het				
5.180	PHKB	C348R	het	.	.	.	
5.181	ACE	T461M	het				
5.181	DMD	R2155W	hom	rs1800273	0.027	0.01	
5.181	DYSF	E488K	het	rs61740288	0.018	0.01	
5.181	IL6	D162V	het	rs2069860	0.006	0.0018	
5.181	PGAM2	I114S	het	rs61756062	0.021	0.030	
5.182	nothing						
5.183	DYSF	A201E	het	rs34999029	0.010	0.01	
5.183	PGAM2	I114S	het	rs61756062	0.021	0.030	
5.183	RYR1	E3578Q	het	rs55876273	0.013	0.010	Yes
5.184	ACADVL	G43D	het	rs2230178	0.011	0.070	
5.184	DYSF	c.2864+1G>A	het	rs199954546		0.0005	
5.184	ETFA	T171I	het	rs1801591	0.062	0.050	
5.184	ETFB	P52L	hom	rs79338777	0.061	0.070	
5.184	ETFB	c.13_14insCTG TGG	het	rs61361626			
5.184	PHKB	Y770C	het	rs16945474	0.080	0.060	
5.185	ACADVL	P65L	het	rs28934585	0.034	0.030	
5.185	CACNA1S	Y299H	het	rs35856559	0.007	0.010	
5.185	CPT2	N311S	het	rs142790440	0.002	0.004	
5.185	DYSF	V398M	het	rs144202114	0.005	0.0023	Yes
5.185	DYSF	R1022Q	het	rs34211915	0.024	0.01	Yes
5.185	DYSF	I1325V	het	rs145401010	0.005	0.0023	Yes
5.185	GAA	V816I	het	rs1800314	0.054	0.080	
5.185	MYLK	M1236V	het	rs113124819	0.001	0.002	
5.185	MYLK	T1085A	het	rs75370906	0.065	0.050	
5.185	PHKB	Y770C	hom	rs16945474	0.080	0.060	
5.185	PYGM	R414G	het	rs11231866	0.061	0.040	
5.185	RYR1	S1342G	het	rs34694816	0.037	0.050	
5.186	ACE	R1279Q	het	rs200754517	0.005		
5.186	CKM	L299V	het	rs150271912	0.000	0.001	
5.186	DMD	T1245I	hom	rs1800269	0.008	0.01	
5.186	ETFA	T171I	het	rs1801591	0.062	0.050	
5.186	ETFB	P52L	hom	rs79338777	0.061	0.070	
5.186	ETFB	c.13_14insCTG TGG	het	rs61361626			
5.186	SCN4A	P1571S	het				Yes
5.187	ETFB	Q237H	hom				
5.187	MYLK	Y1829H	het				
5.188	DYSF	E488K	het	rs61740288	0.018	0.01	
5.188	PHKA1	R821H	het	rs139803629	0.003	0.003	
5.188	RYR1	G2060C	?	rs35364374	0.051	0.030	

5.188	RYR1	P1787L	het	rs34934920	0.017	0.010	
5.189	ACTN3	L398F	het	rs201576110	0.000		
5.189	ETFB	c.13_14insCTG TGG	het				
5.190	DMD	N2912D	het	rs1800278	0.032	0.04	
5.190	DMD	E2910V	het	rs41305353	0.030	0.04	
5.190	GAA	E689K	het	rs1800309	0.030	0.090	
5.191	ETFB	V79I	het	rs140608276	0.003	0.003	
5.191	PHKB	Y770C	het	rs16945474	0.080	0.060	
5.192	ACE	Y244C	het	rs3730025	0.011	0.010	
5.192	DYSF	I865V	het	rs34671418	0.043	0.03	
5.192	DYSF	R1022Q	het	rs34211915	0.024	0.01	Yes
5.192	DYSF	R1331L	het	rs61742872	0.025	0.02	Yes
5.192	ETFB	C96Y	het				
5.192	SIL1	L7V	het	rs11555154	0.060	0.050	
5.193	ETFB	P52L	het	rs79338777	0.061	0.070	
5.193	GYG1	D102H	het	rs143137713	0.001	0.001	
5.193	PHKA2	S1053A	het				
5.193	PHKA2	T651N	het	rs149991825	0.002	0.010	
5.193	SGCB	S114F	het	rs150518260	0.000		
5.193	SIL1	K132Q	het	rs61745568	0.026	0.020	
5.194	ACADVL	L17F	het	rs2230179	0.022	0.020	
5.194	ACE	A261S	het	rs4303	0.032	0.030	
5.194	ACE	D592G	het	rs12709426	0.017	0.020	
5.194	ACE	S32P	het	rs4317	0.052	0.050	
5.194	ACE	S49G	het	rs4318	0.054	0.050	
5.194	ANO5	L785R	het	rs146136277	0.004	0.003	
5.194	CACNA1S	c.5488_5495del	het	rs369242419	0.013		Yes
5.194	CACNA1S	A1271T	het	rs138144724	0.007	0.003	
5.194	DYSF	P233L	het	rs143053635	0.000		Yes
5.194	DYSF	I865V	hom	rs34671418	0.043	0.03	
5.194	DYSF	R1333L	het	rs61742872	0.025	0.02	Yes
5.194	ETFB	c.13_14insCTG TGG	het	rs61361626			
5.194	IGF2	R159H	het	rs61732764	0.011	0.01	
5.194	IL6	V168M	het	rs2069842	0.025	0.02	
5.194	LPIN1	R605H	het	rs145021638	0.001		
5.194	PHKB	Y770C	het	rs16945474	0.080	0.060	
5.194	RYR1	R1109K	het	rs35719391	0.007	0.010	Yes
5.194	RYR1	T2787S	het	rs35180584	0.010	0.010	Yes
5.194	SIL1	K132Q	het	rs61745568	0.026	0.020	
5.195	GAA	E689K	het	rs1800309	0.030	0.090	
5.196	SCN4A	T603R	het				Yes
5.198	PHKA2	G1195R	hom	.	.	.	
5.199	LPIN1	c.2269dupA	hom	.	.	.	Yes
5.199	SIL1	T123I	het	rs115800498	0.006	0.002	
5.200	ANO5	c.898_899insA	het				Yes
5.200	ANO5	c.1000delC	het				Yes
5.201	CACNA1S	R422H	het				Yes
5.201	GAA	E689K	het	rs1800309	0.030	0.090	
5.201	GAA	V816I	het	rs1800314	0.054	0.080	

5.201	MYLK	S1646I	het	.	.	.	
5.202	ACADVL	G43D	het	rs2230178	0.011	0.070	
5.202	CKM	T166M	het	rs17357122	0.006	0.004	
5.202	DYSF	E488K	het	rs61740288	0.018	0.01	
5.202	ENO3	G194V	het	.	.	.	
5.202	PGAM2	I114S	het	rs61756062	0.021	0.030	
5.202	RYR1	V3088M	het	rs145044872	0.000	0.001	Yes
5.203	GYG1	P126S	het	.	.	.	
5.203	LPIN1	V494M	het	rs33997857	0.016	0.010	
5.204	ACADVL	R615Q	het	rs148584617	0.003	0.001	
5.204	CACNA1S	M635V	het	rs201784750	0.000		Yes
5.204	FKRP	A114G	het	rs143793528	0.008	0.01	
5.205	CACNA1S	R498H	het	rs150590855			Yes
5.205	PHKB	M185I	het	rs56257827	0.011	0.010	
5.205	SGCA	T39A	hom	rs137852623	0.000		Yes
5.206	SIL1	T123I	het	rs115800498	0.006	0.002	
5.207	GAA	R89H	het	rs200586324	0.000	.	
5.207	LPIN1	P206A	het	.	0.000	.	
5.207	SIL1	K132Q	het	rs61745568	0.026	0.020	
5.208	PHKA2	I513T	het				
5.209	ACADVL	G523R	het	rs139425622	0.001	0.001	
5.209	ANO5	Y282C	het				
5.209	ETFA	T171I	het	rs1801591	0.062	0.050	
5.209	FKRP	G354W	het				
5.209	RYR1	N759D	het	rs147320363	0.000	0.001	Yes
5.210	ACTN3	A231V	het	rs144340728	0.006	0.004	
5.210	CPT2	P50H	het	rs28936375			
5.210	ETFA	T171I	het	rs1801591	0.062	0.050	
5.210	GAA	D91N	het	rs1800299	0.023	0.020	
5.211	GYS1	M416V	het	rs5447	0.007	0.030	
5.212	DMD	R2155W	hom	rs1800273	0.027	0.01	
5.212	ETFA	T171I	het	rs1801591	0.062	0.050	
5.212	HADHA	L603M	het				
5.212	PHKB	Y770C	het	rs16945474	0.080	0.060	
5.213	ACE	S32P	het	rs4317	0.052	0.050	
5.213	ACE	S49G	het	rs4318	0.054	0.050	
5.214	ACTN3	R829Q	het	rs114618009	0.006	0.010	
5.214	IL6	P32S	het	rs2069830	0.026	0.02	
5.214	MYLK	T1085A	het	rs75370906	0.065	0.050	
5.214	PYGM	R414G	het	rs11231866	0.061	0.040	
5.214	SIL1	K132Q	het	rs61745568	0.026	0.020	
5.215	ACADVL	c.1500_1502dell	het				
5.215	RYR1	S1342G	het	rs34694816	0.037	0.050	
5.215	SIL1	K132Q	het	rs61745568	0.026	0.020	
5.216	CAV3	G56S	het	rs72546667	0.037	0.030	
5.216	ETFB	c.13_14insCTG TGG	het	rs55874945	0.034		
5.216	LPIN1	P610S	het	rs4669781	0.039	0.020	
5.216	PHKB	Y770C	het	rs16945474	0.080	0.060	
5.216	RYR1	S1342G	het	rs34694816	0.037	0.050	
5.217	ACADVL	F376S	het				Yes
5.217	ACADVL	c.1752-1G>A	het				Yes

5.217	ACE	R1286S	het	rs4364	0.029	0.030	
5.217	CACNA1S	M827T	het	rs61238538	0.011	0.010	
5.217	DMD	H2921R	het	rs1800279	0.021	0.01	
5.217	LPIN1	P610S	het	rs4669781	0.039	0.020	
5.217	MYLK	N649I	het				
5.217	MYLK	A128V	het	rs143896146	0.001	0.010	
5.217	PHKB	Y770C	het	rs16945474	0.080	0.060	
5.217	RYR1	Q3751E	het	rs4802584	0.012	0.030	
5.217	SIL1	D63E	het	rs115591710	0.004	0.004	
5.218	ANO5	N52S	het	rs143777403	0.003	0.001	
5.218	CCR2	S357L	het	rs191797612		0.001	
5.218	IL6	V168M	het	rs2069842	0.025	0.02	
5.218	MYLK	T1085A	het	rs75370906	0.065	0.050	
5.218	PYGM	R50*	het	rs116987552	0.002	0.001	Yes
5.218	PYGM	c.772+1G>T	het				Yes
5.219	ACTN3	R902C	het	rs71457732	0.007	0.010	
5.219	GAA	E689K	het	rs1800309	0.030	0.090	
5.219	SIL1	L7V	het	rs11555154	0.060	0.050	
5.220	PHKB	Y770C	het	rs16945474	0.080	0.060	
5.221	ACADVL	L501V	het				
5.221	DYSF	E488K	het	rs61740288	0.018	0.01	
5.221	ETFB	c.13_14insCTG TGG	het	rs61361626			
5.221	RYR1	E3578Q	het	rs55876273	0.013	0.010	Yes
5.221	SIL1	L7V	het	rs11555154	0.060	0.050	
5.450	PGAM2	I114S	het	rs61756062	0.021	0.030	
5.450	RYR1	Q3751E	het	rs4802584	0.012	0.030	
5.430	ACE	R1279Q	het	rs200754517	0.005		
5.430	ETFB	P52L	het	rs79338777	0.061	0.070	
5.430	PHKG2	V70M	het				
5.430	RYR1	R896Q	het	rs147515913	0.000		Yes
5.222	ACADVL	I356V	het	rs150140386	0.004	0.003	
5.222	ACE	R1286S	hom	rs4364	0.029	0.030	
5.222	CAV3	G56S	het	rs72546667	0.037	0.030	
5.222	CKM	M30I	het	rs145633772	0.001	0.001	
5.222	FKRP	V79M	het	rs104894683	0.004	0.0041	
5.222	GAA	V816I	het	rs1800314	0.054	0.080	
5.222	HADHA	Q358K	het	rs2229420	0.023	0.020	
5.222	MYLK	T1763I	het	rs142220417	0.002	0.002	
5.222	PGAM2	I114S	het	rs61756062	0.021	0.030	
5.222	SIL1	Q80R	het	rs35581768	0.008	0.010	
5.223	ACE	Q537R	het				
5.223	ACTN3	R829Q	het	rs114618009	0.006	0.010	
5.223	MYLK	T1085A	het	rs75370906	0.065	0.050	
5.223	PYGM	R414G	het	rs11231866	0.061	0.040	
5.223	SIL1	K132Q	het	rs61745568	0.026	0.020	
5.224	DYSF	E488K	het	rs61740288	0.018	0.01	

Patients run by the Rhabdomyolysis panel, and the variants found in them that remained after described filters had been applied (description refers to protein change unless otherwise indicated)

References

- Aboumoussa, A., J. Hoogendijk, et al. (2008). "Caveolinopathy – New mutations and additional symptoms." *Neuromuscular Disorders* **18**(7): 572-578.
- Adzhubei, I. A., S. Schmidt, et al. (2010). "A method and server for predicting damaging missense mutations." *Nature Methods* **7**(4): 248-249.
- Altshuler, D. L., R. M. Durbin, et al. (2010). "A map of human genome variation from population-scale sequencing." *Nature* **467**(7319): 1061-1073.
- Andersen, D. H. (1956). "Familial cirrhosis of the liver with storage of abnormal glycogen." *Lab Invest* **5**(1): 11-20.
- Anderson, E., S. Berkovic, et al. (2002). "ILAE genetics commission conference report: Molecular analysis of complex genetic epilepsies (vol 43, pg 1262, 2002)." *Epilepsia* **43**(12): 1600-1602.
- Andreasen, C., J. B. Nielsen, et al. (2013). "New population-based exome data are questioning the pathogenicity of previously cardiomyopathy-associated genetic variants." *Eur J Hum Genet* **21**(9): 918-928.
- Andres-Enguix, I., L. J. Shang, et al. (2012). "Functional analysis of missense variants in the TRESK (KCNK18) K⁺ channel." *Scientific Reports* **2**.
- Andresen, B. S., S. Olpin, et al. (1999). "Clear Correlation of Genotype with Disease Phenotype in Very-Long-Chain Acyl-CoA Dehydrogenase Deficiency." *The American Journal of Human Genetics* **64**(2): 479-494.
- Andreu, A. L., G. Nogales-Gadea, et al. (2007). "McArdle disease: molecular genetic update." *Acta Myol* **26**(1): 53-57.
- Angelini, C., M. Fanin, et al. (1998). "Homozygous α -sarcoglycan mutation in two siblings: One asymptomatic and one steroid-responsive mild limb-girdle muscular dystrophy patient." *Muscle & Nerve* **21**(6): 769-775.
- Anttila, V., H. Stefansson, et al. (2010). "Genome-wide association study of migraine implicates a common susceptibility variant on 8q22.1." *Nature Genetics* **42**(10): 869-+.
- Antzelevitch, C., G. D. Pollevick, et al. (2007). "Loss-of-function mutations in the cardiac calcium channel underlie a new clinical entity characterized by ST-segment elevation, short QT intervals, and sudden cardiac death." *Circulation* **115**(4): 442-449.
- Aoyama, T., M. Souri, et al. (1995). "Cloning of human very-long-chain acyl-coenzyme A dehydrogenase and molecular characterization of its deficiency in two patients." *Am J Hum Genet* **57**(2): 273-283.
- Arzel-Hezode, M., D. Sternberg, et al. (2010). "HOMOZYGOSITY FOR DOMINANT MUTATIONS INCREASES SEVERITY OF MUSCLE CHANNELOPATHIES." *Muscle & Nerve* **41**(4): 470-477.
- Baig, S. M., A. Koschak, et al. (2011). "Loss of Ca(v)1.3 (CACNA1D) function in a human channelopathy with bradycardia and congenital deafness." *Nat Neurosci* **14**(1): 77-84.
- Balabanski, L., G. Antov, et al. (2014). "Next-generation sequencing of BRCA1 and BRCA2 in breast cancer patients and control subjects." *Molecular and Clinical Oncology* **2**(3): 435-439.
- Bali, D. S., J. L. Goldstein, et al. (2014). "Variability of disease spectrum in children with liver phosphorylase kinase deficiency caused by mutations in the PHKG2 gene." *Mol Genet Metab* **111**(3): 309-313.

- Bao, Y., P. Kishnani, et al. (1996). "Hepatic and neuromuscular forms of glycogen storage disease type IV caused by mutations in the same glycogen-branching enzyme gene." Journal of Clinical Investigation **97**(4): 941-948.
- Baquero, J. L., R. A. Ayala, et al. (1995). "Hyperkalemic periodic paralysis with cardiac dysrhythmia: A novel sodium channel mutation?" Annals of Neurology **37**(3): 408-411.
- Baulac, S., I. Gourfinkel-An, et al. (1999). "A Second Locus for Familial Generalized Epilepsy with Febrile Seizures Plus Maps to Chromosome 2q21-q33." American Journal of Human Genetics **65**(4): 1078-1085.
- Bean, B. P. (2007). "The action potential in mammalian central neurons." Nat Rev Neurosci **8**(6): 451-465.
- Beard, S. E., Spector, E. B., Seltzer, W. K., Frerman, F. E., Goodman, S. I. (1993). "Mutations in electron transfer flavoprotein:ubiquinone oxidoreductase (ETF:QO) in glutaric acidemia type II (GA2)." clin. res. **41**(271).
- Bendahhou, S., T. R. Cummins, et al. (2000). "A double mutation in families with periodic paralysis defines new aspects of sodium channel slow inactivation." Journal of Clinical Investigation **106**(3): 431-438.
- Berkovic, S. F., S. E. Heron, et al. (2004). "Benign familial neonatal-infantile seizures: characterization of a new sodium channelopathy." Ann Neurol **55**(4): 550-557.
- Bertil, H. (2001). Ion Channels of Excitable Membranes, Sinauer Associates, Inc.
- Bhatia, K. P. (2011). "Paroxysmal Dyskinesias." Movement Disorders **26**(6): 1157-1165.
- Black, D. L. (2003). "Mechanisms of alternative pre-messenger RNA splicing." Annu Rev Biochem **72**: 291-336.
- Blakeley, J. and J. Jankovic (2002). "Secondary paroxysmal dyskinesias." Movement Disorders **17**(4): 726-734.
- Bolduc, V., G. Marlow, et al. (2010). "Recessive Mutations in the Putative Calcium-Activated Chloride Channel Anoctamin 5 Cause Proximal LGMD2L and Distal MMD3 Muscular Dystrophies." The American Journal of Human Genetics **86**(2): 213-221.
- Borsani, G., E. I. Rugarli, et al. (1995). "Characterization of a Human and Murine Gene (CLCN3) Sharing Similarities to Voltage-Gated Chloride Channels and to a Yeast Integral Membrane Protein." Genomics **27**(1): 131-141.
- Brackett, J. C., H. F. Sims, et al. (1995). "Two alpha subunit donor splice site mutations cause human trifunctional protein deficiency." The Journal of Clinical Investigation **95**(5): 2076-2082.
- Brauers, E., A. Dreier, et al. (2010). "Differential Effects of Myopathy-Associated Caveolin-3 Mutants on Growth Factor Signaling." The American Journal of Pathology **177**(1): 261-270.
- Browne, D. L., S. T. Ganchar, et al. (1994). "Episodic ataxia/myokymia syndrome is associated with point mutations in the human potassium channel gene, KCNA1." Nat Genet **8**(2): 136-140.
- Bruno, M. K., M. Hallett, et al. (2004). "Clinical evaluation of idiopathic paroxysmal kinesigenic dyskinesia - New diagnostic criteria." Neurology **63**(12): 2280-2287.
- Bruno, M. K., H.-Y. Lee, et al. (2007). "Genotype-phenotype correlation of paroxysmal nonkinesigenic dyskinesia." Neurology **68**(21): 1782-1789.
- Buermans, H. P. J. and J. T. den Dunnen (2014). "Next generation sequencing technology: Advances and applications." Biochimica et Biophysica Acta (BBA) - Molecular Basis of Disease **1842**(10): 1932-1941.
- Bürk, K., F. J. Kaiser, et al. (2014). "A novel missense mutation in CACNA1A evaluated by in silico protein modeling is associated with non-episodic spinocerebellar ataxia with slow progression." European Journal of Medical Genetics **57**(5): 207-211.
- Burwinkel, B., H. D. Bakker, et al. (1998). "Mutations in the liver glycogen phosphorylase gene (PYGL) underlying glycogenosis type VI." Am J Hum Genet **62**(4): 785-791.

- Burwinkel, B., A. J. Maichele, et al. (1997). "Autosomal glycogenosis of liver and muscle due to phosphorylase kinase deficiency is caused by mutations in the phosphorylase kinase beta subunit (PHKB)." Hum Mol Genet **6**(7): 1109-1115.
- Cacciottolo, M., G. Numitone, et al. (2011). "Muscular dystrophy with marked Dysferlin deficiency is consistently caused by primary dysferlin gene mutations." Eur J Hum Genet **19**(9): 974-980.
- Cagliani, R., G. P. Comi, et al. (2001). "Primary beta-sarcoglycanopathy manifesting as recurrent exercise-induced myoglobinuria." Neuromuscular Disorders **11**(4): 389-394.
- Cagliani, R., F. Fortunato, et al. (2003). "Molecular analysis of LGMD-2B and MM patients: identification of novel DYSF mutations and possible founder effect in the Italian population." Neuromuscular Disorders **13**(10): 788-795.
- Capacchione, J. F. and S. M. Muldoon (2009). "The relationship between exertional heat illness, exertional rhabdomyolysis, and malignant hyperthermia." Anesth Analg **109**(4): 1065-1069.
- Carpenter, D., C. Ringrose, et al. (2009). "The role of CACNA1S in predisposition to malignant hyperthermia." BMC Med Genet **10**(104): 1471-2350.
- Castro, M. J., A. H. Stam, et al. (2009). "First mutation in the voltage-gated Na(V)1.1 subunit gene SCN1A with co-occurring familial hemiplegic migraine and epilepsy." Cephalalgia **29**(3): 308-313.
- Ceravolo, F., S. Messina, et al. (2014). "Myoglobinuria as first clinical sign of a primary alpha-sarcoglycanopathy." European Journal of Pediatrics **173**(2): 239-242.
- Charlier, C., N. A. Singh, et al. (1998). "A pore mutation in a novel KQT-like potassium channel gene in an idiopathic epilepsy family." Nat Genet **18**(1): 53-55.
- Chasman, D. I., M. Schurks, et al. (2011). "Genome-wide association study reveals three susceptibility loci for common migraine in the general population." Nature Genetics **43**(7): 695-U116.
- Chen, J., A. Zou, et al. (1999). "Long QT Syndrome-associated Mutations in the Per-Arnt-Sim (PAS) Domain of HERG Potassium Channels Accelerate Channel Deactivation." Journal of Biological Chemistry **274**(15): 10113-10118.
- Chen, W. J., Y. Lin, et al. (2011). "Exome sequencing identifies truncating mutations in PRRT2 that cause paroxysmal kinesigenic dyskinesia." Nature Genetics **43**(12): 1252-U1116.
- Chen, Y., J. Lu, et al. (2003). "Association between genetic variation of CACNA1H and childhood absence epilepsy." Ann Neurol **54**(2): 239-243.
- Cheng, C. J., S. H. Lin, et al. (2011). "Identification and functional characterization of Kir2.6 mutations associated with non-familial hypokalemic periodic paralysis (vol 286, pg 27425, 2011)." Journal of Biological Chemistry **286**(38): 33707-33707.
- Choi, M., U. I. Scholl, et al. (2009). "Genetic diagnosis by whole exome capture and massively parallel DNA sequencing." Proceedings of the National Academy of Sciences **106**(45): 19096-19101.
- Clarkson, P. M., E. P. Hoffman, et al. (2005). ACTN3 and MLCK genotype associations with exertional muscle damage.
- Clemen, C., H. Herrmann, et al. (2013). "Desminopathies: pathology and mechanisms." Acta Neuropathologica **125**(1): 47-75.
- Colombo, I., G. Finocchiaro, et al. (1994). "Mutations and polymorphisms of the gene encoding the beta-subunit of the electron transfer flavoprotein in three patients with glutaric acidemia type II." Hum Mol Genet **3**(3): 429-435.
- Comi, G. P., F. Fortunato, et al. (2001). "Beta-enolase deficiency, a new metabolic myopathy of distal glycolysis." Ann Neurol **50**(2): 202-207.
- Cox, J. J., F. Reimann, et al. (2006). "An SCN9A channelopathy causes congenital inability to experience pain." Nature **444**(7121): 894-898.
- Cronk, L. B., B. Ye, et al. (2007). "Novel mechanism for sudden infant death syndrome: persistent late sodium current secondary to mutations in caveolin-3." Heart Rhythm **4**(2): 161-166.

- Curran, M. E., I. Splawski, et al. (1995). "A molecular basis for cardiac arrhythmia: HERG mutations cause long QT syndrome." Cell **80**(5): 795-803.
- Dale, R. C., P. Grattan-Smith, et al. (2012). "Microdeletions detected using chromosome microarray in children with suspected genetic movement disorders: a single-centre study." Developmental medicine and child neurology **54**(7): 618-623.
- Damji, K. F., R. R. Allingham, et al. (1996). "Periodic vestibulocerebellar ataxia, an autosomal dominant ataxia with defective smooth pursuit, is genetically distinct from other autosomal dominant ataxias." Arch Neurol **53**(4): 338-344.
- Das, A. M., S. Illsinger, et al. (2006). "Isolated Mitochondrial Long-Chain Ketoacyl-CoA Thiolase Deficiency Resulting from Mutations in the HADHB Gene." Clinical Chemistry **52**(3): 530-534.
- De Fusco, M., R. Marconi, et al. (2003). "Haploinsufficiency of ATP1A2 encoding the Na⁺/K⁺ pump alpha 2 subunit associated with familial hemiplegic migraine type 2." Nature Genetics **33**(2): 192-196.
- De Meirleir, L., S. Seneca, et al. (2003). "Clinical and diagnostic characteristics of complex III deficiency due to mutations in the BCS1L gene." Am J Med Genet A **30**(2): 126-131.
- de Paula, F., M. Vainzof, et al. (2001). "Mutations in the caveolin-3 gene: When are they pathogenic?" American Journal of Medical Genetics **99**(4): 303-307.
- de Vries, B., H. Mamsa, et al. (2009). "Episodic ataxia associated with EAAT1 mutation C186S affecting glutamate reuptake." Arch Neurol **66**(1): 97-101.
- Delcourt, M., F. Riant, et al. (2015). "Severe phenotypic spectrum of biallelic mutations in PRRT2 gene." Journal of Neurology, Neurosurgery & Psychiatry.
- Demos, M. K., V. Macri, et al. (2009). "A novel KCNA1 mutation associated with global delay and persistent cerebellar dysfunction." Movement Disorders **24**(5): 778-782.
- Depienne, C., M. Bugiani, et al. (2013). "Brain white matter oedema due to CIC-2 chloride channel deficiency: an observational analytical study." Lancet Neurol **12**(7): 659-668.
- Desmet, F. O., D. Hamroun, et al. (2009). "Human Splicing Finder: an online bioinformatics tool to predict splicing signals." Nucleic Acids Res **37**(9): 1.
- Deuster, P. A., C. L. Contreras-Sesvold, et al. (2013). "Genetic polymorphisms associated with exertional rhabdomyolysis." Eur J Appl Physiol **113**(8): 1997-2004.
- Devaney, J. M., E. P. Hoffman, et al. (2007). IGF-II gene region polymorphisms related to exertional muscle damage.
- Dichgans, M., T. Freilinger, et al. (2005). "Mutation in the neuronal voltage-gated sodium channel SCN1A in familial hemiplegic migraine." Lancet **366**(9483): 371-377.
- Dichgans, M., T. Freilinger, et al. (2005). "Mutation in the neuronal voltage-gated sodium channel SCN1A in familial hemiplegic migraine." Lancet **366**(9483): 371-377.
- Djemie, T., S. Weckhuysen, et al. (2014). "PRRT2 mutations: exploring the phenotypical boundaries." J Neurol Neurosurg Psychiatry **85**(4): 462-465.
- Dlamini, N., N. C. Voermans, et al. (2013). "Mutations in RYR1 are a common cause of exertional myalgia and rhabdomyolysis." Neuromuscular Disorders **23**(7): 540-548.
- Doering, C. J., J. B. Peloquin, et al. (2007). "The Ca(v)1.4 calcium channel: more than meets the eye." Channels **1**(1): 3-10.
- Dogan, R. I., L. Getoor, et al. (2007). "SplicePort--an interactive splice-site analysis tool." Nucleic Acids Res **35**(Web Server issue): 18.
- Doriguzzi, C., L. Palmucci, et al. (1993). "Exercise intolerance and recurrent myoglobinuria as the only expression of Xp21 Becker type muscular dystrophy." Journal of Neurology **240**(5): 269-271.

- Duarte, S. T., J. Oliveira, et al. (2011). "Dominant and recessive RYR1 mutations in adults with core lesions and mild muscle symptoms." Muscle & Nerve **44**(1): 102-108.
- Duffield, M., G. Rychkov, et al. (2003). "Involvement of helices at the dimer interface in C1C-1 common gating." Journal of General Physiology **121**(2): 149-161.
- Dunnen, J. T. d. and S. E. Antonarakis (2000). "Mutation nomenclature extensions and suggestions to describe complex mutations: A discussion." Human Mutation **15**(1): 7-12.
- Efremov, R. G., A. Leitner, et al. (2015). "Architecture and conformational switch mechanism of the ryanodine receptor." Nature **517**(7532): 39-43.
- Ehret GB, M. P., Rice KM, Bochud M, Johnson AD, Chasman DI (2011). "Genetic variants in novel pathways influence blood pressure and cardiovascular disease risk." Nature **478**(7367): 103-109.
- Emery, A. E. (1991). "Population frequencies of inherited neuromuscular diseases--a world survey." Neuromuscular disorders : NMD **1**(1): 19-29.
- Erro, R., U. M. Sheerin, et al. (2014). "Paroxysmal dyskinesias revisited: A review of 500 genetically proven cases and a new classification." Mov Disord **25**(10): 25933.
- Escayg, A., M. De Waard, et al. (2000). "Coding and noncoding variation of the human calcium-channel beta4-subunit gene CACNB4 in patients with idiopathic generalized epilepsy and episodic ataxia." Am J Hum Genet **66**(5): 1531-1539.
- Evangelidou, P., A. Alexandrou, et al. (2013). "Implementation of high resolution whole genome array CGH in the prenatal clinical setting: advantages, challenges, and review of the literature." Biomed Res Int **346762**(10): 4.
- Faber, C. G., G. Lauria, et al. (2012). "Gain-of-function Nav1.8 mutations in painful neuropathy." Proc Natl Acad Sci U S A **109**(47): 19444-19449.
- Fanin, M., A. Anichini, et al. (2012). "Allelic and phenotypic heterogeneity in 49 Italian patients with the muscle form of CPT-II deficiency." Clin Genet **82**(3): 232-239.
- Farmer, T. W. and V. M. Mustian (1963). "Vestibulocerebellar ataxia. A newly defined hereditary syndrome with periodic manifestations." Arch Neurol **8**: 471-480.
- Feng, J., J. Yan, et al. (2002). "Comprehensive mutation scanning of the dystrophin gene in patients with nonsyndromic X-linked dilated cardiomyopathy." Journal of the American College of Cardiology **40**(6): 1120-1124.
- Fertleman, C. R., M. D. Baker, et al. (2006). "SCN9A mutations in paroxysmal extreme pain disorder: allelic variants underlie distinct channel defects and phenotypes." Neuron **52**(5): 767-774.
- Fialho, D., S. Schorge, et al. (2007). "Chloride channel myotonia: exon 8 hot-spot for dominant-negative interactions." Brain **130**: 3265-3274.
- Fontaine, B., T. S. Khurana, et al. (1990). "HYPERKALEMIC PERIODIC PARALYSIS AND THE ADULT MUSCLE SODIUM-CHANNEL ALPHA-SUBUNIT GENE." Science **250**(4983): 1000-1002.
- Fontaine, B., J. Valesantos, et al. (1994). "MAPPING OF THE HYPOKALEMIC PERIODIC PARALYSIS (HYPOPP) LOCUS TO CHROMOSOME 1Q31-32 IN 3 EUROPEAN FAMILIES." Nature Genetics **6**(3): 267-272.
- Forssman, H. (1961). "HEREDITARY DISORDER CHARACTERIZED BY ATTACKS OF MUSCULAR CONTRACTIONS, INDUCED BY ALCOHOL AMONGST OTHER FACTORS." Acta Medica Scandinavica **170**(5): 517-+.
- Fujii, H. and A. Yoshida (1980). "Molecular abnormality of phosphoglycerate kinase-Uppsala associated with chronic nonspherocytic hemolytic anemia." Proc Natl Acad Sci U S A **77**(9): 5461-5465.
- Furby, A., S. Vicart, et al. (2014). "Heterozygous CLCN1 mutations can modulate phenotype in sodium channel myotonia." Neuromuscular Disorders **24**(11): 953-959.
- Furman, R. E. and R. L. Barchi (1978). "PATHOPHYSIOLOGY OF MYOTONIA PRODUCED BY AROMATIC CARBOXYLIC-ACIDS." Annals of Neurology **4**(4): 357-365.

- Gancher, S. T. and J. G. Nutt (1986). "Autosomal dominant episodic ataxia: a heterogeneous syndrome." Mov Disord **1**(4): 239-253.
- Gardiner, A. R., K. P. Bhatia, et al. (2012). "PRRT2 gene mutations: from paroxysmal dyskinesia to episodic ataxia and hemiplegic migraine." Neurology **79**(21): 2115-2121.
- George, A. L., M. A. Crackower, et al. (1993). "MOLECULAR-BASIS OF THOMSEN DISEASE (AUTOSOMAL DOMINANT MYOTONIA-CONGENITA)." Nature Genetics **3**(4): 305-310.
- Gerin, I., M. Veiga-da-Cunha, et al. (1997). "Sequence of a putative glucose 6-phosphate translocase, mutated in glycogen storage disease type Ib." FEBS Lett **419**(2-3): 235-238.
- Ghezzi, D., C. Viscomi, et al. (2009). "Paroxysmal non-kinesigenic dyskinesia is caused by mutations of the MR-1 mitochondrial targeting sequence." Hum Mol Genet **18**(6): 1058-1064.
- Gillard, E. F., K. Otsu, et al. (1991). "A substitution of cysteine for arginine 614 in the ryanodine receptor is potentially causative of human malignant hyperthermia." Genomics **11**(3): 751-755.
- Gillies, R. L., A. R. Bjorksten, et al. (2008). "Identification of genetic mutations in Australian malignant hyperthermia families using sequencing of RYR1 hotspots." Anaesth Intensive Care **36**(3): 391-403.
- Goldfarb, L. G., P. Vicart, et al. (2004). Desmin myopathy.
- Goldstein, J., S. Austin, et al. Phosphorylase Kinase Deficiency.
- Gonsalves, S. G., D. Ng, et al. (2013). "Using exome data to identify malignant hyperthermia susceptibility mutations." Anesthesiology **119**(5): 1043-1053.
- Gordon, J. W., G. A. Scangos, et al. (1980). "Genetic transformation of mouse embryos by microinjection of purified DNA." Proceedings of the National Academy of Sciences **77**(12): 7380-7384.
- Graves, E. J. and B. S. Gillum (1997). "Detailed diagnoses and procedures, National Hospital Discharge Survey, 1995." Vital Health Stat **13**(130): 1-146.
- Graves, T. D., S. Rajakulendran, et al. (2010). "Nongenetic factors influence severity of episodic ataxia type 1 in monozygotic twins." Neurology **75**(4): 367-372.
- Graves, T. D., S. Rajakulendran, et al. (2010). "Nongenetic factors influence severity of episodic ataxia type 1 in monozygotic twins." Neurology **75**(4): 367-372.
- Green, D. S., L. J. Hayward, et al. (1997). "A proposed mutation, Val781Ile, associated with hyperkalemic periodic paralysis and cardiac dysrhythmia is a benign polymorphism." Ann Neurol **42**(2): 253-256.
- Groom, L., S. M. Muldoon, et al. (2011). "Identical de novo mutation in the type 1 ryanodine receptor gene associated with fatal, stress-induced malignant hyperthermia in two unrelated families." Anesthesiology **115**(5): 938-945.
- Grunert, S. C. (2014). "Clinical and genetical heterogeneity of late-onset multiple acyl-coenzyme A dehydrogenase deficiency." Orphanet J Rare Dis **9**(117): 014-0117.
- Gudkova, A., A. Kostareva, et al. (2013). "Diagnostic Challenge in Desmin Cardiomyopathy With Transformation of Clinical Phenotypes." Pediatric Cardiology **34**(2): 467-470.
- Guth, L. M. and S. M. Roth (2013). "Genetic influence on athletic performance." Curr Opin Pediatr **25**(6): 653-658.
- Han, R. and K. P. Campbell (2007). "Dysferlin and muscle membrane repair." Current Opinion in Cell Biology **19**(4): 409-416.
- Haruna, Y., A. Kobori, et al. (2007). "Genotype-Phenotype Correlations of KCNJ2 Mutations in Japanese Patients With Andersen-Tawil Syndrome." Human Mutation **28**(2).
- Hayashi, T., T. Arimura, et al. (2004). "Identification and functional analysis of a caveolin-3 mutation associated with familial hypertrophic cardiomyopathy." Biochemical and Biophysical Research Communications **313**(1): 178-184.

- Head, S. R., H. K. Komori, et al. (2014). "Library construction for next-generation sequencing: overviews and challenges." Biotechniques **56**(2): 61-64.
- Heinemann, S. H., H. Terlau, et al. (1992). "Calcium channel characteristics conferred on the sodium channel by single mutations." Nature **356**(6368): 441-443.
- Heled, Y., M. S. Bloom, et al. (2007). CM-MM and ACE genotypes and physiological prediction of the creatine kinase response to exercise.
- Helliwell, T. R., A. R. T. Green, et al. (1994). "Hereditary distal myopathy with granulo-filamentous cytoplasmic inclusions containing desmin, dystrophin and vimentin." Journal of the Neurological Sciences **124**(2): 174-187.
- Hendrickx, J., P. Coucke, et al. (1995). "Mutations in the phosphorylase kinase gene PHKA2 are responsible for X-linked liver glycogen storage disease." Hum Mol Genet **4**(1): 77-83.
- Heron, S. E. and L. M. Dibbens (2013). "Role of PRRT2 in common paroxysmal neurological disorders: a gene with remarkable pleiotropy." Journal of Medical Genetics **50**(3): 133-139.
- Hers, H. G. (1959). "[Enzymatic studies of hepatic fragments; application to the classification of glycogenoses]." Rev Int Hepatol **9**(1): 35-55.
- Hicks, D., A. Sarkozy, et al. (2011). A founder mutation in Anoctamin 5 is a major cause of limb girdle muscular dystrophy.
- Hubal, M. J., J. M. Devaney, et al. (2010). CCL2 and CCR2 polymorphisms are associated with markers of exercise-induced skeletal muscle damage.
- Human Genome Sequencing, C. (2004). "Finishing the euchromatic sequence of the human genome." Nature **431**(7011): 931-945.
- Hwang, J. H., F. Zorzato, et al. (2012). "Mapping domains and mutations on the skeletal muscle ryanodine receptor channel." Trends in Molecular Medicine **18**(11): 644-657.
- Imbrici, P., M. C. D'Adamo, et al. (2011). "Episodic ataxia type 1 mutations affect fast inactivation of K⁺ channels by a reduction in either subunit surface expression or affinity for inactivation domain." American Journal of Physiology-Cell Physiology **300**(6): C1314-C1322.
- Indo, Y., R. Glassberg, et al. (1991). "Molecular characterization of variant alpha-subunit of electron transfer flavoprotein in three patients with glutaric acidemia type II--and identification of glycine substitution for valine-157 in the sequence of the precursor, producing an unstable mature protein in a patient." Am J Hum Genet **49**(3): 575-580.
- Isackson, P. J., M. J. Bennett, et al. (2006). "Identification of 16 new disease-causing mutations in the CPT2 gene resulting in carnitine palmitoyltransferase II deficiency." Molecular Genetics and Metabolism **89**(4): 323-331.
- James Kew, C. D. (2010). Ion channels from structure to function.
- Jarvie, T. (2005). "Next generation sequencing technologies." Drug Discovery Today: Technologies **2**(3): 255-260.
- Jen, J. C. (2008). "Hereditary Episodic Ataxias." Year in Neurology 2008 **1142**: 250-253.
- Jen, J. C., J. Wan, et al. (2005). "Mutation in the glutamate transporter EAAT1 causes episodic ataxia, hemiplegia, and seizures." Neurology **65**(4): 529-534.
- Jensen, M. Ø., V. Jogini, et al. (2012). "Mechanism of Voltage Gating in Potassium Channels." Science **336**(6078): 229-233.
- Jiang, Y., A. Lee, et al. (2002). "Crystal structure and mechanism of a calcium-gated potassium channel." Nature **417**(6888): 515-522.
- Jodice, C., E. Mantuano, et al. (1997). "Episodic ataxia type 2 (EA2) and spinocerebellar ataxia type 6 (SCA6) due to CAG repeat expansion in the CACNA1A gene on chromosome 19p." Hum Mol Genet **6**(11): 1973-1978.
- Jurkat-Rott, K. and F. Lehmann-Horn (2007). "Genotype-phenotype correlation and therapeutic rationale in hyperkalemic periodic paralysis." Neurotherapeutics **4**(2): 216-224.

- Kallioniemi, A., O.-P. Kallioniemi, et al. (1992). "Comparative Genomic Hybridization for Molecular Cytogenetic Analysis of Solid Tumors." Science **258**(5083): 818-821.
- Kanno, T., K. Sudo, et al. (1980). "Hereditary deficiency of lactate dehydrogenase M-subunit." Clin Chim Acta **108**(2): 267-276.
- Kassardjian, C. and M. Milone (2014). "Coexistence of DMPK gene expansion and CLCN1 missense mutation in the same patient." Neurogenetics **15**(3): 213-214.
- Kawabe, K., K. Goto, et al. (2004). "Dysferlin mutation analysis in a group of Italian patients with limb-girdle muscular dystrophy and Miyoshi myopathy." European Journal of Neurology **11**(10): 657-661.
- Ke, T., C. R. Gomez, et al. (2009). "Novel CACNA1S mutation causes autosomal dominant hypokalemic periodic paralysis in a South American family." J Hum Genet **54**(11): 660-664.
- Keating, K. E., K. A. Quane, et al. (1994). "Detection of a novel RYR1 mutation in four malignant hyperthermia pedigrees." Hum Mol Genet **3**(10): 1855-1858.
- Kerber, K. A., J. C. Jen, et al. (2007). "A new episodic ataxia syndrome with linkage to chromosome 19q13." Arch Neurol **64**(5): 749-752.
- Kertesz, A. (1967). "Paroxysmal kinesigenic choreoathetosis. An entity within the paroxysmal choreoathetosis syndrome. Description of 10 cases, including 1 autopsied." Neurology **17**(7): 680-690.
- Kikuchi, T., M. Nomura, et al. (2007). "Paroxysmal kinesigenic choreoathetosis (PKC): confirmation of linkage to 16p11-q21, but unsuccessful detection of mutations among 157 genes at the PKC-critical region in seven PKC families." Journal of human genetics **52**(4): 334-341.
- Kimura, H., J. Zhou, et al. (2012). "Phenotype Variability in Patients Carrying KCNJ2 Mutations." Circulation-Cardiovascular Genetics **5**(3): 344-353.
- Kishi, H., T. Mukai, et al. (1987). "Human aldolase A deficiency associated with a hemolytic anemia: thermolabile aldolase due to a single base mutation." Proc Natl Acad Sci U S A **84**(23): 8623-8627.
- Klein, A., S. Lillis, et al. (2012). "Clinical and genetic findings in a large cohort of patients with ryanodine receptor 1 gene-associated myopathies." Human Mutation **33**(6): 981-988.
- Klein, R. J., C. Zeiss, et al. (2005). "Complement Factor H Polymorphism in Age-Related Macular Degeneration." Science **308**(5720): 385-389.
- Koch, M. C., K. Baumbach, et al. (1995). "Paramyotonia congenita without paralysis on exposure to cold: a novel mutation in the SCN4A gene (Val1293Ile)." Neuroreport **6**(15): 2001-2004.
- Koch, M. C., K. Ricker, et al. (1991). "LINKAGE DATA SUGGESTING ALLELIC HETEROGENEITY FOR PARAMYOTONIA-CONGENITA AND HYPERKALEMIC PERIODIC PARALYSIS ON CHROMOSOME-17." Human Genetics **88**(1): 71-74.
- Koch, M. C., K. Steinmeyer, et al. (1992). "THE SKELETAL-MUSCLE CHLORIDE CHANNEL IN DOMINANT AND RECESSIVE HUMAN MYOTONIA." Science **257**(5071): 797-800.
- Kollberg, G., M. Tulinius, et al. (2007). "Cardiomyopathy and exercise intolerance in muscle glycogen storage disease 0." N Engl J Med **357**(15): 1507-1514.
- Kouloumenta, A., M. Mavroidis, et al. (2007). "Proper Perinuclear Localization of the TRIM-like Protein Myospryn Requires Its Binding Partner Desmin." Journal of Biological Chemistry **282**(48): 35211-35221.
- Krahn, M., C. Bérout, et al. (2009). "Analysis of the DYSF mutational spectrum in a large cohort of patients." Human Mutation **30**(2): E345-E375.
- Kubisch, C., T. Schmidt-Rose, et al. (1998). "ClC-1 chloride channel mutations in myotonia congenita: variable penetrance of mutations shifting the voltage dependence." Hum Mol Genet **7**(11): 1753-1760.
- Kubisch, C., B. C. Schroeder, et al. (1999). "KCNQ4, a novel potassium channel expressed in sensory outer hair cells, is mutated in dominant deafness." Cell **96**(3): 437-446.

- Kubota, T., X. Roca, et al. (2011). "A mutation in a rare type of intron in a sodium-channel gene results in aberrant splicing and causes myotonia." Human Mutation **32**(7): 773-782.
- Kullmann, D. N. (2010). "Neurological Channelopathies." Annual Review of Neuroscience, Vol 33 **33**: 151-172.
- LaDuca, H., A. J. Stuenkel, et al. (2014). "Utilization of multigene panels in hereditary cancer predisposition testing: analysis of more than 2,000 patients." Genet Med **16**(11): 830-837.
- Lafreniere, R. G., M. Z. Cader, et al. (2010). "A dominant-negative mutation in the TRESK potassium channel is linked to familial migraine with aura." Nature Medicine **16**(10): 1157-U1501.
- Lagier-Tourenne, C., L. Tranebjaerg, et al. (2003). "Homozygosity mapping of Marinesco-Sjogren syndrome to 5q31." Eur J Hum Genet **11**(10): 770-778.
- Lahoria, R., T. L. Winder, et al. (2014). "Novel ANO5 homozygous microdeletion causing myalgia and unprovoked rhabdomyolysis in an Arabic man." Muscle & Nerve **50**(4): 610-613.
- Lance, J. W. (1977). "FAMILIAL PAROXYSMAL DYSTONIC CHOREOATHETOSIS AND ITS DIFFERENTIATION FROM RELATED SYNDROMES." Annals of Neurology **2**(4): 285-293.
- Lee, E. and N. Chahin A patient with mutation in the SCN4A p.M1592v presenting with fixed weakness, rhabdomyolysis, and episodic worsening of weakness, Muscle Nerve. 2013 Aug;48(2):306-7. doi: 10.1002/mus.23803. Epub 2013 Jun 26.
- Lee, H.-y., Y.-H. Fu, et al. (2015). "Episodic and Electrical Nervous System Disorders Caused by Nonchannel Genes." Annual Review of Physiology **77**(1): null.
- Lee, H.-Y., Y. Huang, et al. (2012). "Mutations in the Gene PRRT2 Cause Paroxysmal Kinesigenic Dyskinesia with Infantile Convulsions." **1**(1): 2-12.
- Lee, H. Y., Y. Xu, et al. (2004). "The gene for paroxysmal non-kinesigenic dyskinesia encodes an enzyme in a stress response pathway." Hum Mol Genet **13**(24): 3161-3170.
- Lee, Y. C., A. Durr, et al. (2012). "Mutations in KCND3 cause spinocerebellar ataxia type 22." Ann Neurol **72**(6): 859-869.
- Leen, W. G., J. Klepper, et al. (2010). "Glucose transporter-1 deficiency syndrome: the expanding clinical and genetic spectrum of a treatable disorder." Brain **133**: 655-670.
- Leen, W. G., J. Klepper, et al. (2010). "Glucose transporter-1 deficiency syndrome: the expanding clinical and genetic spectrum of a treatable disorder." Brain **133**(Pt 3): 655-670.
- Lei, K. J., L. L. Shelly, et al. (1993). "Mutations in the glucose-6-phosphatase gene that cause glycogen storage disease type 1a." Science **262**(5133): 580-583.
- Leipold, E., L. Liebmann, et al. (2013). "A de novo gain-of-function mutation in SCN11A causes loss of pain perception." Nat Genet **45**(11): 1399-1404.
- Lenk, U., R. Hanke, et al. (1994). "Carrier detection in DMD families with point mutations, using PCR-SSCP and direct sequencing." Neuromuscular Disorders **4**(5-6): 411-418.
- Levano, S., M. Vukcevic, et al. (2009). "Increasing the number of diagnostic mutations in malignant hyperthermia." Human Mutation **30**(4): 590-598.
- Li, J. Y., X. L. Zhu, et al. (2012). "Targeted genomic sequencing identifies PRRT2 mutations as a cause of paroxysmal kinesigenic choreoathetosis." Journal of Medical Genetics **49**(2): 76-78.
- Lim, K. H., L. Ferraris, et al. (2011). "Using positional distribution to identify splicing elements and predict pre-mRNA processing defects in human genes." Proc Natl Acad Sci U S A **108**(27): 11093-11098.
- Lindberg, C., C. Sixt, et al. (2012). "Episodes of exercise-induced dark urine and myalgia in LGMD 2I." Acta Neurologica Scandinavica **125**(4): 285-287.

- Liu, Q., Z. Qi, et al. (2012). "Mutations in PRRT2 result in paroxysmal dyskinesias with marked variability in clinical expression." Journal of Medical Genetics **49**(2): 79-82.
- Looi, R. Y., K. J. Goh, et al. (2010). "P1.21 Genetic mutations in dysferlinopathy in a Malaysian population." Neuromuscular Disorders **20**(9–10): 606.
- Ma, L., D. Roman-Campos, et al. (2013). "A novel channelopathy in pulmonary arterial hypertension." N Engl J Med **369**(4): 351-361.
- Maekawa, M., K. Sudo, et al. (1990). "Molecular characterization of genetic mutation in human lactate dehydrogenase-A (M) deficiency." Biochemical and Biophysical Research Communications **168**(2): 677-682.
- Maichele, A. J., B. Burwinkel, et al. (1996). "Mutations in the testis/liver isoform of the phosphorylase kinase gamma subunit (PHKG2) cause autosomal liver glycogenosis in the gsd rat and in humans." Nat Genet **14**(3): 337-340.
- Malfatti, E., J. Nilsson, et al. (2014). "A new muscle glycogen storage disease associated with glycogenin-1 deficiency." Annals of Neurology **76**(6): 891-898.
- Mamoune, A., M. Bahuau, et al. (2014). "A thermolabile aldolase A mutant causes fever-induced recurrent rhabdomyolysis without hemolytic anemia." PLoS Genet **10**(11).
- Manning, B. M., K. A. Quane, et al. (1998). "Identification of Novel Mutations in the Ryanodine-Receptor Gene (RYR1) in Malignant Hyperthermia: Genotype-Phenotype Correlation." The American Journal of Human Genetics **62**(3): 599-609.
- Marchant, C. L., F. R. Ellis, et al. (2004). "Mutation analysis of two patients with hypokalemic periodic paralysis and suspected malignant hyperthermia." Muscle & Nerve **30**(1): 114-117.
- Martiniuk, F., M. Bodkin, et al. (1990). "Identification of the base-pair substitution responsible for a human acid alpha glucosidase allele with lower "affinity" for glycogen (GAA 2) and transient gene expression in deficient cells." Am J Hum Genet **47**(3): 440-445.
- Marziali, A. and M. Akeson (2001). "New DNA sequencing methods." Annu Rev Biomed Eng **3**: 195-223.
- Matthews, E., D. Fialho, et al. (2010). "The non-dystrophic myotonias: molecular pathogenesis, diagnosis and treatment." Brain **133**: 9-22.
- Matthews, E., R. Labrum, et al. (2009). "Voltage sensor charge loss accounts for most cases of hypokalemic periodic paralysis." Neurology **72**(18): 1544-1547.
- Mc, A. B. (1951). "Myopathy due to a defect in muscle glycogen breakdown." Clin Sci **10**(1): 13-35.
- McClatchey, A. I., D. McKenna-Yasek, et al. (1992). "Novel mutations in families with unusual and variable disorders of the skeletal muscle sodium channel." Nat Genet **2**(2): 148-152.
- McClatchey, A. I., J. Trofatter, et al. (1992). "DINUCLEOTIDE REPEAT POLYMORPHISMS AT THE SCN4A LOCUS SUGGEST ALLELIC HETEROGENEITY OF HYPERKALEMIC PERIODIC PARALYSIS AND PARAMYOTONIA-CONGENITA." American Journal of Human Genetics **50**(5): 896-901.
- McClatchey, A. I., P. Van den Bergh, et al. (1992). "Temperature-sensitive mutations in the III–IV cytoplasmic loop region of the skeletal muscle sodium channel gene in paramyotonia congenita." Cell **68**(4): 769-774.
- McNally, E. M., E. de Sá Moreira, et al. (1998). "Caveolin-3 in Muscular Dystrophy." Human Molecular Genetics **7**(5): 871-877.
- Meyerkleine, C., K. Steinmeyer, et al. (1995). "SPECTRUM OF MUTATIONS IN THE MAJOR HUMAN SKELETAL-MUSCLE CHLORIDE CHANNEL GENE (CLCNUI) LEADING TO MYOTONIA." American Journal of Human Genetics **57**(6): 1325-1334.

- Miceli, F., M. V. Soldovieri, et al. (2008). "Gating consequences of charge neutralization of arginine residues in the S4 segment of K(v)7.2, an epilepsy-linked K⁺ channel subunit." *Biophys J* **95**(5): 2254-2264.
- Michot, C., L. Hubert, et al. (2010). "LPIN1 gene mutations: a major cause of severe rhabdomyolysis in early childhood." *Human Mutation* **31**(7): E1564-E1573.
- Milasin, J., F. Muntoni, et al. (1996). "A point mutation in the 5' splice site of the dystrophin gene first intron responsible for X-linked dilated cardiomyopathy." *Hum Mol Genet* **5**(1): 73-79.
- Miller, T. M., M. R. D. da Silva, et al. (2004). "Correlating phenotype and genotype in the periodic paralyses." *Neurology* **63**(9): 1647-1655.
- Milone, M., T. Liewluck, et al. (2012). "Amyloidosis and exercise intolerance in ANO5 muscular dystrophy." *Neuromuscular Disorders* **22**(1): 13-15.
- Minetti, C., F. Sotgia, et al. (1998). "Mutations in the caveolin-3 gene cause autosomal dominant limb-girdle muscular dystrophy." *Nat Genet* **18**(4): 365-368.
- Mizuta, K., S. Tsutsumi, et al. (2007). "Molecular characterization of GDD1/TMEM16E, the gene product responsible for autosomal dominant gnathodiaphyseal dysplasia." *Biochemical and Biophysical Research Communications* **357**(1): 126-132.
- Mohapatra, B., S. Jimenez, et al. (2003). "Mutations in the muscle LIM protein and α -actinin-2 genes in dilated cardiomyopathy and endocardial fibroelastosis." *Molecular Genetics and Metabolism* **80**(1-2): 207-215.
- Monaco, A. P., C. J. Bertelson, et al. (1988). "An explanation for the phenotypic differences between patients bearing partial deletions of the DMD locus." *Genomics* **2**(1): 90-95.
- Monnier, N., V. Procaccio, et al. (1997). "Malignant-hyperthermia susceptibility is associated with a mutation of the alpha 1-subunit of the human dihydropyridine-sensitive L-type voltage-dependent calcium-channel receptor in skeletal muscle." *Am J Hum Genet* **60**(6): 1316-1325.
- Moody, S. and P. Mancias (2013). "Dysferlinopathy Presenting as Rhabdomyolysis and Acute Renal Failure." *Journal of Child Neurology* **28**(4): 502-505.
- Moreau, A., P. Gosselin-Badaroudine, et al. (2015). "Gating pore currents are defects in common with two Nav1.5 mutations in patients with mixed arrhythmias and dilated cardiomyopathy." *The Journal of General Physiology* **145**(2): 93-106.
- Morton, N. E. (1955). "Sequential tests for the detection of linkage." *American Journal of Human Genetics* **7**(3): 277-318.
- Mosharov, E. V., A. Borgkvist, et al. (2015). "Presynaptic effects of levodopa and their possible role in dyskinesia." *Movement Disorders* **30**(1): 45-53.
- Moslehi, R., S. Langlois, et al. (1998). "Linkage of malignant hyperthermia and hyperkalemic periodic paralysis to the adult skeletal muscle sodium channel (SCN4A) gene in a large pedigree." *American Journal of Medical Genetics* **76**(1): 21-27.
- Moslemi, A. R., C. Lindberg, et al. (2010). "Glycogenin-1 deficiency and inactivated priming of glycogen synthesis." *N Engl J Med* **362**(13): 1203-1210.
- Mount, L. A. and S. Reback (1940). "Familial paroxysmal choreoathetosis - Preliminary report on a hitherto undescribed clinical syndrome." *Archives of Neurology and Psychiatry* **44**(4): 841-847.
- Muntoni, F., M. Cau, et al. (1993). "Deletion of the Dystrophin Muscle-Promoter Region Associated with X-Linked Dilated Cardiomyopathy." *New England Journal of Medicine* **329**(13): 921-925.
- Musumeci, O., S. Brady, et al. (2014). "Recurrent rhabdomyolysis due to muscle β -enolase deficiency: very rare or underestimated?" *Journal of Neurology* **261**(12): 2424-2428.
- Musumeci, O., C. Bruno, et al. (2012). "Clinical features and new molecular findings in muscle phosphofructokinase deficiency (GSD type VII)." *Neuromuscular Disorders* **22**(4): 325-330.

- Nakajima, H., N. Kono, et al. (1990). "Genetic defect in muscle phosphofructokinase deficiency. Abnormal splicing of the muscle phosphofructokinase gene due to a point mutation at the 5'-splice site." Journal of Biological Chemistry **265**(16): 9392-9395.
- Nance, J. R. and A. L. Mammen (2015). "Diagnostic evaluation of rhabdomyolysis." Muscle & Nerve: n/a-n/a.
- Neville, B. G. R., F. M. C. Besag, et al. (1998). "Exercise induced steroid dependent dystonia, ataxia, and alternating hemiplegia associated with epilepsy." Journal of Neurology Neurosurgery and Psychiatry **65**(2): 241-244.
- Ng, P. C. and S. Henikoff (2001). "Predicting deleterious amino acid substitutions." Genome Research **11**(5): 863-874.
- Ng, S. B., E. H. Turner, et al. (2009). "Targeted capture and massively parallel sequencing of 12 human exomes." Nature **461**(7261): 272-276.
- Nguyen, K., G. Bassez, et al. (2005). "Dysferlin mutations in LGMD2B, Miyoshi myopathy, and atypical dysferlinopathies." Human Mutation **26**(2): 165-165.
- Nguyen, K., G. Bassez, et al. (2007). "Phenotypic study in 40 patients with dysferlin gene mutations: High frequency of atypical phenotypes." Archives of Neurology **64**(8): 1176-1182.
- Norman, B., M. Esbjörnsson, et al. (2014). ACTN3 genotype and modulation of skeletal muscle response to exercise in human subjects.
- North, K. N., N. Yang, et al. (1999). "A common nonsense mutation results in [alpha]-actinin-3 deficiency in the general population." Nat Genet **21**(4): 353-354.
- Ohshiro-Sasaki, A., H. Shimbo, et al. (2014). "A three-year-old boy with glucose transporter type 1 deficiency syndrome presenting with episodic ataxia." Pediatr Neurol **50**(1): 99-100.
- Okano, H. and S. Yamanaka (2014). "iPS cell technologies: significance and applications to CNS regeneration and disease." Mol Brain **7**(22): 1756-6606.
- Okuda, S., F. Kanda, et al. (2001). "Hyperkalemic periodic paralysis and paramyotonia congenita – A novel sodium channel mutation –." Journal of Neurology **248**(11): 1003-1004.
- Olson, T. M., A. E. Alekseev, et al. (2006). "Kv1.5 channelopathy due to KCNA5 loss-of-function mutation causes human atrial fibrillation." Hum Mol Genet **15**(14): 2185-2191.
- Ophoff, R. A., G. M. Terwindt, et al. (1996). "Familial hemiplegic migraine and episodic ataxia type-2 are caused by mutations in the Ca²⁺ channel gene CACNL1A4." Cell **87**(3): 543-552.
- Ophoff, R. A., G. M. Terwindt, et al. (1996). "Familial hemiplegic migraine and episodic ataxia type-2 are caused by mutations in the Ca²⁺ channel gene CACNL1A4." Cell **87**(3): 543-552.
- Orho, M., N. U. Bosshard, et al. (1998). "Mutations in the liver glycogen synthase gene in children with hypoglycemia due to glycogen storage disease type 0." Journal of Clinical Investigation **102**(3): 507-515.
- Panoutsopoulou, K., I. Tachmazidou, et al. (2013). "In search of low-frequency and rare variants affecting complex traits." Human Molecular Genetics **22**(R1): R16-R21.
- Papponen, H., T. Toppinen, et al. (1999). "Founder mutations and the high prevalence of myotonia congenita in northern Finland." Neurology **53**(2): 297-302.
- Pearson, T., C. Akman, et al. (2013). "Phenotypic Spectrum of Glucose Transporter Type 1 Deficiency Syndrome (Glut1 DS)." Current Neurology and Neuroscience Reports **13**(4): 1-9.
- Pearson, T. A. and T. A. Manolio (2008). "How to interpret a genome-wide association study." Jama **299**(11): 1335-1344.
- Peltonen, L. and V. A. McKusick (2001). "Dissecting Human Disease in the Postgenomic Era." Science **291**(5507): 1224-1229.
- Peroz, D., N. Rodriguez, et al. (2008). "Kv7.1 (KCNQ1) properties and channelopathies." J Physiol **586**(7): 1785-1789.

- Pirone, A., J. Schredelseker, et al. (2010). Identification and functional characterization of malignant hyperthermia mutation T1354S in the outer pore of the Cav α 1S-subunit.
- Piton, A., C. Redin, et al. (2013). "XLID-causing mutations and associated genes challenged in light of data from large-scale human exome sequencing." Am J Hum Genet **93**(2): 368-383.
- Plassart-Schiess, E., L. Lhuillier, et al. (1998). "Functional expression of the Ile693Thr Na⁺ channel mutation associated with paramyotonia congenita in a human cell line." The Journal of Physiology **507**(3): 721-727.
- Pompe, J. C. (1932). "Over idiopathische hypertrophie van het hart." Ned. Tijdschr. Geneesk **76**: 304-312.
- Pons, R., E. Cuenca-León, et al. (2012). "Paroxysmal non-kinesigenic dyskinesia due to a PNKD recurrent mutation: Report of two Southern European families." European Journal of Paediatric Neurology **16**(1): 86-89.
- Poujois, A., J. C. Antoine, et al. Chronic neuromyotonia as a phenotypic variation associated with a new mutation in the KCNA1 gene, J Neurol. 2006 Jul;253(7):957-9. Epub 2006 Mar 6.
- Prelich, G. (2012). "Gene Overexpression: Uses, Mechanisms, and Interpretation." Genetics **190**(3): 841-854.
- Priori, S. G., C. Napolitano, et al. (2001). "Mutations in the cardiac ryanodine receptor gene (hRyR2) underlie catecholaminergic polymorphic ventricular tachycardia." Circulation **103**(2): 196-200.
- Protasi, F., C. Paolini, et al. (2002). "Multiple Regions of RyR1 Mediate Functional and Structural Interactions with α 1S-Dihydropyridine Receptors in Skeletal Muscle." Biophysical Journal **83**(6): 3230-3244.
- Ptacek, L. J., A. George, et al. (1992). "MUTATIONS IN AN S4 SEGMENT OF THE ADULT SKELETAL-MUSCLE SODIUM-CHANNEL CAUSE PARAMYOTONIA-CONGENITA." Neurology **42**(7): 1425-1425.
- Ptacek, L. J., A. L. George, Jr., et al. (1991). "Identification of a mutation in the gene causing hyperkalemic periodic paralysis." Cell **67**(5): 1021-1027.
- Purevsuren, J., T. Fukao, et al. (2009). "Clinical and molecular aspects of Japanese patients with mitochondrial trifunctional protein deficiency." Molecular Genetics and Metabolism **98**(4): 372-377.
- Rabbani, B., N. Mahdieh, et al. (2012). "Next-generation sequencing: impact of exome sequencing in characterizing Mendelian disorders." J Hum Genet **57**(10): 621-632.
- Rabbani, B., M. Tekin, et al. (2014). "The promise of whole-exome sequencing in medical genetics." J Hum Genet **59**(1): 5-15.
- Raben, N., R. Exelbert, et al. (1995). "Functional expression of human mutant phosphofructokinase in yeast: genetic defects in French Canadian and Swiss patients with phosphofructokinase deficiency." American Journal of Human Genetics **56**(1): 131-141.
- Rainier, S., D. Thomas, et al. (2004). "Myofibrillogenesis regulator 1 gene mutations cause paroxysmal dystonic choreoathetosis." Archives of Neurology **61**(7): 1025-1029.
- Raouf, R., K. Quick, et al. (2010). "Pain as a channelopathy." Journal of Clinical Investigation **120**(11): 3745-3752.
- Rayan, D. L. R. and M. G. Hanna (2010). "Skeletal muscle channelopathies: nondystrophic myotonias and periodic paralysis." Current Opinion in Neurology **23**(5): 466-476.
- Rayan, D. L. R., A. Haworth, et al. (2012). "A new explanation for recessive myotonia congenita Exon deletions and duplications in CLCN1." Neurology **78**(24): 1953-1958.
- Rehm, H. L. (2013). "Disease-targeted sequencing: a cornerstone in the clinic." Nat Rev Genet **14**(4): 295-300.

- Remme, C. A. (2013). "Cardiac sodium channelopathy associated with SCN5A mutations: electrophysiological, molecular and genetic aspects." J Physiol **591**(Pt 17): 4099-4116.
- Rios, E. and G. Brum (1987). "Involvement of dihydropyridine receptors in excitation-contraction coupling in skeletal muscle." Nature **325**(6106): 717-720.
- Risch, N. and K. Merikangas (1996). "The Future of Genetic Studies of Complex Human Diseases." Science **273**(5281): 1516-1517.
- Rosales, X. Q., J. M. Gastier-Foster, et al. (2010). "Novel diagnostic features of dysferlinopathies." Muscle & Nerve **42**(1): 14-21.
- Rosenberg, H., M. Davis, et al. (2007). "Malignant hyperthermia." Orphanet J Rare Dis **2**: 21.
- Rosenfeld, J., K. Sloan-Brown, et al. (1997). "A novel muscle sodium channel mutation causes painful congenital myotonia." Annals of Neurology **42**(5): 811-814.
- Rotstein, M., K. Engelstad, et al. (2010). "Glut1 deficiency: Inheritance pattern determined by haploinsufficiency." Annals of Neurology **68**(6): 955-958.
- Rozen, S. and H. Skaletsky (2000). "Primer3 on the WWW for general users and for biologist programmers." Methods in molecular biology (Clifton, N.J.) **132**: 365-386.
- Ryan, D. P., M. R. D. da Silva, et al. (2010). "Mutations in Potassium Channel Kir2.6 Cause Susceptibility to Thyrotoxic Hypokalemic Periodic Paralysis." Cell **140**(1): 88-98.
- Sambuughin, N., J. Capacchione, et al. (2009). "The ryanodine receptor type 1 gene variants in African American men with exertional rhabdomyolysis and malignant hyperthermia susceptibility." Clinical Genetics **76**(6): 564-568.
- Sanaker, P. S., M. Toompuu, et al. (2010). "Differences in RNA processing underlie the tissue specific phenotype of ISCU myopathy." Biochimica et Biophysica Acta (BBA) - Molecular Basis of Disease **1802**(6): 539-544.
- Sanger, F., S. Nicklen, et al. (1977). "DNA sequencing with chain-terminating inhibitors." Proceedings of the National Academy of Sciences of the United States of America **74**(12): 5463-5467.
- Sather, W. A. and E. W. McCleskey (2003). "Permeation and selectivity in calcium channels." Annu Rev Physiol **65**: 133-159.
- Scalco, R., A. Gardiner, et al. (2015). "Rhabdomyolysis: a genetic perspective." Orphanet Journal of Rare Diseases **10**(1): 51.
- Schlingmann, K. P., M. Konrad, et al. (2004). "Salt wasting and deafness resulting from mutations in two chloride channels." N Engl J Med **350**(13): 1314-1319.
- Schneider, S. A., C. Paisan-Ruiz, et al. (2009). "GLUT1 gene mutations cause sporadic paroxysmal exercise-induced dyskinesias." Mov Disord **24**(11): 1684-1688.
- Schneiderbanger, D., S. Johannsen, et al. (2014). "Management of malignant hyperthermia: diagnosis and treatment." Ther Clin Risk Manag **10**: 355-362.
- Scholl, U. I., G. Goh, et al. (2013). "Somatic and germline CACNA1D calcium channel mutations in aldosterone-producing adenomas and primary aldosteronism." Nat Genet **45**(9): 1050-1054.
- Schouten, J. P., C. J. McElgunn, et al. (2002). "Relative quantification of 40 nucleic acid sequences by multiplex ligation-dependent probe amplification." Nucleic Acids Research **30**(12): e57.
- Schwarz, J. M., D. N. Cooper, et al. (2014). "MutationTaster2: mutation prediction for the deep-sequencing age." Nat Meth **11**(4): 361-362.
- Sharma, P., S. Ghavami, et al. (2010). " β -Dystroglycan binds caveolin-1 in smooth muscle: a functional role in caveolae distribution and Ca²⁺ release." Journal of Cell Science **123**(18): 3061-3070.
- Shen, J., Y. Bao, et al. (1996). "Mutations in exon 3 of the glycogen debranching enzyme gene are associated with glycogen storage disease type III that is differentially expressed in liver and muscle." Journal of Clinical Investigation **98**(2): 352-357.

- Shen, X.-M., D. Selcen, et al. (2014). "Mutant SNAP25B causes myasthenia, cortical hyperexcitability, ataxia, and intellectual disability." Neurology **83**(24): 2247-2255.
- Shen, Y., W.-P. Ge, et al. (2015). "Protein mutated in paroxysmal dyskinesia interacts with the active zone protein RIM and suppresses synaptic vesicle exocytosis." Proceedings of the National Academy of Sciences **112**(10): 2935-2941.
- Shen, Y. G., H. Y. Lee, et al. (2011). "Mutations in PNKD causing paroxysmal dyskinesia alters protein cleavage and stability." Human Molecular Genetics **20**(12): 2322-2332.
- Shi, C.-h., S.-l. Sun, et al. (2013). "PRRT2 gene mutations in familial and sporadic paroxysmal kinesigenic dyskinesia cases." Movement Disorders **28**(9): 1313-1314.
- Silveira-Moriyama, L., A. R. Gardiner, et al. (2013). "Clinical features of childhood-onset paroxysmal kinesigenic dyskinesia with PRRT2 gene mutations." Dev Med Child Neurol **55**(4): 327-334.
- Simon, D. B., R. S. Bindra, et al. (1997). "Mutations in the chloride channel gene, CLCNKB, cause Bartter's syndrome type III." Nat Genet **17**(2): 171-178.
- Singh, N. A., C. Charlier, et al. (1998). "A novel potassium channel gene, KCNQ2, is mutated in an inherited epilepsy of newborns." Nat Genet **18**(1): 25-29.
- Singh, N. A., C. Pappas, et al. (2009). "A role of SCN9A in human epilepsies, as a cause of febrile seizures and as a potential modifier of Dravet syndrome." PLoS Genet **5**(9): 18.
- Smeitink, J. A., O. Elpeleg, et al. (2006). "Distinct clinical phenotypes associated with a mutation in the mitochondrial translation elongation factor EFTs." Am J Hum Genet **79**(5): 869-877.
- Smith, Bradley N., N. Ticozzi, et al. (2014). "Exome-wide Rare Variant Analysis Identifies TUBA4A Mutations Associated with Familial ALS." Neuron **84**(2): 324-331.
- Sokolov, S., T. Scheuer, et al. (2007). "Gating pore current in an inherited ion channelopathy." Nature **446**(7131): 76-78.
- Solinas-Toldo, S., S. Lampel, et al. (1997). "Matrix-based comparative genomic hybridization: biochips to screen for genomic imbalances." Genes Chromosomes Cancer **20**(4): 399-407.
- Spadafora, P., M. Liguori, et al. (2012). "CAV3 T78M mutation as polymorphic variant in South Italy." Neuromuscular Disorders **22**(7): 669-670.
- Spiekerkoetter, U. (2010). "Mitochondrial fatty acid oxidation disorders: clinical presentation of long-chain fatty acid oxidation defects before and after newborn screening." J Inherit Metab Dis **33**(5): 527-532.
- Spiekerkoetter, U., B. Sun, et al. (2003). "Molecular and phenotypic heterogeneity in mitochondrial trifunctional protein deficiency due to 2-subunit mutations." Human Mutation **21**(6): 598.
- Spiekerkoetter, U., B. Sun, et al. (2003). "Molecular and phenotypic heterogeneity in mitochondrial trifunctional protein deficiency due to β -subunit mutations." Human Mutation **21**(6): 598-607.
- Splawski, I., K. W. Timothy, et al. (2004). "Ca(V)1.2 calcium channel dysfunction causes a multisystem disorder including arrhythmia and autism." Cell **119**(1): 19-31.
- Steckley, J. L., G. C. Ebers, et al. (2001). "An autosomal dominant disorder with episodic ataxia, vertigo, and tinnitus." Neurology **57**(8): 1499-1502.
- Steinmeyer, K., C. Lorenz, et al. (1994). "Multimeric structure of CIC-1 chloride channel revealed by mutations in dominant myotonia congenita (Thomsen)." The EMBO Journal **13**(4): 737-743.
- Stelzl, U., U. Worm, et al. (2005). "A human protein-protein interaction network: A resource for annotating the proteome." Cell **122**(6): 957-968.
- Stewart, W. F., C. Wood, et al. (2008). "Cumulative lifetime migraine incidence in women and men." Cephalalgia **28**(11): 1170-1178.

- Stojkovic, T., J. Vissing, et al. Muscle glycogenosis due to phosphoglucomutase 1 deficiency, *N Engl J Med*. 2009 Jul 23;361(4):425-7. doi: 10.1056/NEJMc0901158.
- Stowell, K. M. (2014). "DNA testing for malignant hyperthermia: the reality and the dream." *Anesth Analg* **118**(2): 397-406.
- Struyk, A. F. and S. C. Cannon (2007). "A Na⁺ channel mutation linked to hypokalemic periodic paralysis exposes a proton-selective gating pore." *Journal of General Physiology* **130**(1): 11-20.
- Stühmer, W. (1998). [16] Electrophysiologic recordings from *Xenopus* oocytes. *Methods in Enzymology*. P. M. Conn, Academic Press. **Volume 293**: 280-300.
- Stunnenberg, B. C., H. B. Ginjaar, et al. (2010). "Isolated eyelid closure myotonia in two families with sodium channel myotonia." *Neurogenetics* **11**(2): 257-260.
- Swoboda, K. J., B. W. Soong, et al. (2000). "Paroxysmal kinesigenic dyskinesia and infantile convulsions - Clinical and linkage studies." *Neurology* **55**(2): 224-230.
- Szczesna, D., J. Zhao, et al. (2002). Phosphorylation of the regulatory light chains of myosin affects Ca²⁺ sensitivity of skeletal muscle contraction.
- Taroni, F., E. Verderio, et al. (1993). "Identification of a common mutation in the carnitine palmitoyltransferase II gene in familial recurrent myoglobinuria patients." *Nat Genet* **4**(3): 314-320.
- Tarui, S., G. Okuno, et al. (1965). "Phosphofructokinase Deficiency in Skeletal Muscle. A New Type of Glycogenosis." *Biochem Biophys Res Commun* **19**: 517-523.
- Tegtmeyer, L. C., S. Rust, et al. (2014). "Multiple Phenotypes in Phosphoglucomutase 1 Deficiency." *New England Journal of Medicine* **370**(6): 533-542.
- Thomas, K. R. and M. R. Capecchi (1987). "Site-directed mutagenesis by gene targeting in mouse embryo-derived stem cells." *Cell* **51**(3): 503-512.
- Thuillier, L., H. Rostane, et al. (2003). "Correlation between genotype, metabolic data, and clinical presentation in carnitine palmitoyltransferase 2 (CPT2) deficiency." *Human Mutation* **21**(5): 493-501.
- Tomlinson, S. E., M. G. Hanna, et al. (2009). "Clinical neurophysiology of the episodic ataxias: Insights into ion channel dysfunction in vivo." *Clinical Neurophysiology* **120**(10): 1768-1776.
- Tonin, P., C. Bruno, et al. (2009). "Unusual presentation of phosphoglycerate mutase deficiency due to two different mutations in PGAM-M gene." *Neuromuscul Disord* **19**(11): 776-778.
- Torbergson, T. (1975). "A family with dominant hereditary myotonia, muscular hypertrophy, and increased muscular irritability, distinct from myotonia congenita thomsen." *Acta Neurol Scand* **51**(3): 225-232.
- Torkamani, A., K. Bersell, et al. (2014). "De novo KCNB1 mutations in epileptic encephalopathy." *Ann Neurol* **76**(4): 529-540.
- Trabzuni, D., M. Ryten, et al. (2011). "Quality control parameters on a large dataset of regionally dissected human control brains for whole genome expression studies." *Journal of Neurochemistry* **119**(2): 275-282.
- Traverso, M., E. Gazzero, et al. (2008). "Caveolin-3 T78M and T78K missense mutations lead to different phenotypes in vivo and in vitro." *Lab Invest* **88**(3): 275-283.
- Trip, J., G. Drost, et al. (2008). "In tandem analysis of CLCN1 and SCN4A greatly enhances mutation detection in families with non-dystrophic myotonia." *Eur J Hum Genet* **16**(8): 921-929.
- Trudeau, M. M., J. C. Dalton, et al. (2006). Heterozygosity for a protein truncation mutation of sodium channel SCN8A in a patient with cerebellar atrophy, ataxia, and mental retardation, *J Med Genet*. 2006 Jun;43(6):527-30. Epub 2005 Oct 19.
- Tsujino, S., L. A. Rubin, et al. (1994). "An A-to-C substitution involving the translation initiation codon in a patient with myophosphorylase deficiency (McArdle's disease)." *Human Mutation* **4**(1): 73-75.

- Tsujino, S., S. Shanske, et al. (1993). "Molecular genetic heterogeneity of myophosphorylase deficiency (McArdle's disease)." N Engl J Med **329**(4): 241-245.
- Tsujino, S., S. Shanske, et al. (1993). "The molecular genetic basis of muscle phosphoglycerate mutase (PGAM) deficiency." Am J Hum Genet **52**(3): 472-477.
- Tuffery-Giraud, S., C. Saquet, et al. (2005). "Mutation spectrum leading to an attenuated phenotype in dystrophinopathies." Eur J Hum Genet **13**(12): 1254-1260.
- Vahedi, K., C. Depienne, et al. (2009). "Elicited repetitive daily blindness A new phenotype associated with hemiplegic migraine and SCN1A mutations." Neurology **72**(13): 1178-1183.
- Valente, E. M., S. D. Spacey, et al. (2000). "A second paroxysmal kinesigenic choreoathetosis locus (EKD2) mapping on 16q13-q22.1 indicates a family of genes which give rise to paroxysmal disorders on human chromosome 16." Brain **123**: 2040-2045.
- van der Kooij, A. J., W. S. Frankhuizen, et al. (2007). "Limb-girdle muscular dystrophy in the Netherlands: Gene defect identified in half the families." Neurology **68**(24): 2125-2128.
- Van Petegem, F. (2015). "Ryanodine Receptors: Allosteric Ion Channel Giants." Journal of Molecular Biology **427**(1): 31-53.
- Vandyke, D. H., R. C. Griggs, et al. (1975). "HEREDITARY MYOKYMIA AND PERIODIC ATAXIA." Journal of the Neurological Sciences **25**(1): 109-118.
- Vanmolkot, K. R. J., E. Babini, et al. (2007). "The novel p.L1649Q mutation in the SCN1A epilepsy gene is associated with familial hemiplegic migraine: genetic and functional studies. Mutation in brief #957. Online." Human Mutation **28**(5): 522.
- Vatta, M., M. J. Ackerman, et al. (2006). "Mutant caveolin-3 induces persistent late sodium current and is associated with long-QT syndrome." Circulation **114**(20): 2104-2112.
- Veeramah, K. R., J. E. O'Brien, et al. (2012). "De novo pathogenic SCN8A mutation identified by whole-genome sequencing of a family quartet affected by infantile epileptic encephalopathy and SUDEP." Am J Hum Genet **90**(3): 502-510.
- Vicart, S., D. Sternberg, et al. (2005). "Human skeletal muscle sodium channelopathies." Neurological Sciences **26**(4): 194-202.
- Vicart, S., D. Sternberg, et al. (2004). "New mutations of SCN4A cause a potassium-sensitive normokalemic periodic paralysis." Neurology **63**(11): 2120-2127.
- Wagner, S., H. Lerche, et al. (1997). "A novel sodium channel mutation causing a hyperkalemic paralytic and paramyotonic syndrome with variable clinical expressivity." Neurology **49**(4): 1018-1025.
- Wang, D., P. Kranz-Eble, et al. (2000). "Mutational analysis of GLUT1 (SLC2A1) in Glut-1 deficiency syndrome." Human Mutation **16**(3): 224-231.
- Wang, D., J. M. Pascual, et al. (2005). "Glut-1 deficiency syndrome: clinical, genetic, and therapeutic aspects." Ann Neurol **57**(1): 111-118.
- Wang, J.-L., L. Cao, et al. (2011). "Identification of PRRT2 as the causative gene of paroxysmal kinesigenic dyskinesias." Brain : a journal of neurology **134**(Pt 12): 3493-3501.
- Wataya, K., J. Akanuma, et al. (1998). "Two CPT2 mutations in three Japanese patients with carnitine palmitoyltransferase II deficiency: Functional analysis and association with polymorphic haplotypes and two clinical phenotypes." Human Mutation **11**(5): 377-386.
- Waters, M. F., N. A. Minassian, et al. (2006). "Mutations in voltage-gated potassium channel KCNC3 cause degenerative and developmental central nervous system phenotypes." Nat Genet **38**(4): 447-451.

- Weber, Y. G., A. Storch, et al. (2008). "GLUT1 mutations are a cause of paroxysmal exertion-induced dyskinesias and induce hemolytic anemia by a cation leak." Journal of Clinical Investigation **118**(6): 2157-2168.
- Wehling, C., C. Beimgraben, et al. (2007). "Self-assembly of the isolated KCNQ2 subunit interaction domain." FEBS Letters **581**(8): 1594-1598.
- Wehner, M., P. R. Clemens, et al. (1994). "Human muscle glycogenosis due to phosphorylase kinase deficiency associated with a nonsense mutation in the muscle isoform of the alpha subunit." Hum Mol Genet **3**(11): 1983-1987.
- William Bateson, E. R. S., R. C. Punnett (1904). Royal Society. Reports to the Evolution committee. Report II. Experimental Studies in the Physiology of Heredity.
- Williams, M. E., L. M. Marubio, et al. (1994). "Structure and functional characterization of neuronal alpha 1E calcium channel subtypes." Journal of Biological Chemistry **269**(35): 22347-22357.
- Wilmshurst, J. M., S. Lillis, et al. (2010). "RYR1 mutations are a common cause of congenital myopathies with central nuclei." Annals of Neurology **68**(5): 717-726.
- Wu, H., J. A. Cowing, et al. (2006). "Mutations in the gene KCNV2 encoding a voltage-gated potassium channel subunit cause "cone dystrophy with supernormal rod electroretinogram" in humans." Am J Hum Genet **79**(3): 574-579.
- Wu, L., H.-D. Tang, et al. (2014). "PRRT2 truncated mutations lead to nonsense-mediated mRNA decay in Paroxysmal Kinesigenic Dyskinesia." Parkinsonism & related disorders **20**(12): 1399-1404.
- Wycisk, K. A., C. Zeitz, et al. (2006). "Mutation in the auxiliary calcium-channel subunit CACNA2D4 causes autosomal recessive cone dystrophy." Am J Hum Genet **79**(5): 973-977.
- Yamin, C., O. Amir, et al. (2007). ACE ID genotype affects blood creatine kinase response to eccentric exercise.
- Yamin, C., J. Duarte, et al. (2008). "IL6 (-174) and TNFA (-308) promoter polymorphisms are associated with systemic creatine kinase response to eccentric exercise." European Journal of Applied Physiology **104**(3): 579-586.
- Yan, Z., X.-c. Bai, et al. (2015). "Structure of the rabbit ryanodine receptor RyR1 at near-atomic resolution." Nature **517**(7532): 50-55.
- Yang, N., D. G. MacArthur, et al. (2003). "ACTN3 Genotype Is Associated with Human Elite Athletic Performance." The American Journal of Human Genetics **73**(3): 627-631.
- Yang, N. B., S. Ji, et al. (1994). "SODIUM-CHANNEL MUTATIONS IN PARAMYOTONIA-CONGENITA EXHIBIT SIMILAR BIOPHYSICAL PHENOTYPES IN-VITRO." Proceedings of the National Academy of Sciences of the United States of America **91**(26): 12785-12789.
- Yang, X., Y. Zhang, et al. (2013). "Phenotypes and PRRT2 mutations in Chinese families with benign familial infantile epilepsy and infantile convulsions with paroxysmal choreoathetosis." BMC Neurol **13**(209): 1471-2377.
- Yang, Y., Y. Wang, et al. (2004). "Mutations in SCN9A, encoding a sodium channel alpha subunit, in patients with primary erythralgia." J Med Genet **41**(3): 171-174.
- Yao, D., H. Mizuguchi, et al. (2008). "Thermal instability of compound variants of carnitine palmitoyltransferase II and impaired mitochondrial fuel utilization in influenza-associated encephalopathy." Human Mutation **29**(5): 718-727.
- Yates, C. M., I. Filippis, et al. (2014). "SuSPect: Enhanced Prediction of Single Amino Acid Variant (SAV) Phenotype Using Network Features." Journal of Molecular Biology **426**(14): 2692-2701.
- Zalk, R., O. B. Clarke, et al. (2015). "Structure of a mammalian ryanodine receptor." Nature **517**(7532): 44-49.
- Zeharia, A., A. Shaag, et al. (2008). "Mutations in LPIN1 cause recurrent acute myoglobinuria in childhood." Am J Hum Genet **83**(4): 489-494.

- Zhang, X. Y., J. Wen, et al. (2013). "Gain-of-function mutations in SCN11A cause familial episodic pain." Am J Hum Genet **93**(5): 957-966.
- Zhang, Y., H. S. Chen, et al. (1993). "A mutation in the human ryanodine receptor gene associated with central core disease." Nat Genet **5**(1): 46-50.
- Zhou, H., S. Lillis, et al. (2010). "Multi-minicore disease and atypical periodic paralysis associated with novel mutations in the skeletal muscle ryanodine receptor (RYR1) gene." Neuromuscular Disorders **20**(3): 166-173.
- Zhuchenko, O., J. Bailey, et al. (1997). "Autosomal dominant cerebellar ataxia (SCA6) associated with small polyglutamine expansions in the alpha 1A-voltage-dependent calcium channel." Nat Genet **15**(1): 62-69.
- Zuberi, S. M., L. H. Eunson, et al. (1999). "A novel mutation in the human voltage-gated potassium channel gene (Kv1.1) associates with episodic ataxia type 1 and sometimes with partial epilepsy." Brain **122**(Pt 5): 817-825.
- Zutt, R., A. J. van der Kooi, et al. (2014). "Rhabdomyolysis: Review of the literature." Neuromuscular Disorders **24**(8): 651-659.